Aus dem Institut für Phytopathologie
der Christian-Albrechts-Universität zu Kiel

Rhizosphere Processes and Microbial Functions under Successive Wheat Rotational Positions

Dissertation
zur Erlangung des Doktorgrades
der Agrar- und Ernährungswissenschaftlichen Fakultät
der Christian-Albrechts-Universität zu Kiel

vorgelegt von

M.Sc. Mehdi Rashtbari
aus Kharvana, Iran
Kiel, 2024

Dekan: Prof. Dr. Georg Thaller.
1. Berichterstatterin: Jun. Prof. Dr. Baharsadat Razavidezfuly
2. Berichterstatter: Prof. Henning Kage
Tag der mündlichen Prüfung: 03.07.2024

“Published with the approval of the Faculty of Agricultural and Nutritional Sciences”

Summary

Wheat is an important staple crop worldwide, and the increasing demand for wheat requires more intensive cropping systems, such as monoculture. However, continuous cultivation of wheat contributes to a decline in grain yield and quality, possibly due to increased weed infestation and the proliferation of pests and fungal pathogens. Therefore, in the present study, we aimed to investigate 1) the underlying mechanisms that govern the productivity of winter wheat (WW) grown in self-succession as opposed to WW grown after a break crop, oilseed rape, 2) the impact of successive wheat cultivation on glucose release from roots and microbial activity, 3) the effects of continuous wheat rotations on glucose release, microbial growth and activity, and expression of sugar transporter genes. We hypothesized that there would be reduced rhizodeposition in self-successional WW, resulting in distinct changes in the microbial community composition and reduced production of hydrolytic enzymes. We found that the position of WW in the rotation has a significant impact on wheat biomass and also the structure and function of the soil microbiota. The findings underscore the necessity of identifying and characterizing specific compounds in root exudates that trigger soil microorganisms. Therefore, we improved and optimized the protocol of soil glucose imaging - *in situ* imaging method of glucose release and presence of glucose in the area around the root. and adapted this method for the soil environment. The study revealed that regions characterized by high glucose release in wheat roots exhibited heightened microbial activity, indicating a direct correlation between glucose availability and microbial stimulation. Furthermore, the investigation into long-term wheat cultivation demonstrates a notable decrease in both glucose release and enzyme activity, suggesting potential shifts in the microbial environment over time. Third wheat after break crop (W3) exhibited the lowest proportion of hotspots for glucose release in comparison to the first wheat (W1). Concurrently, there was a notable upregulation of the expressions of functional orthologous genes of SWEET family sugar transporters, particularly SWEET1a, in the wheat roots of W3 as opposed to W1. Moreover, total microbial biomass experienced a decline in both the rhizosphere and bulk soils of W3 relative to W1, indicating shifts in the microbial community composition. The research revealed the effect of crop rotational positions on root exudation patterns, and microbial responses, hence shaping the rhizosphere environment and influencing soil properties. Overall, these insights contribute to a comprehensive understanding of the factors influencing soil health and highlight the importance of considering temporal dynamics and intricate relationships between crop rotation and soil microbial responses for sustainable agriculture. This study emphasizes the importance of long-term research into the effects of continuous wheat cultivation on soil health and microbial communities. Enhancing beneficial microorganisms in the rhizosphere is crucial for sustainable agriculture and continued exploration of innovative tools like the glucose imaging method offer new opportunities for soil research, helping us monitor root exudation and microbial responses in field settings.

Zusammenfassung

Weizen ist weltweit ein wichtiges Grundnahrungsmittel, und der steigende Bedarf an Weizen erfordert intensivere Anbausysteme wie Monokulturen. Die kontinuierliche Anbau von Weizen trägt jedoch zu einem Rückgang des Getreideertrags und der Qualität bei, möglicherweise aufgrund erhöhter Unkrautbefall und der Verbreitung von Schädlingen und Pilzpathogenen. Daher haben wir uns in der vorliegenden Studie zum Ziel gesetzt, 1) die zugrunde liegenden Mechanismen zu untersuchen, die die Produktivität von Winterweizen (WW) beeinflussen, der in Selbstfolge angebaut wird im Vergleich zu WW, der nach einer Unterbrechungskultur, Raps, angebaut wird, 2) die Auswirkungen aufeinanderfolgender Weizenkulturen auf die Glukosefreisetzung aus den Wurzeln und die mikrobielle Aktivität zu untersuchen und 3) die Auswirkungen kontinuierlicher Weizenrotationen auf die Glukosefreisetzung, das mikrobielle Wachstum und die Aktivität sowie die Expression von Zuckert ransporter-Genen zu untersuchen. Wir haben die Hypothese aufgestellt, dass es bei selbstfolgender WW eine reduzierte Rhizodeposition geben würde, was zu deutlichen Veränderungen in der mikrobiellen Gemeinschaftszusammensetzung und einer reduzierten Produktion hydrolytischer Enzyme führt. Wir haben festgestellt, dass die Position von WW in der Rotation einen signifikanten Einfluss auf die Weizenbiomasse sowie die Struktur und Funktion der Bodenmikrobiota hat. Die Ergebnisse unterstreichen die Notwendigkeit, spezifische Verbindungen in Wurzelexsudaten zu identifizieren und zu charakterisieren, die Bodenmikroorganismen auslösen. Daher haben wir das Protokoll der Bodenglukose-Bildgebung verbessert und optimiert - eine in-situ-Bildgebungsmethode zur Glukosefreisetzung und zum Vorhandensein von Glukose im Bereich um die Wurzel - und diese Methode für die Bodenumgebung angepasst. Die Studie ergab, dass Regionen mit hoher Glukosefreisetzung in Weizenwurzeln eine erhöhte mikrobielle Aktivität aufweisen, was auf einen direkten Zusammenhang zwischen der Verfügbarkeit von Glukose und der mikrobiellen Stimulation hinweist. Darüber hinaus zeigt die Untersuchung des Langzeitweizenanbaus einen bemerkenswerten Rückgang sowohl der Glukosefreisetzung als auch der Enzymaktivität, was auf potenzielle Verschiebungen in der mikrobiellen Umwelt im Laufe der Zeit hinweist. Der dritte Weizen nach Unterbrechungskultur (W3) zeigte im Vergleich zum ersten Weizen (W1) den niedrigsten Anteil an Hotspots für Glukosefreisetzung. Gleichzeitig gab es eine bemerkenswerte Hochregulation der Expressionen funktional orthologer Gene der SWEET-Familie von Zuckert ransportern, insbesondere SWEET1a, in den Weizenwurzeln von W3 im Vergleich zu W1. Darüber hinaus erlebte die Gesamtzahl der mikrobiellen Biomasse sowohl in der Rhizosphäre als auch in den Bulk-Böden von W3 im Vergleich zu W1 einen Rückgang, was auf Verschiebungen in der mikrobiellen Gemeinschaftszusammensetzung hinweist. Die Forschung hat die Auswirkungen der Anbaupositionen auf die Wurzelexsudationsmuster und mikrobielle Reaktionen aufgedeckt, wodurch die Rhizosphärenumgebung geformt und Bodeneigenschaften beeinflusst wurden. Insgesamt tragen diese Erkenntnisse zu einem umfassenden Verständnis der Faktoren bei, die die Bodengesundheit beeinflussen, und betonen die Bedeutung der Berücksichtigung zeitlicher Dynamiken und komplexer Beziehungen zwischen Fruchtfolge und bodenmikrobiellen Reaktionen für eine nachhaltige Landwirtschaft. Diese Studie unterstreicht die Bedeutung langfristiger Forschung zu den Auswirkungen kontinuierlicher Weizenanbau auf Bodengesundheit und mikrobielle Gemeinschaften. Die Förderung nützlicher Mikroorganismen in der Rhizosphäre ist für eine nachhaltige Landwirtschaft entscheidend, und die fortlaufende Erforschung innovativer Werkzeuge wie der Glukosebildgebungsmethode bietet neue Möglichkeiten für die Bodenforschung und hilft uns, Wurzelexsudation und mikrobielle Reaktionen in Feldumgebungen zu überwachen.

Table of Contents

Tables

Figures

List of Abbreviations

%	percent
˚C	Degree Celsius
µg	Microgram
µ	specific growth rate
µL	Microliter
AEM	anion exchange membrane
AMC	7-amino-4-methyl coumarin
AMC-L	L-leucine-7-amino-4-methylcoumarin hydrochloride
AMF	arbuscular mycorrhizal fungi
ASVs	amplicon sequence variant
ATP	Adenosine triphosphate
BBCH	Biologische Bundesanstalt für Land- und Forstwirtschaft, Bundessortenamt und CHemische Industrie
BCA	Biological control agents
BGU	*β*-glucosidase
BMBF	German Federal Ministry of Education and Research
BonaRes	Boden als nachhaltige Ressource
bp	base pair
BR	basal respiration
BS	bulk soil
C	Carbon
C:N	carbon to nitrogen ratio
CAU	Christian-Albrechts-University of Kiel
cDNA	Complementary DNA
C_m	mineral carbon
C_{mic}	microbial biomass C
CO_2	Carbon dioxide
Da	Dalton
DMSO	Dimethyl sulfoxide
DNA	Deoxyribonucleic acid
DOC	dissolved organic carbon
EA-IRMS	elemental analyzer coupled to an isotope-ratio mass spectrometer
g	gram
Ggt	*Gaeumannomyces graminis* var *tritici*
GLMs	General linear models
GLU	glucose
GMB	growing microbial biomass
h	hour
HEs	Hydrolytic enzymes
IAA	Indole acetic acid (auxin)
K	potassium
kg	kilogram
K_m	the substrate concentration at which the reaction rate is 50% of the Vmax
KW1	oilseed rape
KW2	first wheat plots after oilseed rape
KW4	third wheat plots after oilseed rape
LAP	Leucine aminopeptidase
LMWOS	low-molecular-weight organic substances
MB	microbial biomass
MBC	Microbial biomass carbon
MBP	Microbial biomass phosphorus
MES	4-morpholineethane sulfonic acid
mg	milligram

mM	millimolar
MUF	4-methylumbelliferone
MUF-P	4-methylumbelliferyl-phosphate
MUF-β	4-methylumbelliferyl-β-glucoside
N	Nitrogen
NCBI	National Center for Biotechnology Information
NH_4^+	ammonium
NO_2^-	nitrite
NO_3^-	nitrate
nM	nanomolar
nm	nanometer
N_{min}	mineral nitrogen
N_{mic}	microbial biomass nitrogen
PCoA	principal coordinate analysis
PERMANOVA	Permutational multivariate analysis of variance
PHOS	acid phosphomonoesterase
qCO_2	metabolic quotient
qPCR	Quantitative polymerase chain reaction
RABIT	rapid automated bacterial impedance technique
ROI	region of interest
R_{dia}	root diameter
RH	rhizosphere
RLD	root length density
RNA	Ribonucleic acid
rpm	round per minute
RS	resistance index
RTD	root tissue density
RT-qPCR	Real-Time Polymerase Chain Reaction
S	substrate concentration
SRA	Sequence Read Archive
SD	standard deviation
SIGR	Substrate Induced Growth Respiration
SIR	substrate-induced respiration
SOM	soil organic matter
SRL	specific root length
SWEET	sugars will be eventually effluxed transporter
TAD	Take-All decline
TAL	transcription activator-like
T_g	generation time
t_{lag}	lag period
TMB	total microbial biomass
TN	total extractable nitrogen
TOC	total organic carbon
TRIZMA	Tris(hydroxymethyl)aminomethan
T_t	substrate turnover time
UK	United Kingdom
USA	United States of America
V_{max}	maximum velocity of enzyme activity
W1	first wheat after a break crop
W2	second wheat after a break crop
W3	third wheat after a break crop
WHC	water-holding capacity
WM	wheat monoculture
WW	winter wheat

1 Chapter I: General Introduction

1.1. Introduction

Since its domestication around 10,000 years ago, wheat (*Triticum aestivum*) has played a crucial role in global food security. Wheat now supplies a fifth of food calories and protein to the world's population. It is the most widely cultivated crop in the world, cultivated on 217 million ha annually (Erenstein et al., 2022). Developing countries contribute over 60% to the total wheat production. To meet the demands of a growing population, wheat yield must increase by 60% by 2050. However, the escalating global temperatures pose a threat, projecting a potential 27% yield decrease (FAO, 2018; Ordon et al., 2019). Despite modern pesticide use, diseases and pests result in a global average yield loss of 20% (Serfling et al., 2017). The increasing expenses of treatment, coupled with environmental concerns, underscore the imperative to develop stable, affordable, and non-chemical disease control methods (Ordon et al., 2019).

1.2. Soil-borne Plant Pathogens

In simple terms, plants have two main parts: what we see above the ground, like leaves and stems, and what's below the ground, which is the root system. While the above-ground parts are more noticeable and studied, it's the root system that plays a crucial role in taking up water and nutrients for the plant's health and providing support (Weller et al., 2002). Diseases that target the roots can seriously harm the plant, leading to lower quality and crop yield. These diseases, often found in the soil, can affect plants from their early stages to maturity, causing significant losses by disrupting water and nutrient uptake (Coninck et al., 2015; Panth et al., 2020).

1.3. Take-all disease in wheat

Although extensively studied, take-all disease, induced by the soil-borne fungus *Gaeumannomyces tritici*, persists as the foremost root ailment affecting wheat on a global scale (Freeman and Ward, 2004). *Gaeumannomyces tritici* was formerly known as *Gaeumannomyces graminis* var. *tritici* and belongs to the Magnaporthaceae family. Notably, it also affects other cereals such as barley (*Hordeum vulgare*), rye (*Secale cereale*), and triticale (*Triticosecale*). Unlike other fungal pathogens with root-infecting capabilities, such as *Fusarium*, *Rhizoctonia*, *Verticillium*, and *Pythium* species, which exhibit a broad host spectrum and can infiltrate various plant tissues causing damage, G. *tritici* solely targets roots, confining its host range to cereals (Palma-Guerrero et al., 2021). Because of its ability to infect and grow in both wet and dry conditions it is one of the most important soil-borne diseases of wheat in the world (Kwak & Weller, 2013). Take-all disease is prevalent in temperate wheat-growing regions globally, extending to high-altitude subtropical and tropical areas (Hornby, 1993).

The economic consequence of this disease is substantial due to diminished wheat yield and compromised grain quality; both the direct and indirect outcomes of harm to wheat roots are delineated in Figure 1.2. It is noteworthy that there are currently no available resistant wheat cultivars against take-all, and chemical control remains constrained.

Consequently, control measures primarily hinge on crop rotation, emphasizing the pressing need for innovative control strategies.

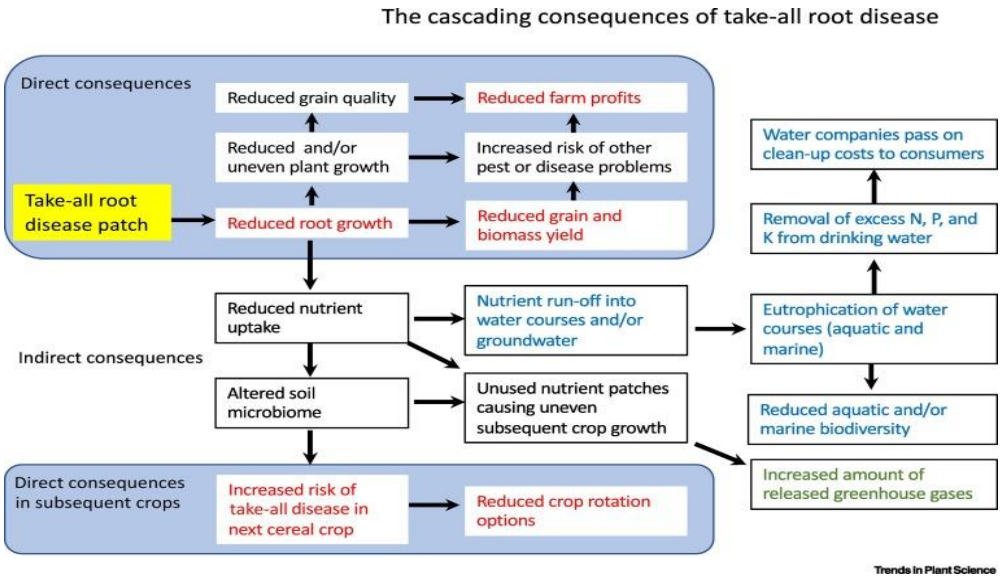

Figure 1.1- The Cascading Direct and Indirect Consequences of Take-All Root Disease (Palma-Guerrero et al., 2021).

1.4. Take-All Control

As already mentioned, the primary and consistently effective control method for managing take-all disease is crop rotation (Wang et al., 2020). Given the specialized nature of G. *tritici* and its reliance on infested host remains for survival and nutrition, this approach is not surprising. A successful crop rotation strategy involves the early and prompt removal of volunteer cereals to maximize the benefits of non-host crop intervals. Additionally, the elimination of grass hosts for the take-all pathogen in alfalfa or legume pastures before returning to wheat or barley is crucial (Kwak et al., 2013). The cultivation of non-susceptible break crops contributes to the reduction of take-all severity by minimizing inoculum (McMillan et al., 2018). For instance, Monaci et al. (2017) observed that winter wheat exhibited greater rootability and root density, along with thinner roots, when grown following alfalfa compared to following barley. Gaiser et al. (2012) demonstrated that spring wheat exhibited greater rooting depth and higher root length density in the subsoil when grown after lucerne compared to after chicory and fescue. An alternative approach to mitigate yield losses due to take-all disease could involve the continuous cultivation of wheat. This practice may trigger what's known as the "take-all decline effect," resulting in decreased severity of the disease or even its undetectability after consecutive years of wheat cultivation. However, it's worth noting that despite these benefits, grain yield tends to be lower compared to wheat grown in rotation with other crops (Cook, 2003; Arnhold et al., 2023).

1.5. Take-All Decline

The process known as take-all decline (TAD), where the incidence of take-all disease decreases when wheat is continuously cultivated in the same field, is a prevalent form of natural suppression of this disease (Hornby et al., 1998). It typically involves a pattern of initially low take-all levels during the early cropping years, followed by disease outbreaks between 2 and 7 years, and ultimately a decline in the disease accompanied by increased yields (Chng et al., 2015).

Certain soils exhibit suppressive characteristics against take-all disease, although the specific reasons for this phenomenon are often unclear. Suppressiveness may stem from effects on the pathogen, host, or the balance of antagonistic microflora in the soil (Cook, 2014). General suppression tends to increase with higher microbial biomass in the soil (Weller et al., 2002). Various mechanisms for specific suppression exist. In general suppression, the beneficial effect is not attributed to any specific microorganism or a particular group; instead, it involves a collective influence of various microbes (Cook 2014). Recently referred to as key species or the core microbiome, these specific microbes drive both the composition and function of the microbiome (Dong et al. 2020). Consequently, general suppression cannot be transferred between different soils, highlighting its non-transferrable nature (Andrade et al. 2011; Kwak and Weller 2013). Conversely, specific suppression is tailored to combat a particular pathogenic microorganism and is facilitated by distinct microbes, albeit utilizing mechanisms similar to those observed in general suppression (Andrade et al. 2011). Research has demonstrated that introducing 1% (w/w) of natural suppressive soil into sterile suppressive soil, inoculated with Ggt, is adequate to convey suppression against take-all disease (Chang et al. 2015; Durán et al. 2017).
Studies related with soil disease suppression are numerous, mainly considering biotic factors associated with the disease incidence diminution as microbial composition (Duran and Mora, 2021); however, the mechanisms involved are multiple and complexly interconnected. In fact, studies of plant–microbe–soil interactions guaranty a better understanding of these processes.

1.6. Rhizosphere

Plant roots form connections with a distinct set of soil microorganisms found in the root vicinity, referred to as the rhizosphere. The rhizosphere surrounding an individual root encompasses a space extending from the root to an indistinct location in the soil. The extent of this zone is influenced by the diffusion of exudates, as well as the developmental stage and biochemical characteristics of the roots, as described by Hinsinger et al. (2005). This area is recognized as one of the most intricate ecosystems globally, housing millions of microbial cells. However, the microbial cell count varies based on the plant's genotype and its growth stages (Singhal et al., 2016). Within the rhizosphere, plants release diverse compounds that serve as chemical attractants for soil microorganisms (Pandey et al., 2017). The initiation of a rhizosphere occurs when the tip of a root enters a soil volume and concludes when that particular section of the root undergoes decay, as outlined by Jones et al. (2004). As roots progress, they develop hairs, branch roots, and, in the case of dicotyledon roots, secondary thickening. The duration of the rhizosphere's existence varies, depending on whether the plant is an annual or perennial crop, and it can endure for multiple years (Watt et al., 2016).
The plant microbiome provides the host plant with additional gene pools, often referred to as the second plant genome or extended genome (Berendsen et al., 2012; Rout and Southworth, 2013). Notably, there has been a growing focus on plant root-associated microbiomes in recent years due to their crucial roles in host nutrition, development, and immunity (Chen et al., 2019). A study demonstrated that plant roots assemble microbial communities in the root zone from the surrounding soil (Fitzpatrick et al., 2018). The microbiota in these compartments can either be beneficial or harmful to the host plant, and any shift in this balance could significantly impact crop production in agricultural ecosystems. Consequently, understanding how root-associated microbial communities respond to soil management practices and the physiological status of the plant is of significant agronomic interest.

Soil, often described as a "microbial seed bank" (Lennon et al., 2011), provides plants with a diverse pool of potential microorganisms. Plants, as a strategy to influence their local growth conditions, can modify the soil environment by releasing bioactive molecules into the rhizosphere, thereby altering edaphic conditions for soil microbiota (Hu et al., 2018). Consequently, distinct plant species or genotypes can attract specific microbiota due to variations in root morphologies and patterns of root exudation (Haichar et al., 2008).

Additionally, the composition of root exudates (Gransee and Wittenmayer, 2000) and the structure of the root-associated microbial community are significantly influenced by the plant's growth stage (Schlemper et al., 2017). Studies utilizing molecular technologies have demonstrated variations in the composition of root-associated microbiomes during plant development (Houlden et al., 20087), suggesting that changes in root exudation may be the underlying cause, even though the compositions and quantities of the root exudates were not explicitly assessed in these studies (Chen et al., 2019).

1.7. Root exudates

Root exudates, comprising a diverse range of carbon-containing metabolites such as sugars, amino acids, and organic acids, impose a substantial carbon cost on the host plant (Marschner, 1995). These exudates also serve as substrates and signalling molecules for microbes, fostering intricate biogeochemical interactions between the host plant and microorganisms (Bais et al., 2006). Among the primary low molecular weight compounds found in root exudates, organic acids have been identified as selective agents influencing the structure of the rhizosphere microbiome. They stimulate the growth of specific microbial populations while inhibiting the development of others (Eilers et al., 2010). Incubation experiments indicate that, compared to carbohydrates, organic acids have a more pronounced impact on the richness and structure of dominant taxa within the soil microbial community (Carvalhais et al., 2011; Shi et al., 2011). Plants employ the secretion of organic acids as a crucial strategy to adapt to low nutrient availability, particularly for nutrients like phosphorus and nitrogen (Chen et al., 2019).

Plants release approximately one-third of their photosynthetic products in the form of rhizodeposits into the soil, establishing the foundation for plant-microbial interactions (Kuzyakov et al., 2003; Bais et al., 2006). Rhizodeposits encompass various components, including the loss of root cap and border cells, the death and lysis of root cells, gaseous emissions, the passive and active release of solutes (root exudates), and the presence of gelatinous material on the root surface (mucigel) (Jones et al., 2009). The process of root exudation serves to stimulate microbial activity (Hinsinger et al., 2009), promotes the production of extracellular enzymes (Asmar et al., 1994), and thereby contributes to the decomposition of soil organic matter (SOM) (Cheng and Coleman, 1990). It's worth noting that the elevated enzyme activity observed in the rhizosphere compared to root-free soil is influenced not only by microbial activity but also by the direct release of enzymes by roots or the lysis of root cells (Jones et al., 2009; Marinari et al., 2014).

Glucose, a prevalent soluble carbohydrate abundant in root exudates, plays a pivotal role in facilitating root adaptation to dynamic environmental conditions (Canarini et al., 2019). Its consistent presence among fluctuations in root exudate composition due to varying soil moisture, temperature, and nutrient availability underscores its significance in driving microbial activity within the rhizosphere (Hütsch et al., 2002). The influence of glucose extends beyond its role as a mere energy source. Studies have suggested its

involvement in modulating root exudation patterns in response to environmental cues, thereby shaping the rhizosphere's microbial community structure (Smith and Read, 2008). For instance, glucose availability has been linked to alterations in microbial diversity and enzymatic activities, influencing nutrient cycling processes and potentially affecting plant nutrient uptake (Qi et al., 2022). Wild et al. (2014) found that glucose can actively engage in soil carbon metabolism processes by serving as both a carbon and energy source. Studies conducted in pure cultures have demonstrated that glucose molecules engage with microbial chemoreceptors, eliciting diverse biochemical responses. This finding holds significance for the study of soil microbes (Kirby, 2009).

1.8. Root exudates and plant pathogen response

A holobiome, a symbiotic relationship between the microbial population and the host plant, is established, and the colonization of beneficial fungi and bacteria holds particular significance for sustainable agricultural production (Vandenkoornhuyse et al., 2015). Plant root exudates exert protective effects by competing for nutrients and producing substances that hinder the growth of pathogenic microorganisms. Through chemotaxis, plant root exudates can attract desired microbes while repelling pathogens. This process contributes to maintaining soil moisture, stabilizing soil aggregates, facilitating nutrient mobilization, and impeding the growth of competing plants (Narula et al., 2012).

Plants face diverse challenges in their natural environment, such as drought, warming and plant pathogens, but they have developed sophisticated strategies to address these issues (Bukovská et al., 2021; Philippot et al., 2013). One fundamental strategy involves synthesizing specialized compounds with unique properties. These compounds serve dual purposes: some act as direct defenses against pests and diseases, while others function as signalling molecules. The signalling molecules alert nearby plants, preparing them to activate their defense mechanisms.

The activation of the plant immune system under the attack of leaf pathogens led to the change of rhizosphere microbial community, indicating that plant immune signals and rhizosphere microbial community assembly are functionally related (Bakker et al. 2018). A strategy employed to enhance plant defense involves the release of secretions by the roots to recruit beneficial microorganisms during pathogen attacks, commonly known as the "cry for help" (Bakker et al., 2018). These signals operate as an SOS call to beneficial soil microbes, fostering collaboration with the plant to alleviate the impacts of environmental stresses (Teklić et al., 2021). Within their chemical arsenal, plants generate diverse compounds that play specific roles in defense and signalling (Dubey et al., 2020; Islam et al., 2021). Importantly, plant roots have evolved similarly to other plant parts. When roots release these compounds, they initiate the recruitment of symbiotic microbes, thereby enhancing the plant's resilience and overall health, particularly in response to environmental stressors (de Vries et al., 2020). Beneficial microbes have the capability to activate plant defense signalling pathways and/or impede the virulence and growth of pathogens by secreting antibiotics, as depicted in Figure 2 (Liu et al., 2020). For instance, upon pathogen invasion, members of the *Chitinophagaceae* and *Flavobacteriaceae* were enriched in the root endosphere, providing protection against plant diseases (Carrión et al., 2019). When attacked by the pathogen *Pythium ultimum*, barley roots increased the secretion of vanillic acid, fumaric acid, and p-coumaric acid, inducing Pseudomonas fluorescens CHA0 to colonize and synthesize the antibiotic 2,4-diacetylphloroglucinol (DAPG) (Jousset et al., 2011).

These findings suggest that plants recruit beneficial microbes that produce antimicrobial compounds when facing pathogenic attacks.
Direct plant defense involves root exudates directly suppressing pathogens and pests. On the other hand, indirect plant defense refers to root exudates playing a role in driving plant-microbe feedbacks for defense. This occurs by altering the rhizosphere microbiome, recruiting beneficial microbes. These beneficial microorganisms, in turn, enhance plant defense through two pathways: firstly, by activating plant defense signaling pathways, and secondly, by secreting antimicrobial compounds that inhibit pathogens (Fig. 1.2; Sun et al., 2021).

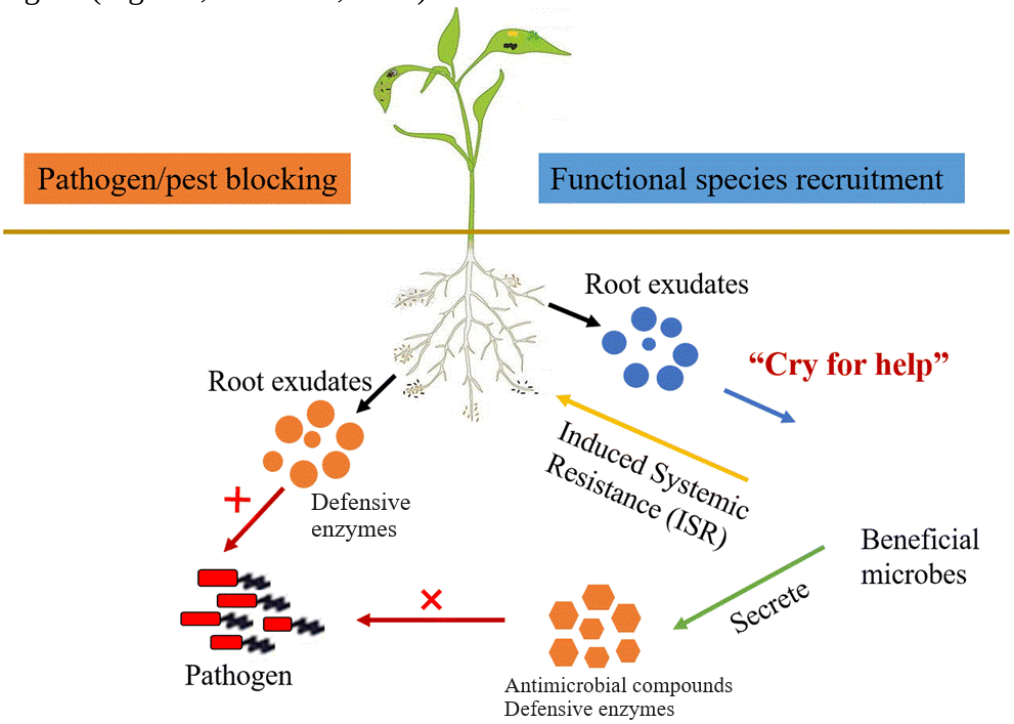

Figure 1.2. Direct and indirect plant defense mechanisms mediated by root exudates (adopted from Sun et al., 2021)

Figure 1.3 illustrates the factors influencing the association between plants and their microbiome, as well as the chemical exudates released by roots to attract microbial species. Biotic factors encompass both beneficial and harmful elements simultaneously. Notably, the host plant releases specific root exudates designed to recruit beneficial microbes. These microbes play a role in providing nutrients, inducing and priming host immunity, and enhancing tolerance under challenging conditions (Afridi et al., 2024).
In response to stress and pathogen attacks, plants engage in complex biochemical processes. For example, barley roots, when infected with the soil-borne pathogenic fungus *Fusarium graminearum*, released elevated amounts of phenolic compounds, including t-cinnamic acids with antifungal properties (Bakker et al., 2018). A similar pattern was observed in sweet basil roots, which released the antifungal compound rosmarinic acid when infected with the oomycete fungus *Pythium ultimum* (Bakker et al., 2018). Nevertheless, root exudates can act as a natural nutrient supply for pathogenic fungi, including *Phytophthora*, *Verticillium*, *Pythium*, *Aphanomyces*, *Sclerotium*, *Fusarium*, and *Rhizoctonia*. Furthermore, a single exudate can attract various species; for instance, the isoflavones released by soybean roots have the capability to attract both *Bradyrhizobium japonicum* (a mutualistic bacterium) and *Phytophthora sojae* (a pathogen) (Song et al., 2021).

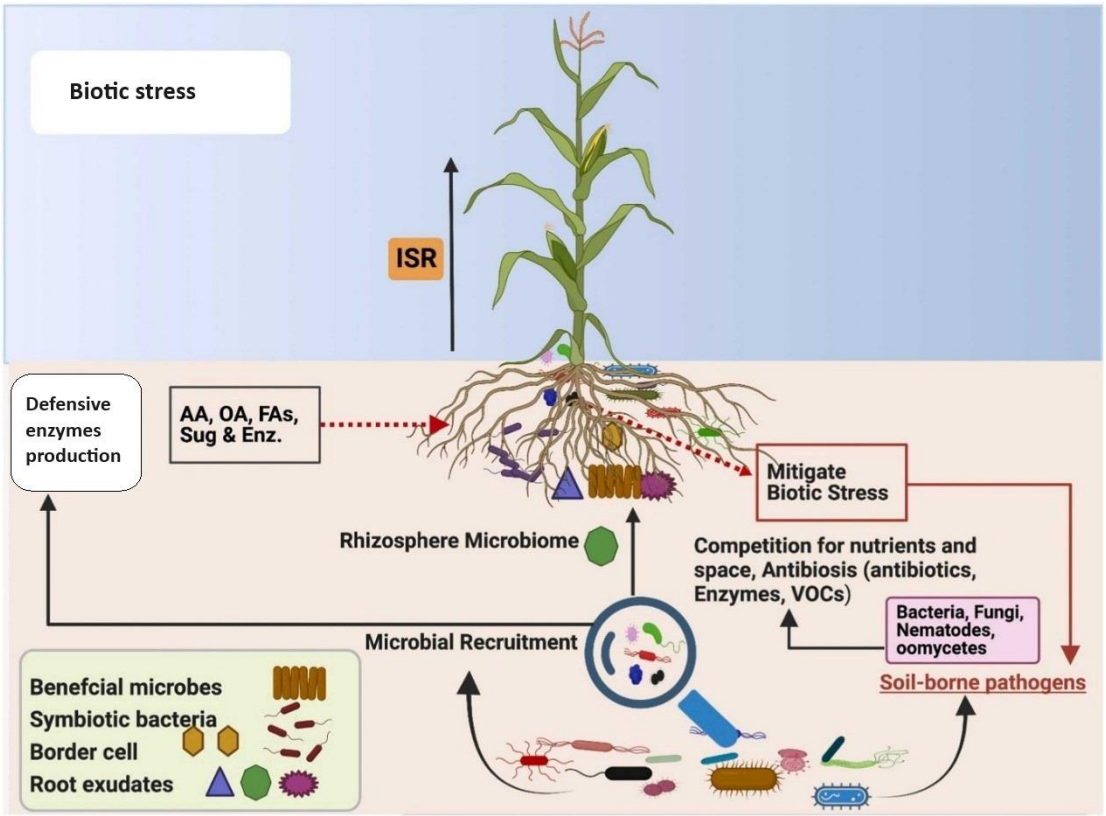

Figure 1.3. factors influencing the association between plants and their microbiome, and the chemical exudates released by roots to attract microbial species (adopted from Afridi et al., 2024)

Rhizospheric microbes serve as biological control agents (BCA) that regulate plant pathogens, ultimately enhancing plant productivity by producing antimicrobial secondary metabolites (Singh et al., 2019) and hydrolytic enzymes (Adesina et al., 2007) and improving nutrient availability (Glick, 2012). The secretion of lytic enzymes by plant growth-promoting rhizobacteria enhances defense capabilities (Upadhyay et al., 2016). Hydrolytic enzymes (HEs) have the ability to break down chemical bonds in a wide range of polymeric compounds, including chitin, proteins, cellulose, hemicelluloses, and phytopathogenic DNA (Jadhav and Sayyed, 2016). By targeting the cell wall, proteins, and DNA of pathogens, HEs effectively control phytopathogens, thereby playing a crucial role in bio-control (Prathap and Ranjitha, 2015).

1.9. Soil microbial functions and enzyme activity

The concept of soil quality is defined as "the capacity of a soil to function, within ecosystem and land use boundaries, to sustain productivity, maintain environmental quality, and promote plant and animal health" (Doran, 1996). Due to its dynamic nature, soil quality requires continuous monitoring over time, and the selection of appropriate indicators depends on the specific objectives of users (Snapp and Morrone, 2008). Soil extracellular enzymes play a crucial role in controlling soil nutrient cycling (Maharjan et al., 2017; Uwituze et al., 2022), and their activities are considered important determinants of soil quality (Sinsabaugh et al., 2008).

Microorganisms play a pivotal role as the most dynamic component in the soil ecosystem, offering timely responses and feedback to its conditions (Toledo et al., 2023; Zhao et al., 2023). The diversity and composition of soil microbial communities are crucial for maintaining soil quality and health. Higher levels of bacteria and fungi in the soil show a positive correlation with the overall well-being of the soil ecosystem

(Liu et al., 2015). Soil extracellular enzymes are predominantly released outside the cell, either by soil microorganisms (Skujinš and Burns, 1976) or plant roots (Burns et al., 2015). They can bind to either the cell or soil particles or diffuse freely in soils (Burns et al., 2015). Soil enzyme activity is generated through the biological activities of the soil fauna, organisms, and plant roots. Moreover, they play a vital role in the C, N, and P cycles within the soil (Fu et al., 2017).

The enzyme activity reflects the trend and intensity of various biochemical processes in the soil, making it more sensitive than changes to the physicochemical properties. Therefore, compared to the physical and chemical indices, ascertaining the changes in the soil enzyme activity is a more intuitive and reliable approach to elucidate the impact of agricultural management on soil quality (Li et al., 2023).

Continuous cropping practices have been observed to adversely impact soil microorganisms. These practices result in a notable decrease in functional strains, including aerobic and nitrogen-fixing bacteria, disrupting the original structure of the soil microbial community and subsequently affecting plant growth (Wang et al., 2018). Furthermore, such practices can inhibit the secretion of antibiotics by bacteria, promoting the proliferation of pathogenic bacteria, thereby increasing the incidence of plant diseases (Zhang et al., 2020). Concurrently, harmful microorganisms release secondary metabolites that attract beneficial microorganisms for their advantage, further disturbing the soil microecology and pushing it towards a state conducive to their survival. This exacerbates challenges associated with continuous cropping. Hence, it is crucial to investigate the impact of continuous wheat cropping on soil microbial and biochemical characteristics for the improvement of cultivation practices and the enhancement of the soil environment (Song et al., 2024).

In recent years, numerous analyses have been conducted analyses on the impact of continuous cropping on enzyme activity; however, the findings were inconsistent. Some studies indicated a peak in enzyme activity with increasing years of planting (Zhang et al., 2021), while others demonstrated a negative correlation between the two (Wang et al., 2022). These discrepancies may be attributed to variations in soil type and plant species. Furthermore, microbial communities play a significant role in maintaining the microecological environment of plant roots through their influence on soil enzyme activity.

1.10. Objectives and Hypotheses

Wheat is an important staple crop worldwide, and the increasing demand for wheat requires more intensive cropping systems, such as monoculture (Gan et al., 2014). However, continuous cultivation of wheat contributes to a decline in grain yield and quality (Debaeke et al., 1996), possibly due to increased weed infestation and the proliferation of agrophages (pests and fungal pathogens) (Woźniak, 2019). Therefore, in the present study, we aimed to investigate 1) the underlying mechanisms that govern the productivity of WW grown in self-succession as opposed to WW grown after a break crop, oilseed rape, 2) the impact of successive wheat cultivation on glucose release from roots and microbial activity, 3) the effects of continuous wheat rotations on glucose release, microbial growth and activity, and expression of sugar transporter genes.

We hypothesized that there would be reduced rhizodeposition in self-successional WW, resulting in distinct changes in the microbial community composition and reduced production of hydrolytic enzymes. The reduced rhizodeposition in self-successional WW would be followed by changes in the microbial community composition and a

decreased microbial activity, influencing nutrient (especially mineral N) uptake by the plant and plant biomass.
Specifically, we focused on the quantification of root growth parameters and the associated biochemical parameters (C and N translocation), enzyme kinetics involved in C, N, and P acquisition as well as on the microbial (bacterial and archaeal) compositions in the rhizosphere (RH) and bulk (BS) soil of WW grown in different rotational positions.

1.11. Experiments, Materials and Methods

1.11.1. Field sites and experimental design

The experiments were conducted in two field sites. The first field experiment located in the Hohenschulen experimental field site (54°19′05″N, 9°58′38″E), which is owned by the Christian-Albrechts-University of Kiel, Germany. The soil at the site was pseudogleyic sandy loam (Luvisol), with 21% clay and 35% silt, 44% sand, a pH of 6.7, and organic carbon content of 1.3%, total nitrogen content of 0.15%, and available phosphorous and potassium contents of 9 $mg.kg^{-1}$ and 15 $mg.kg^{-1}$, respectively (Sieling et al., 2005). The crop rotation trial was established in 1989. It 126 included the factors a) rotational position (rapeseed, first wheat after rapeseed, third wheat grown continuously, b) winter wheat varieties (4 levels), and c) N levels (4 levels). From this trial, we selected following rotational positions containing the winter wheat cultivar "Nordkap" and optimal N-fertilization (240 kg N ha^{-1}): (1) winter oilseed rape–winter wheat (W1) and (2) winter oilseed rape–winter wheat–winter wheat- winter wheat (W3). Each crop rotation element is cultivated every year and each plot is replicated four times in incomplete blocks.
The second field site is located near Harste (51°36′23.5″N, 9°51′55.8″E, 142 m above sea level) in Central Germany and the soil type is a silty loam Luvisol derived from Loess (IUSS Working Group WRB, 2015). Long-term (1991–2020) mean annual precipitation is 624 mm and mean annual temperature is 9.4°C (DWD, 2022). The crop rotation trial was established in 2006 (Koch et al., 2018) and includes nine crop rotations, out of which two with winter wheat were included in this study: (1) wheat monoculture (WM) and (2) winter oilseed rape–winter wheat–winter wheat– grain pea–sugar beet–winter wheat. From the latter, the first (W1) and second wheat (W2) after oilseed rape as break crop were considered. Each crop rotation element is cultivated every year with the winter wheat cultivar "Nordkap" and each plot is replicated three times in incomplete blocks.

1.11.2. Rhizobox Experiments

1.11.2.1. Greenhouse

For the rhizobox experiment conducted in the greenhouse with transparent rhizoboxes (20 × 20 × 3 cm), soil samples were collected from the Ap horizon (0-20 cm) of soil at the Hohenschulen experimental field from six different plots at the beginning of the growing season. The soil samples were collected from W1 and W3. After filling the rhizoboxes with soil samples, healthy seeds of the wheat cultivar 'Nordkap' were selected and sterilized before being germinated on wet filter paper for three days at room temperature. Soil moisture was monitored gravimetrically every two days and adjusted to maintain 70% water holding capacity (WHC) throughout the two-month experiment by adding sterile distilled water as needed. Due to the limited space and resources in the rhizoboxes, plants were harvested at two time points: four weeks (t1, BBCH 13) and eight weeks (t2, BBCH 29) after sowing through destructive sampling.

This approach ensured a consistent and comparable temporal assessment of enzyme activities and plant root exudates in W1 and W3.

1.11.2.2. Outdoor rhizotron experiment

Soil was collected in September 2021 from the Experimental Farm Hohenschulen, Faculty of Agricultural and Nutritional Sciences, Christian-Albrechts-University of Kiel. Composite soil samples for rhizobox experiments were taken from oilseed rape (KW1), first (KW2) and third wheat (KW4) plots (N = 4 replications). We conducted an outdoor rhizotron experiment using newly designed rhizotrons with a height of 100 cm, width of 35 cm and inner thickness of 2.5 cm (Reichel et al., 2022). The rhizotrons were placed on the campus of Forschungszentrum Jülich, Germany. All rhizotrons were kept inclined at 45^{o} to facilitate root growth along the lower side of the rhizotrons. Winter wheat seeds were germinated on petri dishes with sterile filter paper for 24 h in the dark at 23 ^{o}C. Subsequently, one germinated seed was sown into each rhizotron. The plants were not fertilized for the duration of the experiment. The plants were harvested at the stem elongation stage (BBCH 30).

1.11.3. Biochemical soil analyses

At harvest, soil samples were stored at -25 °C before analysis of mineral N, dissolved organic carbon (DOC), and total extractable nitrogen (TN) and were quantified with a total organic C (TOC) analyzer (TOC-V + ASI-V + TNM, Shimadzu, Japan). The chloroform-fumigation extraction (CFE) method was used to estimate microbial biomass C and N.

1.11.4. Soil imaging methods

Zymography was performed to measure β-glucosidase activity, following the protocol developed by Razavi et al., (2019). The membranes were soaked in the fluorescent solution and then directly applied to the root-exposing side of the rhizoboxes and covered with aluminium foil to avoid exposure to light and drying out. After one hour of incubation, the membranes were quickly removed, cleaned with a soft brush and exposed to UV light of 355 nm wavelength excitation in a dark room.

1.11.4.1. Method development: *in situ* glucose imaging

Soil glucose imaging is a method used to visualize and quantify the amount of glucose exuded from plant roots. This method was developed and optimized based on the protocols developed by McLaughlin and Boyer (2004) and Voothuluru et al. (2018) and is useful for studying plant root exudation and interactions with the surrounding soil. The process involves preparing a reaction mixture solution by dissolving phosphate powder (Sigma P7994) in distilled water to make a 100 mL buffer solution of 0.05 M (pH 7.4). To this solution, 1.7 unit/ml of glucose oxidase from *Aspergillus niger* (Sigma G7141), 1.5 unit/ml of peroxidase from horseradish (Sigma P8125), and 200 μM of Ampliflu red (Sigma 90101) dissolved in 60 μL of Dimethylsulfoxide were added.
Polyamide membrane filters with a diameter of 20 cm and a pore size of 0.45 mm (Tao Yuan, China) were cut to fit the size of the rhizobox and then saturated with the prepared reaction mixture solution. These membranes are then attached to the rooted side of each rhizobox. After an optimal incubation time (one hour for wheat), the membranes were quickly removed and placed in a dark room under UV light of 355 nm wavelength.
The magenta-colored area on the membrane indicates the presence of glucose exudation, as hydrogen peroxide was generated from a reaction between glucose and

glucose oxidase enzymes. Horseradish peroxidase then catalyses the conversion of colorless Ampliflu red into magenta colored and fluorescent resorufin (Zhou et al., 1997).

1.11.4.2. Installing root windows and *in situ* glucose imaging

At the tillering stage (BBCH 28) under the field condition, the root windows were built at an angle of 90° to the soil surface next to the wheat plants. Root windows (30 × 30 cm) consisting of a transparent acrylic sheet (3-5 mm thick) were fixed in place by two vertical steel rods and backfilled with soil to remove air gaps.

1.11.4.3. Calibration and image analysis

All images were captured using a Canon EOS 6D digital camera with a Canon lens EF 24–105 mm 1: 4L IS II USM. For image processing, individual 4 cm^2 membranes were soaked in MUF and AMC solutions of varying concentrations (0, 0.2, 0.5, 1, 2, 4, 6, 8, and 10 mM for MUF, and 0, 0.1, 0.2, 1, 2, 4 and 5 mM for AMC), then exposed to UV light in the same way as the samples. Calibrated values were used to quantify the colour intensity and relate enzyme activity to the grey value. Fluorescent signals of MUF/AMC on an area basis were calculated based on the volume of substrate solution taken up by a fixed membrane size. The images were processed and analysed using the ImageJ software package. Mean+2SD was applied to identify and separate hotspots within each image. The rhizosphere extent of each root was calculated from the root surface for mature roots (>2 cm from the tip) and root tips (0–2 cm) for glucose release and β-glucosidase activity (soil zymograms) (Bilyera et al., 2021).

1.11.5. Enzyme kinetics, substrate affinity, and catalytic efficiency

The soil samples were collected in a conical tube and stored at 5 °C. soil samples were taken from three soil compartments, i.e., rhizosphere soil (RH) sampled with microspatulas from ≤ 5 mm away from the rhizosphere of primary roots, root-free bulk soil (BS) and the loosely attached soil to the roots after shaking off the plant roots as root-affected soil samples (RA). The kinetics of hydrolytic enzymes involved in C, N, and P cycles were measured by fluorimetric microplate assays of 4-methylumbelliferone (MUF) and 7-amino-4-methyl coumarin (AMC) (Dorodnikov et al., 2009).

1.11.6. Basal respiration and substrate-induced respiration

The MicroResp™ system (Chapman et al., 2007) was utilized to measure basal respiration (BR) and substrate-induced respiration (SIR). For BR, we used distilled water, while SIR was measured using glucose as a readily available C source.

1.11.7. Expression analysis of SWEET sugar transporters by RT-qPCR

Total RNA from wheat leaf and root tissues was extracted with TRIzol® reagent (Thermo Fisher Scientific, Germany) according to the manufacturer's instructions. Quality and concentration control of total RNA were performed using gel electrophoresis and NanoVue Plus Spectrophotometer (GE Healthcare Life Science), respectively. Total RNA samples of three independent biological replicates were used for further experimentation. Complementary DNA (cDNA) was synthesized from 1 µg total RNA in 20 µl reaction volume using RevertAid First Strand cDNA Synthesis Kit (Thermo Fisher Scientific, Germany) at 42 °C for 1 h.

1.11.8. Kinetics of the substrate-induced respiration

Total and active microbial biomass was characterized by Substrate Induced Growth Respiration (SIGR) (Blagodatskaya et al., 2014).

1.11.9. Data analysis

All the statistical analyses were performed in SAS v.9.2. Significant differences measured and calculated parameters between W1 and W3 soil samples were confirmed by Two-Way ANOVA after checking normality and homogeneity of variance values. A probability of $p < 0.05$ was used as the significance level between treatment comparisons. Error bars indicate the standard error of the means.

1.12. Results and Discussion

1.12.1 Study 1: Effect of preceding crop legacy on root growth dynamics, rhizosphere processes and microbial interactions

There was a strong response of root growth traits to WW rotational position with an overall reduction in RLD of 29 % and 31 % for KW2 and KW4, respectively, mainly in the upper 30 cm of the soil (Fig. 1.4a). However, even at a greater depth (60-100 cm), KW1 had the highest difference in RLD compared with KW4. At this depth, KW2 increased its RLD greater than KW4, which had the lowest values of all three rotational positions. Similarly, KW1 had the highest RTD of all rotational positions, with 58 % and 48 % higher RTD values than KW2 and KW4, respectively (Fig. 1.4b). These differences were apparent in both the topsoil and the subsoil. Overall, KW1 had thicker roots with an R_{dia} of 0.28 mm compared to 0.25 mm and 0.24 mm for KW2 and KW4, respectively, a trend that was observed throughout the soil profile (Fig. 1.4c). Finally, KW2 and KW4 increased their SRL by 28 % and 33 % compared to KW1, with significant differences along the complete soil profile (Fig. 1.4d).

More ammonium (NH_4^+) and nitrate (NO_3^-) were found in the RH compared to BS and in the 0-30 cm soil layer compared to subsoil layers. The rotational position of WW strongly affected mineral N, with a 42 % and 48 % lower NH_4^+ concentration in KW1 overall compared to KW2 and KW4, respectively (Fig. 1.5a). In particular, in the uppermost soil depth of KW1, there was much less NH_4^+ than in the same depth of KW2 (-54 %) and KW4 (-58 %). In addition, a similarly lower NO_3^- content was found in KW1 (-49 % and -36 % compared to KW2 and KW4, Fig. 1.5b). Microbial biomass C (C_{mic}) and N (N_{mic}) were also highly impacted by the rotational position, as shown in Fig. 6. C_{mic} was lower by 37 % and 43 % in KW1 compared to KW2 and KW4, respectively (Fig. 1.6a). N_{mic} values of KW1 were 50 % and 57 % lower than those of KW2 and KW4 (Fig. 1.6b).

The rotational position also had a major influence on DOC levels. KW1 soil had 68 % and 150 % higher DOC concentrations than KW2 and KW4, respectively (Fig. 1.7). A significant main effect of soil compartment was shown, with a 74 % higher DOC content in the RH compared to BS. Interestingly, the DOC level in the RH of KW1 at both subsoil depths (30-60 and 60-100 cm) was 1.7 and 4.1 times higher than KW2 and KW4, respectively (Fig. 1.7). Similar DOC concentrations were observed in the BS in the rotational position and at all three soil depths.

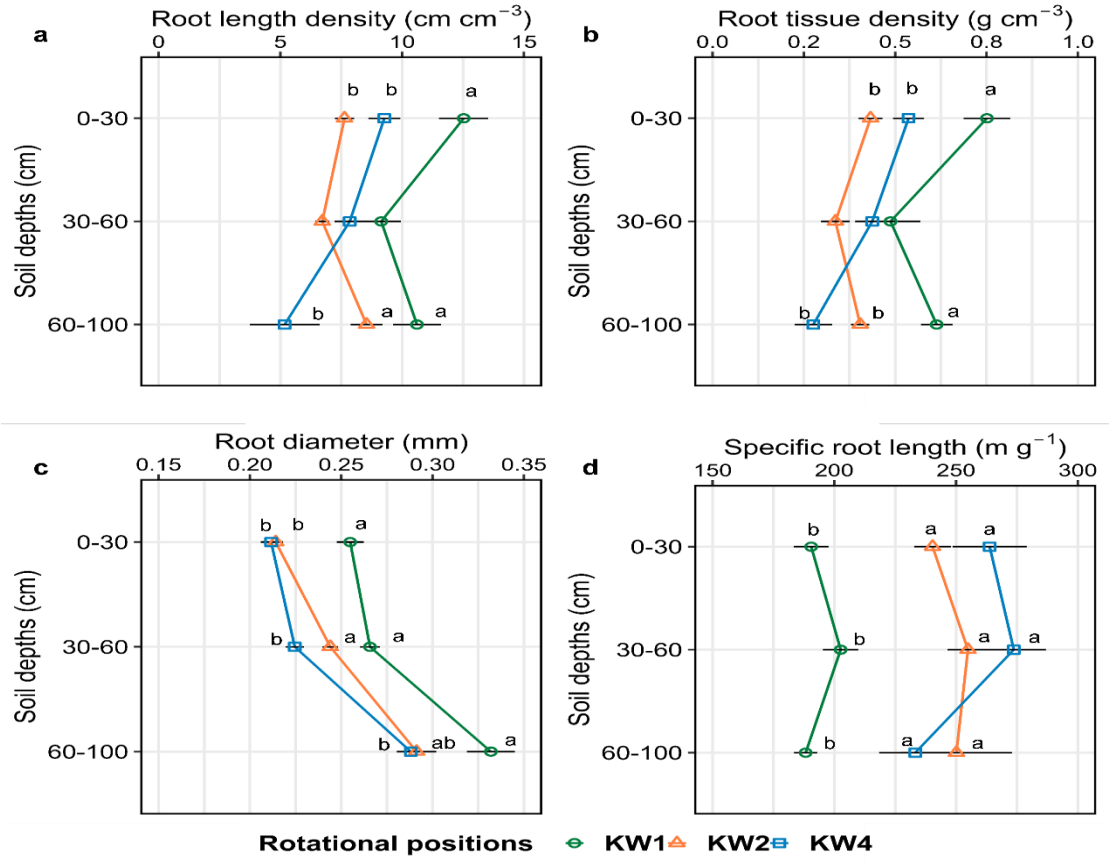

Figure 1.4. Effect of the rotational positions on root length density (a), root tissue density (b), average root diameter (c) and specific root length (d) of the following winter wheat at the onset of stem elongation (BBCH 30) at soil depths 0-30 cm, 30-60 cm and 60-100 cm). KW1 = first wheat, KW2 = second wheat, and KW4 = fourth wheat after oilseed rape in soil from the experimental farm Hohenschulen in Kiel, Germany. Within each soil depth, different lowercase letters denote significant differences between rotational positions at $p \leq 0.05$ according to ANOVA with Bonferroni correction for multiple comparisons. No letters indicate non-significant differences.

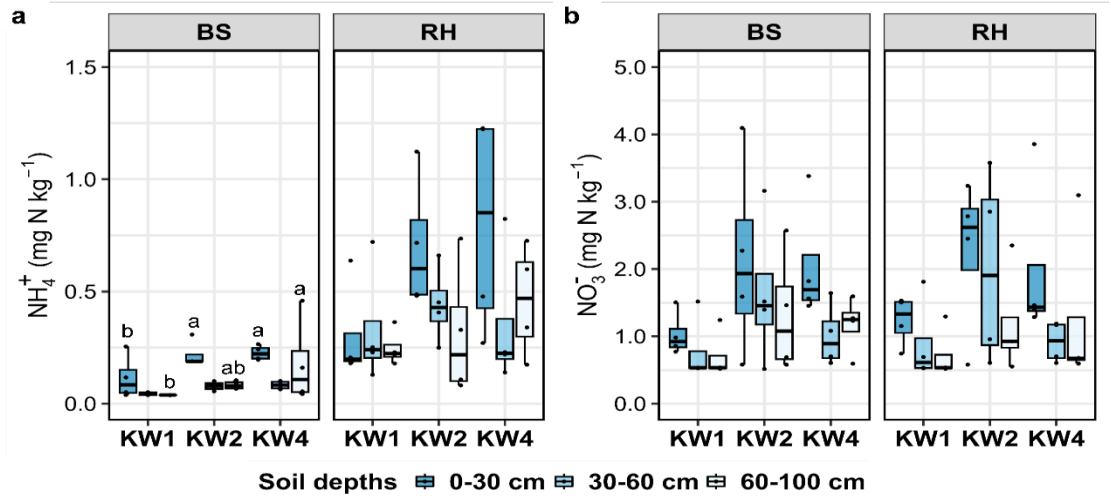

Figure 1.5. Effect of the rotational positions on soil NH_4^+-N (a) and NO_3^--N (b) of the following winter wheat at onset of stem elongation (BBCH 30) at soil depths 0-30 cm, 30-60 cm and 60-100 cm and two soil compartments bulk soil (BS) and rhizosphere soil (RH). KW1 = first wheat, KW2 = second wheat, and KW4 = fourth wheat after oilseed rape in soil from the experimental farm Hohenschulen in Kiel, Germany. Within each soil depth and soil compartment, different lowercase letters denote significant differences between rotational positions at $p \leq 0.05$ according to ANOVA with Bonferroni correction for multiple comparisons. No letters indicate non-significant differences.

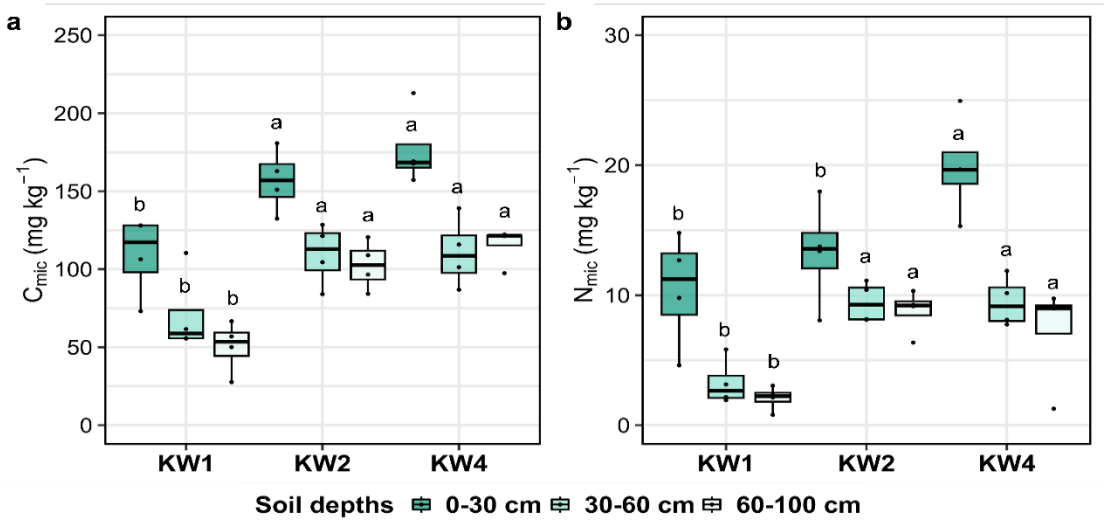

Figure 1.6. Effect of the rotational positions on microbial biomass carbon (C_{mic}, a) and microbial biomass nitrogen (N_{mic}, b) of the following winter wheat at onset of stem elongation (BBCH 30) at soil depths 0-30 cm, 30-60 cm and 60-100 cm. KW1 = first wheat, KW2 = second wheat, and KW4= fourth wheat after oilseed rape in soil from the experimental farm Hohenschulen in Kiel, Germany. Within each soil depth, different lowercase letters denote significant differences between rotational positions at $p \leq 0.05$ according to ANOVA with Bonferroni correction for multiple comparisons. No letters indicate non-significant differences.

The main components of the microbial community composition at the phylum level were *Actinobacteriota*, *Proteobacteria*, *Chloroflexi*, *Gemmatimonadota*, and *Crenarchaeota*. The relative abundance of several taxa from *Acidobacteriota*, *Gemmatimonadota*, *Nitrospirota*, and *Chloroflexi* was significantly affected by the rotational position in the BS and RH soils and at different soil depths. While in the BS of the plants, the relative abundance of *Acidobacteriota* was not significantly different, we recorded a significantly higher relative abundance of *Acidobacteriota* in the RH of the topsoil and subsoil of KW1 compared to both KW2 and KW4 (Fig. 1.8a). A decreasing relative abundance of *Gemmatimonadota* in KW4 compared to KW1 was found in both soil compartments, while the difference between KW1 and KW2 remained insignificant (Fig. 1.8b). With regard to *Nitrospirota*, KW1 and KW2 had similar relative abundances in both BS and the RH (Fig. 1.8c). In the RH, the relative abundance of *Nitrospirota* was significantly lower in both the topsoil and subsoil of KW2 compared to KW4. Finally, in KW1 and KW2, there was a much lower relative abundance of *Chloroflexi* compared to KW4, and this difference was consistently found in BS and RH soil (Fig. 1.8d).

Successively grown WW appeared to prioritize soil exploration, shaping a thinner and less dense root system, as indicated by its higher SRL, lower R_{dia}, and RTD. Increasing the proportion of WW in the rotation led to a clear reduction in biomass of the following WW. We provide evidence of an early onset of reduced biomass growth and onset of early root senescence in successively grown WW. This reduction was associated with changes in microbial activity and composition (Fig. 1.7) in WW rotations, coupled with changes in root growth (Fig. 1.4). The decrease in plant dry weight for successive WW rotations was of a similar magnitude for both aboveground and belowground plant parts. In response to biotic and abiotic stresses, the specific root length (SRL) of plants tend to increase (Kramer-Walter et al., 2016; Kaloterakis et al., 2021; Spitzer et al., 2021), while root length density (RLD) and average root diameter (Rdia) are reduced (Kramer-Walter et al., 2016; Lopez et al., 2023). Kelly et al. (2022) found higher SRL in WW landraces grown in low nutrient availability conditions, while landraces with a

higher proportion of coarse roots were linked to higher extractable C pools in the rhizosphere. Root diameter is considered an important feature that enhances root exudation, and thicker absorptive roots have been shown to increase mycorrhizal colonization (Wen et al., 2019). Consistent with this, we observed important root plastic responses influenced by the preceding crop history. Root plastic responses associated with higher biomass and RLD during early growth stages lead to increased ability for nutrient and water uptake, dry matter accumulation, and thus yield (Chen et al., 2020). The reduction of root length and root mass across the soil profile confers changes to the soil organic carbon pool through reduced inflow of dead root material as well as root exudation to the soil, which in turn decelerates mineralization processes (De Deyn et al., 2008; Cong et al., 2014).

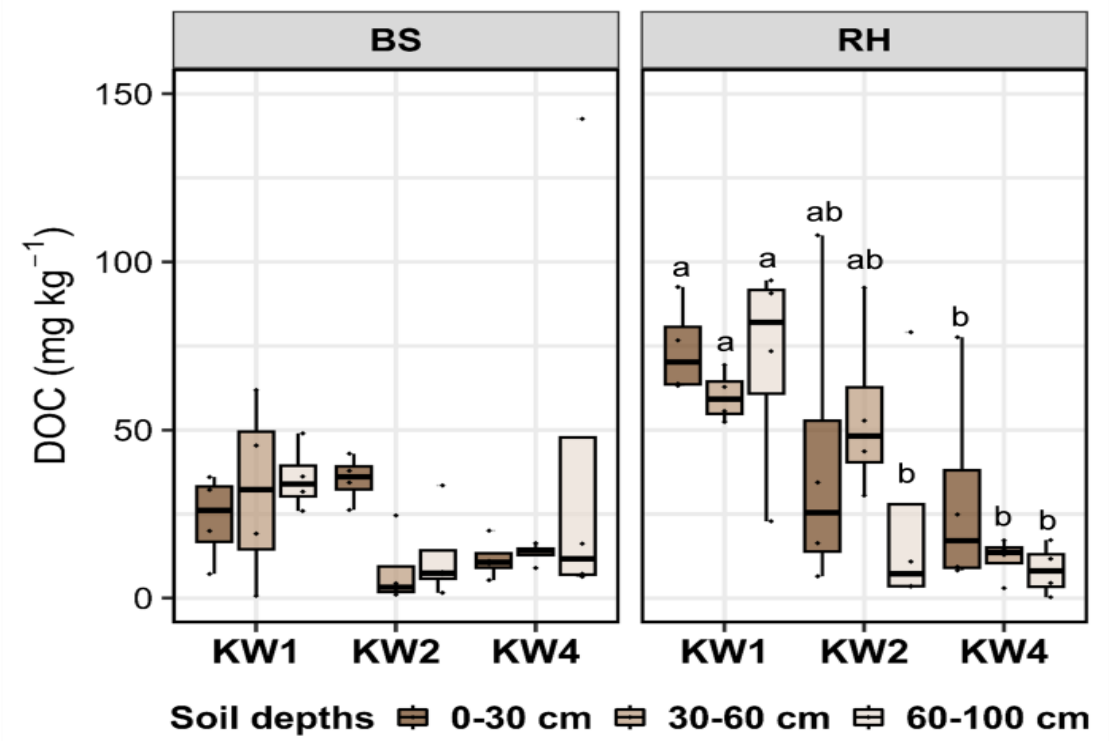

Figure 1.7. Effect of the rotational positions on dissolved organic carbon (DOC) of the following winter wheat at onset of stem elongation (BBCH 30), at soil depths 0-30 cm, 30-60 cm and 60-100 cm and in two soil compartments bulk soil (BS) and rhizosphere soil (RH). KW1 = first wheat, KW2 = second wheat, and KW4 = fourth wheat after oilseed rape in soil from the experimental farm Hohenschulen in Kiel, Germany. Within each soil depth and soil compartment, different lowercase letters denote significant differences between rotational positions at $p \leq 0.05$ according to ANOVA with Bonferroni correction for multiple comparisons. No letters indicate non-significant differences.

In a recent field experiment, Yang et al. (2022) found that microbial biomass C (C_{mic}) and N (N_{mic}) increased with increasing wheat (WW) dry matter throughout the growth period. However, the highest plant biomass-yielding rotational position KW1 had much lower Cmic and Nmic values at all three soil depths. Typically, higher root biomass is associated with increased microbial biomass (Lange et al., 2015). However, changes in microbial diversity may be more accurately associated with changes in root biomass, explaining the observed trends (Fig. 1.7) in this experiment (Ren et al., 2017). Hansen et al. (2019) observed a similar decline in Cmic when oilseed rape was introduced to successive wheat monocultures, and attributed this effect to the biocidal qualities of its secondary metabolite isothiocyanate. Successively grown WW has a clear soil legacy

with increased microbial biomass. The high initial DOC content of the soil induced rapid regrowth of microbes following the initial adjustment of the water holding capacity (WHC) and therefore N immobilization which could have affected plant growth.

Results showed that the root system of KW1, stimulated microbial activity and increased the release of glucose and leucine, which can be directly utilized by microbes. This enables KW1-selected microbes to use dissolved organic C (DOC) and N in the rhizosphere more effectively compared to successively grown WW (Fig. 1.5, Fig. 1.6). It has been shown that plants have a decreased capacity to utilize low molecular weight C under intense microbial competition, with DOC content driving this interaction (Kuzyakov & Jones, 2006; Song et al., 2020). Labile carbon is considered critical for maintaining the pathogen suppressive qualities of agricultural soils irrespective of the total soil organic matter content (Bongiorno et al., 2019), which would explain the generally lower Ggt prevalence in soil after oilseed rape cultivation (Jenkyn et al., 2014).

The higher richness of bacterial taxa (ASVs, amplicon sequence variants) in the bulk soil of KW4 compared to KW1 and KW2 suggests that successive wheat cultivation selects a broader spectrum of bacteria that are better adapted to the specific soil conditions (Mayer et al., 2019). Previous research by Hilton et al. (2018) has observed that preceding crops affect the microbial communities in the wheat rhizosphere. This is most likely due to the continuous secretion of exudates of similar quality that preferentially stimulate specific groups of microbes (Jones et al., 2019; Wen et al., 2022). This is most likely due to the continuous secretion of exudates of similar quality that preferentially stimulate specific groups of microbes (Jones et al., 2019; Wen et al., 2022). We observed differences in the relative abundance of bacteria at the phylum level (Fig. 1.8) that shifted the spectrum of interactions of microbes and wheat with potential imbalance or dysbiosis effect. The microbial community structure of KW1 and KW2 were more similar compared to KW4 (Fig. 1.8b). It appears that the higher rate of WW residue return in the soil of WW monocropping leads to the prevalence of an unfavorable soil microbial community that is associated with early growth reduction and biomass loss. The prevalence of bacterial taxa with lower secretion of extracellular enzymes that foster the acquisition of carbon and nitrogen created a competitive environment for both plants and microbes, resulting in less mineral nitrogen being taken up by KW2.

The observed alterations in root growth patterns, microbial activity, and soil dynamics in response to successive wheat (WW) cultivation underline the pivotal role of root exudates and secretions in shaping soil microbial communities and influencing plant performance. The diminished biomass growth and early onset of root senescence in successively grown WW indicate a complex interplay between root plastic responses and the soil microbial environment. The root system of the first rotational position (KW1) emerges as a key player, stimulating microbial activity and enhancing the release of glucose and leucine, which are crucial substrates for microbial utilization. This microbial stimulation and efficient utilization of dissolved organic carbon (DOC) and nitrogen (N) in the rhizosphere by KW1-selected microbes highlight the importance of specific root exudates in fostering a beneficial microbial community.

The findings underscore the necessity of identifying and characterizing specific compounds in root exudates that trigger soil microorganisms, as they play a pivotal role in shaping the microbial community structure and influencing nutrient dynamics. The glucose imaging method, developed as a result of this investigation, emerges as a valuable tool for probing the intricate dynamics of root exudation, providing a means

to visualize and quantify the release of critical substrates that drive microbial activity. The ability to discern the nuances of root-microbe interactions enhances our understanding of soil legacy effects and offers insights into sustainable agricultural practices by emphasizing the importance of managing root exudation for fostering a resilient and beneficial soil microbiome.

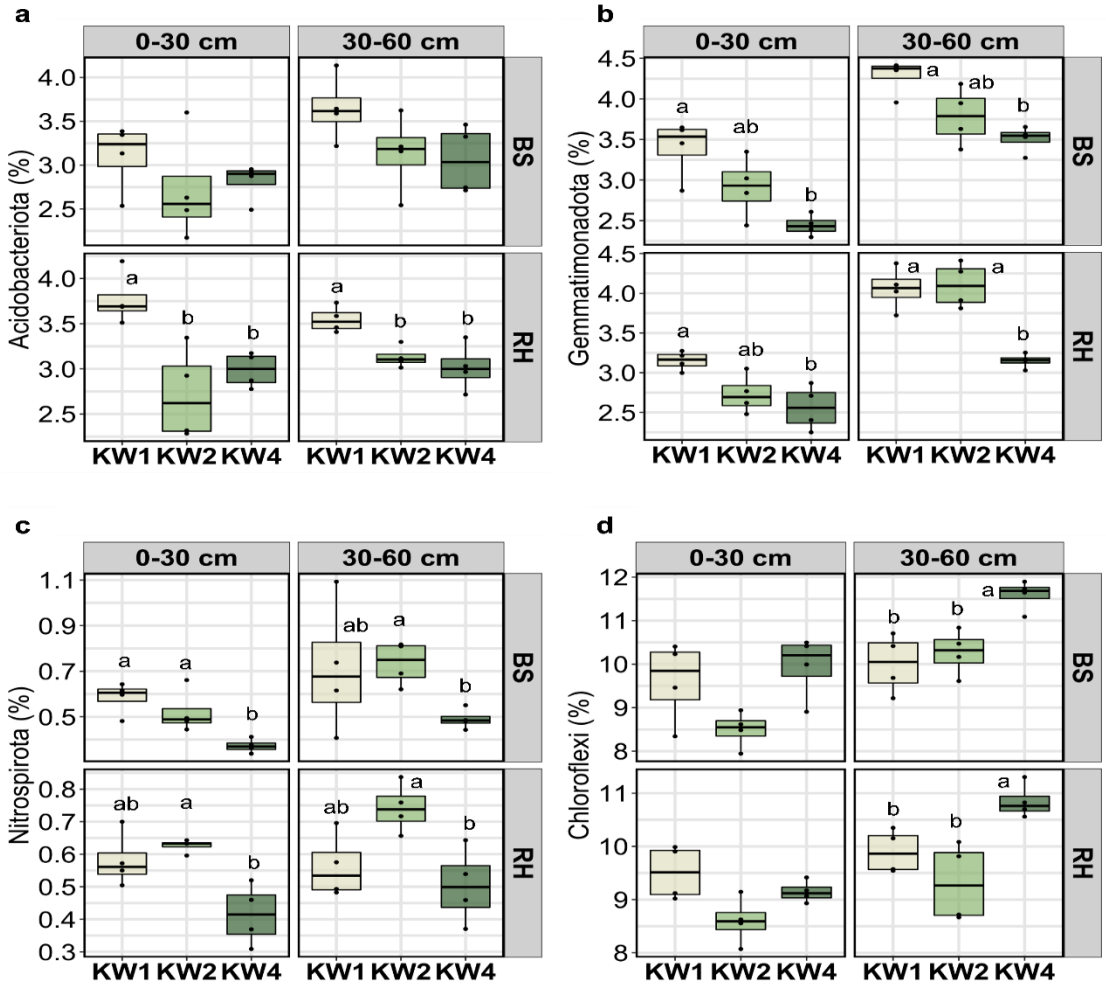

Figure 1.8. Effect of the rotational positions on the relative abundance of (a) *Acidobacteriota*, (b) *Gemmatimonadota*, (c) *Nitrospirota* and (d) *Chloroflexi* at soil depths 0-30 cm and 30-60 cm, in the two soil compartments bulk soil (BS) and rhizosphere (RH). KW1 = first wheat, KW2 = second wheat, and KW4 = fourth wheat after oilseed rape in field soil from the experimental farm Hohenschulen in Kiel, Germany. Within each soil depth and soil compartment, different lowercase letters denote significant differences between rotational positions at $p \leq 0.05$ according to ANOVA with Bonferroni correction for multiple comparisons. No letters indicate non-significant differences.

1.12.2. Study 2: methodological innovations to study the rhizosphere processes

Glucose, the primary compound in exudates as an easy available sugar, is among the soluble carbohydrates that are adjusted by the roots to adapt to osmotic conditions (Sharp et al., 1990; Spollen et al., 2008; Voothuluru et al., 2016). Soil glucose imaging is a method used to visualize and quantify the amount of glucose exuded from plant roots. This method was optimized based on the protocols developed by McLaughlin and Boyer (2004) and Voothuluru et al. (2018) and is useful for studying plant root exudation and interactions with the surrounding soil.

In situ glucose imaging was performed for AMF-inoculated and AMF non-inoculated rhizoboxes, which were divided into three drought- and three optimum conditions. Soybean seeds were sterilized with 70% ethanol and 10% hydrogen peroxide, and rinsed thrice with distilled water (Ibiang et al., 2017). These sterilized seeds were germinated on wet filter paper in a petri dish for three days before transplanting into rhizoboxes. Treatments with and without AMF were set up in separate boxes. Zymography and glucose imaging were performed in different rhizoboxes to avoid cross effects of the two imaging methods. Thus, soil was packed in 24 transparent rhizoboxes (20 × 20 × 3 cm). The experiment consisted of four treatments (drought vs. optimum, AMF vs. no-AMF), each of which was replicated thrice to measure zymography.

In glucose imaging, decreasing the release of glucose was demonstrated in color bars in which white color showed the highest glucose exudation. Under optimum conditions, glucose was mainly exuded along the roots and root tips (Fig. 1.9). On the contrary, under drought condition, glucose exudation was more focused on the root tips. However, a higher release of glucose was observed in the rhizosphere under AMF-drought than control-drought.

In line with our hypothesises, glucose exudation highly relied on moisture condition, as suggested by Vancura and Hovadik (1965) and Calvo et al. (2019). Under optimum condition, glucose was homogeneously exuded along the root as well as root tips, but drought dramatically reduced glucose exudation along with a total decrease in exudation (Liese et al., 2018), especially from the mature part of the root (Fig. 1). Remarkably, AMF strongly boosted glucose hotspots in comparison to non-mycorrhizal plants. Glucose exuded from root characterized by lability and ready utilization can be directly absorbed by AMF as a C source (Bago et al., 2000; Bücking et al., 2008) to stimulate AMF hyphae branching and lengthening. On the other hand, AMF may contribute to glucose release, for instance, by the expression of β-glucosidase and mobilizing oligo- and polysaccharides or glycosylated compounds. Therefore, the enhanced glucose exudation was attributed to the concomitant direct secretion from plant roots or product of β-glucosidase activity within rhizosphere. This accelerated glucose availability within the mycorrhizosphere (Kraigher *et al.*, 2013), the zone of influence in the vicinity of fungal hyphae (Tarafdar and Marschner, 1994), which compensates C deprivation of rhizobiota due to drought (Asensio et al., 2021).

The results obtained from the glucose imaging method provide compelling evidence of its efficacy in elucidating the nuanced dynamics of glucose exudation under varying moisture conditions and mycorrhizal associations. The method effectively captured the spatial distribution of glucose release along the roots and root tips, highlighting distinct patterns in response to both optimal and drought conditions. Notably, the visualization of glucose hotspots demonstrated the strong influence of arbuscular mycorrhizal fungi (AMF) on boosting glucose exudation, presenting a novel aspect of the method's utility in unraveling plant-microbe interactions.

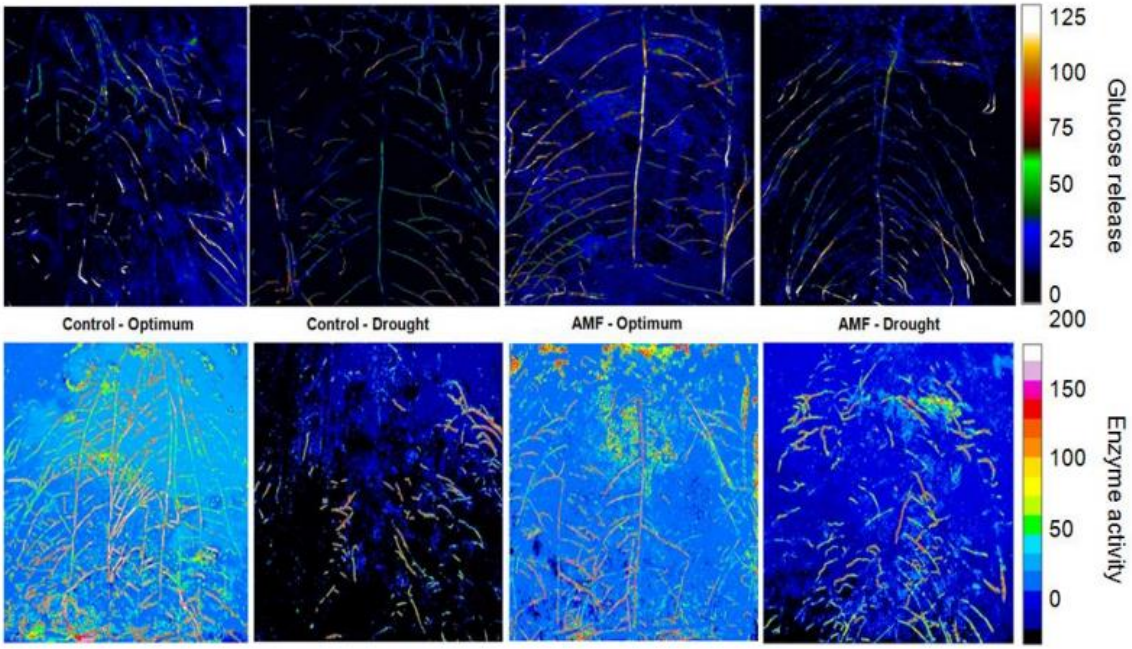

Figure 1.9. Upper row shows glucose release (nmol/cm^2), for treatment with and without AMF (control), under optimum and drought conditions. Lower row: shows zymograms of acid phosphomonoesterase (pmol cm^{-2} h $^{-1}$).

The observed changes in glucose exudation under AMF-drought conditions compared to control-drought further emphasize the method's sensitivity to variations in environmental factors. The ability to discern differences in glucose release attributed to direct root secretion and β-glucosidase activity within the rhizosphere showcases the method's capacity to provide detailed insights into the molecular processes influencing glucose dynamics. These findings lay a solid foundation for extending the application of the glucose imaging method to diverse plant species, such as wheat, and investigating the impact of successive cultivation on glucose release and enzyme activity. The method's success in capturing these intricate dynamics positions it as a valuable tool for advancing our understanding of plant responses to environmental stress and mycorrhizal associations, with potential applications in optimizing agricultural practices for enhanced plant-microbe interactions and sustainable crop production. This prompted the initiation of a subsequent experiment aimed at rigorously assessing how the dynamic relationship between these factors is influenced over successive wheat cropping cycles.

1.12.3. Study 3: glucose release and enzyme activity affected by successive wheat cultivation

The spatial distribution of glucose release and β-glucosidase activity was found to be influenced by successive wheat plantation, particularly at t2, as shown in Figure 1.11. Furthermore, at t2, W3 exhibited the lowest proportion of glucose release hotspots, covering 1.83% of the total soil surface area. This represents a 31.7% decline compared to W1 ($p<0.05$) (see Figure 1.11).

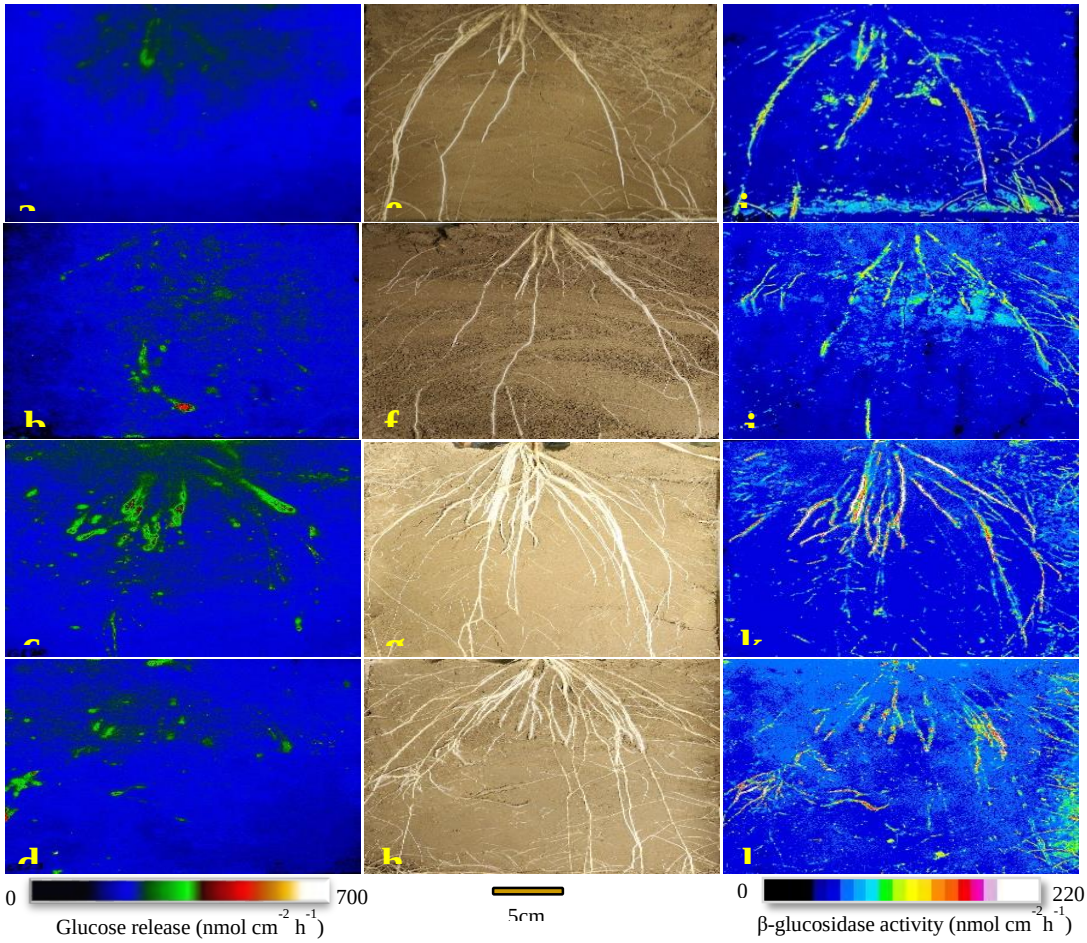

Figure 1.11. Spatial distribution of glucose release (a-d); β-glucosidase activity (i-l) and original images of the wheat root (e-h) at T1W1 (top row), T1W3 (second row), T2W1 (third row), T2W3 (lower row), respectively (T1: four weeks (BBCH 13), and T2: eight weeks after sowing (BBCH 29); W1: first and W3: third wheat after break crop.

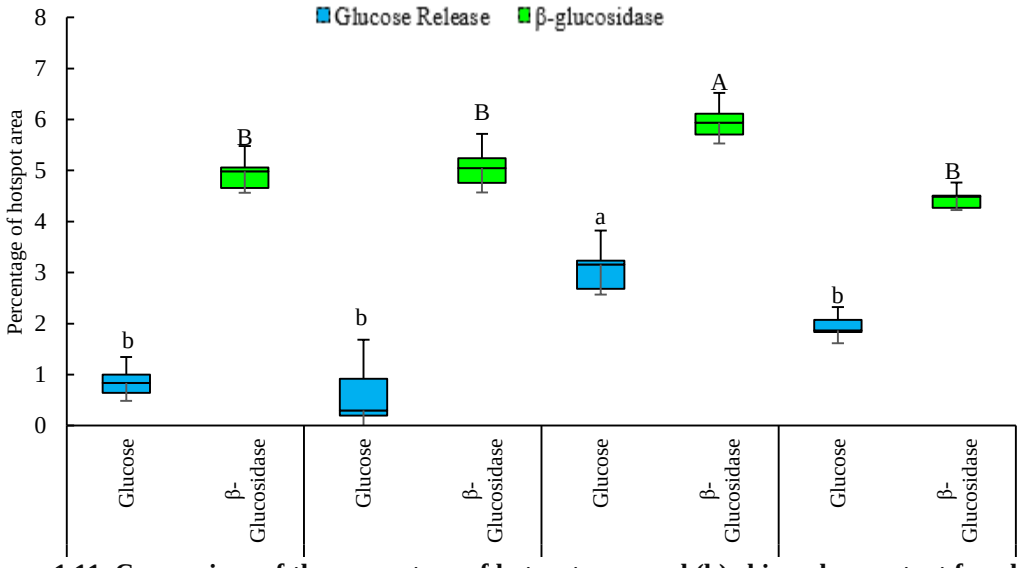

Figure 1.11. Comparison of the percentage of hotspot area and (b) rhizosphere extent for glucose release and β-glucosidase activity in the first (W1) and third (W3) wheat after break crop at two sampling dates (T1: four weeks (BBCH 13), and T2: eight weeks after sowing (BBCH 29)). Lower-case letters denote significant differences between treatments in terms of glucose release and upper-case letters denote significant differences between treatments in terms of β-glucosidase activity according to two- way ANOVA at $p<0.05$.

The results showed that W3 wheat plants had a consistently lower in glucose release rate in both root tips and mature roots, especially at t2, compared to W1 ($p<0.05$). At t1, glucose release at wheat root tips decreased by 19.4% in W3 compared to W1. However, at t2, W1 had higher glucose release at root tips with 403.3 $nmol^{-1}$ cm^{-2}, while W3 resulted in 20% lower glucose release. A similar trend was observed for glucose release from mature roots, which decreased by 18.5% and 17.4% at t1 and t2, respectively, in W3 compared to W1 (Fig. 1.12). The wheat crop rotational positions minimally affected β-glucosidase activity at t1 for both root tips and mature roots. Subsequently, at t2, a noticeable declining trend in enzyme activity was observed from W1 to W3, leading to an 11.4% decrease in root tip activity and a 13.6% decrease in mature root enzyme activity. W1 displayed higher enzyme activity for root tips (153.85 nmol $MUFcm^{-2}h^{-1}$) and mature roots (159.64 nmol $MUFcm^{-2}h^{-1}$) ($p<0.01$; Fig. 1.12). Thus, the highest glucose release at T2 was accompanied by the highest β-glucosidase activity.

Soil basal respiration increased at t2, but no significant difference was observed between W1 and W3 ($p<0.01$). W1 exhibited higher basal respiration by 0.114 µg CO2 $g^{-1}h^{-1}$, which was 10.5% higher than that observed in W3. At both sampling times, the microbial quotient in W3 was significantly higher compared to W1, with higher microbial quotient observed at t2 in W3, which was 0.018 µg CO_2-C mg^{-1} MBC h^{-1}, indicating a ~28% increase compared to W1 at the same sampling date ($p<0.01$; Fig. 1.13).

In accordance with our hypothesis, successive wheat cultivation resulted in a substantial reduction in glucose release from roots and a decrease in rhizosphere expansion at t2 (as depicted in Figs. 1.10, 1.11, and 1.12). However, this trend was not observed in plants at t1. The age of the plant is an essential factor that determines the extent and type of exudation (Olanrewaju et al., 2019), which varies throughout its life cycle (Gargallo-Garriga et al., 2018). As plants progress through their life cycle, the composition and quantity of root exudates can vary substantially (Gargallo-Garriga et al., 2018). The observed discrepancy between t1 and t2 may be attributed, in part, to the evolving physiological state of the plant, influencing its exudation patterns (Ulrich et al., 2022). A growing body of research indicates that root exudates play a crucial role in shaping the special microbial communities within the rhizosphere (Huang et al., 2014; Paterson et al., 2007). Subsequently, these plant-associated microorganisms have the potential to exert influence on both plant growth and overall plant health. Also, decaying roots create a favourable environment for necrotrophic pathogens and contribute to increasing fungal colonization (Häffner et al., 2014; Olanrewaju et al., 2019) and can modify the fungal community within the rhizosphere, leading to the proliferation of host-specific pathogenic fungi at the cost of beneficial fungi associated with plant health (Wu et al., 2016).

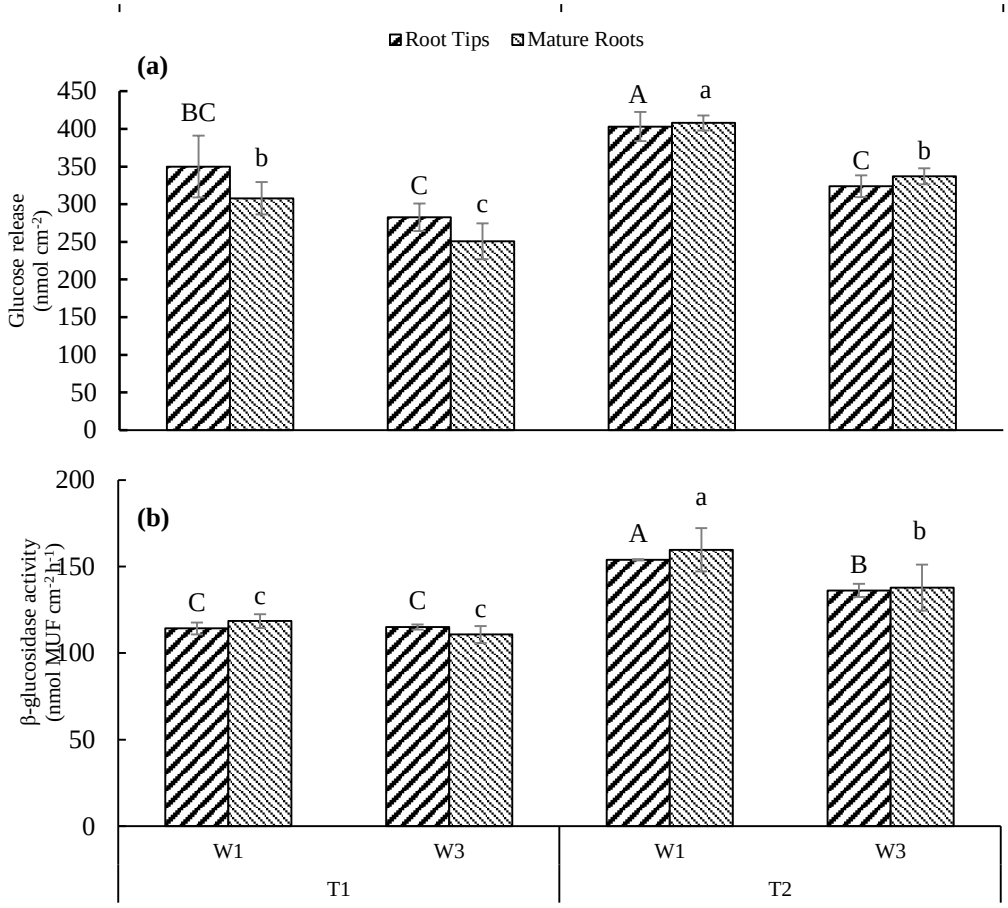

Figure 1.12. (a) Glucose releasing rate and (b) β-glucosidase activity in the first (W1) and third (W3) wheat after break crop at two sampling times (T1: four weeks (BBCH 13), and T2: eight weeks after sowing (BBCH 29)). Lower-case letters denote significant differences between treatments for mature root and upper-case letters denote significant differences between treatments for root tips according to two-way ANOVA at p<0.05.

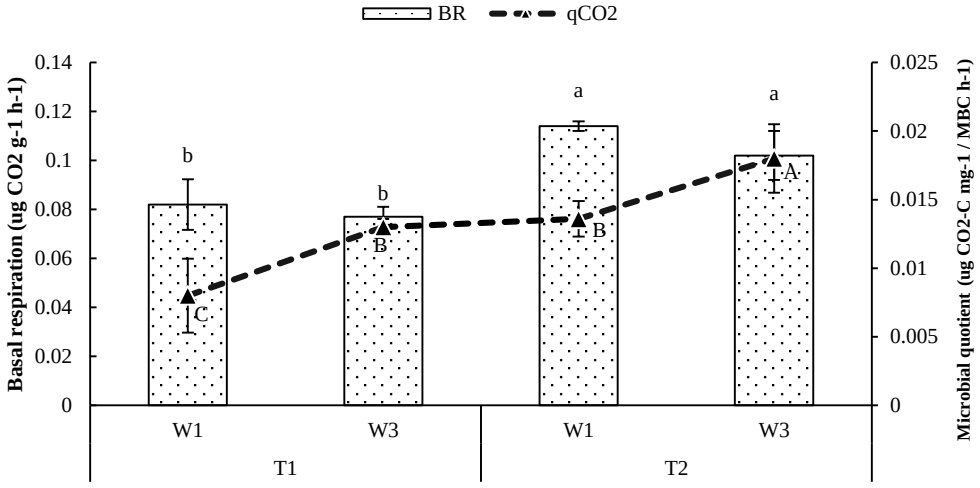

Figure 1.13. Basal respiration (bar charts) and microbial quotient values (dashed line) in wheat rhizosphere soil in the first (W1) and third (W3) wheat after break crop at two sampling times (T1: four weeks (BBCH 13), and T2: eight weeks after sowing (BBCH 29)). Lower-case letters denote significant differences between treatments in terms of basal respiration and upper-case letters denote significant differences between treatments in terms of microbial quotient according to two-way ANOVA at p<0.05.

The decrease in glucose release from wheat roots (as observed in Fig. 1.11) coupled with a decrease in C availability due to root senescence, leads to competition for C in the rhizosphere among beneficial microbes and soil-borne pathogens (Bressan and Figueiredo, 2008). Plant root exudates contain a variety of compounds, including sugars, that can have antimicrobial properties and regulate the microbial community in the soil (Dennis et al., 2010). Jalali and Suryanarayana (1971) showed that healthy wheat plants secrete considerably higher amounts of glucose than infected plants. The lower concentrations of released glucose in W3 were confirmed by its lower proportion of hotspot and lower rhizosphere extent during t2 (as illustrated in Figs. 1.10 and 1.11). This suggests that the plant's rhizosphere development and activity, as reflected by the extent and intensity of hotspots, may have played a role in the observed differences in glucose release between W3 and the other treatments. Root exudates, such as glucose, substantially affect the initiation and development of plant-microbe interactions in the rhizosphere (Hage-Ahmed et al., 2013). Therefore, the composition and extent of root exudates will affect soil-borne pathogens differently (Jones et al., 2004). Bakker et al., (2013) reported that pathogens have sophisticated mechanisms to receive sugar fluxes from the host plant. Moreover, pathogens can modify the expression of the SWEET family of sugar transporters to obtain the sugars necessary for their growth (Chen et al., 2010). The plant, by reducing rhizosphere size, is engineering density gradients of soil biochemical properties to establish a protection zone against pathogen invasion. In other words, plants can regulate their glucose release and modify plant-pathogen interactions towards a healthy relationship.

Overall, this study sheds light on the rhizosphere processes in successive wheat cultivation, revealing a significant impact on root processes. Specifically, the reduction in the release rate of key root exudates, notably glucose, alters the competitive dynamics on the root surface. The observed decrease in glucose release, coupled with constrained rhizosphere expansion, leads to a substantial reduction in microbial biomass C, resulting in lower enzyme activity. Maintaining the expansion of the rhizosphere is a plant strategy under biotic stress since the rhizosphere and its hotspots are essential microbial habitats that determine the processes, dynamics, and cycling of C in terrestrial ecosystems. The findings of this study suggest that successive wheat cultivation changes root primary compound exudation, leading to declining glucose release, creating a harsh environment for beneficial soil microbes and accelerating root senescence, ultimately resulting in wheat yield decline.

In the next section, we delve into the intricate mechanisms governing the modulation of rhizosphere processes in field conditions. Building upon the insights gained from the preceding study on successive wheat cultivation, this chapter aims to unravel the underlying dynamics of glucose release controlled by sugar transporters in wheat plants. By conducting field experiments, we aim to explore the direct impact of altered root exudation patterns, particularly the reduction in glucose release, on microbial growth and enzyme activity around the root. The field conditions provide a realistic and dynamic environment, allowing us to investigate how changes in root primary compound exudation, specifically glucose, influence the rhizosphere microbial community. Through this exploration, we seek to elucidate the intricate interplay between sugar transporters, microbial dynamics, and enzyme activity, contributing to a comprehensive understanding of the regulatory mechanisms that shape the rhizosphere environment in wheat plants and its implications for overall plant health and productivity.

1.12.4. Study 4: A SWEET challenge: less sugars for rhizospheric microbiome under the successive wheat rotation

The spatial pattern of glucose release was affected by continuous wheat cultivation (Fig. 1.14). W3 had the lowest proportion of hotspots for glucose release with 1.35 % of the total soil surface area, indicating a 17.7 % decline compared to W1 ($p<0.05$) (Fig. 1.15a). Glucose release rate for wheat root tips and mature roots showed that W3 demonstrated a consistent decrease in both compartments compared to W1 and the highest glucose release at root tips was obtained in W1 with 593.5 $nmol^{-1}$ cm^{-2} ($p<0.05$). However, as shown in Figure 2b, glucose release increased enormously in root tips compared to mature roots in W1 and W3. In W1, glucose release at wheat root tips increased by 30.2 % compared to mature roots, while in W3, root tips had 35.6 % higher glucose release than mature roots (Fig. 1.15b).

Results showed that the expressions of functional orthologous genes of SWEET1a in wheat roots were significantly upregulated in W3 compared to W1. The expressions of these orthologous genes were also checked by real-time quantitative PCR. It was found that these genes were upregulated under continuous wheat cultivation (Fig. 1.16a). However, there was a reverse expression pattern for SWEET genes in wheat plant leaves in W3 compared to W1. We found downregulation of genes, especially for SWEET 2a. Also, all orthologous genes of SWEET13 showed downregulation in continuous wheat cultivation compared to W1 (Fig. 1.16b).

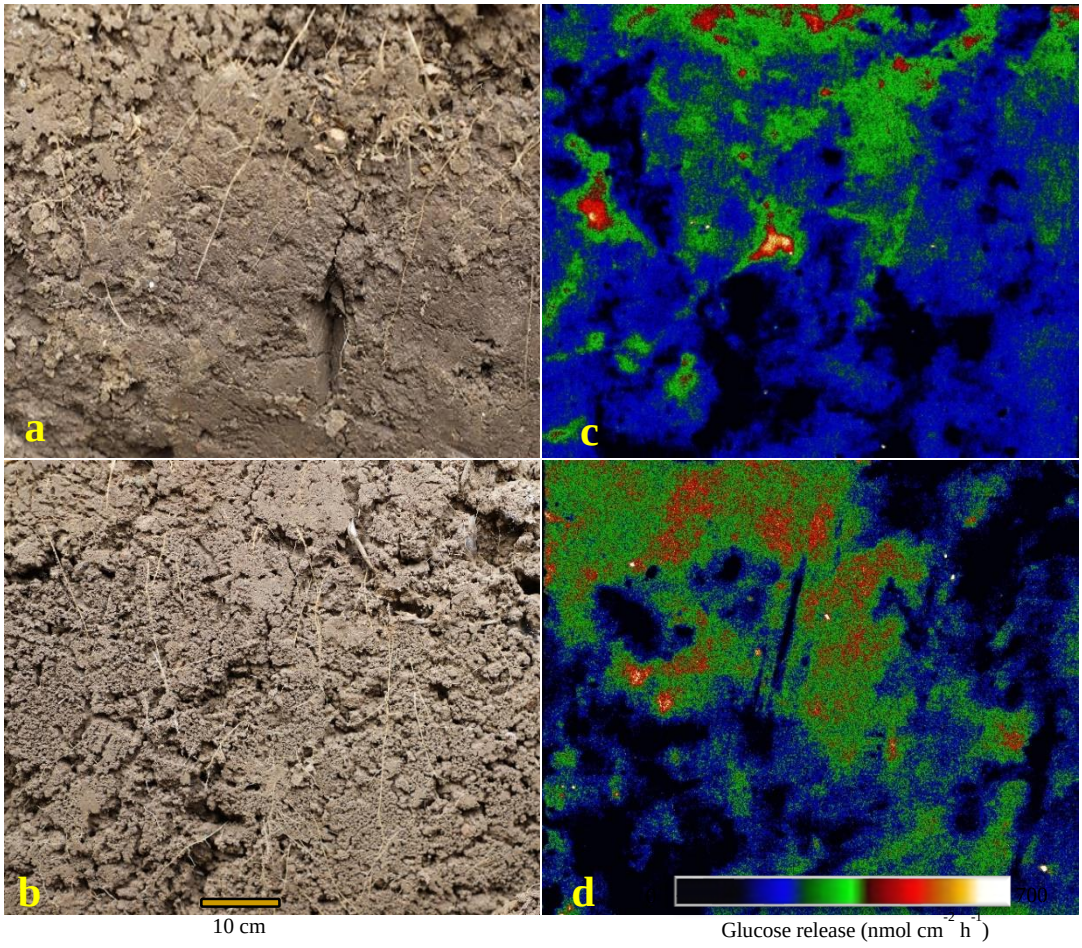

Figure 1.14. Original images of the wheat root (a, b) and spatial distribution of glucose release (c, d) at W1 (top row) and W3 (lower row), respectively (W1: first and W3: third wheat after break crop).

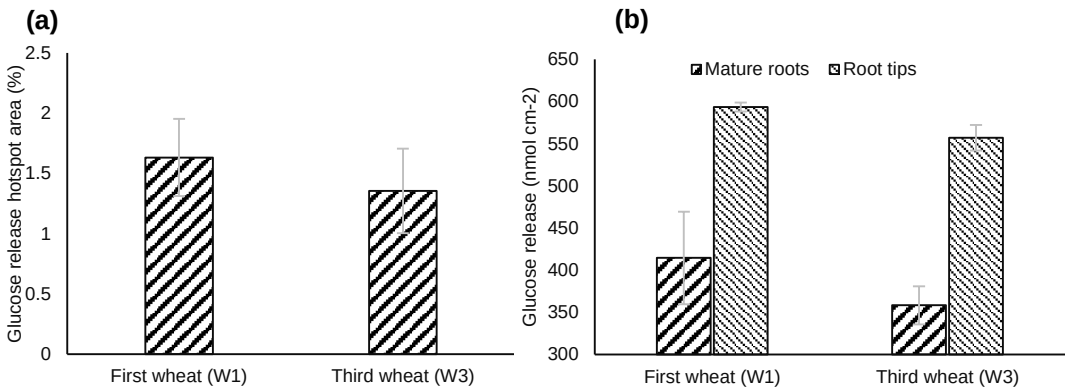

Figure 1.15. (a) Comparison of the percentage of hotspot area and (b) mean glucose releasing rate in the whole area and region of interest (ROI) in the first (W1) and third (W3) wheat after break crop. Error bars represent standard error of means (n = 4).

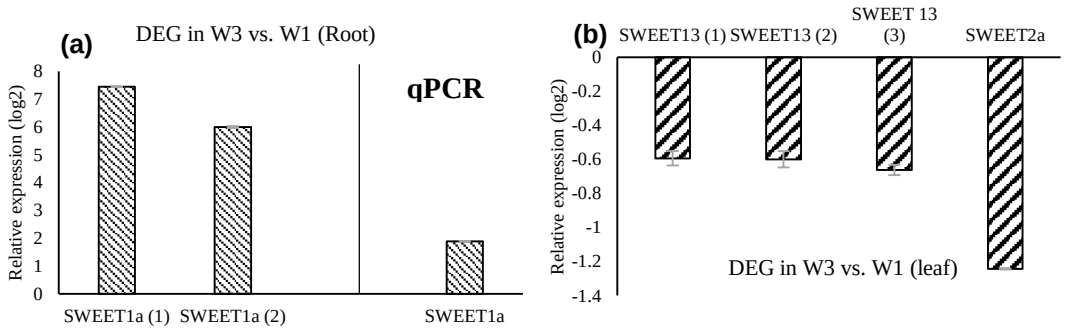

Figure 1.16. Relative expression of differentially expressed SWEET genes in wheat (a) roots and (b) leaves in W3 vs. W1 (W1: first and W3: third wheat after break crop). Error bars represent standard error of means.

Total microbial biomass dropped by 11.8 and 4.8 % in W3 in the rhizosphere and bulk soils compared to W1 (respectively; Fig. 1.17a). The Growing microbial biomass in the rhizosphere soil of W1 was about five times higher than W3, and different crop rotations did not affect growing microbial biomass in bulk soil compartment (Fig. 1.17b). The GMB/TMB ratio was also strongly affected by crop rotation, and W1 had the higher ratios in both rhizosphere and bulk soil (0.14 and 0.002, respectively; Fig. 1.17c). The specific growth rates (μ) considerably increased in W3 in the rhizosphere compartment compared to W1 (0.17 and 0.23 h^{-1}) and both W1 and W3 had similar specific growth rates in bulk soil samples (about 0.26 h^{-1}; Fig. 1.17d). Despite a slower specific growth rate, a seven times shorter lag period was observed in W1 vs W3 rhizosphere soil. Similar lag periods were observed for bulk soil samples in W1 and W3 (15.49 and 15.64 h, respectively; Fig. 1.17e). Generation time of actively growing microbial community-consuming substrate during incubation of soils with glucose and nutrients in W3 declined by 24.2 % compared to W1 in rhizosphere soil and the difference in Tg in bulk soil for W1 and W3 was negligible (2.66 and 2.58 h, respectively; Fig. 1.17f).

Root secretion and exudates play a pivotal role in modulating the interplay between roots and soil microorganisms (Mommer et al., 2016). Glucose stands as the predominant sugar synthesized within the root systems of wheat plants (Yahya et al., 2021). However, the collection of glucose from natural soil settings is challenging due to their intricate chemical associations with the soil matrix, coupled with the concurrent release of microbial exudates (Yahya et al., 2021). Therefore, in the current

investigation, we used a novel method to *in situ* localization and quantification of glucose released from wheat roots (Hoang-Rashtbari et al., 2022). Results showed that continuous wheat cultivation affected wheat root glucose release (Figs. 1.14, 1.115a). The observed differences in glucose release between W1 and W3 underscore the impact of crop rotation on root exudation patterns. The substantial reduction in glucose hotspots in W3 compared to W1 could be attributed to changes in root physiology and exudation processes. This result aligns with Chen et al. (2022) who have highlighted the role of crop rotation in altering root exudation patterns. This indicates that the development and activity of the plant's rhizosphere, as demonstrated by the intensity of hotspots, potentially contributed to the observed variations in glucose release between W3 and W1.

The observed differential expression of SWEET genes in wheat roots and leaves highlights the intricate interplay between crop rotation and plant-microbe interactions. The expressions of functional orthologous genes of SWEET1a in wheat roots were significantly upregulated in W3 compared to W1 which further confirmed by real-time quantitative PCR (Fig. 1.16a). SWEET1a, belonging to clade I of the SWEET family, acts as a low affinity (Km ~100 mM) glucose-specific carrier with a passive diffusion manner and involved in the redistribution of sugars within the root system and in the uptake of glucose into unloading cells as part of the sugar unloading mechanism in sink organs (Chen et al., 2010; Ho et al., 2019). The upregulation of these genes in W3 wheat roots may reflect the need for energy and carbon sources required for nutrient uptake and root development. Also, this upregulation could be linked to altered root exudation patterns and the demand for nutrient acquisition in the rhizosphere of W3 (Wen et al., 2022).

Conversely, the expressions of functional orthologous genes of SWEET13 and SWEET2a in wheat leaves were significantly downregulated in W3 compared to W1 (Fig. 1.16b). These genes are involved in in the export of sugars (such as glucose and sucrose) produced during photosynthesis from the mesophyll cells of wheat leaves to other plant tissues (Breia et al., 2021) and may play important roles in sugar partitioning during seed development (Xie et al., 2019). SWEET2 transporters retrieve sugars from the cytosol to the vacuole to limit their leakage to the extracellular space where they may feed the pathogen (Chen et al., 2015). This downregulation, especially for SWEET2a, could reflect a complex response to changes in root exudation and nutrient availability, potentially impacting plant growth and stress responses. Also, downregulation of these genes may indicate a decreased sugar export from the source tissues (leaves) to the rest of the plant and might be a result of reduced photosynthetic activity or altered resource allocation in continuous wheat cultivation. This is consistent with Zhang et al. (2021) who reported decrease in photosynthesis rate and efficiency in monoculture compared to intercropping and crop rotation.

In summary, our study offers novel insights into the complex interplay between continuous wheat cultivation, root exudation patterns, microbial dynamics, gene expression, and enzymatic activities within the rhizosphere and bulk soil compartments. Notably, our research introduced a pioneering approach by conducting glucose imaging in the field setting for the first time, shedding light on the dynamics of glucose release from wheat roots. The decline in glucose release observed under continuous wheat cultivation (W3) compared to the first wheat after a break crop (W1) underscores the significance of root exudates in shaping rhizosphere interactions. This shift in glucose release could be linked to altered root physiology and exudation processes, potentially reflecting the plant's strategy to create a less favorable environment for potential pathogens. The differential expression of SWEET genes in wheat roots and leaves

further adds to the novelty of our findings. The upregulation of SWEET1a orthologous genes in W3 roots suggests a demand for energy and carbon sources for nutrient uptake, while the downregulation of certain genes in leaves could indicate shifts in resource allocation strategies.

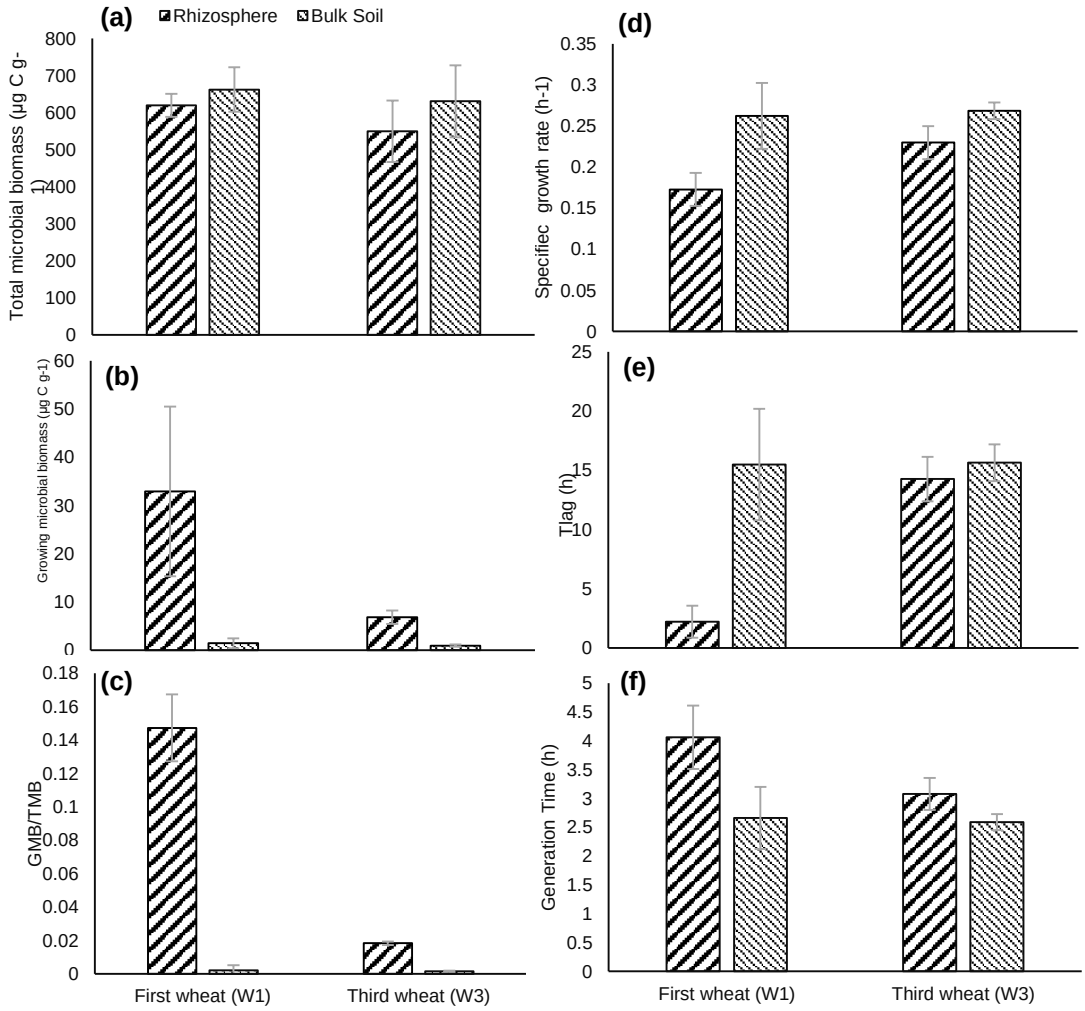

Figure 1.17- Total microbial biomass (TMB) (a), actively growing microbial biomass (GMB) (b), Specific growth rates (µ) of soil microorganisms (d), their lag time (T_{lag}) (e) and generation time (T_g) (f) in rhizosphere and bulk soil samples of the first (W1) and third (W3) wheat after break crop during incubation at 25°C. Error bars represent standard error of means (n = 3).

Our study not only contributes to the understanding of how continuous wheat cultivation shapes plant-soil-microbe interactions but also introduces novel techniques, like *in situ* glucose imaging, to assess these interactions in the field. These insights carry implications for sustainable agricultural practices, nutrient cycling, and ecosystem health. By revealing the complex cascade of effects triggered by continuous cultivation, we provide valuable perspectives for optimizing management strategies and maintaining productive ecosystems in the face of evolving agricultural practices.

In the upcoming section, our focus shifts to the distinctive silty loam (loess) soil conditions, diverging from our previous experiments conducted in sandy loam soil. This shift is motivated by the desire to investigate whether similar trends in enzyme activity and microbial growth, as observed in the silty loam soil, persist in the loess soil environment. Our study aims to bridge this knowledge gap by unravelling the enzyme kinetics patterns influenced by varying crop rotation scenarios. Building on the insights

gained from continuous wheat cultivation, root exudation dynamics, and gene expression in sandy loam soil, we extend our investigations to understand how these factors interact within the rhizosphere and bulk soil compartments in the context of loess soil. This comparative analysis will contribute to a more comprehensive understanding of the universal and soil-specific factors shaping plant-soil-microbe interactions, providing valuable insights for sustainable agricultural practices and ecosystem management.

1.12.5. Study 5: different crop rotation scenarios affected enzyme kinetics pattern in a loess soil

Soil samples were collected from the field site is located near Harste with soil type of silty loam Luvisol derived from Loess from three wheat rotational positions (W1, W2 and WM). At t1, different wheat rotational positions had a substantial impact on the total microbial biomass in the rhizosphere compartment, with a 42.5% and 42.8% decrease in WM compared to W2 and W1, respectively. Notably, the bulk soil exhibited a higher total microbial biomass than the rhizosphere soil at t1 in WM and t2 in W1 and WM (Fig. 1.18a). The trend in growing microbial biomass varied at both t1 and t2. In both sampling times, the rhizosphere soil showed significantly higher growing microbial biomass compared to the bulk soil. While wheat monoculture significantly increased growing microbial biomass at t1, by t2, the rhizosphere soil of W1 exhibited approximately 2.5 times higher growth compared to WM. Crop rotations did not have a significant effect on growing microbial biomass in the bulk soil compartment (Fig. 1.18b).

Wheat rotational positions significantly influenced the maximum rate (V_{max}) of extracellular enzymes in the rhizosphere, root-affected, and bulk soil (p<0.01; Fig. 1.18). In terms of α-glucosidase activity at t1, continuous wheat cultivation markedly increased the enzyme activity in all sampling compartments. Notably, at t2, the rhizosphere soil exhibited the highest V_{max} value compared to both bulk soil (BS) compartment (Fig. 1.19a). For β-glucosidase activity. In the second sampling time, WM significantly decreased β-glucosidase activity in all studied compartments. The lowest V_{max} was observed in wheat monoculture with values of 56.67 and 67.98 nmol MUF $g^{-1}h^{-1}$ in BS and RH compartments, respectively (Fig. 1.19b).

Leucine aminopeptidase activity displayed an increasing trend from bulk soil to rhizosphere soil. In the bulk soil (BS) at t1, W1 exhibited the highest V_{max} at 114.4 nmol AMC $g^{-1}h^{-1}$, with a 29.8% and 15.9% decrease in W2 and WM, respectively (Fig. 1.119c). In contrast to the other studied enzymes, wheat monoculture led to a substantial increase in acid phosphatase compared to the first and second wheat after the break crop. In rhizosphere (RH) compartment, WM demonstrated the highest enzyme activity at t2, with values of 73.8 and 83.1 nmol MUF $g^{-1}h^{-1}$, respectively. At the second sampling time, W1 displayed the lowest acid phosphatase activity in RH (Fig. 1.19d).

At t2, the rhizosphere (RH) exhibited the most efficient α-glucosidase with low substrate affinity in both W1 and WM. Additionally, the bulk soil in WM displayed the lowest catalytic efficiency. Throughout both sampling times, W2 resulted in the lowest catalytic efficiency overall (Fig. 1.20a). For β-glucosidase, there was a decreasing trend in K_m values from bulk soil to rhizosphere soil in all wheat rotational positions. At t2, the RH compartment in W1 had the highest catalytic efficiency, reaching 4.4 nmol MUF µmol substrate$^{-1}h^{-1}$. With plant growth, wheat monoculture resulted in lower enzyme efficiency, and there were no significant differences between W2 and WM (Fig. 1.20b). The same trend was observed for catalytic efficiency values for leucine aminopeptidase at the second sampling time. W1 in the RH compartment exhibited the

highest catalytic efficiency, and continuous wheat cultivation led to a decline in enzyme efficiency (Fig. 1.20c). A different trend was observed for catalytic efficiency and K_m values for acid phosphatase, where wheat monoculture at both sampling times led to more efficient enzymes. At t2, RH soil in WM had the highest catalytic efficiency values, reaching 2.9 nmol MUF µmol substrate^{-1}h^{-1}, corresponding to a 38.6% and 6.2% increase compared to W1 and W2, respectively (Fig. 1.20d).

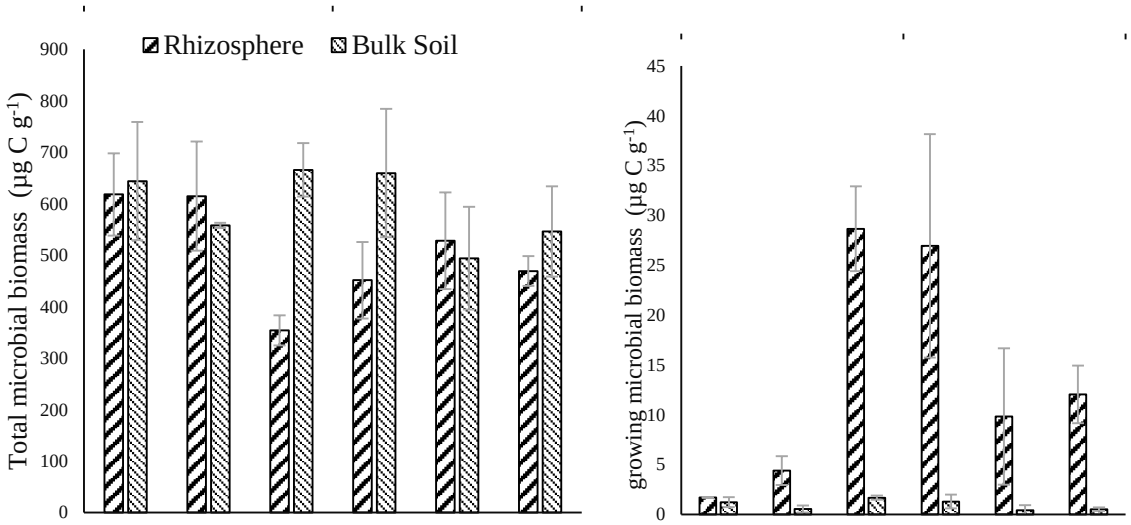

Figure 1.18. Total microbial biomass (TMB) (a), actively growing microbial biomass (GMB) (b), in different wheat soil compartments (BS: bulk soil, RH: rhizosphere) in the first (W1), second (W2) winter wheat after oilseed rape break crop and long-term wheat monoculture (WM) at two sampling times, T1 (BBCH 29) and T2 (BBCH 59). Error bars represent standard error of means (n = 3) according to ANOVA at p<0.05.

This study unravels dynamic shifts in microbial biomass, growth, and activity influenced by various wheat rotational positions across two sampling times (t1 and t2; Fig. 1.18), revealing the intricate interplay between crop rotation and soil microbial ecology. Previous studies, including those by Venter et al. (2016) and Sun et al. (2023), support the complexity of this relationship. While wheat monoculture enhanced microbial growth in the rhizosphere at t1, a notable shift occurred by t2. The rhizosphere soil of W1 (first year wheat) exhibited a remarkable growth increase, surpassing WM by approximately 2.5 times (Fig. 1.17). This hints at an adaptive and growth-promoting effect of W1 on the rhizosphere microbiome, consistent with Liu et al. (2023) observations of enhanced microbial activity in rotational systems compared to monoculture. These findings underscore the temporal dynamics and intricate relationships between wheat rotational positions and microbial responses, emphasizing the need for a comprehensive understanding of soil microbial communities in sustainable agricultural practices.

At t1, WM increased activity across all compartments (Fig. 1.19), potentially reflecting readily available resources for this readily degradable substrate (Sinsabaugh et al., 2002). However, at t2, WM exhibited the lowest activity, suggesting potential resource depletion or changes in microbial community composition in the monoculture system (Yahya et al., 2021). Notably, the rhizosphere consistently displayed higher activity compared to bulk soil, highlighting the localized enrichment of enzymes due to root exudates (Dhungaha et al., 2023). While the rhizosphere displayed the most efficient enzyme (low K_m) at t2 in both W1 and WM, WM bulk soil had the lowest efficiency throughout the study, suggesting potential spatial and temporal variability in enzyme efficiency within the different compartments and wheat rotations (Wang et al., 2023).

WM showed variable effects on β-glucosidase activity. At t1, WM had the highest activity in the rhizosphere, displaying the highest catalytic efficiency. However, this advantage diminished by t2, with W1 rhizosphere exhibiting the highest efficiency, potentially indicating efficient utilization of complex carbohydrates by specific microbial groups (Sinsabaugh et al., 2002). By t2, WM displayed the lowest activity in all compartments, suggesting potential limitations or shifts in resource availability in the monoculture over time. The decline in β-glucosidase activity in WM at t2, coupled with lower efficiency compared to W1 rhizosphere, indicates potential limitations or shifts in resource availability for the monoculture system over time.

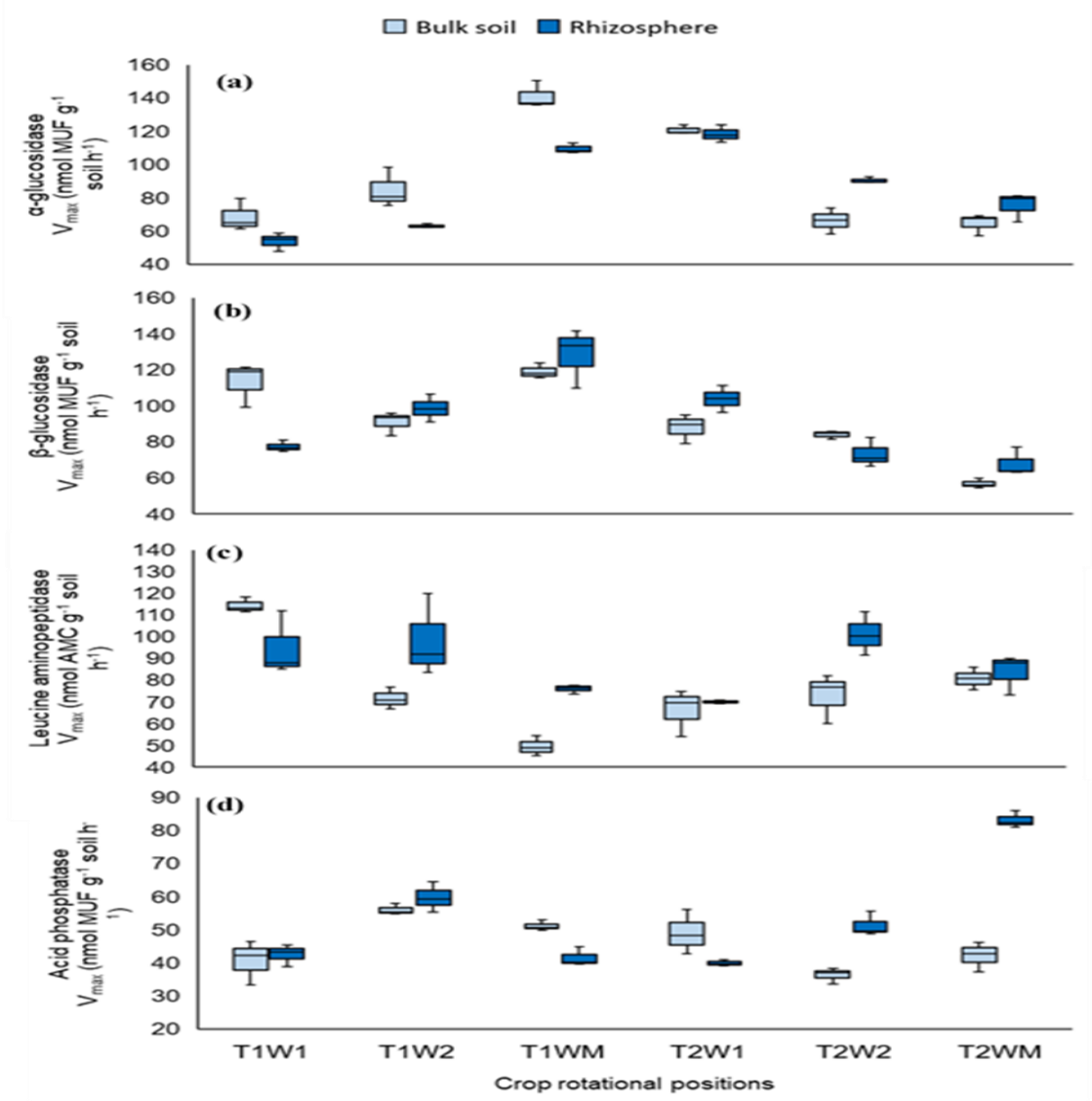

Figure 1.19. V_{max} values of α-glucosidase (a), β-glucosidase (b), leucine aminopeptidase (c) and acid phosphatase (d) in different wheat soil compartments (BS: bulk soil, RH: rhizosphere) in the first (W1), second (W2) winter wheat after oilseed rape break crop and long-term wheat monoculture (WM) at two sampling times, T1 (BBCH 29) and T2 (BBCH 59). Error bars represent standard error of means (n = 3) according to ANOVA at $p<0.05$.

In conclusion, our investigation into the distinct silty loam (loess) soil conditions, diverging from previous experiments in sandy loam soil, has uncovered notable differences in enzyme activity, microbial growth, and related dynamics. The identified trends underscore the necessity for further in-depth exploration using advanced techniques such as imaging and gene expression analysis. These methodologies will

provide a more comprehensive understanding of the unique characteristics and mechanisms at play in silty loam soil. This imperative next step in research will not only deepen our insights into plant-soil-microbe interactions but also contribute valuable knowledge essential for the development of targeted and sustainable agricultural practices in diverse soil environments.

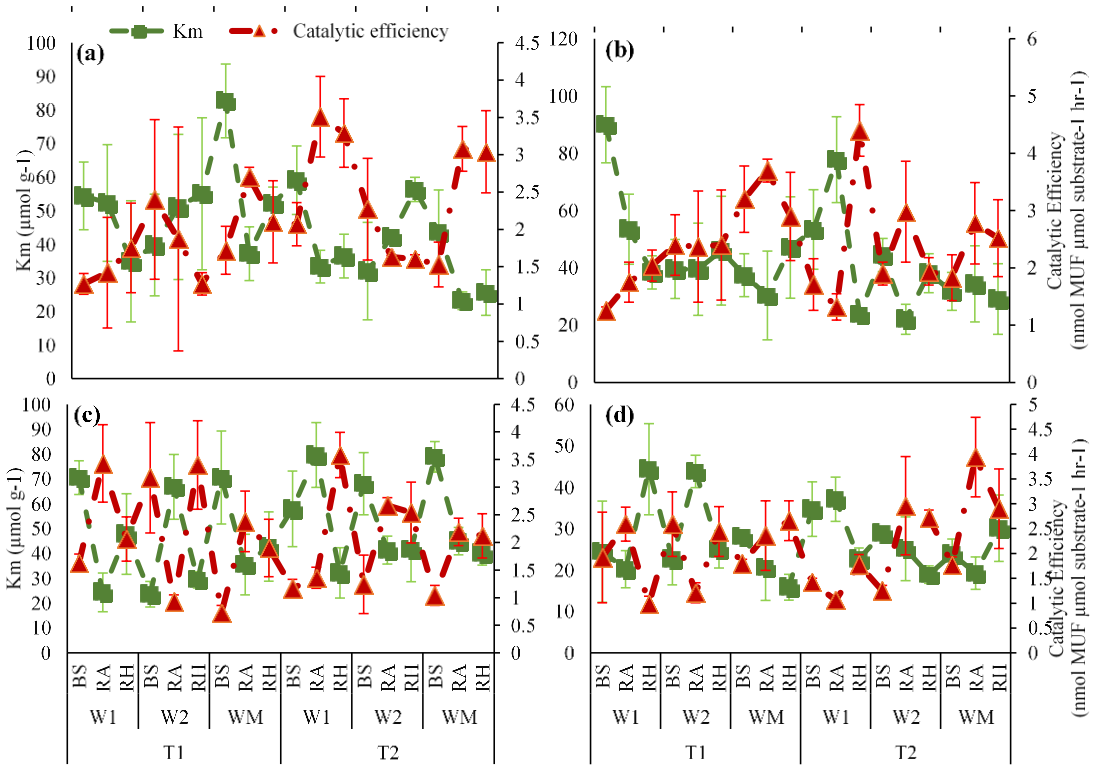

Figure 1.20. K_m values and catalytic efficiency of α-glucosidase (a), β-glucosidase (b), leucine aminopeptidase (c) and acid phosphatase (d) in different wheat soil compartments (BS: bulk soil, RH: rhizosphere) in the first (W1), second (W2) winter wheat after oilseed rape break crop and long-term wheat monoculture (WM) at two sampling times, T1 (BBCH 29) and T2 (BBCH 59). Error bars represent standard error of means (n = 3) according to ANOVA at p<0.05.

1.13. Summary of the main results of the studies

In this thesis, at first, we investigated the underlying mechanisms that govern the productivity of WW grown in self-succession as opposed to WW grown after a break crop, such as oilseed rape. We found significant biomass decline in successively grown winter wheat (WW) and also contrasting root plastic responses in response to successive WW rotational positions. The lower dissolved organic carbon (DOC) observed in the rhizosphere of successively grown winter wheat (WW) was found to be associated with microbial nitrogen (N) immobilization. Additionally, the rotational position of winter wheat strongly influenced the activity of carbon (C) and nitrogen (N)-acquiring enzymes. This rotational effect extended to the microbial community composition, indicating that the position of winter wheat in the rotation has a significant impact on the structure and function of the soil microbiota. These findings highlight the intricate connections between plant rotations, rhizosphere processes, and microbial dynamics, providing valuable insights for understanding and managing soil health in agricultural systems (Study 1).

The findings underscore the necessity of identifying and characterizing specific compounds in root exudates that trigger soil microorganisms, as they play a pivotal role

in shaping the microbial community structure and influencing nutrient dynamics. Glucose, the primary compound in exudates as an easily available sugar, is among the soluble carbohydrates that are adjusted by the roots to adapt to osmotic conditions. Therefore, we improved and optimized the protocol of soil glucose imaging - *in situ* imaging method of glucose release and presence of glucose in the area around the root. and adapted this method for the soil environment. The results obtained from the glucose imaging method provide compelling evidence of its efficacy in elucidating the nuanced dynamics of glucose exudation under varying moisture conditions and mycorrhizal associations. The method's success in capturing these intricate dynamics positions it as a valuable tool for advancing our understanding of plant responses to environmental stress (Study 2).

In the subsequent experiment, we aimed at thoroughly assessing how the dynamic relationship between these factors is influenced over successive wheat cropping cycles in a rhizobox experiment. The newly developed glucose imaging method proved to be a powerful tool for *in situ* visualization of glucose within the soil matrix. The study revealed that regions characterized by high glucose release exhibited heightened microbial activity, indicating a direct correlation between glucose availability and microbial stimulation. Interestingly, the distribution of glucose release along the wheat root is found to be heterogeneous, emphasizing the spatial complexity of root exudation patterns. Furthermore, the investigation into long-term wheat cultivation demonstrates a notable decrease in both glucose release and enzyme activity, suggesting potential shifts in the microbial environment over time. Importantly, the study underscores that successive wheat cultivation induces alterations in the exudation of root primary compounds, shedding light on the dynamic nature of plant-soil interactions in response to continuous cropping practices (Sudy 3).

Building upon the insights gained from the preceding study on successive wheat cultivation, we aimed to investigate the intricate mechanisms governing the modulation of rhizosphere processes in field conditions. In the context of continuous wheat cultivation, several key observations emerged. Firstly, W3 exhibited the lowest proportion of hotspots for glucose release in comparison to W1. Concurrently, there was a notable upregulation of the expressions of functional orthologous genes of SWEET family sugar transporters, particularly SWEET1a, in the wheat roots of W3 as opposed to W1. This shift in gene expression patterns suggests dynamic responses in the plant's molecular processes under prolonged wheat cultivation. Moreover, total microbial biomass experienced a decline in both the rhizosphere and bulk soils of W3 relative to W1, indicating shifts in the microbial community composition. Further accentuating these differences, β-glucosidase activity displayed a higher maximum velocity (V_{max}) in soil samples from W1 across all compartments studied compared to W3 samples. The reduced glucose release in W3 underscores the pivotal role of root exudates in shaping rhizosphere interactions and influencing microbial community dynamics during continuous wheat cultivation. Additionally, variations in SWEET gene expression in wheat roots and leaves signal potential adjustments in nutrient uptake and resource allocation strategies, providing valuable insights into the intricate interplay between plant physiology, root exudation, and microbial responses in the context of sustained wheat cultivation (Study 4).

Expanding on the insights obtained from sandy loam soil, we have extended our research endeavors to delve into the intricate interactions within the rhizosphere and bulk soil compartments, particularly within the distinct context of loess soil. Recognizing the inherent differences between soil types, our investigation aims to unravel how key factors such as enzyme kinetics patterns and microbial growth operate

in the unique environmental conditions of loess soil. The catalytic efficiency exhibited a consistent decline with successive wheat rotations, reflecting a downward trend from the root to bulk soil compartments. Notably, the rhizosphere (RH) compartment displayed the highest enzyme activity, and there was a discernible decrease in enzyme activities from the rhizosphere to the bulk soil compartments. Regarding wheat monoculture (WM), an initial decrease in rhizosphere biomass was observed, which, however, transitioned into the promotion of microbial growth compared to other rotations. This dual effect underscored the potential for both suppression and adaptation within the microbiome under continuous wheat cultivation. In summary, our findings indicate that sustained wheat cultivation not only suppressed microbial activity and functional efficiency but also resulted in lower enzyme activity, accompanied by the production of less efficient enzymes.

1.14. Conclusions and perspectives

The collective findings from the five studies underscore the profound impact of continuous wheat cultivation and successive rotations on soil microbial dynamics, enzymatic activities, and overall plant performance. The research revealed the importance of considering rotational positions, root exudation patterns, and microbial responses in shaping the rhizosphere environment and influencing soil health. Studies highlight the soil legacy from preceding crops, linking reduced root growth and labile carbon availability to decreased microbial and enzymatic activities in successive wheat rotations. The introduction of a glucose imaging method proves valuable for understanding nuanced dynamics of glucose exudation, shedding light on plant responses to environmental stress. Successive wheat cultivation significantly alters rhizosphere processes, resulting in declines in glucose release and creating a less favorable environment for beneficial soil microbes. The complex interplay between continuous wheat cultivation, root exudation patterns, gene expression, and enzymatic activities is explored, emphasizing the need for sustainable agricultural practices that account for the intricate dynamics of plant-soil-microbe interactions. Overall, these insights contribute to a comprehensive understanding of the factors influencing soil health and highlight the importance of considering temporal dynamics and intricate relationships between crop rotation and soil microbial responses for sustainable agriculture.

These studies provide several key perspectives that could shape future research and agricultural practices. Firstly, there is a need for continued investigation into the long-term impacts of continuous wheat cultivation and successive rotations on soil health and microbial communities. Understanding the persistent effects and potential shifts in soil dynamics over extended periods is crucial for designing sustainable agricultural systems.

The identified role of root exudates in shaping rhizosphere interactions emphasizes the importance of crop selection and management practices that optimize nutrient availability and microbial activity. Developing strategies to enhance beneficial microorganisms and their functions in the rhizosphere could contribute to improved soil health and plant performance. The introduction of innovative tools, such as the glucose imaging method, opens avenues for further advancements in soil research. Continued exploration of techniques will enhance our ability to monitor and understand the intricate dynamics of root exudation and microbial responses in real-world field settings.

Additionally, the findings highlight the complexity and adaptability of microbial communities in response to different rotational positions and continuous cropping.

Further research could delve into the underlying mechanisms of microbial adaptation and explore how these communities can be harnessed to promote sustainable agricultural practices. Ultimately, these perspectives underscore the importance of holistic approaches that integrate plant physiology, microbial ecology, and soil chemistry to inform more resilient and environmentally friendly agricultural systems. By incorporating these insights, researchers and practitioners can work towards developing strategies that balance crop productivity with long-term soil health and ecosystem sustainability.

1.15. References

Adesina M. F., Lembke A., Costa R., Speksnijder A., Smalla K. (2007). Screening of bacterial isolates from various European soils for *in vitro* antagonistic activity towards *Rhizoctonia solani* and *Fusarium oxysporum*: site dependent composition and diversity revealed. *Soil Biol. Biochem*. 39, 2818–2828. 10.1016/j.soilbio.2007.06.004

Afridi, M.S., Kumar, A., Javed, M.A., Dubey, A., de Medeiros, F.H.V., Santayo, G. 2024. Harnessing root exudates for plant microbiome engineering and stress resistance in plants. Microbiological Research. 279: 127567.

Asmar, F., Eiland, F., Nielsen. 1994. Effect of extracellular enzyme activities on solubilization rate of soil organic nitrogen. Biol. Fertility Soils, 17 (1994), pp. 32-38.Bago, B., Pfeffer, P.E. & Shachar-Hill, Y., 2000. Carbon metabolism and transport in arbuscular mycorrhizas. *Plant Physiol*. 124, 949–958.

Bais HP, Weir TL, Perry LG, Gilroy S, Vivanco JM. The role of root exudates in rhizosphere interactions with plants and other organisms. Annu Rev Plant Biol. 2006;57:233–66.

Bakker, P., Berendsen, R., Doornbos, R., Wintermans, P., Pieterse, C., 2013. The rhizosphere revisited: root microbiomics. Front. Plant Sci. 4:165. doi:10.3389/fpls.2013.00165

Bakker, P., Berendsen, R., Doornbos, R., Wintermans, P., Pieterse, C., 2013. The rhizosphere revisited: root microbiomics. Front. Plant Sci. 4:165. doi:10.3389/fpls.2013.00165

Bakker, P.A., Pieterse, C.M.J., Jonge, R.D., Berendse, R.L. 2018. The Soil-Borne Legacy. Cell 172. 1178-1180.

Berendsen RL, Pieterse CMJ, Bakker PAHM. The rhizosphere microbiome and plant health. Trends Plant Sci. 2012;17(8):478–86.

Bongiorno, G., Postma, J., Bünemann, E.K., Brussaard, L., de Goede, R.G.M., Mäder, P., Tamm, L., Thuerig, B., 2019. Soil suppressiveness to *Pythium ultimum* in ten European long-term field experiments and its relation with soil parameters. Soil Biology and Biochemistry 133, 174–187. doi:10.1016/j.soilbio.2019.03.012

Breia R, Conde A, Badim H, Fortes AM, Gerós H, Granell A. Plant SWEETs: from sugar transport to plant-pathogen interaction and more unexpected physiological roles. Plant Physiol. 2021 Jun 11;186(2):836-852. doi: 10.1093/plphys/kiab127.

Bressan, W., Figueiredo, J.E.F., 2008. Efficacy and dose–response relationship in biocontrol of Fusarium disease in maize by Streptomyces spp. Eur. J. Plant Pathol. 120(3), 311-316. doi:10.1007/s10658-007-9220-y

Bücking, H., Abubaker, J., Govindarajulu, M., Tala, M., Pfeffer, P.E., Nagahashi, G., Lammers, P., Shachar-Hill, Y., 2008. Root exudates stimulate the uptake and metabolism of organic carbon in germinating spores of Glomus intraradices. *New Phytologist* 180, 684– 695.

Burns RG, DeForest JL, Marxsen J, Sinsabaugh RL, Stromberger ME, Wallenstein MD, et al. Soil enzymes in a changing environment: current knowledge and future directions. Soil Biol Biochem. (2013) 58:216–34. doi: 10.1016/j.soilbio.2012.11.009

Calvo OC, Franzaring J, Schmid I, Fangmeier A, 2019. Root exudation of carbohydrates and cations from barley in response to drought and elevated CO2. *Plant and Soil* 438, 127–142.

Canarini, A., Kaiser, C., Merchant, A., Richter, A., Wanek, W., 2019. Root Exudation of Primary Metabolites: Mechanisms and Their Roles in Plant Responses to Environmental Stimuli. Front. Plant Sci. 10. doi:10.3389/fpls.2019.00157

Carrión VJ, Perez-Jaramillo J, Cordovez V, Tracanna V, de Hollander M, Ruiz-Buck D, Mendes LW, van Ijcken WFJ, Gomez-Exposito R, Elsayed SS, Mohanraju P, Arifah A, van der

Oost J, Paulson JN, Mendes R, van Wezel GP, Medema MH, Raaijmakers JM (2019) Pathogen-induced activation of disease-suppressive functions in the endophytic root microbiome. Science 366:606–612. https://doi.org/10.1126/science.aaw9285

Carvalhais LC, Dennis PG, Fedoseyenko D, Hajirezaei MR, Borriss R, von Wiren N. Root exudation of sugars, amino acids, and organic acids by maize as affected by nitrogen, phosphorus, potassium, and iron deficiency. J Plant Nutr Soil Sci. 2011;174(1):3–11.

Chen, L.-Q., Hou, B.-H., Lalonde, S., Takanaga, H., Hartung, M. L., Qu, X.-Q., Guo, W.-J., Kim, J.-G., Underwood, W., Chaudhuri, B., Chermak, D., Antony, G., White, F. F., Somerville, S. C., Mudgett, M. B., & Frommer, W. B. (2010). Sugar transporters for intercellular exchange and nutrition of pathogens. Nature, 468(7323), 527-532. https://doi.org/10.1038/nature09606

Chen, L.Q., Hou, B.H., Lalonde, S., Takanaga, H., Hartung, M., Qu, X.Q., Guo, W.J., Kim, J.G., Underwood, W., Chaudhuri, B., Chermak, D., Antony, G., White, F.F., Somerville, S.C., Mudgett, M.B., Frommer, W., 2010. Sugar transporters for intercellular exchange and nutrition of pathogens. Nature. 468, 527–532. doi:10.1038/nature09606

Chen, S., Waghmode, T.R., Sun, R. *et al.* Root-associated microbiomes of wheat under the combined effect of plant development and nitrogen fertilization. *Microbiome* **7**, 136 (2019). https://doi.org/10.1186/s40168-019-0750-2

Chen, Y., Palta, J., Prasad, P.V.V., Siddique, K.H.M., 2020. Phenotypic variability in bread wheat root systems at the early vegetative stage. BMC Plant Biology 20, 1–16. doi:10.1186/s12870-020-02390-8

Chng, S., Cromey, M.G., Dodd, S.L. *et al.* Take-all decline in New Zealand wheat soils and the microorganisms associated with the potential mechanisms of disease suppression. *Plant Soil* **397**, 239–259 (2015). https://doi.org/10.1007/s11104-015-2620-4

Cong, W.F., van Ruijven, J., Mommer, L., De Deyn, G.B., Berendse, F., Hoffland, E., 2014. Plant species richness promotes soil carbon and nitrogen stocks in grasslands without legumes. Journal of Ecology 102, 1163–1170. doi:10.1111/1365-2745.12280

Coninck BD, Timmermans P, Vos C, Cammue BPA, Kazan K. 2015. What lies beneath: belowground defense strategies in plants. Trends in Plant Science 20: 91–101.

Cook JR. 2003. Take-all of wheat. Physiological and Molecular Plant Pathology 62: 73–86.

Curl, E.A., Truelove, B. (1986). Root Exudates. In: The Rhizosphere. Advanced Series in Agricultural Sciences, vol 15. Springer, Berlin, Heidelberg. https://doi.org/10.1007/978-3-642-70722-3_3

De Deyn, G.B., Cornelissen, J.H.C., Bardgett, R.D., 2008. Plant functional traits and soil carbon sequestration in contrasting biomes. Ecology Letters 11, 516–531. 38 doi:10.1111/j.1461-0248.2008.01164.x

De Veris, F.T., Griffiths, R.I., Knight, C.G., Nicolitch, O., Williams, A. 2020. Harnessing rhizosphere microbiomes for drought-resilient crop production. Science, 368 (2020), pp. 270-274, 10.1126/science.aaz5192

Dennis P.G., Miller, A.J., Hirsch, P.R., 2010. Are root exudates more important than other sources of rhizodeposits in structuring rhizosphere bacterial communities? FEMS Microbiol. Ecol. 72 (3), 313–327. https://doi.org/10.1111/j.1574-6941.2010.00860.x

Doran JW, Jones AJ. *Methods for Assessing Soil Quality. SSSA Spec. Publ. 49*. Madison, WI: SSSA (1996).

Dubey, A., Kumar, A., Khan, M.L. (2020). Role of Biostimulants for Enhancing Abiotic Stress Tolerance in Fabaceae Plants. In: Hasanuzzaman, M., Araújo, S., Gill, S. (eds) The Plant Family Fabaceae. Springer, Singapore. https://doi.org/10.1007/978-981-15-4752-2_8

Eilers KG, Lauber CL, Knight R, Fierer N. Shifts in bacterial community structure associated with inputs of low molecular weight carbon compounds to soil. Soil Biol Biochem. 2010;42(6):896–903.

Fitzpatrick CR, Copeland J, Wang PW, Guttman DS, Kotanen PM, Johnson MTJ. Assembly and ecological function of the root microbiome across angiosperm plant species. Proc Natl Acad Sci U S A. 2018;115(6):E1157–65.

Freeman, J. and Ward, E. (2004), *Gaeumannomyces graminis*, the take-all fungus and its relatives. Molecular Plant Pathology, 5: 235-252. https://doi.org/10.1111/j.1364-3703.2004.00226.x

Fu, H., Zhang, G., Zhang, F., Sun, Z., Geng, G., and Li, T. (2017). Effects of continuous tomato monoculture on soil microbial properties and enzyme activities in a solar greenhouse. *Sustainability* 9:317.

Gaiser, T., Perkons, U., Küpper, P. M., Puschmann, D. U., Peth, S., Kautz, T., et al. (2012). Evidence of improved water uptake from subsoil by spring wheat following lucerne in a temperate humid climate. Field Crops Res. 126, 56–62. doi: 10.1016/j.fcr.2011.09.019

Gargallo-Garriga, A., Preece, C., Sardans, J., Oravec, M., Urban, O., Peñuelas, J., 2018. Root exudate metabolomes change under drought and show limited capacity for recovery. Sci. Rep. 8(1), 12696. doi:10.1038/s41598-018-30150-0

Gerlach M. Introduction of Ophiobolus graminis into new polders and its decline. Netherlands Journal of Plant Pathology 1968;74(Suppl. 2): 1–97.

Glick B. R. (2012). Plant growth-promoting bacteria: mechanisms and applications. *Scientifica* 12, 1–15. 10.6064/2012/963401

Gransee A, Wittenmayer L. Qualitative and quantitative analysis of water-soluble root exudates in relation to plant species and development. J Plant Nutr Soil Sci. 2000;163(4):381–5.

Häffner, E., Karlovsky, P., Splivallo, R., Traczewska, A., and Diederichsen, E., 2014. ERECTA, salicylic acid, abscisic acid, and jasmonic acid modulate quantitative disease resistance of Arabidopsis thaliana to Verticillium longisporum. BMC Plant Biol. 14(1), 85. doi:10.1186/1471-2229-14-85

Hage-Ahmed, K., Moyses, A., Voglgruber, A., Hadacek, F., Steinkellner, S., 2013. Alterations in Root Exudation of Intercropped Tomato Mediated by the Arbuscular Mycorrhizal Fungus Glomus mosseae and the Soilborne Pathogen *Fusarium oxysporum* f.sp. lycopersici. J Phytopathol. 161(11-12), 763-773. doi:https://doi.org/10.1111/jph.12130.

Hage-Ahmed, K., Moyses, A., Voglgruber, A., Hadacek, F., Steinkellner, S., 2013. Alterations in Root Exudation of Intercropped Tomato Mediated by the Arbuscular Mycorrhizal Fungus Glomus mosseae and the Soilborne Pathogen *Fusarium oxysporum* f.sp. lycopersici. J Phytopathol. 161(11-12), 763-773. doi:https://doi.org/10.1111/jph.12130.

Haichar FE, Marol C, Berge O, Rangel-Castro JI, Prosser JI, Balesdent J, Heulin T, Achouak W. Plant host habitat and root exudates shape soil bacterial community structure. ISME J. 2008;2(12):1221–30.

Hansen, J.C., Schillinger, W.F., Sullivan, T.S., Paulitz, T.C., 2019. Soil Microbial Biomass and Fungi Reduced with Canola Introduced into Long-Term Monoculture Wheat Rotations. Front. Microbiol. 10:1488. doi: 10.3389/fmicb.2019.01488doi:10.3389/fmicb.2019.01488

Hansen, J.C., Schillinger, W.F., Sullivan, T.S., Paulitz, T.C., 2019. Soil microbial biomass and fungi reduced with canola introduced into long-term monoculture wheat rotations. Frontiers in Microbiology 10, 1488. doi:10.3389/fmicb.2019.01488

Hargreaves, S.K., Hofmockel, K.S., 2014. Physiological shifts in the microbial community drive changes in enzyme activity in a perennial agroecosystem. Biogeochemistry. 117(1), 67-79. doi:10.1007/s10533-013-9893-6

Hilton, S., Bennett, A.J., Chandler, D., Mills, P., Bending, G.D., 2018. Preceding crop and seasonal effects influence fungal, bacterial and nematode diversity in wheat and oilseed rape rhizosphere and soil. Applied Soil Ecology 126, 34–46. doi:10.1016/j.apsoil.2018.02.007

Hinsinger P, Gobran GR, Gregory PJ, Wenzel WW (2005) Rhizosphere geometry and heterogenity arising from root-mediated physical and chemical processes. *New Phytologist* **168**, 293–303.

Hinsinger, P., Bengough, A.G., Vetterlein, D. *et al.* Rhizosphere: biophysics, biogeochemistry and ecological relevance. *Plant Soil* **321**, 117–152 (2009). https://doi.org/10.1007/s11104-008-9885-9

Ho LH, Klemens PAW, Neuhaus HE, Ko HY, Hsieh SY, Guo WJ. SlSWEET1a is involved in glucose import to young leaves in tomato plants. J Exp Bot. 2019 Jun 28;70(12):3241-3254. doi: 10.1093/jxb/erz154.

Hoang, D. T. T., Rashtbari, M., Anh, L. T., Wang, S., Tu, D. T., Hiep, N. V., & Razavi, B. S. (2022). Mutualistic interaction between arbuscular mycorrhiza fungi and soybean roots enhances drought resistant through regulating glucose exudation and rhizosphere expansion.

Soil Biology and Biochemistry, 171, 108728. https://doi.org/https://doi.org/10.1016/j.soilbio.2022.108728
Hornby, D. (1983) Suppressive soils. Annu. Rev. Phytopathol. 21, 65–85
Hornby, D. (1983) Suppressive soils. Annu. Rev. Phytopathol. 21, 65–85.
Hornby, D., Bateman, G.L., Gutteridge, R.J., Lucas, P., Osbourn, A.E., Ward, E. and Yarham, D.J. (1998) Take all Disease of Cereals: a Regional Perspective. Wallingford, UK: CABI International
Hornby, D., Bateman, G.L., Gutteridge, R.J., Lucas, P., Osbourn, A.E., Ward, E. and Yarham, D.J. (1998) Take all Disease of Cereals: a Regional Perspective. Wallingford, UK: CABI International
Houlden A, Timms-Wilson TM, Day MJ, Bailey MJ. Influence of plant developmental stage on microbial community structure and activity in the rhizosphere of three field crops. FEMS Microbiol Ecol. 2008;65(2):193–201.
Hu LF, Robert CAM, Cadot S, Zhang X, Ye M, Li BB, Manzo D, Chervet N, Steinger T, van der Heijden MGA, et al. Root exudate metabolites drive plant-soil feedbacks on growth and defense by shaping the rhizosphere microbiota. Nat Commun. 2018;9:2738.
Huang, X. F., Chaparro, J. M., Reardon, K. F., Zhang, R., Shen, Q., Vivanco, J. M. 2014. Rhizosphere interactions: root exudates, microbes, and microbial communities. Botany. 92, 267–275. https://doi.org/10.1139/cjb-2013-0225
Hütsch, B.W., Augustin, J., Merbach, W., 2002. Plant rhizodeposition — an important source for carbon turnover in soils. J. Plant. Nutr. Soil Sci. 165(4), 397-407. doi:https://doi.org/10.1002/1522-2624(200208)165:4<397::AID-JPLN397>3.0.CO;2-C
Ibiang, Y.B., Mitsumoto, H., and Sakamoto, K., 2017. Bradyrhizobia and arbuscular mycorrhizal fungi modulate manganese, iron, phosphorus, and polyphenols in soybean (Glycine max (L.) Merr.) under excess zinc. *Environ. Exp. Bot.* 137, 1–13.
Islam, M.S., Fahad, S., Hossain, A., et al. 2021. Legumes under Drought Stress: Plant Responses, Adaptive Mechanisms, and Management Strategies in Relation to Nitrogen Fixation Eng. Toler. Crop Plants Abiotic Stress (2021), pp. 179-207, 10.1201/9781003160717-9
Jadhav H. P., Sayyed R. Z. (2016). Hydrolytic enzymes of rhizospheric microbes in crop protection. *MOJ Cell Sci. Rep.* 3, 135–136. 10.15406/mojcsr.2016.03.00070
Jalali, B.L., Suryanarayana, D., 1971. Shift in the carbohydrate spectrum of root exudates of wheat in relation to its root-rot disease. Plant Soil. 34, 261-267. https://doi.org/10.1007/BF01372783
Jenkyn, J.F., Gutteridge, R.J. and White, R.P. (2014), Effects of break crops, and of wheat volunteers growing in break crops or in set-aside or conservation covers, all following crops of winter wheat, on the development of take-all (*Gaeumannomyces graminis* var. *tritici*) in succeeding crops of winter wheat. Ann Appl Biol, 165: 340-363. https://doi.org/10.1111/aab.12139
Jones DL, Hodge A, Kuzyakov Y (2004) Plant and mycorrhizal regulation of rhizodeposition. *New Phytologist* **163**, 459–480.
Jones, D. L., Nguyen, C., & Finlay, R. D. (2009). Carbon flow in the rhizosphere: carbon trading at the soil–root interface. Plant and Soil, 321(1), 5-33. https://doi.org/10.1007/s11104-009-9925-0
Jones, D.L., Hodge, A., Kuzyakov, Y., 2004. Plant and mycorrhizal regulation of rhizodeposition. New Phytol. 163(3), 459-480. doi:10.1111/j.1469-8137.2004.01130.x
Jones, D.L., Nguyen, C. & Finlay, R.D. Carbon flow in the rhizosphere: carbon trading at the soil–root interface. *Plant Soil* **321**, 5–33 (2009). https://doi.org/10.1007/s11104-009-9925-0
Jones, P., Garcia, B.J., Furches, A., Tuskan, G.A., Jacobson, D., 2019. Plant host-associated mechanisms for microbial selection. Frontiers in Plant Science 10, 1–14. doi:10.3389/fpls.2019.00862
Jousset A, Rochat L, Lanoue A, Bonkowski M, Keel C, Scheu S (2011) Plants respond to pathogen infection by enhancing the antifungal gene expression of root-associated bacteria. Mol Plant-Microbe Interact 24:352–358. https://doi.org/10.1094/MPMI

Kaloterakis, N., van Delden, S.H., Hartley, S., De Deyn, G.B., 2021. Silicon application and plant growth promoting rhizobacteria consisting of six pure Bacillus species alleviate salinity stress in cucumber (Cucumis sativus L). Scientia Horticulturae 288, 110383. doi:10.1016/J.SCIENTA.2021.110383

Katan J, Greenberger A, Alon H, Grinstein A. 1976. Solar heating by polyethylene mulching for the control of disease caused by soil-borne pathogen. Disease Control and Pest Management 66: 683–688.

Kelly, C., Haddix, M.L., Byrne, P.F., Cotrufo, M.F., Schipanski, M., Kallenbach, C.M., Wallenstein, M.D., Fonte, S.J., 2022. Divergent belowground carbon allocation patterns of winter wheat shape rhizosphere microbial communities and nitrogen cycling activities. Soil Biology and Biochemistry 165, 108518. doi:10.1016/j.soilbio.2021.108518

Kirby, J.R. 2009. Chemotaxis-Like Regulatory Systems: Unique Roles in Diverse Bacteria. Annu. Rev. Microbiol. 63, 45–59. Doi:0066-4227/09/1013-0045$20.00.

Kraigher, H., Bajc, M., Grebenc, T., 2013. Chapter 8 - mycorrhizosphere complexity. In: Matyssek, N.C.R., Cudlin, P., Mikkelsen, T.N., Tuovinen, J.P., Wieser, G., Paoletti, E. (eds): Developments in environmental science. *Elsevier*, pp 151–177.

Kramer-Walter, K.R., Bellingham, P.J., Millar, T.R., Smissen, R.D., Richardson, S.J., Laughlin, D.C., 2016. Root traits are multidimensional: specific root length is independent from root tissue density and the plant economic spectrum. Journal of Ecology 104, 1299–1310. doi:10.1111/1365-2745.12562

Kuzyakov, Y., Jones, D.L., 2006. Glucose uptake by maize roots and its transformation in the rhizosphere. Soil Biology and Biochemistry 38, 851–860. doi:10.1016/j.soilbio.2005.07.012

Kuzyakov, Y., Raskatov, A., Kaupenjohann M. 2003. Turnover and distribution of root exudates of Zea mays. Plant Soil, 254 (2003), pp. 317-327

Kwak Y-S, Weller DM. 2013. Take-all of wheat and natural disease suppression: a review. The Plant Pathology Journal 29: 125–135.

Lange, M., Eisenhauer, N., Sierra, C.A., Bessler, H., Engels, C., Griffiths, R.I., Mellado-Vázquez, P.G., Malik, A.A., Roy, J., Scheu, S., Steinbeiss, S., Thomson, B.C., Trumbore, S.E., Gleixner, G., 2015. Plant diversity increases soil microbial activity and soil carbon storage. Nature Communications 6, 6707. doi:10.1038/ncomms7707

Lennon JT, Jones SE. Microbial seed banks: the ecological and evolutionary implications of dormancy. Nat Rev Microbiol. 2011;9(2):119–30.

Liese, R., Lübbe, T., Albers, N.W., Meier, I.C., 2018. The mycorrhizal type governs root exudation and nitrogen uptake of temperate tree species. *Tree Physiology* 38, 83–95.

Liu H, Brettell LE, Qiu Z, Singh BK (2020) Microbiome-mediated stress resistance in plants. Trends Plant Sci 25:733–743. https://doi.org/10.1016/j.tplants.2020.03.014

Liu, L., Sun, C., Liu, S., Chai, R., Huang, W., Liu, X., et al. (2015). Bioorganic fertilizer enhances soil suppressive capacity against bacterial wilt of tomato. *PLoS One* 10:e0121304. doi: 10.1371/journal.pone.0121304

Lopez, G., Ahmadi, S.H., Amelung, W., Athmann, M., Ewert, F., Gaiser, T., Gocke, M.I., Kautz, T., Postma, J., Rachmilevitch, S., Schaaf, G., Schnepf, A., Stoschus, A., Watt, M., Yu, P., Seidel, S.J., 2023. Nutrient deficiency effects on root architecture and root-to-shoot ratio in arable crops. Frontiers in Plant Science 13, 1–18. doi:10.3389/fpls.2022.1067498

Maharjan M, Sanaullah M, Razavi BS, Kuzyakov Y. Effect of land use and management practices on microbial biomass and enzyme activities in subtropical top-and sub-soils. *Appl Soil Ecol*. (2017) 113:22–8. doi: 10.1016/j.apsoil.2017.01.008

Marinari, S., Moscateli., C., Grego, S. 2014. Enzymes at plant-soil interface. L. Gianfreda, M.A. Rao (Eds.), Enzymes in Agricultural Sciences, OMICS Group eBooks, USA (2014), pp. 94-109.

Marschner H. Mineral Nutrition of Higher Plants. In: Marschner H, editor. Mineral Nutrition of Higher Plants. 2nd ed. London: Academic Press; 1995. p. 681–861.

Mayer, Z., Sasvári, Z., Szentpéteri, V., Rétháti, B.P., Vajna, B., Posta, K., 2019. Effect of long-term cropping systems on the diversity of the soil bacterial communities. Agronomy 9, 1–10. doi:10.3390/agronomy9120878

Mazzola, M., 2002. Mechanisms of natural soil suppressiveness to soilborne diseases. Antonie Van Leeuwenhoek 81, 557–564 (2002). https://doi.org/10.1023/A:1020557523557
McLaughlin, J.E. & Boyer, J.S., 2004. Glucose localisation in maize ovaries when kernel number decreases at low water potential and sucrose is fed to the stems. *Annals of Botany* 94, 75– 86.
McMillan, V.E., Canning, G., Moughan, J. *et al.* Exploring the resilience of wheat crops grown in short rotations through minimising the build-up of an important soil-borne fungal pathogen. *Sci Rep* **8**, 9550 (2018). https://doi.org/10.1038/s41598-018-25511-8
Mommer LKirkegaard Jvan Ruijven J (2016) Root-root interactions: towards a rhizosphere framework Trends in Plant Science 21:209–217. https://doi.org/10.1016/j.tplants.2016.01.009
Monaci, E., Polverigiani, S., Neri, D., Bianchelli, M., Santilocchi, R., Toderi, M., et al. (2017). Effect of contrasting crop rotation systems on soil chemical, biochemical properties and plant root growth in organic farming: first results. *Ital J. Agron.* 12, 364–374. doi: 10.4081/ija.2017.831
Narula, N., E. Kothe, R.K. Behl. 2012. Role of root exudates in plant-microbe interactions. J. Appl. Bot. Food Qual., 82 (2012), pp. 122-130
Nicole B. Schmid, Ricardo F.H. Giehl, Stefanie Döll, Hans-Peter Mock, Nadine Strehmel, Dierk Scheel, Xiaole Kong, Robert C. Hider, Nicolaus von Wirén. 2014. Feruloyl-CoA 6′-Hydroxylase1-Dependent Coumarins Mediate Iron Acquisition from Alkaline Substrates in Arabidopsis, *Plant Physiology*, Volume 164, Issue 1, January 2014, Pages 160–172.
Olanrewaju, O.S., Ayangbenro, A.S., Glick, BR., Babalola, O.O., 2019. Plant health: feedback effect of root exudates-rhizobiome interactions. Appl. Microbiol. Biotechnol. 103(3), 1155-1166. doi:10.1007/s00253-018-9556-6
P. Bukovská, M. Rozmoš, M. Kotianová, K. Gančarčíková, M. Dudáš, H. Hršelová, J. Jansa. 2021. Arbuscular mycorrhiza mediates efficient recycling from soil to plants of nitrogen bound in chitin Front. Microbiol., 12 (2021), pp. 1-16, 10.3389/fmicb.2021.574060
Palma-Guerrero, J., Chancellor, T., Spong, J., Canning, G., Hammond, J., McMillan, V.E., Hammond-Kosack, K.E. 2021. Take-All Disease: New Insights into an Important Wheat Root Pathogen. Trends in Plant Science, August 2021, Vol. 26, No. 8: 836-839.
Pandey, P.; Irulappan, V.; Bagavathiannan, M.V.; Senthil-Kumar, M. Impact of combined abiotic and biotic stresses on plant growth and avenues for crop improvement by exploiting physio-morphological traits. *Front. Plant Sci.* **2017**, *8*, 537
Panth M, Hassler SC, Baysal-Gurel F. 2020. Methods for Management of Soilborne Diseases in Crop Production. Agriculture 10: 16.
Paterson, E., Gebbing, T., Abel, C., Sim, A., Telfer, G. 2007. Rhizodeposition shapes rhizosphere microbial community structure in organic soil. New Phytol. **173**, 600–610. https://doi.org/10.1111/j.1469-8137.2006.01931.x
Prathap M., Ranjitha K. B. D. (2015). A critical review on plant growth promoting rhizobacteria. *J. Plant Pathol. Microbiol*. 6, 1–4. 10.4172/2157-7471.1000266
Qi, B., Zhang K., Qin, S., Lyu, D., He, J. 2022. Glucose addition promotes C fixation and bacteria diversity in C-poor soils, improves root morphology, and enhances key N metabolism in apple roots. PLoS One. 19;17(1):e0262691. doi: 10.1371/journal.pone.0262691
Ren, C., Chen, J., Deng, J., Zhao, F., Han, X., Yang, G., Tong, X., Feng, Y., Shelton, S., Ren, G., 2017. Response of microbial diversity to C:N:P stoichiometry in fine root and microbial biomass following afforestation. Biology and Fertility of Soils 53, 457–468. doi:10.1007/s00374-017-1197-x
Rothrock CS. 1987. Take-all of wheat as affected by tillage and wheat-soybean doublecropping. Soil Biology and Biochemistry 19: 307–311.
Rout ME, Southworth D. The root microbiome influences scales from molecules to ecosystems: the unseen majority. Am J Bot. 2013;100(9):1689–91.
Schlemper TR, Leite MFA, Lucheta AR, Shimels M, Bouwmeester HJ, van Veen JA, Kuramae EE. Rhizobacterial community structure differences among sorghum cultivars in different growth stages and soils. FEMS Microbiol Ecol. 2017;93(8):1–11.

Sharp, R.E., Hsiao, T.C., Silk, W.K., 1990. Growth of the maize primary root at low water potentials. II. Role of growth and deposition of hexose and potassium in osmotic adjustment. *Plant Physiol* 93, 1337–1346.
Shi SJ, Richardson AE, O'Callaghan M, DeAngelis KM, Jones EE, Stewart A, Firestone MK, Condron LM. Effects of selected root exudate components on soil bacterial communities. FEMS Microbiol Ecol. 2011;77(3):600–10.
Singh, B. N., Hidangmayum, A., Singh, A., Shera, S. S., & Dwivedi, P. (2019). *Secondary metabolites of plant growth promoting rhizomicroorganisms* (pp. 391-404). Berlin, Germany:: Springer.
Singhal, P.; Jan, A.T.; Azam, M.; Haq, Q.M.R. Plant abiotic stress: A prospective strategy of exploiting promoters as alternative to overcome the escalating burden. *Front. Life Sci.* **2016**, *9*, 52–63.
Sinsabaugh RL, Lauber CL, Weintraub MN, Ahmed B, Allison SD, Crenshaw C, et al. Stoichiometry of soil enzyme activity at global scale. *Ecol Lett.* (2008) 11:1252–64. doi: 10.1111/j.1461-0248.2008. 01245.x
Skujinš J, Burns RG. Extracellular enzymes in soil. *CRC Crit Rev Microbiol.* (1976) 4:383–421. doi: 10.3109/10408417609102304
Smith, S.E., Read, D., 2008. The Symbionts Forming Arbuscular Mycorrhizas. Mycorrhizal Symbiosis 3rd Edn. London: Academic Press, 13–41. https://doi.org/10.1016/B978-0-12-370526-6.X5001-6
Snapp SS, Morrone VL. Soil quality assessment. In: Logsdon S, Clay D, Moore D, Tsegaye T, editors. *Soil Science Step-by-Step Field Analysis.* Madison, WI: Soil Science Society of America (2008). p. 79–96.
Soil extracellular enzymes control the soil nutrient cycling, and their activities have been suggested as important determinant of soil quality (Uwituze et al., 2022). They are primarily secreted outside the cell by soil microorganisms (10) or plant roots (11), and they can bind to either the cell or soil particles or diffuse freely in soils (11).
Song R, Zhu WZ, Li H and Wang H (2024) Impact of wine-grape continuous cropping on soil enzyme activity and the composition and function of the soil microbial community in arid areas. *Front. Microbiol.* 15:1348259. doi: 10.3389/fmicb.2024.1348259
Song, C., Jin, K., Raajimakers, J. 2021. Designing a home for beneficial plant microbiomes. Current Opinion in Plant Biology. 62: 102025.
Song, X., Razavi, B.S., Ludwig, B., Zamanian, K., Zang, H., Kuzyakov, Y., Dippold, M.A., Gunina, A., 2020. Combined biochar and nitrogen application stimulates enzyme activity and root plasticity. Science of the Total Environment 735, 139393. doi:10.1016/j.scitotenv.2020.139393
Spitzer, C.M., Lindahl, B., Wardle, D.A., Sundqvist, M.K., Gundale, M.J., Fanin, N., Kardol, P., 2021. Root trait–microbial relationships across tundra plant species. New Phytologist 229, 1508–1520. doi:10.1111/nph.16982
Spollen, W.G., Tao, W., Valliyodan, B., Chen, K., Hejlek, L.G., Kim, J.J., Lenoble, M.E., Zhu, J., Bohnert, H.J., Henderson, D,, Schachtman, D.P., Davis, G.E., Springer, G.K., Sharp, R.E., Nguyen, H.T., 2008. Spatial distribution of transcript changes in the maize primary root elongation zone at low water potential. *BMC Plant Biol* 8, 32.
Sun, H., Jiang, S., Jiang, C., Wu, C., Gao, M., Wang, Q. 2021. A review of root exudates and rhizosphere microbiome for crop production. *Environ Sci Pollut Res* **28**, 54497–54510 (2021). https://doi.org/10.1007/s11356-021-15838-7
Tarafdar, J.C., Marschner, H., 1994. Efficiency of VAM hyphae in utilization of organic phosphorus by wheat plants. *Soil Sci Plant Nutr* 40, 593–600.
Toledo, S., Bondaruk, V. F., Yahdjian, L., Oñatibia, G. R., Loydi, A., and Alberti, J. (2023). Environmental factors regulate soil microbial attributes and their response to drought in rangeland ecosystems. *Sci. Total Environ.* 892:164406. doi: 10.1016/j.scitotenv.2023.164406
Ulrich, D. E. M., Clendinen, C. S., Alongi, F., Mueller, R. C., Chu, R. K., Toyoda, J., Gallegos-Graves, V., Goemann, H. M., Peyton, B., Sevanto, S., Dunbar, J. 2022. Root exudate composition reflects drought severity gradient in blue grama (Bouteloua gracilis). Sci Rep. 22;12(1):12581. doi: 10.1038/s41598-022-16408-8. PMID: 35869127; PMCID: PMC9307599.

Upadhyay S. K., Singh G., Singh D. P. (2016). Mechanism and understanding of PGPR: an approach for sustainable agriculture under a biotic stresses, in *Microbes and Environmental Management*, eds Singh J. S., Singh D. P. (Stadum: Studium Press Pvt. Ltd;), 225–254.
Uwituze Y, Nyiraneza J, Fraser TD, Dessureaut-Rompré J, Ziadi N and Lafond J (2022) Carbon, Nitrogen, Phosphorus, and Extracellular Soil Enzyme Responses to Different Land Use. *Front. Soil Sci.* 2:814554. doi: 10.3389/fsoil.2022.814554
Vancura, V., Hovadik, A., 1965. Root exudates of plants II. Composition of root exudates of some vegetables. *Plant Soil* 22, 21–32.
Vandenkoornhuyse, P., Quaiser, A., Duhamel, M., Le Van, A. and Dufresne, A. (2015), The importance of the microbiome of the plant holobiont. New Phytol, 206: 1196-1206. https://doi.org/10.1111/nph.13312
Vaughan, M. M., Christensen, S., Schmelz, E. A., Huffaker, A., Mcauslane, H. J., Alborn, H. T., Romero, M., Allen, L. H., and Teal, P. E. A. (2015) Accumulation of terpenoid phytoalexins in maize roots is associated with drought tolerance. *Plant Cell Environ*, 38: 2195–2207. doi: 10.1111/pce.12482.
Vheng, W., Coleman, D.C. 1990. Effect of living roots on soil organic matter decomposition. Soil Biol. Biochem., 22 (1990), pp. 781-787
Voothuluru, P., Anderson, J.C., Sharp, R.E., Peck, S.C., 2016. Plasma membrane proteomics in the maize primary root growth zone: novel insights into root growth adaptation to water stress. *Plant, Cell & Environment* 39, 2043-2054.
Voothuluru, P., Braun, D.M., Boyer, J.S., 2018. An in vivo imaging assay detects spatial variability in glucose release from plant roots. *Plant Physiology* 178, 1002–1010.
Walker, J. (1981) Taxonomy of take-all fungi and related genera and species. In Biology and Control of Take-All (Asher, M.J.C. and Shipton, P.J., eds). London: Academic Press, pp. 15–74
Walker, J.L. (1975) Take-all diseases of Gramineae: a review of recent work. Rev. Plant Pathol. 54, 113–144
Wang, J. T., Zhang, Y. B., Xiao, Q., and Zhang, L. M. (2022). Archaea is more important than bacteria in driving soil stoichiometry in phosphorus deficient habitats. *Sci. Total Environ.* 827:154417. doi: 10.1016/j.scitotenv.2022.154417
Wang, R., Xiao, Y., Lv, F., Hu, L., Wei, L., Yuan, Z., et al. (2018). Bacterial community structure and functional potential of rhizosphere soils as influenced by nitrogen addition and bacterial wilt disease under continuous sesame cropping. *Appl. Soil Ecol.* 125, 117–127.
Watt M., Kirkegaard J. A., Passioura J. B. (2006) Rhizosphere biology and crop productivity—a review. *Australian Journal of Soil Research* **44**, 299-317.
Weller DM, Raaijmakers JM, Gardener BBM, Thomashow LS. 2002. Microbial populations responsible for specific soil suppressiveness to plant pathogens. Annual Review of Phytopathology 40: 309–348.
Wen, T., Yu, G.H., Hong, W.D., Yuan, J., Niu, G.Q., Xie, P.H., Sun, F.S., Guo, L.D., Kuzyakov, Y., Shen, Q.R., 2022. Root exudate chemistry affects soil carbon mobilization via microbial community reassembly. Fundamental Research 2, 697–707. doi:10.1016/j.fmre.2021.12.016
Wen, T., Yu, G.H., Hong, W.D., Yuan, J., Niu, G.Q., Xie, P.H., Sun, F.S., Guo, L.D., Kuzyakov, Y., Shen, Q.R., 2022. Root exudate chemistry affects soil carbon mobilization via microbial community reassembly. Fundamental Research 2, 697–707. doi:10.1016/j.fmre.2021.12.016
Wen, Z., White, P.J., Shen, J. and Lambers, H. (2022), Linking root exudation to belowground economic traits for resource acquisition. New Phytol, 233: 1620-1635. https://doi.org/10.1111/nph.17854
Wild, B., Schnecker, J., Alves, R.J., Baruskov, P., Bartya, J., Čapek, P., Gentsch, N., Gittel, A., Guggenberger, G., Lashchinskiy, N., Mikutta, R., Rusalimova, O., Šantrůčková, H., Shibistova, T., Urich. T., Watzka, M., Zrazhevskaya, G., Richter, A. 2014. Input of easily available organic C and N stimulates microbial decomposition of soil organic matter in arctic permafrost soil. Soil Biol. Biochem. 75: 143-151. https://doi.org/10.1016/j.soilbio.2014.04.014.

Wilkes, M.A., Marschall, D.R., Copeland, L. 1999. Hydroxamic acids in cereal roots inhibit the growth of take-all. Soil biology and biochemistry. 31(13): 1831-1836.
Wu, L., Chen, J., Wu, H., Wang, J., Wu, Y., Lin, S., Khan, M.U., Zhang, Z., Lin, W. 2016. Effects of consecutive monoculture of *Pseudostellaria heterophylla* on soil fungal community as determined by pyrosequencing. Sci Rep. 24; 6:26601. doi: 10.1038/srep26601. PMID: 27216019; PMCID: PMC4877567.
Xie H, Wang D, Qin Y, Ma A, Fu J, Qin Y, Hu G, Zhao J (2019) Genome-wide identification and expression analysis of SWEET gene family in *Litchi chinensis* reveal the involvement of *LcSWEET2a/3b* in early seed development. BMC Plant Biol **19**: 499.
Yahya M, Islam Eu, Rasul M, Farooq I, Mahreen N, Tawab A, Irfan M, Rajput L, Amin I and Yasmin S (2021) Differential Root Exudation and Architecture for Improved Growth of Wheat Mediated by Phosphate Solubilizing Bacteria. *Front. Microbiol.* 12:744094. doi: 10.3389/fmicb.2021.744094
Yang, Y., Li, M., Wu, J., Pan, X., Gao, C., Tang, D.W.S., 2022. Impact of combining long-term subsoiling and organic fertilizer on soil microbial biomass carbon and nitrogen, soil enzyme activity, and water use of winter wheat. Frontiers in Plant Science 12, 1–13. doi:10.3389/fpls.2021.788651
Yin C, Mueth N, Hulbert S, Schlatter D, Paulitz TC, Schroeder K, Prescott A, Dhingra A. 2017. Bacterial communities on wheat grown under long-term conventional tillage and no-till in the Pacific Northwest of the United States. Phytobiomes Journal 1: 83–90
Zhang J, Shuang S, Zhang L, Xie S and Chen J (2021) Photosynthetic and Photoprotective Responses to Steady-State and Fluctuating Light in the Shade-Demanding Crop *Amorphophallus xiei* Grown in Intercropping and Monoculture Systems. *Front. Plant Sci.* 12:663473. doi: 10.3389/fpls.2021.663473
Zhang, Y., Guo, R., Li, S., Chen, Y., Li, Z., He, P., et al. (2021). Effects of continuous cropping on soil, senescence, and yield of Tartary buckwheat. *Agron. J.* 113, 5102–5113.
Zhao, J. Y., Xie, X., Jiang, Y. Y., Li, J. X., Fu, Q., Qiu, Y. B., et al. (2023). Effects of simulated warming on soil microbial community diversity and composition across diverse ecosystems. *Sci. Total Environ.* 911:168793.
Zhiwen Wang, Qin Peng, Xiang Gao, Shan Zhong, Yuan Fang, Xinling Yang, Yun Ling, and Xili Liu. 2020. Novel Fungicide 4-Chlorocinnamaldehyde Thiosemicarbazide (PMDD) Inhibits Laccase and Controls the Causal Agent of Take-All Disease in Wheat, *Gaeumannomyces graminis* var. *tritici*. *Journal of Agricultural and Food Chemistry* 2020 *68* (19), 5318-5326.DOI: 10.1021/acs.jafc.0c01260

1.16. Contribution to the included manuscripts

The Ph.D. thesis is a cumulative study, which comprises three published, one submitted and one in preparation manuscripts elaborated in cooperation with various co-authors. The extent of the doctoral candidate's contribution to the manuscripts is assessed on the following scale:

A. Has contributed to the work (0-33%); B. Has made a substantial contribution (34-66%); C. Did the majority of the work independently (67-100%)

Study 1. Nikolaos Kaloterakis, ***Mehdi Rashtbari***, Bahar S. Razavi, Andrea Braun-Kiewnick3, Adriana Giongo, Kornelia Smalla, Charlotte Kummer, Sirgit Kummer, Rüdiger Reichel, Nicolas Brüggemann. 2024. Preceding crop legacy modulates the early growth of winter wheat by influencing root growth dynamics, rhizosphere processes, and microbial interactions. Soil Biology and Biochemistry 191 (2024) 109343.

Conceptual design	A
Planning	A
Implementation	B
Preparation of the manuscript	B

Study 2. Duyen Thi Thu Hoang[1], ***Mehdi Rashtbari[1]***, Luu The Anh, Shang Wang, Dang Thanh Tu, Nguyen Viet Hiep, Bahar S. Razavi. 2022. Mutualistic interaction between arbuscular mycorrhiza fungi and soybean roots enhances drought resistant through regulating glucose exudation and rhizosphere expansion. Soil Biology and Biochemistry 171 (2022) 108728

Conceptual design	A
Planning	A
Implementation	B
Preparation of the manuscript	B

Study 3. ***Mehdi Rashtbari***, Andrea Braun-Kiewnick, Kornelia Smalla, Bahar S. Razavi. 2024. Glucose Release and Enzyme Activity Are Affected by Successive Wheat Cultivation and Plant Developmental Stage. Geoderma

Conceptual design	A
Planning	B
Implementation	C
Preparation of the manuscript	C

Study 4. ***Mehdi Rashtbari***, Seyed Sajjad Hoseini, Ahmad Samir Azimi, Markus Schemmel, Zheng Zhou, Lingyue Han, Daguang Cai, Bahar S. Razavi. 2024. Glucose Release Controlled by Sugar Transporters in Wheat Plant Modulates Microbial Growth and Enzyme Activity Around the Root. Submitted

Conceptual design	A
Planning	A
Implementation	C
Preparation of the manuscript	C

Study 5. ***Mehdi Rashtbari***, Seyed Sajjad Hoseini, Dennis Grunwald, Kessica Arnhold, Hans-Josef Koch, Bahar S. Razavi. 2024. Different Crop Rotation Scenarios Affected Enzyme Kinetics Pattern in a Loess Soil. In Preparation

Conceptual design	A
Planning	A
Implementation	C
Preparation of the manuscript	C

2 Chapter II: Publications and Manuscripts

2.1. Study 1: Preceding crop legacy modulates the early growth of winter wheat by influencing root growth dynamics, rhizosphere processes, and microbial interactions

Nikolaos Kaloterakis[1], Mehdi Rashtbari[2], Bahar S. Razavi[2], Andrea Braun-Kiewnick[3], Adriana Giongo[3], Kornelia Smalla[3], Charlotte Kummer[1], Sirgit Kummer[1], Rüdiger Reichel[1], Nicolas Brüggemann[1]

[1]Institute of Bio- and Geosciences, Agrosphere (IBG-3), Forschungszentrum Jülich GmbH, 52428 Jülich, Germany
[2]Department of Soil and Plant microbiome, Institute for phytopathology, Christian-Albrechts-University of Kiel, 24118, Kiel, Germany
[3]Institute for Epidemiology and Pathogen Diagnostics, Julius Kühn Institute (JKI) – Federal Research Centre for Cultivated Plants, 38104, Braunschweig, Germany

Status: Published in Soil Biology and Biochemistry 191 (2024) 109343

2.1.1. Abstract

Successive winter wheat (WW) rotations are associated with a substantial yield decline, and the underlying mechanisms remain elusive. An outdoor experiment was set up using sandy loam soil. WW was grown in rhizotrons, in soil after oilseed rape (KW1), after one season of WW (KW2), and after three successive seasons of WW (KW4). We applied zymography and harvested the plants at the stem elongation stage to observe changes in the activity of β-glucosidase (BGU) and leucine aminopeptidase (LAP), as well as using glucose (GLU) imaging to observe glucose release patterns in the rhizosphere of WW. Several biochemical and microbial properties of the bulk soil and the rhizosphere of the rotational positions were measured. KW2 and KW4 exhibited reduced plant biomass compared to KW1. There was a higher root length density and root mean diameter, as well as a lower specific root length for KW1 compared to KW2 and KW4. KW1 soil had a lower mineral N concentration and microbial biomass carbon (C) and nitrogen (N) than KW2 and KW4, which translated to a lower plant C:N ratio. A greater rhizosphere extent of BGU and LAP across the soil profile was also visible for KW1 compared to KW2 and KW4 using zymography. Lower dissolved organic C and hotspot areas of GLU in the rhizosphere of successive WW might explain shifts in the microbial community composition, possibly leading to a dysbiosis with the soil microbes in the rhizosphere. Soil depth and rotational position explained most of the variance in the soil microbial communities. The relative abundance of *Acidobacteriota*, *Gemmatimonadota*, *Nitrospirota*, and *Chloroflexi* significantly varied among the rotational positions. Our results highlight the effect of WW rotational positions on soil

and plant properties, as well as microbial community dynamics, and provide evidence for the pathways driving biomass decline in successively grown WW.

2.1.2. Introduction

Due to its high economic importance, higher proportions of winter wheat (WW) are added to crop rotations by growing two or more WW crops after a break crop (Kwak & Weller, 2013). The positive effects of adding non-cereal break crops to the rotation have been well established. On a global scale, up to 40 % of the cultivated wheat is grown successively, with only a late summer fallow as a break (Angus et al., 2015; Yin et al., 2022). However, growing WW successively in the same field increases the risk of soil-borne infections, such as the take-all disease caused by *Gaeumannomyces graminis* var *tritici* (Ggt, recently re-named *Gaeumannomyces tritici*), which is the most important soil-borne fungal pathogen of WW, causing root rotting and significant yield losses (Cook, 2003; Kwak & Weller, 2013). Plant yield is negatively affected by the self-succession of wheat in the same field (Sieling & Christen, 2015) due to the increased incidence of Ggt (Smagacz et al., 2016). The take-all disease persists in wet and dry conditions and can cause a yield decline of up to 50 % (Palma-Guerrero et al., 2021). However, it has been recently demonstrated that the yield reduction is evident in a dry year with no obvious Ggt infection (Arnhold et al., 2023a). Adding non-cereal break crops to the rotation, such as oilseed rape, has been shown to enhance the yield of the following WW (Angus et al., 2015; Weiser et al., 2018). Nevertheless, the complex interactions between pre-crop plants and microorganisms in the rhizosphere remain unclear.

WW allocates 20-30 % of the assimilated carbon (C) belowground through the root (Kuzyakov & Domanski, 2000), known as rhizodeposition. Rhizodeposition shapes a dynamic and heterogeneous microenvironment in the rhizosphere, which is estimated to extend between 0.5 mm and 4 mm for different plant species (Kuzyakov & Razavi, 2019) and to be governed by mutualistic, parasitic, and neutral interactions between roots and soil microorganisms (Pausch & Kuzyakov, 2017). Root exudates are a highly influential pool of organic compounds with a low molecular weight, referred to as rhizodeposits, which are secreted into the rhizosphere. They provide a nutrient source for soil microbes, stimulating their activity, but also acting as signals for both mutualists and parasites, with consequences for plant health (Hernández-Calderón et al., 2018; Mohan et al., 2020). The efflux of primary metabolites to the soil due to root exudation creates a plant C source, which fuels microbial growth and nutrient mineralization, affecting plant performance and health. Soil microbes, in turn, influence root exudation by producing extracellular enzymes and polymeric substances (Costa et al., 2018; Korenblum et al., 2020). Both processes require significant amounts of energy and are therefore an investment from both the plant and microbial sides to stimulate their nutrient acquisition as well as proliferation in the soil (Costa et al., 2018; Canarini et al., 2019). For plants, this can be exhibited as the stimulation of root growth. Plants also excrete secondary metabolites (e.g. flavonoids) into their rhizosphere in response to biotic stress and herbivores to induce systemic resistance (ISR; Vlot et al., 2020; Pang et al., 2021). Labile soil organic matter (SOM) and nitrogen (N) mineralization following enhanced enzymatic activity (e.g. protein and cellulose-degrading enzymes) are thus mediated by root exudation and indirectly increase plant nutrient uptake (Meier et al., 2017). These interactions can induce changes in the root system architecture and, in turn, influence nutrient and water uptake (Galloway et al., 2020).

WW shapes its rhizosphere microbial community through rhizodeposition (Wen et al., 2022), enhancing nutrient uptake and plant performance. In particular, oilseed rape and

legumes as preceding crops have been associated with the selection of beneficial microbial taxa, and the suppression of pathogenic microbial taxa, in WW (Vujanovic et al., 2012). This is mainly due to differences in the residue quality that affect its decomposition process (Kerdraon et al., 2019). WW residues mainly contain cellulose and have a higher lignin content than oilseed rape, decelerating their decomposition rate (Pascault et al., 2010). In addition to the soil legacy effect of the residues of the preceding crop, glucose release in the rhizosphere of the growing WW, which is affected by root growth and functioning, can shape microbial communities and, therefore, affect the productivity of WW (Qi et al., 2022). Glucose is the most abundant monosaccharide in the root exudates of WW (Yahya et al., 2021) and is a readily available C source for the soil microbiome. As such, it can fuel both mutualistic, competitive, and pathogenic interactions between soil microorganisms and plants that might affect plant productivity (Philippot et al., 2013). Besides root pathogens that can directly affect plant health, such as Ggt, the prevalence of other detrimental microorganisms in the rhizosphere can compete with roots for available nutrients (Kuzyakov & Xu, 2013). This leads to reduced root growth and exudation, which further increases the C cost for the soil microbial community, creating negative plant–soil feedback (Cortois et al., 2016; Bennett & Klironomos, 2019). Diversified WW rotations with oilseed rape as a preceding crop are known to increase WW yield compared to successively grown WW (Kirkegaard et al., 2008; Ramanauskienė et al., 2018). Most studies show a positive effect on WW pathogen suppression, soil structure, and a high residual N content after oilseed rape harvest (Sieling & Christen, 2015; Weiser et al., 2018; Hilton et al., 2018), although these positive effects have not always been consistently observed (Arnhold et al., 2023b).

Our study aimed to investigate the underlying mechanisms that govern the productivity of WW grown in self-succession as opposed to WW grown after a break crop, such as oilseed rape. Specifically, we focused on the quantification of root growth parameters and the associated biochemical parameters (C and N translocation) as well as on the microbial (bacterial and archaeal) compositions in the rhizosphere (RH) and bulk (BS) soil of WW grown in different rotational positions. We hypothesized that there would be reduced rhizodeposition in self-successional WW, resulting in distinct changes in the microbial community composition and reduced production of hydrolytic enzymes. The reduced rhizodeposition in self-successional WW would be followed by changes in the microbial community composition and a decreased microbial activity, influencing nutrient (especially mineral N) uptake by the plant and plant biomass.

To test these hypotheses, an outdoor rhizotron experiment was conducted, contrasting three rotational positions of WW. We combined zymography and glucose (GLU) imaging on WW at the onset of stem elongation to observe changes in the activity of two important C- and N-acquiring enzymes, β-glucosidase (BGU), and leucine aminopeptidase (LAP) as well as glucose release in its rhizosphere. We also combined soil biochemical and microbiome analyses to assess nutrient and C availability as well as microbial community composition in the rhizosphere of WW and to understand the mechanisms underlying WW performance in those rotational positions.

2.1.3. Methods

2.1.3.1. Experimental design

The soil was collected in September 2021 from the experimental farm Hohenschulen, Faculty of Agricultural and Nutritional Sciences, Kiel University, 54°19′05″N, 9°58′38″E, Germany. The crop rotation trial was established in 1989. It included the following factors: a) rotational position (oilseed rape, first wheat after oilseed rape,

third wheat grown continuously), b) WW varieties (4 levels), and c) N fertilization levels (4 levels). Composite soil samples for rhizobox experiments were taken from oilseed rape (KW1), first wheat plots (KW2), and third wheat plots (KW4) (N = 4 replications) containing the WW cultivar "Nordkap" (SAATEN-UNION GmbH, Isernhagen, Germany) and optimal N fertilization (240 kg N ha^{1}). Soil was collected from the topsoil (0-30 cm) and subsoil (30-50 cm) and sieved to 2 mm. The residues of the preceding crop were not removed from the soil before sampling, and the field was ploughed after sampling. The crop rotations are referred to as rotational positions hereinafter. After the harvest of the different preceding crops, the plant residues remained on the field. The soil is a Cambic Luvisol of sandy loam texture (44 % sand, 35 % silt, and 21 % clay; Sieling et al., 2005). The lack of effervescence in our soil samples after adding 10 % HCl indicated the absence of carbonates, which was confirmed by an average $\delta^{13}C$ value of -26.92 ‰ of soil samples analyzed before the start of the experiment. Table 1 shows some important initial soil biochemical parameters specific to the three rotational positions.

We conducted an outdoor rhizotron experiment (May 4, 2022 to June 30, 2022) using newly designed rhizotrons with a height of 100 cm, a width of 35 cm, and an inner thickness of 2.5 cm (Reichel et al., 2022). Each rhizotron was wrapped in a 50-mm-thick, aluminum-coated Rockwool foil to reduce soil temperature fluctuations inside the rhizotron. Bulk density was adjusted to 1.35 g cm^{-3} and deionized water was added to adjust soil moisture to 70 % water-holding capacity (215 g H_2O soil kg^{-1}) at the onset of the experiment. The plants were subsequently rain-fed throughout the experiment. The rhizotrons were placed on the campus of Forschungszentrum Jülich, Germany. All rhizotrons were consistently inclined at 45° to facilitate root growth along the lower side of the rhizotrons. WW seeds (cultivar "Nordkap") were germinated on petri dishes with sterile filter paper for 24 h in the dark at 23 °C. One germinated seed was subsequently sown into each rhizotron. The plants were not fertilized for the duration of the experiment. The plants were harvested at the stem elongation stage (BBCH 30).

2.1.3.2. Above and belowground plant growth analyses

The aerial plant parts were split at harvest into pseudostems (hereinafter referred to as stems) and leaves. The lower sides of the rhizotrons were then removed, and images of the root system along the soil profile were taken with a camera (DSLR Nikon D3500 Kit AF-P VR 18-55mm, Nikon Corp., Tokyo, Japan). The soil profile was then divided into three layers (0-30 cm, 30-60 cm, and 60-100 cm), and soil samples were taken from two soil compartments, i.e. RH sampled with microspatulas from ≤ 5 mm away from the rhizosphere of primary roots and root-free BS. We pooled and mixed subsamples to form a composite sample, and then split it into several parts to ensure sufficient soil was collected for every planned analysis. For analysis of microbial biomass C and N (C_{mic} and N_{mic}), we sampled root-affected soil from a distance between 5 mm and 20 mm away from the rhizoplane of primary roots. This measure was taken to ensure that a sufficient amount of soil (20 g per sample) was sampled to be used for this specific analysis. The roots were then retrieved after washing off the soil through a 1 mm sieve and stored in 30 % ethanol. They were scanned at 600 dpi (Epson Perfection V800 Photo, Epson, Japan) and analyzed with WinRhizo® software (Regent Instruments Inc., Quebec, Canada) for the following root growth traits: root length, average root diameter (R_{dia}), root surface area, and root volume. The roots were split into seven diameter classes: 0-0.05 mm, 0.05-0.1 mm, 0.1-0.5 mm, 0.5-1 mm, 1-1.5 mm, 1.5-2 mm, and ≥ 2 mm. Using these root growth traits, we computed the root length density (RLD), the specific root length (SRL), and the proportion of root length

for the seven root diameter classes. Estimates of root tissue density (RTD) were made as described in Rose (2017). All plant materials were oven-dried at 60 °C to constant weight (maximum three days) to record their dry weight. Ball-milled (MM 400, Retsch, Germany) above and belowground plant samples, as well as soil samples, were weighed into tin capsules (HEKAtech, Wegberg, Germany) to determine the C and N content using an elemental analyzer coupled to an isotope-ratio mass spectrometer (EA-IRMS, Flash EA 2000, coupled to Delta V Plus; Thermo Fisher Scientific Inc., Waltham, MA, USA).

2.1.3.3. Biochemical soil analyses

At harvest, soil samples were stored at -25 °C before analysis of mineral N, dissolved organic carbon (DOC), and total extractable nitrogen (TN). For the analysis, they were thawed and extracted using 0.01 M $CaCl_2$ (soil-to-solution ratio of 1:4 w:v), vortexed, shaken horizontally for 2 h at 200 rpm, centrifuged for 15 min at 690 × g, and filtrated through 0.45 µm PP-membrane filters (Ø 25 mm; DISSOLUTION ACCESSORIES, ProSense B.V., Munich, Germany). Soil solution was stored overnight at 4 °C before DOC and TN analysis. Ammonium (NH_4^+) was measured by continuous-flow analysis (Flowsys, Alliance Instruments GmbH, Freilassing, Germany). Nitrate (NO_3^-) and sulfate (SO_4^{2-}) were measured by ion chromatography (Metrohm 850 Professional IC Anion – MCS, Metrohm AG, Herisau, Switzerland). Mg was measured by inductively coupled plasma optical emission spectroscopy (iCAP 6500; Thermo Fisher Scientific Inc., Waltham, MA, USA). The pH was measured in the same solution using a glass pH electrode (SenTix® 940, WTW, Xylem Analytics, Weilheim, Germany). DOC and TN were quantified with a total organic C (TOC) analyzer (TOC-V + ASI-V + TNM, Shimadzu, Japan). Using 0.01 M calcium acetate lactate (CAL) instead of $CaCl_2$ and following the same extraction protocol, the plant-available phosphorus (P_{CAL}) and potassium (K_{CAL}) were measured with inductively coupled plasma optical emission spectroscopy (ICP-OES, iCAP 6500; Thermo Fisher Scientific Inc., Waltham, MA, USA).

The chloroform-fumigation extraction (CFE) method was used to estimate microbial biomass C and N. Ten grams of fresh soil stored at 4 °C were weighed in beakers and placed inside a desiccator. They were incubated with ethanol-free chloroform (80 ml) at room temperature for 24 h. Soil samples were then extracted with 0.01 M $CaCl_2$ and analyzed with a TOC analyzer, as described previously. Non-fumigated soil samples were extracted using the same protocol. The difference between extracted C and N from fumigated and non-fumigated soil samples was used to calculate C_{mic} and N_{mic}, using the correction factors 0.45 and 0.4 as the extractable parts of C_{mic} (kEC) and N_{mic} (kEN), respectively (Wu et al., 1990; Joergensen, 1996).

2.1.3.4. Glucose imaging

Soil glucose imaging was applied to all rhizoboxes according to Hoang et al. (2022). Accordingly, phosphate powder (Sigma P7994) was dissolved in distilled water to make a 100 mL buffer solution with a concentration of 0.05 M (pH 7.4). Added to the solution were 1.7 unit/ml glucose oxidase from *Aspergillus niger* (Sigma G7141), 1.5 unit/ml peroxidase from horseradish (Sigma P8125), and 200 µM Ampliflu red (Sigma 90101, Sigma-Aldrich, Darmstadt, Germany) dissolved in 60 µL dimethylsulfoxide. Installed rhizotrons were gently removed to avoid cutting roots. Polyamide membrane filters (pore size 0.45 mm – Tao Yuan, China) were cut into 10×20 cm strips. These membranes were saturated with the prepared reaction mixture solution before being attached to the rooted area. After 20 minutes of incubation (an optimal incubation time

was tested in advance; time may differ between plant species (Hoang et al., 2022)), membranes were quickly removed, placed in a dark container, and immediately transferred to the dark room under UV light with a wavelength of 355 nm. The magenta-colored area on the membrane indicated glucose exudation as hydrogen peroxide generated from a reaction between glucose and glucose oxidase enzymes, which was catalyzed by horseradish peroxidase to convert colorless Ampliflu red into magenta-colored resorufin (Zhou et al., 1997).

2.1.3.5. Zymography

Zymography (BGU and LAP activity) was performed according to the protocol developed by Razavi et al. (2019). A 4-methylumbelliferyl-β-glucoside (MUF-β) and L-leucine-7-amino-4-methylcoumarin hydrochloride (AMC-L) (Sigma Aldrich, Germany) solutions were prepared in MES buffer ($C_6H_{13}NO_4SNa_{0.5}$, Sigma-Aldrich, Darmstadt, Germany) and TRIZMA ($C_4H_{11}NO_3 \cdot HCl$, $C_4H_{11}NO_3$, Sigma-Aldrich, Darmstadt, Germany), respectively, to make a fluorescent solution of 12 mM. The same polyamide membrane filters (Tao Yuan, China) with a pore size of 0.45 mm were selected to reduce enzyme diffusion through the pores (Razavi et al., 2016). The membranes were soaked in the fluorescent solution and then directly applied to the root-exposed side of the rhizoboxes before being subsequently covered with aluminum foil to avoid exposure to light and drying out. After one hour of incubation, the membranes were quickly removed, cleaned with a soft brush, and exposed to UV light with an excitation wavelength of 355 nm in a dark room.

All images were taken with a digital camera (Canon EOS 6D, Canon Inc.) and a Canon lens EF 24–105 mm 1: 4L IS II USM with the setting of aperture and shutter speed at f/5.6 and 1/10 sec (for glucose imaging) and 1/8 sec (for zymography), respectively. The calibration lines for glucose imaging were prepared by soaking a 4 cm^2 membrane in a glucose solution at respective concentrations of 0 mM, 2 mM, 4 mM, 6 mM, 8 mM, and 10 mM. The membranes were soaked in the respective reaction mixture solution in the same way as mentioned above. Fluorescent signals of glucose release on an area basis were calculated based on the volume of substrate solution taken up by a fixed membrane size.

Zymography processing was calibrated by soaking individual 4 cm^2 membranes in MUF solution at respective concentrations of 0 mM, 0.2 mM, 0.5 mM, 1 mM, 2 mM, 4 mM, 6 mM, 8 mM, and 10 mM. These membranes were exposed to UV light in the same way as the samples. Calibrated values were used to quantify the color intensity and to link BGU activity to the grey value. Fluorescent signals of MUF on an area basis were calculated based on the volume of substrate solution taken up by a fixed membrane size.

The image processing and analysis were conducted using the software package ImageJ. The hotspot percentage was calculated based on the pixel size proportion of the hot area to the entire image. In other words, hotspot areas were determined to have the 25 % higher pixel-wise enzyme activities after subtracting background values at zero concentration of the calibration line from all zymograms and glucose release images (Ma et al., 2018). Meanwhile, the rhizosphere extent of each root was calculated from the root surface. The rhizosphere extent was determined for root segments for the following parameters: 1) glucose release and 2) BGU and leucine aminopeptidase activity (soil zymograms). To measure the rhizosphere extent, five horizontal transects (angle to the root ~90°) were randomly drawn across five randomly selected roots for the glucose release image and BGU zymogram using ImageJ. In total, this yielded 25

lines per image as pseudo-replicates, and their mean was used for each rhizobox (as a true replicate) (Bilyera et al., 2021).

2.1.3.6. Enzyme kinetics and turnover time

The kinetics of hydrolytic enzymes involved in C and N cycles were measured by fluorimetric microplate assays of 4-methylumbelliferone (MUF) and 7-amino-4-methyl coumarin (AMC) (Dorodnikov et al., 2009). A fluorogenic substrate based on MUF and one type based on AMC were used to assess enzymatic activities: 4-methylumbelliferyl-β-D-glucoside to detect BGU activity; L-Leucine-7-amino-4-methylcoumarin to detect LAP activity. All substrates and chemicals were purchased from Sigma-Aldrich (Darmstadt, Germany).

According to German et al. (2011), 1.0 g of soil was suspended in 50 mL of distilled water, of which 50 µL aliquots were pipetted into labeled wells of a 96-well microplate (Thermo Fisher, Denmark). A 50 µL buffer (MES/Trizma) and 100 µL respective substrate solution were then added to each well. The activity of enzymes was measured at three time points: 30 min, 60 min, and 120 min using CLARIOstar Plus (BMG LABTECH, Germany) at an excitation wavelength of 355 nm and an emission wavelength of 460 nm. We determined enzyme activities over a range of substrate concentrations from low to high (0 µmol g^{-1} soil, 20 µmol g^{-1} soil, 40 µmol g^{-1} soil, 60 µmol g^{-1} soil, 80 µmol g^{-1} soil, 100 µmol g^{-1} soil, 200 µmol g^{-1} soil, and 400 µmol g^{-1} soil) to ensure the appropriate saturating concentration.

Enzyme activities (V_{max}) were denoted as released MUF/AMC in nmol per g dry soil per hour (nmol MUF/AMC g^{-1} soil h^{-1}) (Awad et al., 2012), and the affinity constant for each enzyme (K_m) was expressed in µmol substrate per g dry soil (µmol g^{-1} soil). Simultaneously, MUF/AMC concentrations of 0 nM, 10 nM, 20 nM, 30 nM, 40 nM, 50 nM, 100 nM, and 200 nM were prepared to calibrate the measurement. The Michaelis-Menten equation was used to determine the parameters of the activity of the enzyme (V):

$$V = \frac{V_{max}[S]}{K_m[S]} \quad (1)$$

where V_{max} is the maximum enzyme activity (a function of enzyme concentration), S is the substrate concentration, and K_m is the substrate concentration at half-maximal enzyme activity. Both V_{max} and K_m parameters were approximated by the Michaelis–Menten equation (1) with the non-linear regression routine of SigmaPlot (v. 12.3). Catalytic efficiency was calculated as the V_{max}-to-K_m ratio (Panikov et al., 1992). The substrate turnover rate was calculated by equation (2), where T_t is the turnover time (hours) (Zhang et al., 2020).

$$T_t = \frac{K_m \times [S]}{V_{max} + [S]} \quad (2)$$

2.1.3.7. Soil DNA extraction and 16S rRNA gene amplicon sequencing

The distinct microbial communities (bacteria and archaea) were accessed using a metabarcoding approach (16S rRNA amplicon sequencing). Total DNA was extracted from 0.5 g of BS and RH soil samples using the FastDNA SpinKit for Soil (MP Biomedicals Fast Prep-24 5G) according to the manufacturer's instructions. This included weighing the soil into the 2 mL bead-beating tubes containing the lysis matrix. After adding 978 µL sodium phosphate buffer and 122 µL of the MT buffer provided by the kit, samples were vortexed and adjusted for bead beating using the FastPrep-24 (2 x 30 s with a 5-min rest, speed 4). Samples were kept on ice until 250 µL of PPS (protein precipitation solution) were added. Extraction was performed according to the manufacturer's protocol, and DNA was eluted in 100 µL of DES water.

The quantity and integrity of the DNA were checked by Nanodrop and on 0.8% agarose gels, respectively. The libraries from the 16S rRNA gene amplicon using Uni341F and Uni806R primers and Illumina adaptors (Illumina, San Diego, USA) were performed at Novogene (UK) using Illumina MiSeq v2 (2 × 250 bp) chemistry according to the manufacturer's instructions (Illumina, San Diego, USA). Unassembled raw amplicon data were deposited in the National Center for Biotechnology Information (NCBI) Sequence Read Archive (SRA) under BioProject PRJNA942109.

2.1.3.8. Amplicon sequence analyses

The soil sample sequences were analyzed and categorized using the Divisive Amplicon Denoising Algorithm (DADA2 v.1.12.1 pipeline; Callahan et al., 2016) in R (R Core Team, 2019). The "FilterAndTrimmed" function was utilized for the quality trimming and filtering processes. Reads of less than 100 bp were discarded, and two expected errors were permitted for each read. The subsequent steps involved error inference, denoising, and chimera removal. Following quality filtering, denoising, and chimera removal, the 16S rRNA gene amplicon depths of 48 samples produced 1,558,139 high-quality 16S rRNA gene reads, or 32,461 per sample. The amplicon sequencing variations (ASVs) were assigned taxonomically using the SILVA database version 138 (Quast et al., 2013) and then imported into the phyloseq tool in R (McMurdie & Holmes, 2013). Unassigned ASVs at the phylum level and any remaining ASVs identified as chloroplasts, mitochondria, or eukaryotes were omitted from the studies. Amplicon sequencing yielded 46,725 unique ASVs.

2.1.3.9. Statistical analysis

General linear models (GLMs) were used to test the difference between the means of the response variables at a significance threshold of $\alpha = 0.05$. The factors in the GLM were rotational position (KW1, KW2, and KW4), soil compartment (BS, RH), and soil depth (0-30 cm, 30-60 cm, and 60-100 cm). The Shapiro–Wilk and Levene tests as well as a visual inspection of QQ plots were used to test for normality of the residual distribution and homogeneity of variance, respectively. Pairwise comparisons were made for soil chemical and enzymatic data using Bonferroni correction to identify differences between the response variables. Data transformation was performed when the assumptions of GLM failed. Yeo–Johnson (Yeo & Johnson, 2000), Box–Cox (Box-Cox, 1964), and log transformations were used. The transformation used for a certain variable is mentioned in the respective table. Correlation analysis was performed using Pearson's correlation for the response variable and for every level of the rotational position of WW (KW1, KW2, and KW4). Since the soil sampling for microbiome data was performed only for soil depths of 0-30 cm and 30-60 cm, we calculated correlation coefficients for these two depths only, excluding the 60-100 cm layer from our analysis. Where applicable, we also show the variables related to BS and RH. The abovementioned statistical analyses were performed with IBM SPSS Statistics for Windows, version 23 (IBM Corp., Armonk, N.Y., USA). Graphs were generated with the *ggplot2* package in R (v4.2.1; R Core Team 2022).

Relative abundances, alpha and beta diversities, and statistical tests were determined in R using specialized R package functions. Rarefaction analysis within the vegan R package examined the sequencing depth (Oksanen et al., 2020). The rarefaction curves tended to reach a plateau, indicating that the sequencing method supplied sufficient sequences to cover most of the sample diversity. Microbial sequences were rarefied for the lowest number of sequences identified among all samples, generating a dataset with 22,158 sequences per sample. The alpha diversity indices were computed for each

rarefied sample using the *phyloseq* (McMurdie & Holmes, 2013) and *microbiome* (Lahti et al., 2017) R packages. Using 10,000 permutations, Kruskal–Wallis tests were employed to evaluate for statistically significant changes in alpha diversity. The microbial composition of samples was assessed after transformation to relative abundance. The differences in phyla and taxa across samples were visualized using the *phyloseq* package (McMurdie & Holmes, 2013). Permutational multivariate analysis of variance (PERMANOVA) was performed to identify significant differences in the WW microbial community composition. The beta diversity of the microbial communities was visualized by a principal coordinate analysis (PCoA) using the Bray–Curtis distance.

2.1.4. Results

2.1.4.1. Effects of rotational position, soil compartment, and soil depth on winter wheat growth

The preceding crop history had a pronounced effect on the biomass of the following WW. KW2 and KW4 plants had 43 % and 45 % reduced dry weight, respectively, compared to KW1 (Table S2.1.1; Fig. 2.1.1a). The decline in wheat dry weight was attributed to a reduction in root and stem biomass for KW2, and root, stem, and leaf biomass for KW4 when compared to KW1 (Fig. 2.1.1a). Higher shoot N concentration resulted in a lower C:N ratio for KW1 compared to KW2 and KW4 (Table S1; Fig. 2.1.1b). In all rotational positions, there was a similar C:N ratio increase within roots, stems, and leaves (Table S2.1.2).

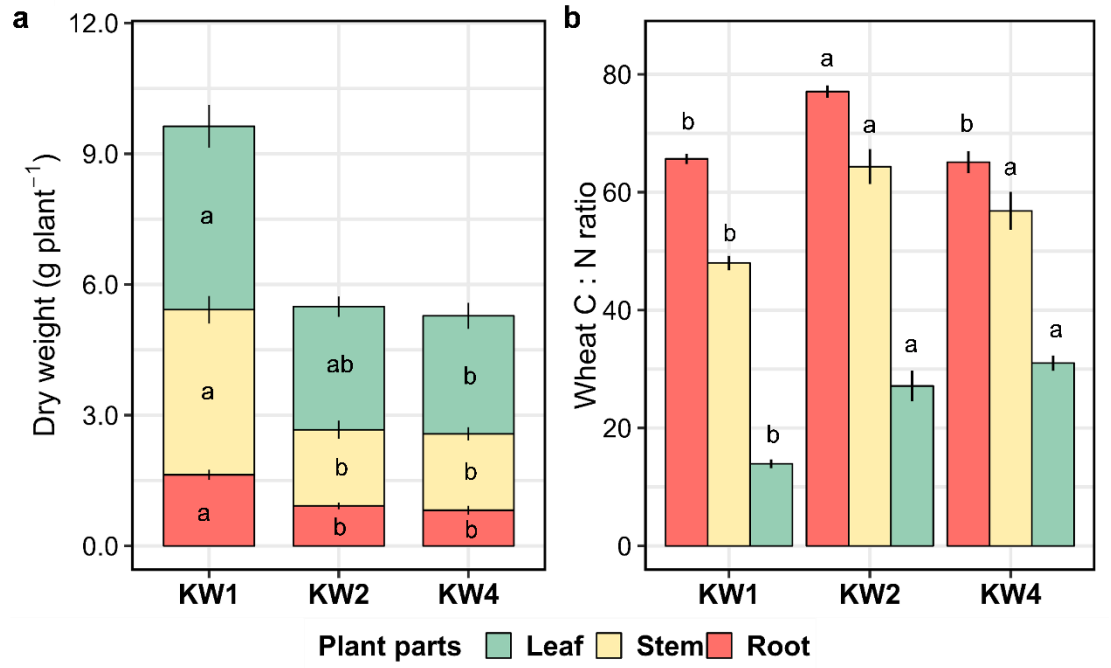

Figure 2.1.1. Effect of the rotational positions on root, stem, leaf dry weight (a) and C:N ratio (b) of the following winter wheat at onset of stem elongation (BBCH 30). KW1 = first wheat, KW2 = second wheat, and KW4 = fourth wheat after oilseed rape in soil from the experimental farm Hohenschulen in Kiel, Germany. Within each plant part, different lowercase letters denote significant differences between rotational positions at $p \leq 0.05$ according to ANOVA with Bonferroni correction for multiple comparisons.

There was a strong response of root growth traits to WW rotational position with an overall reduction in RLD of 29 % and 31 % for KW2 and KW4, respectively, mainly in the upper 30 cm of the soil (Table S2; Fig. 2.1.2a). However, even at a greater depth (60-100 cm), KW1 had the highest difference in RLD compared with KW4. At this

depth, KW2 increased its RLD greater than KW4, which had the lowest values of all three rotational positions. Similarly, KW1 had the highest RTD of all rotational positions, with 58 % and 48 % higher RTD values than KW2 and KW4, respectively (Table S2.1.2; Fig. 2.1.2b). These differences were apparent in both the topsoil and the subsoil. Overall, KW1 had thicker roots with an R_{dia} of 0.28 mm compared to 0.25 mm and 0.24 mm for KW2 and KW4, respectively, a trend that was observed throughout the soil profile (Table S2.1.2, Fig. 2.1.2c). The R_{dia} of all three rotational positions increased at greater soil depth (Table S2.1.2). Finally, KW2 and KW4 increased their SRL by 28 % and 33 % compared to KW1, with significant differences along the complete soil profile (Table S2.1.2, Fig. 2.1.2d).

2.1.4.2. Effects of rotational position, soil compartment, and soil depth on biochemical soil properties

More ammonium (NH_4^+) and nitrate (NO_3^-) were found in the RH compared to BS and in the 0-30 cm soil layer compared to subsoil layers (Table S2.1.3). The rotational position of WW strongly affected mineral N, with a 42 % and 48 % lower NH_4^+ concentration in KW1 overall compared to KW2 and KW4, respectively (Fig. 2.1.3a). In particular, in the uppermost soil depth of KW1, there was much less NH_4^+ than in the same depth of KW2 (-54 %) and KW4 (-58 %). In addition, a similarly lower NO_3^- content was found in KW1 (-49 % and -36 % compared to KW2 and KW4, Fig. 2.1.3b). Microbial biomass C (C_{mic}) and N (N_{mic}) were also highly impacted by the rotational position, as shown in Fig. 4. C_{mic} was lower by 37 % and 43 % in KW1 compared to KW2 and KW4, respectively (Fig. 2.1.4a). N_{mic} values of KW1 were 50 % and 57 % lower than those of KW2 and KW4 (Fig. 2.1.4b). Most C_{mic} and N_{mic} were found in the topsoil (Table S2.1.2).

The rotational position also had a major influence on DOC levels (Table S2.1.3). KW1 soil had 68 % and 150 % higher DOC concentrations than KW2 and KW4, respectively (Fig. S2.1.2). A significant main effect of soil compartment was shown, with a 74 % higher DOC content in the RH compared to BS. Interestingly, the DOC level in the RH of KW1 at both subsoil depths (30-60 and 60-100 cm) was 1.7 and 4.1 times higher than KW2 and KW4, respectively (Fig. S2.1.2). Similar DOC concentrations were observed in the BS in the rotational position and at all three soil depths.

2.1.4.3. Effects of rotational position, soil compartment, and soil depth on extracellular enzymes activities

The maximum reaction rate (V_{max}) of BGU was higher in KW2 compared to KW4 (by 27 %). No differences were observed between BS and RH, while higher values were observed in the first 30 cm of the soil profile (Table S2.1.4). The interaction between rotational position, soil compartment, and soil depth revealed a 91 % and 169 % higher BGU V_{max} in the RH of KW1 at 30-60 cm and 60-100 cm of the subsoil, respectively, compared to KW4. In contrast, KW2 and KW4 had a higher BGU V_{max} in the topsoil compared to KW1 (by 83 % and 89 %, respectively; Fig. S2.1.5a). The response of the BGU substrate affinity (K_m) to the rotational position revealed a 64 % and 68 % reduction in affinity for KW2 and KW4 compared to KW1, which was evident in all soil layers (Fig. S2.1.5b). A higher catalytic efficiency (K_a) was observed in KW1 compared to KW2 and KW4, while a lower substrate turnover time (Tt) was seen in KW1 and KW2 compared to KW4 (Table S2.1.4). The V_{max} of the leucine aminopeptidase (LAP) of KW1 equaled that of KW2 and was 32 % higher than that of KW4 (Fig. S2.1.5c). It was also increased in BS compared to RH, with no obvious differences in its response between soil depths. Higher values of V_{max} were observed in

the BS of KW1 in the subsoil layers compared to KW2 and KW4. Soil compartment had a significant effect, with LAP affinity increasing in the RH compared to BS (Table S2.1.4). LAP K_m was also affected by the rotational position, as shown in Fig. S5d. KW2 had a much higher LAP affinity in the RH than BS, while it did not fluctuate significantly between the two soil compartments for KW1 and KW4. LAP K_m was higher in KW1 compared to KW4 in the BS (58 %) and RH (76 %) (Fig. S2.1.5d). Finally, both K_a and Tt were increased in KW4 compared to KW1 and KW2 (Table S2.1.4).

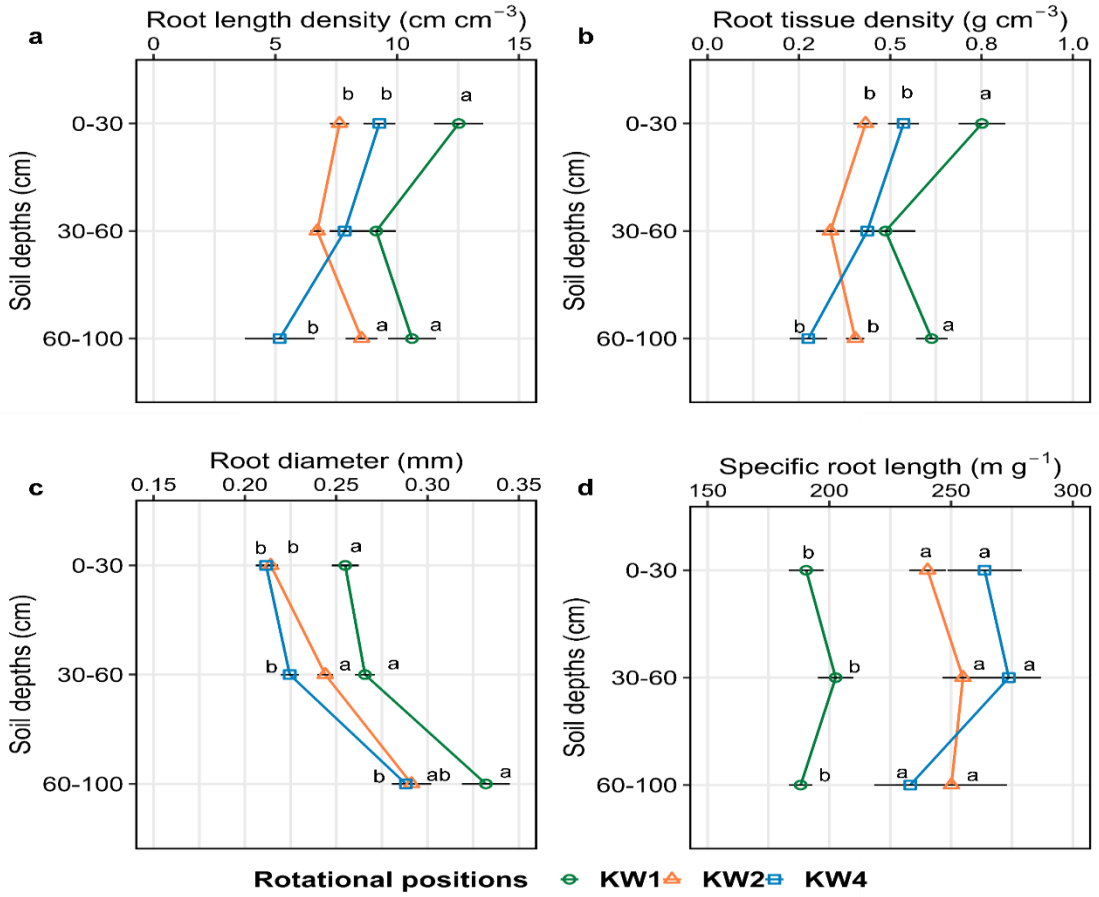

Figure 2.1.2. Effect of the rotational positions on root length density (a), root tissue density (b), average root diameter (c) and specific root length (d) of the following winter wheat at the onset of stem elongation (BBCH 30) at soil depths 0-30 cm, 30-60 cm and 60-100 cm). KW1 = first wheat, KW2 = second wheat, and KW4 = fourth wheat after oilseed rape in soil from the experimental farm Hohenschulen in Kiel, Germany. Within each soil depth, different lowercase letters denote significant differences between rotational positions at $p \leq 0.05$ according to ANOVA with Bonferroni correction for multiple comparisons. No letters indicate non-significant differences.

Zymography revealed significant differences between WW rotations (Table S2.1.5), with the BGU rhizosphere extent of KW1 averaging 5.3 mm compared with 2.5 mm for KW2 and KW4. This response was mainly driven by major differences in the lowest soil depth, where the rhizosphere extent for BGU was 9 mm compared to 4 mm for KW2 and 3 mm for KW4 (Fig. 2.1.5a). In a similar manner, the rhizosphere extent for LAP was, on average, 0.36 mm for KW1, which was significantly higher than for KW4 (0.16 mm, Fig. 2.1.5b). We found a similar, though insignificant, trend of a reduced LAP rhizosphere extent for KW2 (0.19 mm). In terms of BGU and LAP activity, there were no pronounced differences among the fixed factors of the experiment (Fig. 2.1.5c, d). The same was true for the BGU hotspot area, with a decreasing hotspot area percentage at greater soil depths that was nonetheless insignificant (Fig. 2.1.5e). Lastly,

the LAP hotspot area for KW1 was 96 % higher than KW2 in the deep subsoil of 60-100 cm (Fig. 2.1.5f).

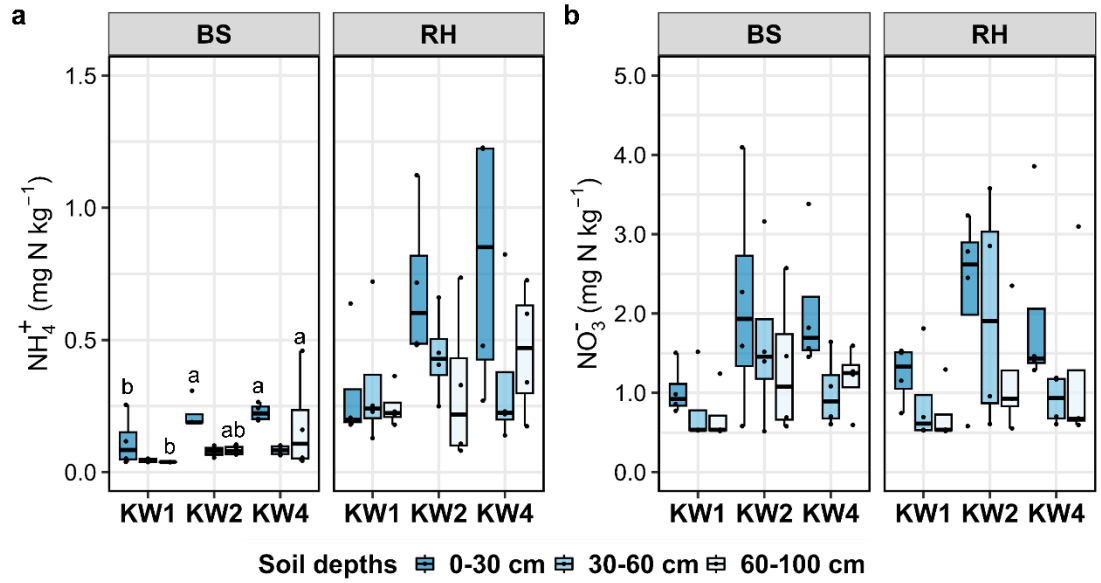

Figure 2.1.3. Effect of the rotational positions on soil NH_4^+-N (a) and NO_3^--N (b) of the following winter wheat at onset of stem elongation (BBCH 30) at soil depths 0-30 cm, 30-60 cm and 60-100 cm and two soil compartments bulk soil (BS) and rhizosphere soil (RH). KW1 = first wheat, KW2 = second wheat, and KW4 = fourth wheat after oilseed rape in soil from the experimental farm Hohenschulen in Kiel, Germany. Within each soil depth and soil compartment, different lowercase letters denote significant differences between rotational positions at $p \leq 0.05$ according to ANOVA with Bonferroni correction for multiple comparisons. No letters indicate non-significant differences.

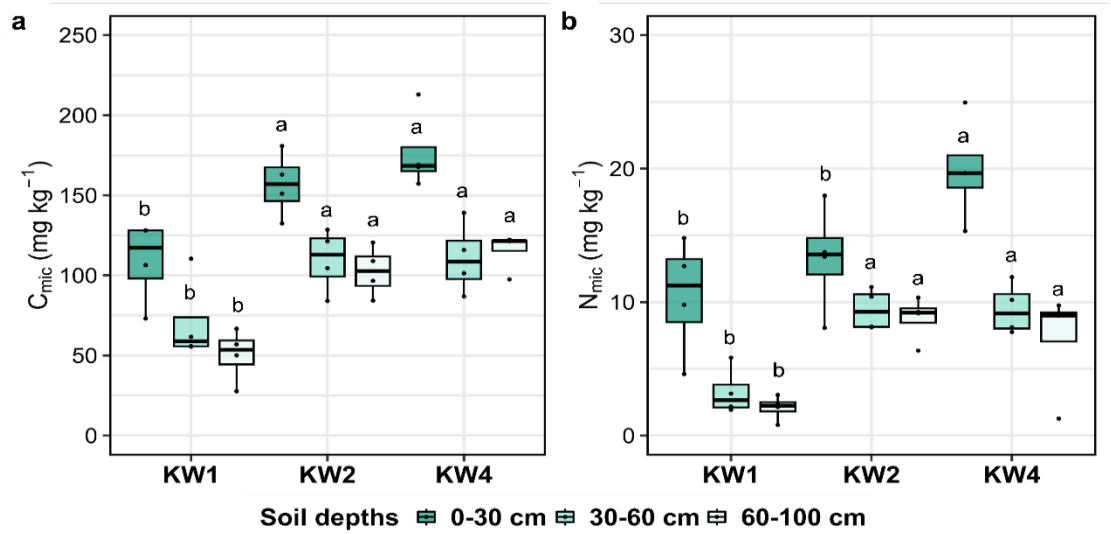

Figure 2.1.4. Effect of the rotational positions on microbial biomass carbon (C_{mic}, a) and microbial biomass nitrogen (N_{mic}, b) of the following winter wheat at onset of stem elongation (BBCH 30) at soil depths 0-30 cm, 30-60 cm and 60-100 cm. KW1 = first wheat, KW2 = second wheat, and KW4= fourth wheat after oilseed rape in soil from the experimental farm Hohenschulen in Kiel, Germany. Within each soil depth, different lowercase letters denote significant differences between rotational positions at $p \leq 0.05$ according to ANOVA with Bonferroni correction for multiple comparisons. No letters indicate non-significant differences.

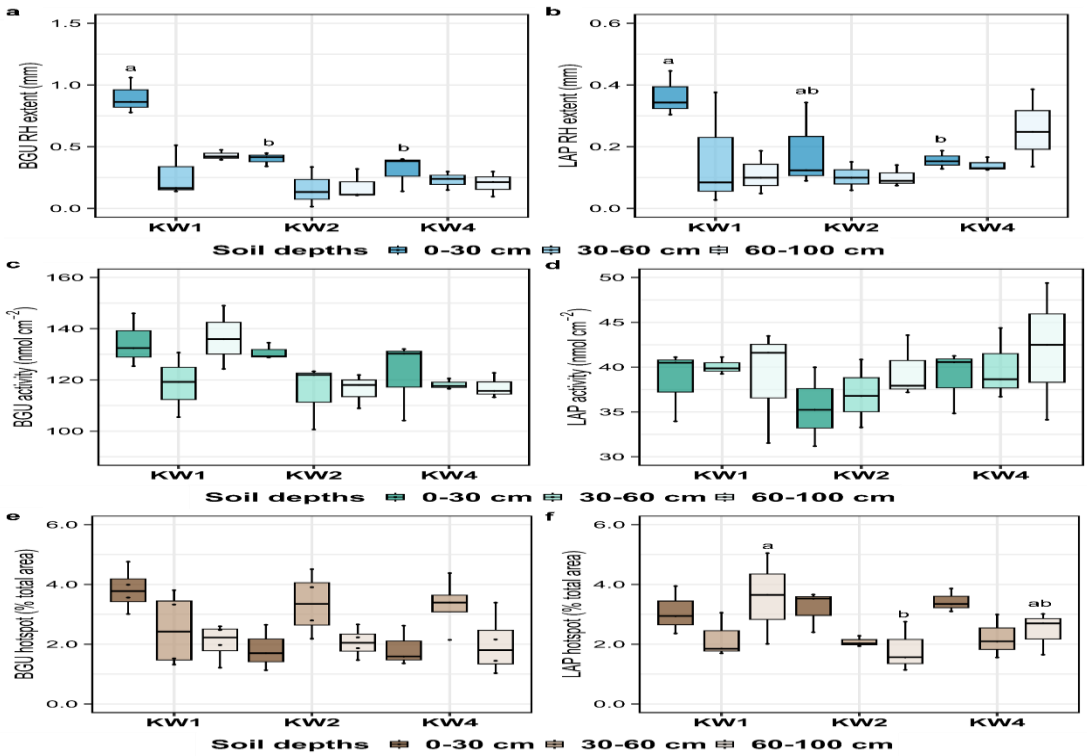

Figure 2.1.5. Effect of the rotational positions on rhizosphere extent (RH), activity and hotspot percentage of *β*-glucosidase (BGU) (a, c, e) and leucine aminopeptidase (LAP) (b, d, f) of the following winter wheat at onset of stem elongation (BBCH 30) at soil depths 0-30 cm, 30-60 cm and 60-100 cm. KW1 = first wheat, KW2 = second wheat, and KW4 = fourth wheat after oilseed rape in soil from the experimental farm Hohenschulen in Kiel, Germany. Within each soil depth and soil compartment, different lowercase letters denote significant differences between rotational positions at $p \leq 0.05$ according to ANOVA with Bonferroni correction for multiple comparisons. No letters indicate non-significant differences.

Glucose (GLU) imaging revealed significant differences between the GLU rhizosphere extent and hotspot area between the three soil layers (Table S2.1.5). This trend followed that of the root growth data. We also observed a decreasing rhizosphere extent for GLU in successively grown WW that was, however, insignificant (Fig. 2.1.6a). The same was found for GLU release per surface area (Fig. 2.1.6b), with a lower relative amount of GLU release in KW2 and KW4, although there was no significant main effect of the rotational position. However, a significant decline was recorded in the GLU hotspot area in the 60-100 cm layer of the soil profile in KW2 (-53 %) compared to KW1 (Fig. 2.1.6c).

2.1.4.4. Effects of rotational position, soil compartment, and soil depth on microbial community structure and composition

A significant difference in species richness between KW1 and KW4 was observed in the BS compartment and in the uppermost 30 cm of soil, where KW4 presented a higher number of species than KW1 (Fig. S2.1.6a). Interestingly, there was no influence on the microbial community diversity and species evenness distribution expressed as the Pielou index and Shannon index, respectively (Fig. S2.1.7a, b). The soil depth had a main effect on the beta diversity parameters (Fig. S2.1.6b). According to the PERMANOVA results, the rotational position explained 10.5 % of the variation ($F = 3.51$; $p < 0.001$) in the microbial community, while soil depth explained 12.3 % of the variation observed ($F = 5.97$; $p < 0.001$).

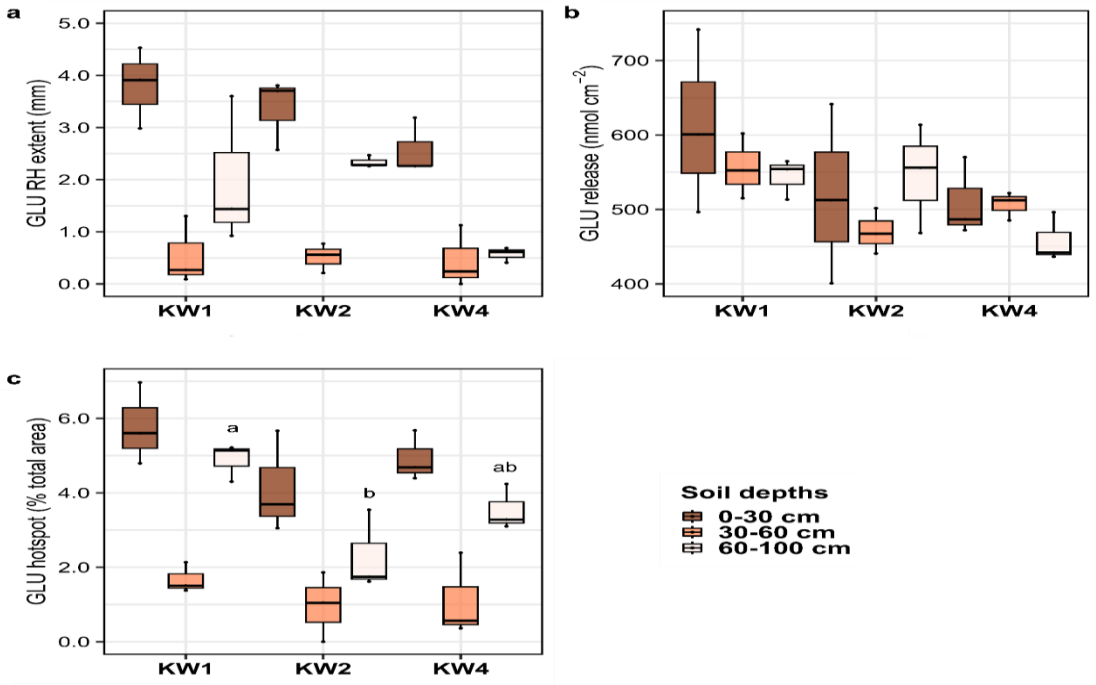

Figure 2.1.6. Effect of the rotational positions on glucose rhizosphere extent (RH, a), release (b) and hotspot percentage (c) of the following winter wheat at onset of stem elongation (BBCH 30) at soil depths 0-30 cm, 30-60 cm and 60-100 cm. KW1 = first wheat, KW2 = second wheat, and KW4 = fourth wheat after oilseed rape in soil from the experimental farm Hohenschulen in Kiel, Germany. Within each soil depth and soil compartment, different lowercase letters denote significant differences between rotational positions at $p \leq 0.05$ according to ANOVA with Bonferroni correction for multiple comparisons. No letters indicate non-significant differences.

The main components of the microbial community composition at the phylum level were *Actinobacteriota*, *Proteobacteria*, *Chloroflexi*, *Gemmatimonadota*, and *Crenarchaeota*. The relative abundance of several taxa from *Acidobacteriota*, *Gemmatimonadota*, *Nitrospirota*, and *Chloroflexi* was significantly affected by the rotational position in the BS and RH soils and at different soil depths. While in the BS of the plants, the relative abundance of *Acidobacteriota* was not significantly different, we recorded a significantly higher relative abundance of *Acidobacteriota* in the RH of the topsoil and subsoil of KW1 compared to both KW2 and KW4 (Fig. 2.1.7a). A decreasing relative abundance of *Gemmatimonadota* in KW4 compared to KW1 was found in both soil compartments, while the difference between KW1 and KW2 remained insignificant (Fig. 2.1.7b). With regard to *Nitrospirota*, KW1 and KW2 had similar relative abundances in both BS and the RH (Fig. 2.1.7c). In the RH, the relative abundance of *Nitrospirota* was significantly lower in both the topsoil and subsoil of KW2 compared to KW4. Finally, in KW1 and KW2, there was a much lower relative abundance of *Chloroflexi* compared to KW4, and this difference was consistently found in BS and RH soil (Fig. 2.1.7d).

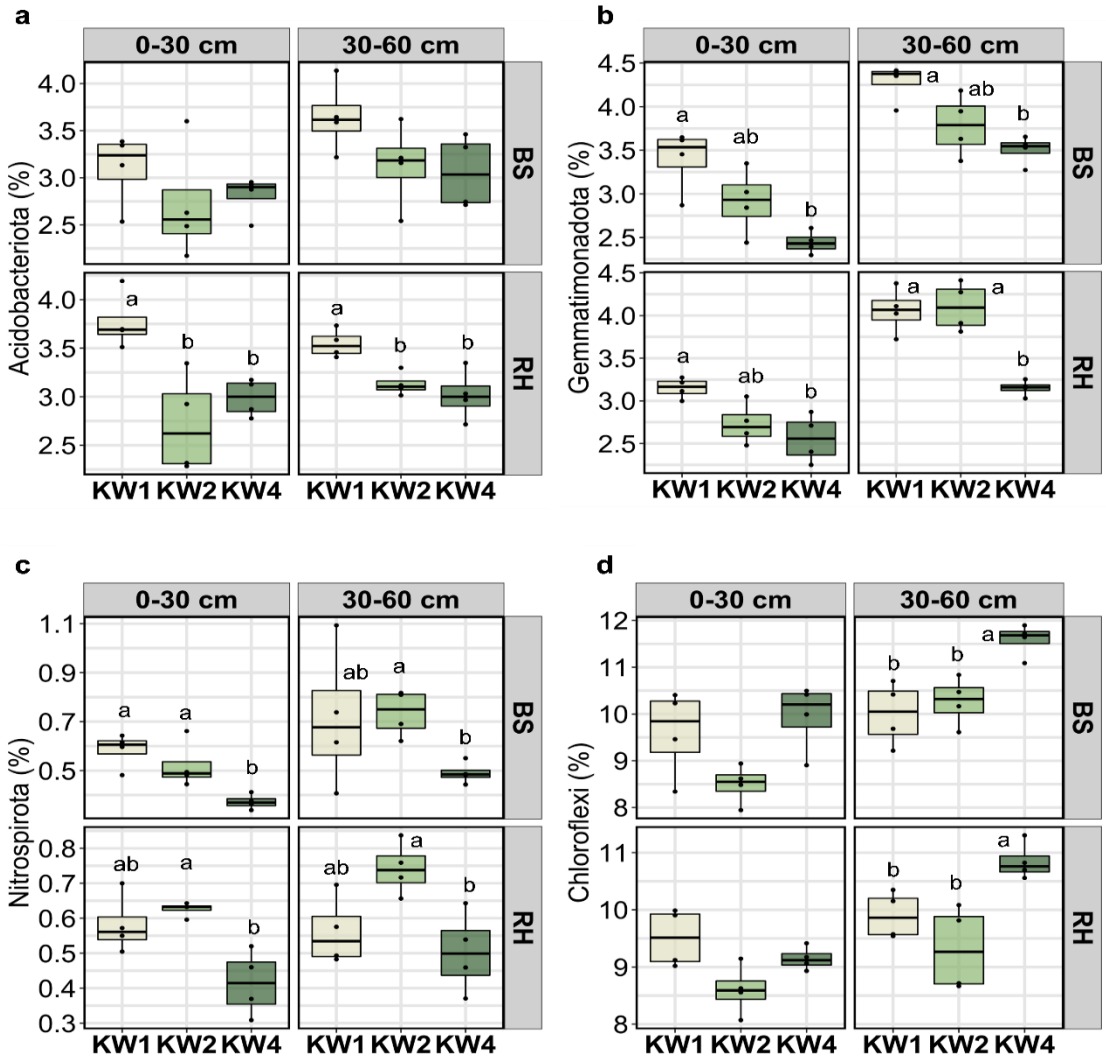

Figure 2.1.7. Effect of the rotational positions on the relative abundance of (a) *Acidobacteriota*, (b) *Gemmatimonadota*, (c) *Nitrospirota* and (d) *Chloroflexi* at soil depths 0-30 cm and 30-60 cm, in the two soil compartments bulk soil (BS) and rhizosphere (RH). KW1 = first wheat, KW2 = second wheat, and KW4 = fourth wheat after oilseed rape in field soil from the experimental farm Hohenschulen in Kiel, Germany. Within each soil depth and soil compartment, different lowercase letters denote significant differences between rotational positions at $p \leq 0.05$ according to ANOVA with Bonferroni correction for multiple comparisons. No letters indicate non-significant differences.

In order to examine the relationship between the measured parameters in each rotational position and their influence on the different bacterial phyla, we conducted correlation analyses (Tables S2.1.9-S2.1.11). At 0-30 cm, the root dry weight of KW1 was negatively correlated with the relative abundance of *Gemmatimonadota* in the rhizosphere compartment. At 30-60 cm, it was positively correlated with the soil NO_3^- content in the BS, K_{CAL} in the RH, and the relative abundance of *Nitrospirota* in the RH, but negatively correlated with *Chloroflexi* in the RH and *Acidobacteriota* in the BS (Table S2.1.9). For KW4, the root dry weight was negatively correlated with the relative abundance of *Chloroflexi* in the RH and *Nitrospirota* in the RH (Table S2.1.11). For KW1 and at 30-60 cm, DOC was positively correlated with P_{CAL} in the RH. DOC was also positively correlated with both the BGU and LAP reaction rates in the BS. Finally, DOC positively correlated with the relative abundance of *Nitrospirota* in the RH (Table S2.1.9). For KW2 and at 0-30 cm, DOC was negatively correlated with K_{CAL}

in the BS. In the RH, there was a negative correlation between DOC and C_{mic} and a positive correlation between DOC and the relative abundance of *Acidobacteriota*. As for KW4, there was a negative correlation between DOC in the RH and BGU rhizosphere extent (Table S2.1.11). C_{mic} exhibited a positive correlation with the LAP hotspot at 0-30 cm of KW1, while it was negatively correlated with *Gemmatimonadota* in the BS. At 30-60 cm, it was positively correlated with both NO_3^- of the RH and N_{mic} (Table S2.1.9). C_{mic} of KW2 was negatively correlated with both *Chloroflexi* and *Acidobacteriota* in the RH at 0-30 cm. In the subsoil, it was negatively correlated with DOC in the RH (Table S2.1.10). Finally, in the topsoil of KW4, C_{mic} was positively correlated with both NH_4^+ and NO_3^- in the RH and BS, respectively (Table S2.1.11).

2.1.5. Discussion

2.1.5.1. Root plastic responses drive nutrient supply and plant biomass accumulation in winter wheat rotations

Successively grown WW appeared to prioritize soil exploration, shaping a thinner and less dense root system, as indicated by its higher SRL, lower R_{dia}, and RTD. It should be noted that the overall RLD and SRL followed a similar trend for each measured diameter class in the rotational positions. In a field trial with silty loam soil, Arnhold et al. (2023b) found no differences in RLD between the first WW after oilseed rape, the second WW after oilseed rape, and WW monoculture at the end of tillering. However, when they measured RLD during late flowering in a year with high summer precipitation, the wheat after oilseed rape had a significantly higher RLD than the successively grown WW in the topsoil. In the sandy loam soil of our study, we documented an early reduction in RLD in successive WW rotations during the relatively dry period of the trial (Fig. S2.1.1). Therefore, the soil type and environmental conditions are strong determinants of the effect of the WW rotational position on its plant biomass accumulation.

Differences in root growth patterns might explain the more efficient N, P, and K uptake in KW1, leading to lower mineral N, P, and K concentrations in the soil of KW1 at BBCH 30 and, therefore, an increased N, P, and K supply to the plants, which is reflected in the lower C:N ratios of KW1 compared to KW2 and KW4 (Fig. 2.1.1a, b; Table S2.1.6). A higher N uptake by maize plants was previously found in diversified crop rotations (maize, soybean, three-year wheat rotation with red clover and rye cover crops) and was associated with a higher C and N enzymatic activity of soil microbes (Bowles et al., 2022). In our study, there was a positive correlation between the root dry weight and the K_{CAL} in the topsoil of KW1, but this was not the case for KW2 and KW4. In the topsoil, the SRL of KW1 was negatively correlated with NH_4^+ in the RH and K_{CAL} (Table S2.1.9). The SRL of plants tends to increase under biotic and abiotic stresses (Kramer-Walter et al., 2016; Kaloterakis et al., 2021; Spitzer et al., 2021), while RLD and R_{dia} are reduced (Kramer-Walter et al., 2016; Lopez et al., 2023). Accordingly, the SRL of KW2 was negatively correlated with RLD and the root dry weight (Table S2.1.10). Kelly et al. (2022) found a higher SRL in WW landraces grown under conditions of low nutrient availability, while landraces with a higher proportion of coarse roots were associated with higher extractable C pools in the RH. The higher NH_4^+ was positively correlated with the R_{dia} of KW1, especially in the subsoil (Table S2.1.9). KW1 is also associated with high residual mineral N in the soil after harvest (10-20 kg N ha^{-1}) that is readily available for uptake by KW1 (Weiser et al., 2018). Our data suggest that this available N stimulated the early growth of KW1, enabling the vigorous establishment and exploitation of the rhizobox soil volume. Due to their initial

root growth reduction, KW2 and KW4 did not fully utilize the N reservoir of the soil, resulting in higher mineral N in the soil at the end of the experiment.

2.1.5.2. High microbial biomass and low labile carbon in the soil of successive winter wheat rotations induce nitrogen immobilization

In a recent field experiment, Yang et al. (2022) found that C_{mic} and N_{mic} increased in parallel with WW dry matter accumulation throughout the growth period. In our experiment, the highest plant biomass-yielding rotational position, KW1, had much lower C_{mic} and N_{mic} values at all three soil depths, confirming the results of the aforementioned study. Typically, higher root biomass is associated with increased microbial biomass (Lange et al., 2015). However, changes in root biomass may be more accurately linked to changes in microbial diversity, thus explaining the trends observed (Fig. S2.1.6) in this experiment (Ren et al., 2017). Hansen et al. (2019) reported a similar decline in C_{mic} when oilseed rape was introduced into successive wheat monocultures and attributed this effect to the biocidal properties of its secondary metabolite, isothiocyanate. The initial soil biochemical properties of the three rotational positions (Table 1) showed a higher C_{mic} in the soil of KW4 and a higher C_{mic}:N_{mic} ratio for KW2 compared to KW1. The higher C_{mic}, C_{mic}:N_{mic} ratio, and lower soil mineral N indicate a significant initial N limitation of the soil microbial community of successively grown WW. The high initial DOC content of the soil (Table 2.1.1) induced rapid microbial regrowth after the initial adjustment of the water-holding capacity (WHC), resulting in N immobilization that may have affected plant growth. The higher C_{mic} measured at the end of the experiment was not utilized as an N source (i.e. mineralization of microbial biomass and N release) by KW2 and KW4, leading to lower plant biomass and a higher plant C:N ratio.

2.1.5.3. Microbial activity in the rhizosphere of winter wheat is highly dependent on its rotational position

The combination of zymography with the quantification of enzyme kinetic parameters complemented each other and improved our understanding of the microbial activity and the nutrient transformations in the RH of WW. Zymography is an invaluable technique to demonstrate the dynamics of enzymatic activity at very small spatial scales (Razavi et al., 2019; Guber et al., 2021). Soil microbes in successive WW rotations invested less in BGU and LAP secretion compared to those in the RH of KW1, especially in the subsoil. The absence of the main effect of soil depth on soil enzymatic activity, together with the high root growth and DOC content in the subsoil, imply that the soil microbes sustained their metabolic function at greater depth. This was evident for all three rotational positions.

The zymograms of BGU and LAP showed a narrower rhizosphere extent in the topsoil of KW2 and KW4 compared to KW1 (Fig. 2.1.5). This suggests that the root system of KW1 stimulated microbial activity, increasing glucose and leucine release, which can be directly utilized by microbes. As a result, the microbes in the RH of KW1 (and partially of KW2) (such as taxa belonging to the *Gemmatimonadota*, *Acidobacteriota*, and *Nitrospirota*) were able to utilize the DOC and N in the RH more effectively than the microbes in the RH of KW4 (Fig. 2.1.3, Fig. S2.1.2). Plants as well as bacteria and archaea (Singh et al., 2016; Bilyera et al., 2021) produce BGU, an enzyme important in the first step of cellulose degradation, which is the major component of plant cell walls. Microbes have a weaker ability to utilize low molecular weight C when competing with plants for available nutrients, with DOC content being a strong determinant of the outcome of this interaction (Kuzyakov & Jones, 2006; Song et al., 2020).

Complementing our findings on the DOC of the RH, we found a larger glucose hotspot area in KW1 compared to KW2 and KW4. Labile C is considered critical for maintaining the pathogen-suppressive qualities of agricultural soils, irrespective of the total soil organic matter content (Bongiorno et al., 2019), which could have confounded the biocidal soil legacy of oilseed rape.
Depth-specific comparisons revealed differences in the activity of the previous C- and N-cycling soil enzymes between all three rotational positions. Interestingly, BGU activity was significantly higher in the RH and in the topsoil of KW2 and KW4 than in KW1. This pattern could be explained by the accumulation of less labile organic matter from the wheat residues in the uppermost soil layers in successively grown WW (Cenini et al., 2016; Ni et al., 2020; Luan et al., 2022), which may have stimulated the growth of cellulose-degrading microbes. This, in turn, led to higher BGU activity in the topsoil and C_{mic} throughout the soil profile (Zhao & Zhang, 2018; Reichel et al., 2022). Soil microorganisms thus synthesize BGU in response to the presence of a decomposable substrate that must be degraded (Turner et al., 2002; Veres et al., 2015).
The larger LAP hotspot area in KW1 compared to successively grown WW indicates a larger overall rhizosphere size, which affects a larger soil volume and thus induces positive soil feedback for KW1. This may have contributed to the observed N limitation of successively grown WW. Protein-derived N accounts for 40 % of total soil N and is a crucial N source for microbes and plants, but it is also a precursor for mineral N production that is available for plant uptake (Rillig et al., 2007; Paungfoo-Lonhienne et al., 2008; Näsholm et al., 2009). It is likely that these differences in the form of organic N in the soil of the rotational position stimulated LAP activity in KW1 and repressed it in successively grown WW, with an increasing size of effect from KW2 to KW4. Emmet et al. (2020) showed that plant N uptake and LAP activity are coupled in sunflower (*Helianthus annuus* L.), buckwheat (*Fagopyrum esculentum* Moench), Sudan grass (*Sorghum* x *drummondii* (Nees ex Steud.) Millsp. & Chase), Japanese millet (*Echinochloa esculenta* (A. Braun) H. Scholz), and maize (*Zea mays* subsp. *mays* L.) during flowering, and attributed this to the priming of soil organic N that is available for plant uptake. We observed that higher concentrations of DOC and NH_4^+ were accompanied by higher LAP activity and substrate affinity in the RH (Fig. S2.1.5, Fig. 2.1.5). However, the literature is inconclusive regarding the impact of inorganic N on LAP activity (Cenini et al., 2016; Shi et al., 2016).

2.1.5.4. The rotational position of WW shapes the soil microbial community composition

The higher richness of bacterial taxa in the BS of KW4 compared to KW1 and KW2 suggests that successive wheat cultivation selects a broader spectrum of bacteria that are better adapted to the specific soil conditions (Mayer et al., 2019). Previous research has shown that preceding crops affect the microbial communities in the wheat rhizosphere (Hilton et al., 2018; Babin et al., 2019). Oilseed rape is known to recruit microbial taxa that enhance the growth of the following WW (Vujanovic et al., 2012). This might be linked to the control that the preceding crops exert over the quantity and quality of the secreted exudates, leading to changes in the relative abundance of certain taxa (Jones et al., 2019; Wen et al., 2022). In addition, we observed only minor differences between BS and RH soil compartments, which is in contrast to other studies reporting pronounced differences between soil- and root-associated communities (Schreiter et al., 2014; Bziuk et al., 2021). These findings suggest that our non-destructive sampling technique using microspatulas may have been constrained by the distance at which we were able to collect soil samples from the vicinity of the plant

roots (≤ 5 mm). Although more precise techniques, such as the wet needle technique (Tian et al., 2020) or Stomacher blending to wash off tightly adhering soil particles directly from the roots, could provide a better distinction between BS and RH microbial communities, they are mainly suitable for only very small sample sizes in terms of soil weight, or they require more root material. Nevertheless, we aimed for a compromise in sampling RH and BS to be able to link all gathered data, i.e. soil biochemical, enzymatic, and microbial community data.

We observed shifts in the bacterial composition at the phylum level between different WW rotational positions (Fig. 2.1.7) that might explain a potential imbalance or dysbiosis effect in successively grown WW, leading to less efficient nutrient uptake and lower plant biomass yields. In general, the microbial community structures of KW1 and KW2 were more similar compared to KW4 (Fig. S2.1.6b). It appears that the higher rate of WW residue return in the soil of WW monocropping may have favored a higher species richness, resulting in microbial taxa competing for slowly degradable C sources (straw) but causing less efficient plant nutrient supply and thus an early reduction of plant growth.

In more detail, we observed a higher relative abundance of *Acidobacteriota* in the RH of KW1 throughout the soil profile compared to KW2 and KW4. *Acidobacteriota* is considered a keystone phylum in the RH of wheat (Kavamura et al., 2020). Bacteria belonging to this phylum have been found to induce auxin (IAA) production in *Arabidopsis*, increase iron uptake following siderophore synthesis, and secrete exopolysaccharides, forming biofilms (Kielak et al., 2016; Kalam et al., 2020). In the subsoil of KW2, the high microbial biomass was negatively associated with the relative abundance of *Acidobacteriota* (Tables S2.1.9-S2.1.10), which was not the case for KW1, thus highlighting the rotational position-specific effect on supporting the proliferation of certain bacterial phyla. *Chloroflexi* and *Nitrospirota* are considered to be NO_2^- oxidizers, contributing to nitrification and, therefore, soil NO_3^- production (Pivato et al., 2021; Yuan et al., 2023). *Nitrospirota* was more prevalent in KW1 and KW2 compared to KW4 in the RH. In the topsoil of KW1, we found that *Nitrospirota* was negatively associated with *Chloroflexi* in the RH (Table S2.1.9), indicating a competition for the same resources. In a rape–rice rotation, Yuan et al. (2023) correlated the relative abundance of *Nitrospirota* to urease activity, which generates NH_4^+ and, therefore, allows N turnover due to nitrification. We found that KW1 formed a more extensive root system and accumulated more N in its biomass. It could thus exploit the newly produced NH_4^+ and NO_3^- more effectively than KW2 and KW4, leading to an increase in biomass in KW1. These findings suggest functional differences in the bacterial communities of the rotational positions, underscoring the dynamic biochemical soil processes that lowered the performance of successively grown wheat.

Understanding the shape of the fungal communities of the rotational positions would help us to better comprehend the complex plant–microbe interactions. Woo et al. (2022) found a strong effect of the rotational position of wheat grown after pea on shaping bacterial and fungal diversity. In another study, fungal community composition responded more than bacterial composition to crop rotation, with a higher relative abundance of beneficial microbes in rotation canola compared to oilseed rape monocropping (Town et al., 2023). Finally, differences in the stability of bacterial and fungal necromass (reflected in the stability between peptides and chitin/chitosan) could determine the mineralization rate of immobilized N by microorganisms and, therefore, the subsequent mineral N release (Camenzind et al., 2023) that is available for uptake by WW.

2.1.6. Conclusions

In this study, three rotational positions of WW were contrasted to assess their impact on soil microbial dynamics, extracellular enzymatic activity, and the performance of WW. We linked the activities of C-acquiring (BGU) and N-acquiring (LAP) enzymes to changes in biochemical soil processes and microbiome community in the RH of successive WW rotations. The reduced root growth and labile C in the RH of successive WW rotations led to decreased microbial and enzymatic activity and, finally, plant nutrient uptake and biomass accumulation. Our results greatly increase our understanding of the preceding crop's soil legacy, which drives the reduction in biomass growth during the early growth of WW.

2.1.7. Data availability statement

The data have been uploaded to the BonaRes Repository for Soil and Agricultural Research Data; https://doi.org/10.20387/bonares-67q1-90wr. Raw amplicon data were deposited in the National Center for Biotechnology Information (NCBI) Sequence Read Archive (SRA) under BioProject PRJNA942109.

2.1.8. Author contributions

NK and NB conceived the study. NB and RR designed the rhizotron prototypes. NK prepared the materials and conducted the experiment. NK, CK and SK performed the sample acquisition and sample analyses (plant, biochemical). CK and SK supported the sample acquisition and sample analyses. MR performed the zymography, glucose imaging and destructive soil analysis for enzyme kinetic parameters and prepared the methodology for the enzymatic analyses. ABK and AG performed the amplicon sequencing analyses and prepared the methodology for amplicon sequencing analyses. NK and NB interpreted the data and wrote the manuscript. NK and NB prepared the draft. NK, MR, BR, ABK, AG, KS, RR and NB provided constructive feedback and revised the manuscript.

2.1.9. Funding

This work was funded by the German Federal Ministry of Education and Research (BMBF) in the framework of the funding initiative "Rhizo4Bio - Importance of the Rhizosphere for the Bioeconomy", project "RhizoWheat" (grant number 031B0910B).

2.1.11. Acknowledgements

The authors acknowledge Henning Kage, Nora Honsdorf and Katharina Pronkow (at the Christian-Albrechts-University of Kiel, CAU) for providing the soil and seed material for the experiment, as well as the technical support of Holger Wissel in the soil and plant C and N analyses.

2.1.11. References

Angus, J.F., Kirkegaard, J.A., Hunt, J.R., Ryan, M.H., Ohlander, L., Peoples, M.B., 2015. Break crops and rotations for wheat. Crop and Pasture Science 66, 523–552. doi:10.1071/CP14252

Arnhold, J., Grunwald D., Braun-Kiewnick A., Koch H.J., 2023a. Effect of crop rotational position and nitrogen supply on root development and yield formation of winter wheat. Front. Plant Sci. 14. doi:10.3389/fpls.2023.1265994

Arnhold, J., Grunwald, D., Kage, H., Koch, H.J., 2023b. No differences in soil structure under winter wheat grown in different crop rotational positions. Canadian Journal of Soil Science. 00, 1-8. doi:10.1139/cjss-2023-0030

Awad, Y.M., Blagodatskaya, E., Ok, Y.S., Kuzyakov, Y., 2012. Effects of polyacrylamide, biopolymer, and biochar on decomposition of soil organic matter and plant residues as determined by 14C and enzyme activities. European Journal of Soil Biology 48, 1–10. doi:10.1016/j.ejsobi.2011.09.005

Babin, D., Deubel, A., Jacquiod, S., Sørensen, S.J., Geistlinger, J., Grosch, R., Smalla, K., 2019. Impact of long-term agricultural management practices on soil prokaryotic communities. Soil Biology and Biochemistry 129, 17–28. doi:https://doi.org/10.1016/j.soilbio.2018.11.002

Bennett, J.A., Klironomos, J., 2019. Mechanisms of plant–soil feedback: interactions among biotic and abiotic drivers. New Phytologist 222, 91–96. doi:10.1111/nph.15603

Bilyera, N., Zhang, X., Duddek, P., Fan, L., Banfield, C.C., Schlüter, S., Carminati, A., Kaestner, A., Ahmed, M.A., Kuzyakov, Y., Dippold, M.A., Spielvogel, S., Razavi, B.S., 2021. Maize genotype-specific exudation strategies: An adaptive mechanism to increase microbial activity in the rhizosphere. Soil Biology and Biochemistry 162, 108426. doi:10.1016/J.SOILBIO.2021.108426

Bongiorno, G., Postma, J., Bünemann, E.K., Brussaard, L., de Goede, R.G.M., Mäder, P., Tamm, L., Thuerig, B., 2019. Soil suppressiveness to *Pythium ultimum* in ten European long-term field experiments and its relation with soil parameters. Soil Biology and Biochemistry 133, 174–187. doi:10.1016/j.soilbio.2019.03.012

Bowles, T.M., Jilling, A., Morán-Rivera, K., Schnecker, J., Grandy, A.S., 2022. Crop rotational complexity affects plant-soil nitrogen cycling during water deficit. Soil Biology and Biochemistry 166, 108552. doi:https://doi.org/10.1016/j.soilbio.2022.108552

Box, G.E.P., Cox, D.R., 1964. An Analysis of Transformations. Journal of the Royal Statistical Society: Series B (Methodological) 26, 211–243. doi:10.1111/J.2517-6161.1964.TB00553.X

Bziuk, N., Maccario, L., Douchkov, D., Lueck, S., Babin, D., Sørensen, S.J., Schikora, A., Smalla, K., 2021. Tillage shapes the soil and rhizosphere microbiome of barley—but not its susceptibility towards Blumeria graminis f. sp. hordei. FEMS Microbiology Ecology 97, fiab018. doi:10.1093/femsec/fiab018

Callahan, B.J., Mcmurdie, P.J., Rosen, M.J., Han, A.W., Johnson, A.J.A., Holmes, S.P., 2016. DADA2: High-resolution sample inference from Illumina amplicon data. Nature Methods 13, 581–583. doi:10.1038/nmeth.3869

Camenzind, T., Mason-Jones, K., Mansour, I., Rillig, M.C., Lehmann, J., 2023. Formation of necromass-derived soil organic carbon determined by microbial death pathways. Nature Geoscience 16, 115–122. doi:10.1038/s41561-022-01100-3

Canarini, A., Kaiser, C., Merchant, A., Richter, A., Wanek, W., 2019. Root exudation of primary metabolites: Mechanisms and their roles in plant responses to environmental stimuli. Frontiers in Plant Science 10, 157. doi:10.3389/fpls.2019.00157

Cenini, V.L., Fornara, D.A., McMullan, G., Ternan, N., Carolan, R., Crawley, M.J., Clément, J.C., Lavorel, S., 2016. Linkages between extracellular enzyme activities and the carbon and nitrogen content of grassland soils. Soil Biology and Biochemistry 96, 198–206. doi:10.1016/j.soilbio.2016.02.015

Cook, R.J., 2003. Take-all of wheat. Physiological and Molecular Plant Pathology 62, 73–86. doi:10.1016/S0885-5765(03)00042-0

Cortois, R., Schröder-Georgi, T., Weigelt, A., van der Putten, W.H., De Deyn, G.B., 2016. Plant–soil feedbacks: role of plant functional group and plant traits. Journal of Ecology 104, 1608–1617. doi:10.1111/1365-2745.12643

Costa, O.Y.A., Raaijmakers, J.M., Kuramae, E.E., 2018. Microbial extracellular polymeric substances: Ecological function and impact on soil aggregation. Frontiers in Microbiology 9, 1–14. doi:10.3389/fmicb.2018.01636

Dorodnikov, M., Blagodatskaya, E., Blagodatsky, S., Marhan, S., Fangmeier, A., Kuzyakov, Y., 2009. Stimulation of microbial extracellular enzyme activities by elevated CO2 depends on soil aggregate size. Global Change Biology 15, 1603–1614. doi:10.1111/J.1365-2486.2009.01844.X

Emmett, B.D., Buckley, D.H., Drinkwater, L.E., 2020. Plant growth rate and nitrogen uptake shape rhizosphere bacterial community composition and activity in an agricultural field. New Phytologist 225, 960–973. doi:10.1111/nph.16171

Galloway, A.F., Knox, P., Krause, K., 2020. Sticky mucilages and exudates of plants: putative microenvironmental design elements with biotechnological value. New Phytologist 225, 1461–1469. doi:10.1111/nph.16144

German, D.P., Chacon, S.S., Allison, S.D., 2011. Substrate concentration and enzyme allocation can affect rates of microbial decomposition. Ecology 92, 1471–1480. doi:10.1890/10-2028.1

Guber, A., Blagodatskaya, E., Juyal, A., Razavi, B.S., Kuzyakov, Y., Kravchenko, A., 2021. Time-lapse approach to correct deficiencies of 2D soil zymography. Soil Biology and Biochemistry 157, 108225. doi:10.1016/j.soilbio.2021.108225

Hansen, J.C., Schillinger, W.F., Sullivan, T.S., Paulitz, T.C., 2019. Soil microbial biomass and fungi reduced with canola introduced into long-term monoculture wheat rotations. Frontiers in Microbiology 10, 1488. doi:10.3389/fmicb.2019.01488

Hernández-Calderón, E., Aviles-Garcia, M.E., Castulo-Rubio, D.Y., Macías-Rodríguez, L., Ramírez, V.M., Santoyo, G., López-Bucio, J., Valencia-Cantero, E., 2018. Volatile compounds from beneficial or pathogenic bacteria differentially regulate root exudation, transcription of iron transporters, and defense signaling pathways in Sorghum bicolor. Plant Molecular Biology 96, 291–304. doi:10.1007/s11103-017-0694-5

Hilton, S., Bennett, A.J., Chandler, D., Mills, P., Bending, G.D., 2018. Preceding crop and seasonal effects influence fungal, bacterial and nematode diversity in wheat and oilseed rape rhizosphere and soil. Applied Soil Ecology 126, 34–46. doi:10.1016/j.apsoil.2018.02.007

Hoang, D.T.T., Rashtbari, M., Anh, L.T., Wang, S., Tu, D.T., Hiep, N.V., Razavi, B.S., 2022. Mutualistic interaction between arbuscular mycorrhiza fungi and soybean roots enhances drought resistant through regulating glucose exudation and rhizosphere expansion. Soil Biology and Biochemistry 171, 108728. doi:10.1016/J.SOILBIO.2022.108728

Joergensen, R.G., 1996. The fumigation-extraction method to estimate soil microbial biomass: Calibration of the kEC value. Soil Biology and Biochemistry 28, 25–31. doi:10.1016/0038-0717(95)00102-6

Jones, P., Garcia, B.J., Furches, A., Tuskan, G.A., Jacobson, D., 2019. Plant host-associated mechanisms for microbial selection. Frontiers in Plant Science 10, 1–14. doi:10.3389/fpls.2019.00862

Kaloterakis, N., van Delden, S.H., Hartley, S., De Deyn, G.B., 2021. Silicon application and plant growth promoting rhizobacteria consisting of six pure *Bacillus* species alleviate salinity stress in cucumber (*Cucumis sativus* L). Scientia Horticulturae 288, 110383. doi:10.1016/J.SCIENTA.2021.110383

Kerdraon, L., Balesdent, M.-H., Barret, M., Laval, V., Suffert, F., 2019. Crop Residues in Wheat-Oilseed Rape Rotation System: a Pivotal, Shifting Platform for Microbial Meetings. Microbial Ecology 77, 931–945. doi:10.1007/s00248-019-01340-8

Kelly, C., Haddix, M.L., Byrne, P.F., Cotrufo, M.F., Schipanski, M., Kallenbach, C.M., Wallenstein, M.D., Fonte, S.J., 2022. Divergent belowground carbon allocation patterns of winter wheat shape rhizosphere microbial communities and nitrogen cycling activities. Soil Biology and Biochemistry 165, 108518. doi:10.1016/j.soilbio.2021.108518

Kirkegaard, J., Christen, O., Krupinsky, J., Layzell, D., 2008. Break crop benefits in temperate wheat production. Field Crops Research 107, 185–195. doi:https://doi.org/10.1016/j.fcr.2008.02.010

Korenblum, E., Dong, Y., Szymanski, J., Panda, S., Jozwiak, A., Massalha, H., Meir, S., Rogachev, I., Aharoni, A., 2020. Rhizosphere microbiome mediates systemic root metabolite exudation by root-to-root signaling. Proceedings of the National Academy of Sciences of the United States of America 117, 3874–3883. doi:10.1073/pnas.1912130117

Kramer-Walter, K.R., Bellingham, P.J., Millar, T.R., Smissen, R.D., Richardson, S.J., Laughlin, D.C., 2016. Root traits are multidimensional: specific root length is independent

from root tissue density and the plant economic spectrum. Journal of Ecology 104, 1299–1310. doi:10.1111/1365-2745.12562

Kuzyakov, Y., Jones, D.L., 2006. Glucose uptake by maize roots and its transformation in the rhizosphere. Soil Biology and Biochemistry 38, 851–860. doi:10.1016/j.soilbio.2005.07.012

Kuzyakov, Y., Domanski, G., 2000. Carbon input by plants into the soil. Review. Journal of Plant Nutrition and Soil Science 163, 421–431. doi:10.1002/1522-2624(200008)163:4<421::AID-JPLN421>3.0.CO;2-R

Kuzyakov, Y., Razavi, B.S., 2019. Rhizosphere size and shape: Temporal dynamics and spatial stationarity. Soil Biology and Biochemistry 135, 343–360. doi:10.1016/j.soilbio.2019.05.011

Kuzyakov, Y., Xu, X., 2013. Competition between roots and microorganisms for nitrogen: Mechanisms and ecological relevance. New Phytologist 198, 656–669. doi:10.1111/nph.12235

Kwak, Y.S., Weller, D.M., 2013. Take-all of wheat and natural disease suppression: A review. Plant Pathology Journal 29, 125–135. doi:10.5423/PPJ.SI.07.2012.0112

Lahti L., Shetty S., et al. 2017. Microbiome: Tools for microbiome analysis in R. Version. Available at: https://github.com/microbiome/microbiome/

Lange, M., Eisenhauer, N., Sierra, C.A., Bessler, H., Engels, C., Griffiths, R.I., Mellado-Vázquez, P.G., Malik, A.A., Roy, J., Scheu, S., Steinbeiss, S., Thomson, B.C., Trumbore, S.E., Gleixner, G., 2015. Plant diversity increases soil microbial activity and soil carbon storage. Nature Communications 6, 6707. doi:10.1038/ncomms7707

Lopez, G., Ahmadi, S.H., Amelung, W., Athmann, M., Ewert, F., Gaiser, T., Gocke, M.I., Kautz, T., Postma, J., Rachmilevitch, S., Schaaf, G., Schnepf, A., Stoschus, A., Watt, M., Yu, P., Seidel, S.J., 2023. Nutrient deficiency effects on root architecture and root-to-shoot ratio in arable crops. Frontiers in Plant Science 13, 1–18. doi:10.3389/fpls.2022.1067498

Luan, H., Liu, Y., Huang, S., Qiao, W., Chen, J., Guo, T., Zhang, Xiaojia, Guo, S., Zhang, Xuemei, Qi, G., 2022. Successive walnut plantations alter soil carbon quantity and quality by modifying microbial communities and enzyme activities. Frontiers in Microbiology 13, 1–14. doi:10.3389/fmicb.2022.953552

Ma, X., Zarebanadkouki, M., Kuzyakov, Y., Blagodatskaya, E., Pausch, J., Razavi, B.S., 2018. Spatial patterns of enzyme activities in the rhizosphere: Effects of root hairs and root radius. Soil Biology and Biochemistry 118, 69–78. doi:10.1016/J.SOILBIO.2017.12.009

Mayer, Z., Sasvári, Z., Szentpéteri, V., Rétháti, B.P., Vajna, B., Posta, K., 2019. Effect of long-term cropping systems on the diversity of the soil bacterial communities. Agronomy 9, 1–10. doi:10.3390/agronomy9120878

McMurdie, P.J., Holmes, S., 2013. Phyloseq: An R package for reproducible interactive analysis and graphics of microbiome census data. PLoS ONE 8, e61217. doi:10.1371/journal.pone.0061217

Meier, I.C., Finzi, A.C., Phillips, R.P., 2017. Root exudates increase N availability by stimulating microbial turnover of fast-cycling N pools. Soil Biology and Biochemistry 106, 119–128. doi:10.1016/j.soilbio.2016.12.004

Mohan, S., Kiran Kumar, K., Sutar, V., Saha, S., Rowe, J., Davies, K.G., 2020. Plant root-exudates recruit hyperparasitic bacteria of phytonematodes by altered cuticle aging: implications for biological control strategies. Frontiers in Plant Science 11, 763. doi:10.3389/fpls.2020.00763

Näsholm, T., Kielland, K., Ganeteg, U., 2009. Uptake of organic nitrogen by plants. New Phytologist 182, 31–48. doi:10.1111/j.1469-8137.2008.02751.x

Ni, X., Liao, S., Tan, S., Peng, Y., Wang, D., Yue, K., Wu, F., Yang, Y., 2020. The vertical distribution and control of microbial necromass carbon in forest soils. Global Ecology and Biogeography 29, 1829–1839. doi:10.1111/geb.13159

Oksanen J., Kindt R., Legendre P., O'Hara B., Simpson G.L., Solymos P., Stevens, M.H.H., Wagner, H., 2020. Vegan: community ecology package. Available at: https://CRAN.R-project.org/package=vegan

Palma-Guerrero, J., Chancellor, T., Spong, J., Canning, G., Hammond, J., McMillan, V.E., Hammond-Kosack, K.E., 2021. Take-all disease: new insights into an important wheat root pathogen. Trends in Plant Science 26, 836–848. doi:10.1016/j.tplants.2021.02.009

Pang, Z., Chen, J., Wang, T., Gao, C., Li, Z., Guo, L., Xu, J., Cheng, Y., 2021. Linking Plant Secondary Metabolites and Plant Microbiomes: A Review. Frontiers in Plant Science 12, 621276. doi:10.3389/fpls.2021.621276

Panikov, N.S., Blagodatsky, S.A., Blagodatskaya, J. V., Glagolev, M. V., 1992. Determination of microbial mineralization activity in soil by modified Wright and Hobbie method. Biology and Fertility of Soils 14, 280–287. doi:10.1007/BF00395464

Pascault, N., Cécillon, L., Mathieu, O., Hénault, C., Sarr, A., Lévêque, J., Farcy, P., Ranjard, L., Maron, P.A., 2010. *In situ* Dynamics of Microbial Communities during Decomposition of Wheat, Rape, and Alfalfa Residues. Microbial Ecology 60, 816–828. doi:10.1007/s00248-010-9705-7

Paungfoo-Lonhienne, C., Lonhienne, T.G.A., Rentsch, D., Robinson, N., Christie, M., Webb, R.I., Gamage, H.K., Carroll, B.J., Schenk, P.M., Schmidt, S., 2008. Plants can use protein as a nitrogen source without assistance from other organisms. Proceedings of the National Academy of Sciences of the United States of America 105, 4524–4529. doi:10.1073/pnas.0712078105

Pausch, J., Kuzyakov, Y., 2017. Carbon input by roots into the soil: Quantification of rhizodeposition from root to ecosystem scale. Global Change Biology 24, 1–12. doi:10.1111/gcb.13850

Philippot, L., Raaijmakers, J.M., Lemanceau, P., Van Der Putten, W.H., 2013. Going back to the roots: The microbial ecology of the rhizosphere. Nature Reviews Microbiology 11, 789–799. doi:10.1038/nrmicro3109

Pivato, B., Semblat, A., Guégan, T., Jacquiod, S., Martin, J., Deau, F., Moutier, N., Lecomte, C., Burstin, J., Lemanceau, P., 2021. Rhizosphere bacterial networks, but not diversity, are impacted by pea-wheat intercropping. Frontiers in Microbiology 12, 1–13. doi:10.3389/fmicb.2021.674556

Qi, B., Zhang, K., Qin, S., Lyu, D., He, J., 2022. Glucose addition promotes C fixation and bacteria diversity in C-poor soils, improves root morphology, and enhances key N metabolism in apple roots. PLOS ONE 17, e0262691.

Quast, C., Pruesse, E., Yilmaz, P., Gerken, J., Schweer, T., Yarza, P., Peplies, J., Glöckner, F.O., 2013. The SILVA ribosomal RNA gene database project: Improved data processing and web-based tools. Nucleic Acids Research 41, 590–596. doi:10.1093/nar/gks1219

R Core Team. 2016. R: a language and environment for statistical computing. Vienna, Austria: R Foundation for Statistical Computing.

Ramanauskienė, J., Semaškienė, R., Jonavičienė, A., Ronis, A., 2018. The effect of crop rotation and fungicide seed treatment on take-all in winter cereals in Lithuania. Crop Protection 110, 14–20. doi:https://doi.org/10.1016/j.cropro.2018.03.011

Razavi, B.S., Zarebanadkouki, M., Blagodatskaya, E., Kuzyakov, Y., 2016. Rhizosphere shape of lentil and maize: Spatial distribution of enzyme activities. Soil Biology and Biochemistry 96, 229–237. doi:10.1016/J.SOILBIO.2016.02.020

Razavi, B.S., Zhang, X., Bilyera, N., Guber, A., Zarebanadkouki, M., 2019. Soil zymography: Simple and reliable? Review of current knowledge and optimization of the method. Rhizosphere 11, 100161. doi:10.1016/J.RHISPH.2019.100161

Reichel, R., Kamau, C.W., Kumar, A., Li, Z., Radl, V., Temperton, V.M., Schloter, M., Brüggemann, N., 2022. Spring barley performance benefits from simultaneous shallow straw incorporation and top dressing as revealed by rhizotrons with resealable sampling ports. Biology and Fertility of Soils 58, 375–388. doi:10.1007/s00374-022-01624-1

Ren, C., Chen, J., Deng, J., Zhao, F., Han, X., Yang, G., Tong, X., Feng, Y., Shelton, S., Ren, G., 2017. Response of microbial diversity to C:N:P stoichiometry in fine root and microbial biomass following afforestation. Biology and Fertility of Soils 53, 457–468. doi:10.1007/s00374-017-1197-x

Rillig, M.C., Caldwell, B.A., Wösten, H.A.B., Sollins, P., 2007. Role of proteins in soil carbon and nitrogen storage: Controls on persistence. Biogeochemistry 85, 25–44. doi:10.1007/s10533-007-9102-6

Rose, L., 2017. Pitfalls in root trait calculations: How ignoring diameter heterogeneity can lead to overestimation of functional traits. Frontiers in Plant Science 8, 1–5. doi:10.3389/fpls.2017.00898

Shi, Y., Sheng, L., Wang, Z., Zhang, X., He, N., Yu, Q., 2016. Responses of soil enzyme activity and microbial community compositions to nitrogen addition in bulk and microaggregate soil in the temperate steppe of Inner Mongolia. Eurasian Soil Science 49, 1149–1160. doi:10.1134/S1064229316100124

Schreiter, S., Ding, G.-C., Heuer, H., Neumann, G., Sandmann, M., Grosch, R., Kropf, S., Smalla, K., 2014. Effect of the soil type on the microbiome in the rhizosphere of field-grown lettuce. Frontiers in Microbiology 5, 144. doi: 10.3389/fmicb.2014.00144

Sieling, K., 2005. Growth stage-specific application of slurry and mineral N to oilseed rape, wheat and barley. Journal of Agricultural Science 142, 495–502. doi:10.1017/S0021859604004757

Sieling, K., Christen, O., 2015. Crop rotation effects on yield of oilseed rape, wheat and barley and residual effects on the subsequent wheat. Archives of Agronomy and Soil Science 61, 1531–1549. doi:10.1080/03650340.2015.1017569

Singh, G., Verman, A.K., Kumar, V., 2016. Catalytic properties, functional attributes and industrial applications of b -glucosidases. 3 Biotech 6, 1–14. doi:10.1007/s13205-015-0328-z

Smagacz, J., Kozieł, M., Martyniuk, S., 2016. Soil properties and yields of winter wheat after long-term growing of this crop in two contrasting rotations. Plant, Soil and Environment 62, 566–570. doi:10.17221/582/2016-PSE

Song, X., Razavi, B.S., Ludwig, B., Zamanian, K., Zang, H., Kuzyakov, Y., Dippold, M.A., Gunina, A., 2020. Combined biochar and nitrogen application stimulates enzyme activity and root plasticity. Science of the Total Environment 735, 139393. doi:10.1016/j.scitotenv.2020.139393

Spitzer, C.M., Lindahl, B., Wardle, D.A., Sundqvist, M.K., Gundale, M.J., Fanin, N., Kardol, P., 2021. Root trait–microbial relationships across tundra plant species. New Phytologist 229, 1508–1520. doi:10.1111/nph.16982

Town, J.R., Dumonceaux, T., Tidemann, B., Helgason, B.L., 2023. Crop rotation significantly influences the composition of soil, rhizosphere, and root microbiota in canola (*Brassica napus* L.). Environmental Microbiome 18, 1–14. doi:10.1186/s40793-023-00495-9

Turner, B.L., Hopkins, D.W., Haygarth, P.M., Ostle, N., 2002. β-Glucosidase activity in pasture soils. Applied Soil Ecology 20, 157–162. doi:https://doi.org/10.1016/S0929-1393(02)00020-3

Veres, Z., Kotroczó, Z., Fekete, I., Tóth, J.A., Lajtha, K., Townsend, K., Tóthmérész, B., 2015. Soil extracellular enzyme activities are sensitive indicators of detrital inputs and carbon availability. Applied Soil Ecology 92, 18–23. doi:https://doi.org/10.1016/j.apsoil.2015.03.006

Vlot, A.C., Sales, J.H., Lenk, M., Bauer, K., Brambilla, A., Sommer, A., Chen, Y., Wenig, M., Nayem, S., 2020. Systemic propagation of immunity in plants. New Phytologist 229, 1234–1250. doi:10.1111/nph.16953

Vujanovic, V., Mavragani, D., Hamel, C., 2012. Fungal communities associated with durum wheat production system: A characterization by growth stage, plant organ and preceding crop. Crop Protection 37, 26–34. doi:https://doi.org/10.1016/j.cropro.2012.02.006

Weiser, C., Fuß, R., Kage, H., Flessa, H., 2018. Do farmers in Germany exploit the potential yield and nitrogen benefits from preceding oilseed rape in winter wheat cultivation? Archives of Agronomy and Soil Science 64, 25–37. doi:10.1080/03650340.2017.1326031

Wen, T., Yu, G.H., Hong, W.D., Yuan, J., Niu, G.Q., Xie, P.H., Sun, F.S., Guo, L.D., Kuzyakov, Y., Shen, Q.R., 2022. Root exudate chemistry affects soil carbon mobilization via microbial community reassembly. Fundamental Research 2, 697–707. doi:10.1016/j.fmre.2021.12.016

Woo, S.L., De Filippis, F., Zotti, M., Vandenberg, A., Hucl, P., Bonanomi, G., 2022. pea-wheat rotation affects soil microbiota diversity, community structure, and soil borne Pathogens. Microorganisms 10, 370. doi:10.3390/microorganisms10020370

Wu, J., Joergensen, R.G., Pommerening, B., Chaussod, R., Brookes, P.C., 1990. Measurement of soil microbial biomass C by fumigation-extraction—an automated procedure. Soil Biology and Biochemistry 22, 1167–1169. doi:10.1016/0038-0717(90)90046-3

Yahya, M., Islam, E. ul, Rasul, M., Farooq, I., Mahreen, N., Tawab, A., Irfan, M., Rajput, L., Amin, I., Yasmin, S., 2021. Differential root exudation and architecture for improved growth of wheat mediated by phosphate solubilizing bacteria. Frontiers in Microbiology 12, 1–23. doi:10.3389/fmicb.2021.744094

Yang, Y., Li, M., Wu, J., Pan, X., Gao, C., Tang, D.W.S., 2022. Impact of combining long-term subsoiling and organic fertilizer on soil microbial biomass carbon and nitrogen, soil enzyme activity, and water use of winter wheat. Frontiers in Plant Science 12, 1–13. doi:10.3389/fpls.2021.788651

Yeo, I.N.K., Johnson, R.A., 2000. A new family of power transformations to improve normality or symmetry. Biometrika 87, 954–959. doi:10.1093/biomet/87.4.954

Yin, C., Schlatter, D., Hagerty, C., Hulbert, S., Paulitz, T.C., 2022. Disease-induced assemblage of the rhizosphere fungal community in successive plantings of wheat. Phytobiomes Journal. doi:10.1094/pbiomes-12-22-0101-r

Yuan, L., Gao, Y., Mei, Y., Liu, J., Kalkhajeh, Y.K., Hu, H., Huang, J., 2023. Effects of continuous straw returning on bacterial community structure and enzyme activities in rape-rice soil aggregates. Scientific Reports 13, 2357. doi:10.1038/s41598-023-28747-1

Zhao, S., Zhang, S., 2018. Linkages between straw decomposition rate and the change in microbial fractions and extracellular enzyme activities in soils under different long-term fertilization treatments. PLoS ONE 13, e0202660. doi:10.1371/journal.pone.0202660

Zhang, X., Kuzyakov, Y., Zang, H., Dippold, M.A., Shi, L., Spielvogel, S., Razavi, B.S., 2020. Rhizosphere hotspots: Root hairs and warming control microbial efficiency, carbon utilization and energy production. Soil Biology and Biochemistry 148, 107872. doi:10.1016/j.soilbio.2020.107872

Zhou, M., Diwu, Z., Panchuk-Voloshina, N., Haugland, R.P., 1997. A stable nonfluorescent derivative of resorufin for the fluorometric determination of trace hydrogen peroxide: applications in detecting the activity of phagocyte NADPH oxidase and other oxidases. Analytical Biochemistry 253, 162–168. doi:10.1006/ABIO.1997.2391

2.1.12. Graphical abstract

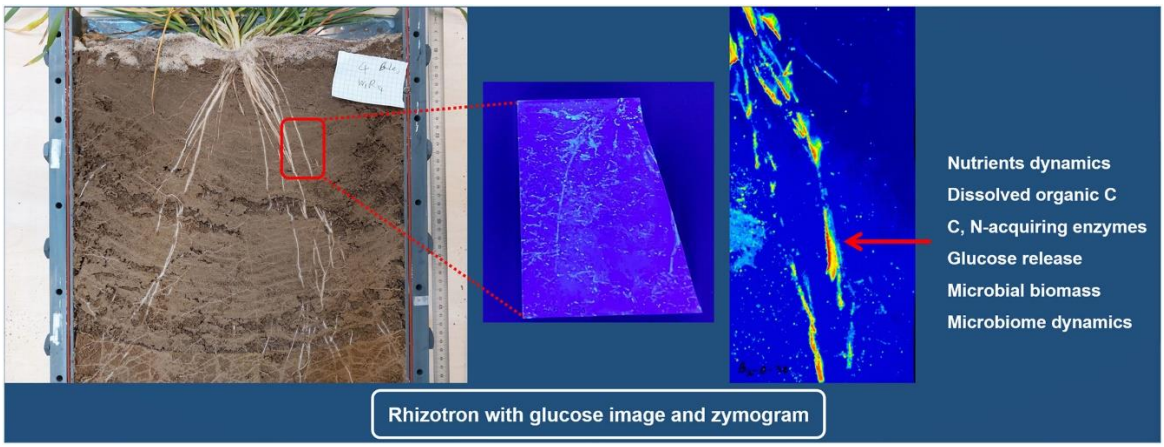

2.1.13. Supplementary material

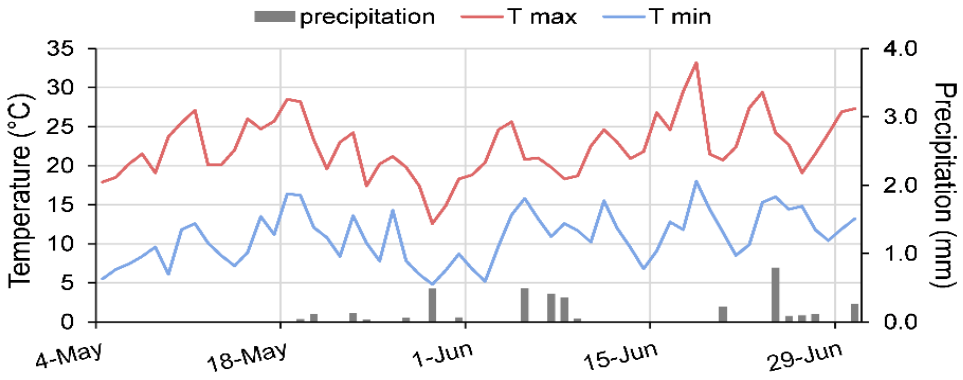

Figure S2.1.1. Minimum, maximum temperature and precipitation fluctuations throughout the course of the experiment.

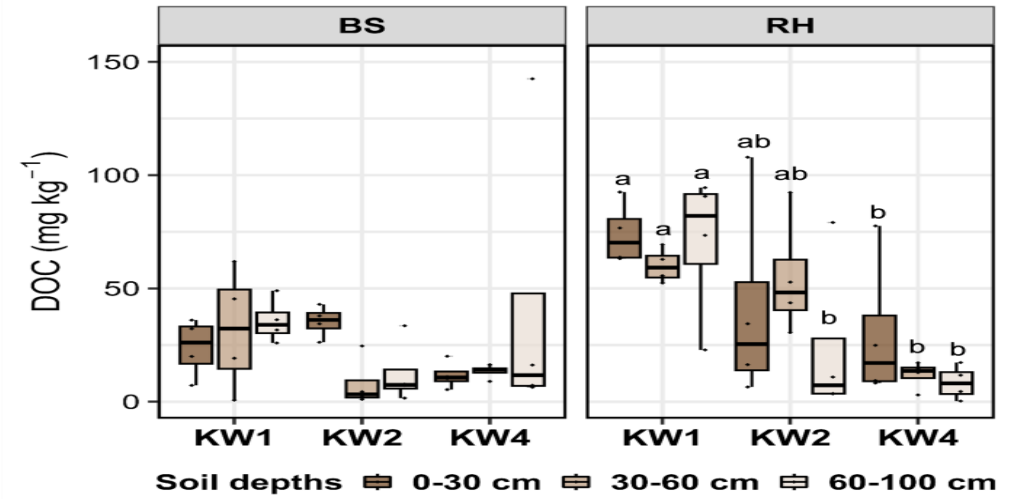

Figure S2.1.2. Effect of the rotational positions on dissolved organic carbon (DOC) of the following winter wheat at onset of stem elongation (BBCH 30), at soil depths 0-30 cm, 30-60 cm and 60-100 cm and in two soil compartments bulk soil (BS) and rhizosphere soil (RH). KW1 = first wheat, KW2 = second wheat, and KW4 = fourth wheat after oilseed rape in soil from the experimental farm Hohenschulen in Kiel, Germany.

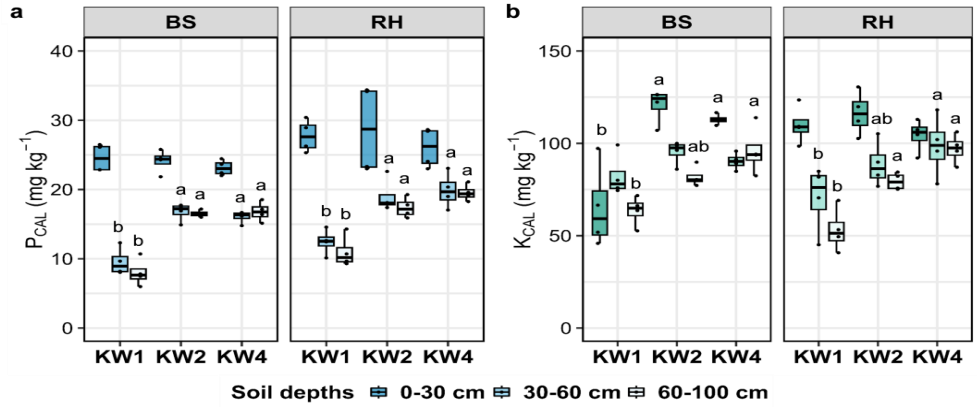

Figure S2.1.3. Effect of the rotational positions on dissolved organic carbon soil P_{cal} (a) and soil K_{cal} (b) of the following winter wheat at onset of stem elongation (BBCH 30) at the three soil depths 0-30 cm, 30-60 cm and 60-100 cm and in two soil compartments bulk soil (BS) and rhizosphere soil (RH). KW1 = first wheat, KW2 = second wheat, and KW4 = fourth wheat after oilseed rape in soil from the experimental farm Hohenschulen in Kiel, Germany. Uppercase letters denote significant differences between rotational positions.

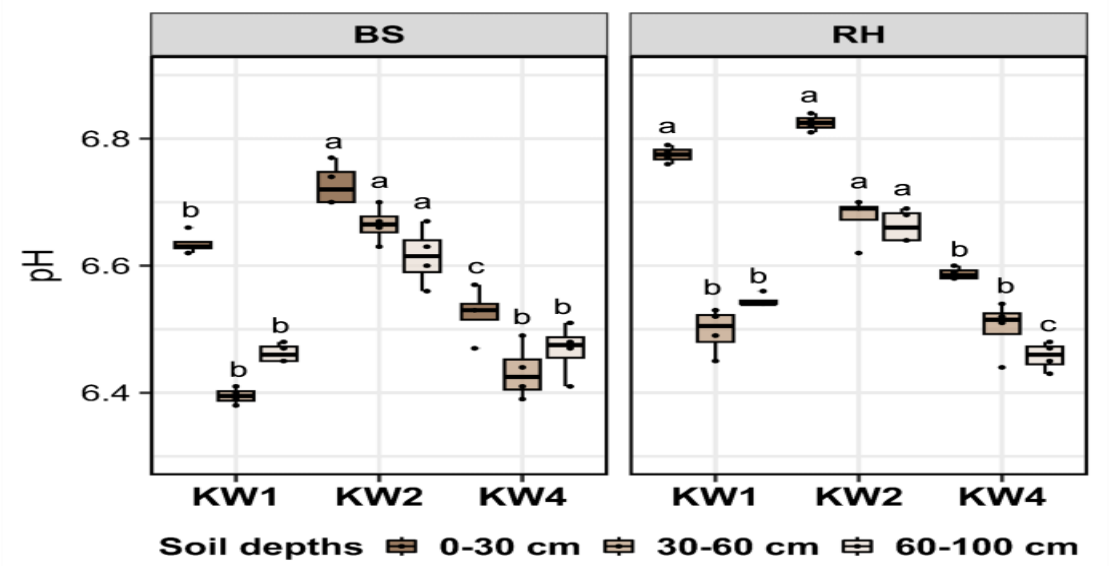

Figure S2.1.4. Effect of the rotational positions on dissolved organic carbon soil pH of the following winter wheat at onset of stem elongation (BBCH 30) at the three soil depths 0-30 cm, 30-60 cm and 60-100 cm and in two soil compartments bulk soil (BS) and rhizosphere soil (RH). KW1 = first wheat, KW2 = second wheat, and KW4= fourth wheat after oilseed rape in soil from the experimental farm Hohenschulen in Kiel, Germany. Uppercase letters denote significant differences between rotational positions.

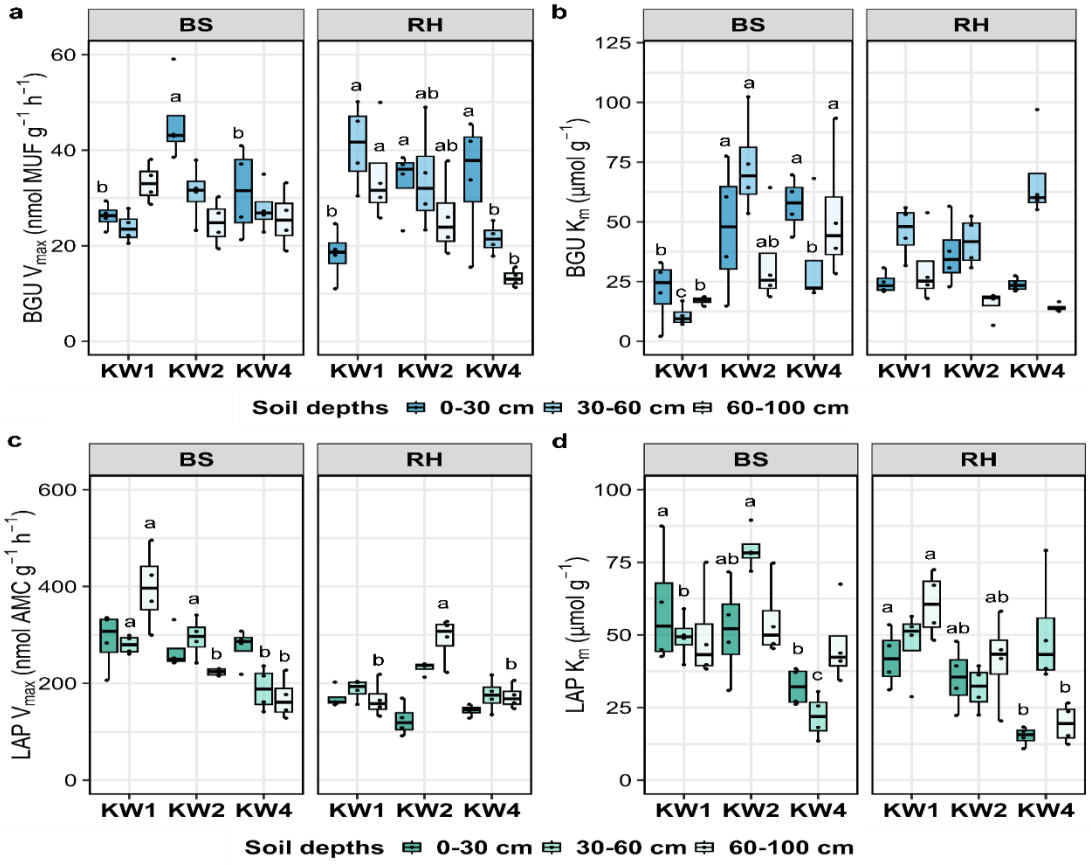

Figure S2.1.5. Effect of the rotational positions on maximum velocity (V_{max}) and enzyme affinity (K_m) of *β*-glucosidase (BGU) (a and b) and leucine aminopeptidase (LAP) (c and d) of the following winter wheat at onset of stem elongation (BBCH 30), at soil depths 0-30 cm, 30-60 cm and 60-100 cm and in two soil compartments bulk soil (BS) and rhizosphere soil (RH). KW1 = first wheat, KW2 = second wheat, and KW4 = fourth wheat after oilseed rape in soil from the experimental farm Hohenschulen in Kiel, Germany.

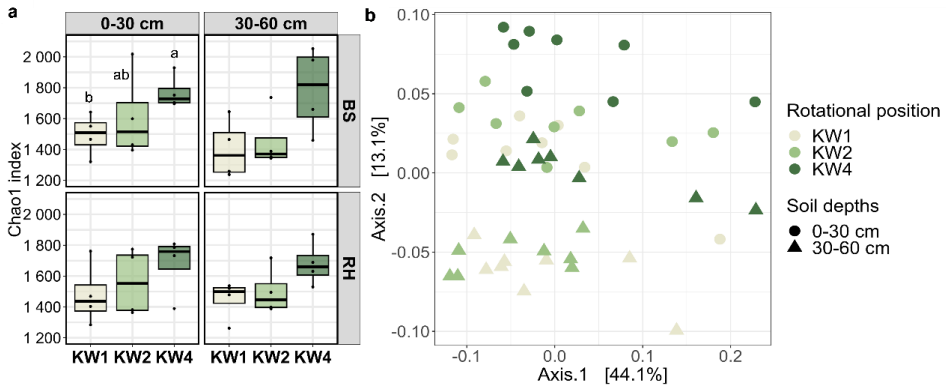

Figure S2.1.6. Effect of the rotational positions on the microbial alpha diversity index Chao1 (a) and PCoA plots of beta diversity (b) of the following winter wheat at onset of stem elongation (BBCH 30), at soil depths 0-30 cm and 30-60 cm, and in two soil compartments bulk soil (BS) and rhizosphere soil (RH). KW1 = first wheat, KW2 = second wheat, and KW4 = fourth wheat after oilseed rape in soil from the experimental farm Hohenschulen in Kiel, Germany.

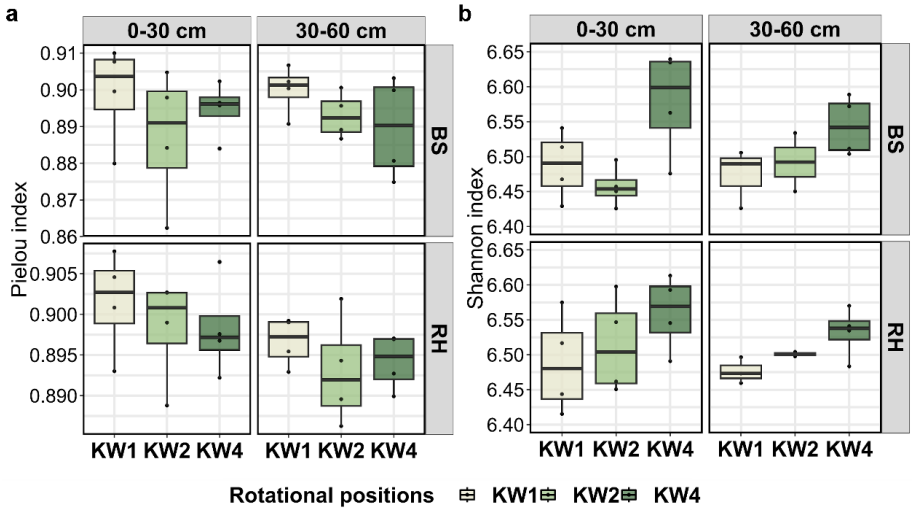

Figure S2.1.7. Effect of the rotational positions on the microbial alpha diversity indices ((a) Pielou and (b) Shannon) of the following winter wheat at onset of stem elongation (BBCH 30), at soil depths 0-30 cm and 30-60 cm, and in two soil compartments bulk soil (BS) and rhizosphere soil (RH). KW1 = first wheat, KW2 = second wheat, and KW4 = fourth wheat after oilseed rape in soil from the experimental farm Hohenschulen in Kiel, Germany.

Table S2.1.1. Impact of rotational position (Rot_pos), plant part (Plant_part) and their interactions on winter wheat total dry weight (Plant DW) as well as total C:N ratio (Plant C:N). For the individual dry weight and C:N ratio of the plant parts (root, stem and leaf) the main effect of rotational position in mentioned. Log transformation was used for Plant DW. Significant values at $p \leq 0.05$ are indicated in bold.

ANOVA results		Plant DW		Root DW		Stem DW		Leaf DW	
	d.f.	F	*p* value	F	*p* value	F	*p* value	F	*p* value
Rot_pos	2	31.08	< 0.001	20.45	< 0.001	24.83	< 0.001	5.43	0.028
Plant_part	2	53.52	< 0.001						
Rot_pos * Plant_part	4	2.13	0.104						
		Plant C:N		Root C:N		Stem C:N		Leaf C:N	
	d.f.	F	*p* value	F	*p* value	F	*p* value	F	*p* value
Rot_pos	2	34.95	< 0.001	25.83	< 0.001	9.20	0.007	24.80	< 0.001
Plant_part	2	391.90	< 0.001						
Rot_pos * Plant_part	4	6.07	0.001						

Table S2.1.2. Impact of rotational position (Rot_pos), soil depth (Depth) and their interactions on root length density (RLD), root tissue density (RTD), root diameter (Rdia), specific root length (SRL), microbial biomass carbon (C_{mic}) and microbial biomass nitrogen (Nmic). The Box-Cox transformation was used for Rida. Significant values at $p \leq 0.05$ are indicated in bold.

ANOVA results		RLD		RTD		Rdia	
	d.f.	F	*p* value	F	*p* value	F	*p* value
Rot_pos	2	15.16	< 0.001	18.52	< 0.001	35.83	< 0.001
Depth	2	4.77	0.017	8.80	0.001	1.94	0.163
Rot_pos * Depth	4	3.438	0.021	3.07	0.033	0.83	0.516
		SRL		C_{mic}		N_{mic}	
	d.f.	F	*p* value	F	*p* value	F	*p* value
Rot_pos	2	22.71	< 0.001	25.45	< 0.001	17.66	< 0.001
Depth	2	100.71	< 0.001	27.11	< 0.001	28.25	< 0.001
Rot_pos * Depth	4	3.09	0.032	0.57	0.686	2.09	0.109

Table S2.1.3. Impact of rotational position (Rot_pos), soil depth (Depth), soil compartment (Comp) and their interactions on soil $N\text{-}NH_4^+$, $N\text{-}NO_3^-$, dissolved organic carbon (DOC) and total nitrogen (TN). The Yeo-Johnson transformation was used for $N\text{-}NH_4^+$, $N\text{-}NO_3^-$ while the Box-Cox transformation was used for DOC and TN. Significant values at $p \leq 0.05$ are indicated in bold.

ANOVA results		$N\text{-}NH_4^+$		$N\text{-}NO_3^-$		DOC		TN	
	d.f.	F	*p* value	F	*p* value	F	*p* value	F	*p* value
Rot_pos	2	10.50	< 0.001	6.97	0.002	10.53	< 0.001	3.80	0.029
Depth	2	11.32	< 0.001	6.87	0.002	1.21	0.307	0.10	0.908
Comp	1	89.81	< 0.001	0.04	0.847	6.61	0.013	21.63	< 0.001
Rot_pos * Depth	4	0.92	0.459	0.21	0.929	0.98	0.426	2.59	0.047
Rot_pos * Comp	2	0.85	0.434	0.09	0.917	3.73	0.030	0.27	0.761
Depth * Comp	2	0.46	0.637	0.20	0.817	2.34	0.106	1.00	0.376
Rot_pos * Depth * Comp	4	0.61	0.655	0.11	0.977	1.96	0.114	0.31	0.873

Table S2.1.4. Impact of rotational position (Rot_pos), soil depth (Depth), soil compartment (Comp) and their interactions on maximum velocity (V_{max}), enzyme substrate affinity (K_m), catalytic efficiency (K_a) and turnover time (Tt) of *β*-glucosidase (BGU V_{max}, BGU K_m, BGU K_a, BGU Tt) and leucine aminopeptidase (LAP V_{max}, LAP K_m, LAP K_a, LAP Tt). The Yeo-Johnson transformation was used for BGU K_m, BGU K_a, BGU Tt, LAP K_a and LAP Tt. Significant values at $p \leq 0.05$ are indicated in bold.

ANOVA results		BGU V_{max}		BGU K_m		BGU K_a		BGU Tt	
	d.f.	F	*p* value	F	*p* value	F	*p* value	F	*p* value
Rot_pos	2	5.33	0.008	10.14	< 0.001	12.59	< 0.001	7.56	0.001
Depth	2	3.21	0.048	7.71	0.001	3.45	0.039	2.16	0.125
Comp	1	0.77	0.384	0.18	0.674	0.29	0.589	1.38	0.245
Rot_pos * Depth	4	8.44	< 0.001	2.41	0.060	2.33	0.068	9.15	< 0.001
Rot_pos * Comp	2	2.34	0.106	14.87	< 0.001	10.35	< 0.001	1.25	0.295
Depth * Comp	2	3.27	0.046	8.83	< 0.001	3.77	0.029	1.72	0.189
Rot_pos * Depth * Comp	4	3.74	0.009	4.06	0.006	4.96	0.002	5.27	0.001
		LAP V_{max}		LAP K_m		LAP K_a		LAP Tt	
	d.f.	F	*p* value	F	*p* value	F	*p* value	F	*p* value
Rot_pos	2	16.75	< 0.001	18.75	< 0.001	8.27	0.001	6.84	0.002
Depth	2	2.44	0.097	2.40	0.100	0.41	0.665	1.99	0.147
Comp	1	75.14	< 0.001	14.71	< 0.001	0.89	0.350	59.71	< 0.001
Rot_pos * Depth	4	5.58	0.001	1.13	0.353	3.14	0.022	6.28	< 0.001
Rot_pos * Comp	2	13.32	< 0.001	6.08	0.004	10.39	< 0.001	11.98	< 0.001
Depth * Comp	2	7.67	0.001	0.92	0.405	1.85	0.168	10.27	< 0.001
Rot_pos * Depth * Comp	4	10.57	< 0.001	8.55	< 0.001	13.30	< 0.001	11.88	< 0.001

Table S2.1.5. Impact of rotational position (Rot_pos), soil depth (Depth) and their interactions on glucose rhizosphere extent (GLU RH extent), activity (GLU activity), hotspot area (GLU hotspot), *β*-glucosidase rhizosphere extent (BGU RH extent), activity (BGU activity), hotspot area (BGU hotspot), leucine aminopeptidase rhizosphere extent (LAP extent), activity (LAP activity) and hotspot percentage (LAP hotspot). The Yeo-Johnson transformation was used for GLU RH extent. Significant values at p ≤ 0.05 are indicated in bold.

ANOVA results		GLU RH extent		GLU activity		GLU hotspot	
	d.f.	F	*p* value	F	*p* value	F	*p* value
Rot_pos	2	3.16	0.066	3.26	0.062	7.27	0.005
Depth	2	15.89	< 0.001	0.72	0.502	37.27	< 0.001
Rot_pos * Depth	4	0.56	0.696	0.80	0.543	0.80	0.544
		BGU RH extent		BGU activity		BGU hotspot	
	d.f.	F	*p* value	F	*p* value	F	*p* value
Rot_pos	2	15.11	0.000	2.91	0.081	0.33	0.726
Depth	2	15.82	0.000	3.13	0.068	3.40	0.056
Rot_pos * Depth	4	3.793	0.021	1.11	0.384	1.87	0.159
		LAP RH extent		LAP activity		LAP hotspot	
	d.f.	F	*p* value	F	*p* value	F	*p* value
Rot_pos	2	1.70	0.211	0.93	0.412	1.18	0.329
Depth	2	2.65	0.098	0.68	0.521	3.99	0.037
Rot_pos * Depth	4	2.52	0.077	0.19	0.940	1.29	0.310

Table S2.1.6. Impact of rotational position (Rot_pos), soil depth (Depth), soil compartment (Comp) and their interactions on plant accessible P (soil P_{cal}), K (soil K_{cal}) and pH. Significant values at p ≤ 0.05 are indicated in bold.

ANOVA results		soil P_{cal}		soil K_{cal}		pH	
	d.f.	F	*p* value	F	*p* value	F	*p* value
Rot_pos	2	36.32	< 0.001	36.16	< 0.001	277.98	< 0.001
Depth	2	148.44	< 0.001	32.94	< 0.001	191.22	< 0.001
Comp	1	28.60	< 0.001	0.15	0.698	88.22	< 0.001
Rot_pos * Depth	4	11.89	< 0.001	3.46	0.014	20.04	< 0.001
Rot_pos * Comp	2	0.45	0.639	1.56	0.219	8.62	0.001
Depth * Comp	2	0.53	0.589	3.06	0.055	6.09	0.004
Rot_pos * Depth * Comp	4	0.51	0.729	6.85	< 0.001	2.13	0.090

Table S2.1.7. Impact of rotational position (Rot_pos), soil depth (Depth) and their interactions on root length proportion for six fine-root diameter classes. Significant values at p ≤ 0.05 are indicated in bold.

Soil cm	Root diameter ≤ 0.05 mm %			Root diameter 0.05 - 0.1 mm %		
	KW1	KW2	KW4	KW1	KW2	KW4
0-30	0.96 ± 0.10	0.87 ± 0.08	0.84 ±	7.94 ± 1.21 b	11.0 ± 1.04 ab	14.11 ±
30-60	1.05 ± 0.13	0.81 ± 0.12	1.09 ±	8.90 ± 1.03 b	6.15 ± 1.07 b	12.28 ±
60-100	1.10 ± 0.17	0.91 ± 0.12	0.79 ±	3.13 ± 0.33	3.20 ± 0.41	5.62 ±
ANOVA	Rotational	F = 2.3; P =		Rotational	F = 19.1; P <	
	Depth	F = 0.56; P =		Depth	F = 48.6; P <	
	Two-way	F = 1.2; P =		Two-way	F = 3.3; P = 0.026	

Soil depth cm	Root diameter 0.1 - 0.5 mm %			Root diameter 0.5 - 1 mm %		
	KW1	KW2	KW4	KW1	KW2	KW4
0-30	85.55 ± 1.31	84.98 ± 1.30	82.01 ±	4.35 ± 0.31 a	2.64 ± 0.25 b	2.77 ±
30-60	85.01 ± 1.54	89.70 ± 1.23 a	83.59 ±	4.29 ± 0.32	2.99 ± 0.30	2.88 ±
60-100	87.02 ± 1.17	89.62 ± 0.79	87.04 ±	7.62 ± 0.82 a	5.73 ± 0.78 b	6.11 ±
ANOVA	Rotational	F = 9.2; P =		Rotational	F = 11.6; P <	
	Depth	F = 8.4; P =		Depth	F = 47.3; P <	
	Two-way	F = 1.9; P =		Two-way	F = 0.1; P = 0.971	
Soil depth cm	Root diameter 1 - 1.5 mm %			Root diameter 1.5 - 2 mm %		
	KW1	KW2	KW4	KW1	KW2	KW4
0-30	0.92 ± 0.10 a	0.43 ± 0.05 ab	0.24 ±	0.22 ± 0.04 a	0.07 ± 0.02 b	0.03 ±
30-60	0.63 ± 0.08 a	0.32 ± 0.04 ab	0.15 ±	0.10 ± 0.02 a	0.02 ± 0.01 ab	0.01 ±
60-100	0.95 ± 0.19 a	0.47 ± 0.11 b	0.39 ±	0.15 ± 0.05 a	0.05 ± 0.02 b	0.04 ±
ANOVA	Rotational	F = 26.9; P <		Rotational	F = 25.9; P <	
	Depth	F = 4.6; P =		Depth	F = 5.1; P = 0.013	
	Two-way	F = 0.4; P =		Two-way	F = 1.6; P = 0.202	

Table S2.1.8. Impact of rotational position (Rot_pos), soil depth (Depth) and their interactions on root length proportion for the coarse root diameter class. Significant values at p ≤ 0.05 are indicated in bold.

Soil depth cm	Root diameter ≥ 2 mm %		
	KW1	KW2	KW4
0-30	0.06 ± 0.02 a	0.01 ± 0.00 b	0.00 ± 0.00 c
30-60	0.02 ± 0.01	0.00 ± 0.00	0.00 ± 0.00
60-100	0.04 ± 0.02	0.01 ± 0.00	0.01 ± 0.00
ANOVA	Rotational position	F = 11.5; P < 0.001	
	Depth	F = 2.6; P = 0.094	
	Two-way	F = 1.1; P = 0.364	

Table S2.1.9. Pearson correlation coefficients of the correlations of plant growth, biochemical and microbial response variables of KW1 at 0-30 cm and 30-60 cm. Asterisks indicate significant correlation coefficients at: *$p \leq 0.05$; **$p \leq 0.01$; ***$p \leq 0.001$.

0-30 cm / 30-60 cm	DW root	NH_4^+ RH	NH_4^+ BS	NO_3^- RH	NO_3^- BS	DOC RH	DOC BS	pH RH	pH BS	P RH	P BS	K RH	K BS	BGU V_{max} RH	BGU V_{max} BS	LAP V_{max} RH	LAP V_{max} BS	C_{mic}	N_{mic}	RLD	SRL	Rdia	Chloroflexi RH	Chloroflexi BS	Gemmatimonadota RH	Gemmatimonadota BS	Acidobacteriota RH	Acidobacteriota BS	Nitrospirota RH	Nitrospirota BS	BGU extent	BGU hotspot	LAP extent	LAP hotspot	GLU extent	GLU hotspot
DW root		-0.17	-0.44	0.51	.963*	0.93	0.58	0.88	-0.72	0.85	0.61	.950*	-0.22	-0.83	0.72	-0.46	0.40	0.38	0.55	0.91	0.32	0.47	-.967*	-0.77	0.77	0.06	-0.10	-.966*	.988*	0.03	-0.70	0.75	-0.21	-0.10	0.07	-0.19
NH_4^+ RH	-0.75		0.93	0.58	-0.05	0.17	-0.84	0.29	-0.20	0.37	0.67	-0.06	0.91	-0.07	-0.81	-0.27	-0.92	-0.02	-0.06	-0.56	-.959*	0.67	0.05	0.61	-0.21	0.49	.968*	0.38	-0.04	0.32	0.94	-0.20	0.98	0.95	-0.94	-0.81
NH_4^+ BS	-0.21	0.64		0.47	-0.28	-0.09	-.980*	-0.04	0.16	0.07	0.43	-0.39	0.79	0.07	-0.94	0.07	-.995**	0.06	-0.04	-0.74	-0.90	0.36	0.37	0.85	-0.54	0.60	0.94	0.65	-0.34	0.47	0.97	-0.26	0.95	0.91	-0.90	-0.75
NO_3^- RH	0.56	-0.14	0.66		0.70	0.78	-0.38	0.64	-0.27	0.76	0.89	0.40	0.27	-0.84	-0.13	-0.03	-0.53	0.71	0.75	0.24	-0.33	0.52	-0.45	0.15	0.00	0.83	0.73	-0.28	0.55	0.74	0.25	0.69	0.73	0.80	-0.82	-0.94
NO_3^- BS	-0.17	-0.51	-0.55	-0.38		.971*	0.40	0.84	-0.58	0.87	0.70	0.86	-0.22	-0.95	0.60	-0.28	0.22	0.59	0.74	0.85	0.27	0.43	-0.89	-0.59	0.58	0.32	0.07	-0.87	0.95	0.30	-0.52	0.88	0.03	0.13	-0.17	-0.41
DOC RH	0.68	-0.20	-0.16	0.20	-0.68		0.24	0.93	-0.69	.958*	0.84	0.88	0.02	-0.92	0.43	-0.41	0.05	0.50	0.65	0.72	0.03	0.63	-0.90	-0.49	0.60	0.35	0.26	-0.81	.950*	0.28	-0.34	0.78	0.22	0.32	-0.36	-0.58
DOC BS	-0.35	0.40	-0.37	-0.75	-0.31	0.37		0.23	-0.35	0.11	-0.27	0.56	-0.68	-0.16	.959*	-0.25	.980*	-0.10	0.04	0.80	0.81	-0.17	-0.54	-0.94	0.70	-0.61	-0.87	-0.77	0.50	-0.52	-0.98	0.29	-0.92	-0.88	0.86	0.70
pH RH	0.62	-0.87	-0.90	-0.26	0.41	0.39	0.10		-0.89	.986*	0.87	0.94	0.27	-0.72	0.33	-0.71	0.03	0.17	0.34	0.59	-0.17	0.84	-0.94	-0.54	0.76	0.11	0.29	-0.77	0.94	-0.01	-0.29	0.50	0.27	0.36	-0.40	-0.62
pH BS	0.35	-0.86	-0.89	-0.37	0.77	-0.05	-0.08	0.90		-0.81	-0.65	-0.90	-0.38	0.35	-0.32	0.94	-0.19	0.28	0.10	-0.45	0.21	-0.86	0.87	0.64	-0.91	0.32	-0.09	0.70	-0.80	0.44	0.73	-0.12	0.25	0.15	-0.11	0.14
P RH	-0.29	-0.19	0.08	0.08	0.78	-0.90	-0.69	-0.15	0.28		0.93	0.88	0.29	-0.79	0.25	-0.61	-0.10	0.30	0.45	0.55	-0.22	0.82	-0.89	-0.42	0.64	0.27	0.41	-0.71	0.91	0.16	-0.14	0.57	0.42	0.51	-0.54	-0.74
P BS	0.83	-0.33	0.38	0.90	-0.51	0.58	-0.51	0.06	-0.20	-0.27		0.64	0.52	-0.72	-0.11	-0.48	-0.46	0.34	0.44	0.24	-0.50	0.85	-0.67	-0.06	0.36	0.51	0.71	-0.41	0.70	0.36	0.31	0.46	0.78	0.84	-0.86	-0.96
K RH	-0.79	0.28	-0.43	-0.92	0.53	-0.56	0.52	-0.01	0.25	0.26	-.999**		0.00	-0.66	0.63	-0.71	0.38	0.09	0.28	0.79	0.14	0.66	-.998**	-0.80	0.91	-0.14	-0.07	-0.93	.977*	-0.21	-0.75	0.52	-0.28	-0.18	0.15	-0.11
K BS	0.30	-0.28	-0.74	-0.53	-0.15	0.70	0.74	0.70	0.42	-0.73	-0.11	0.15		0.21	-0.75	-0.54	-0.74	-0.42	-0.43	-0.61	-.980*	0.75	0.02	0.44	0.01	0.09	0.78	0.37	-0.08	-0.09	1.000*	-0.50	0.83	0.77	-0.74	-0.55
BGU V_{max} RH	0.25	-0.37	0.36	0.68	0.39	-0.47	-.993**	-0.13	0.10	0.77	0.41	-0.42	-0.78		-0.41	0.03	0.00	-0.80	-0.89	-0.72	-0.19	-0.33	0.71	0.32	-0.30	-0.60	-0.24	0.69	-0.80	-0.58	0.31	-0.95	-0.25	-0.35	0.38	0.61
BGU V_{max} BS	0.82	-0.54	-0.45	0.12	-0.35	0.93	0.25	0.70	0.32	-0.72	0.54	-0.50	0.77	-0.34		-0.13	0.91	0.18	0.32	0.93	0.86	-0.16	-0.63	-0.92	0.65	-0.36	-0.76	-0.86	0.62	-0.27	-0.99	0.55	-0.78	-0.72	0.69	0.48
LAP V_{max} RH	0.51	0.16	0.33	0.46	-0.93	0.88	0.23	-0.08	-0.50	-0.84	0.70	-0.70	0.33	-0.33	0.65		-0.13	0.57	0.42	-0.19	0.36	-0.84	0.67	0.52	-0.84	0.50	-0.09	0.47	-0.56	0.64	0.31	0.22	0.78	0.84	-0.86	-0.96
LAP V_{max} BS	0.44	-0.77	-0.19	0.38	0.68	-0.35	-0.84	0.40	0.61	0.72	0.27	-0.26	-0.38	0.85	-0.05	-0.48		-0.16	-0.06	0.69	0.85	-0.34	-0.36	-0.86	0.57	-0.67	-0.95	-0.62	0.31	-0.56	-0.95	0.17	-0.97	-0.94	0.93	0.80
C_{mic}	0.58	-0.16	0.64	1.000**	-0.37	0.20	-0.75	-0.24	-0.35	0.08	0.91	-0.92	-0.52	0.68	0.14	0.46	0.39		.981*	0.42	0.30	-0.20	-0.16	0.11	-0.30	0.84	0.23	-0.24	0.30	0.90	-0.18	0.89	0.38	0.47	-0.50	-0.71
N_{mic}	0.68	-0.47	0.38	0.93	-0.04	0.09	-0.89	0.03	0.00	0.29	0.84	-0.85	-0.49	0.83	0.17	0.22	0.69	0.93		0.57	0.34	-0.08	-0.35	-0.06	-0.10	0.77	0.18	-0.42	0.48	0.82	-0.28	.958*	0.28	0.37	-0.41	-0.63
RLD	0.95	-0.91	-0.33	0.49	0.15	0.44	-0.50	0.71	0.57	-0.01	0.69	-0.66	0.20	0.43	0.68	0.21	0.69	0.51	0.72		0.69	0.07	-0.81	-0.86	0.67	-0.07	-0.46	-.955*	0.83	-0.01	-0.89	0.78	-0.50	-0.41	0.38	0.13
SRL	0.51	-0.92	-0.52	0.13	0.75	-0.19	-0.60	0.69	0.85	0.55	0.15	-0.12	-0.03	0.60	0.18	-0.48	0.93	0.14	0.49	0.76		-0.65	-0.16	-0.60	0.18	-0.25	-0.86	-0.49	0.18	-0.08	-.999*	0.46	-0.87	-0.81	0.79	0.61
Rdia	-0.19	0.67	.994**	0.64	-0.64	-0.06	-0.29	-0.89	-0.93	-0.03	0.40	-0.45	-0.66	0.27	-0.37	0.42	-0.28	0.63	0.34	-0.34	-0.60		-0.65	-0.17	0.58	0.04	0.58	-0.34	0.60	-0.15	0.67	0.02	0.96	0.99	-0.99	-0.99
Chloroflexi RH	-0.26	0.78	0.46	-0.03	-0.89	0.45	0.62	-0.54	-0.80	-0.74	0.05	-0.08	0.20	-0.65	0.09	0.69	-0.93	-0.04	-0.39	-0.56	-.961*	0.55		0.78	-0.88	0.08	0.04	0.94	-.989*	0.14	0.71	-0.57	0.22	0.12	-0.08	0.18
Chloroflexi BS	-0.23	0.80	0.62	0.15	-0.92	0.40	0.45	-0.64	-0.89	-0.66	0.17	-0.20	0.03	-0.49	0.03	0.72	-0.85	0.14	-0.23	-0.52	-0.95	0.70	.981*		-0.89	0.56	0.65	0.91	-0.73	0.52	1.000**	-0.35	0.85	0.79	-0.76	-0.57
Gemmatimonadota RH	-.952*	0.70	-0.02	-0.76	0.13	-0.49	0.60	-0.42	-0.23	0.08	-0.90	0.89	0.00	-0.51	-0.62	-0.43	-0.58	-0.78	-0.87	-0.93	-0.54	-0.02	0.34	0.24		-0.54	-0.31	-0.84	0.80	-0.60	-.999*	0.17	-0.82	-0.75	0.73	0.53
Gemmatimonadota BS	-0.56	0.16	-0.65	-.999**	0.35	-0.17	0.77	0.25	0.35	-0.11	-0.89	0.91	0.55	-0.70	-0.11	-0.43	-0.41	-.999**	-0.94	-0.50	-0.16	-0.63	0.06	-0.12	0.77		0.69	0.17	0.05	.980*	0.44	0.57	0.86	0.91	-0.92	-0.99
Acidobacteriota RH	-0.59	0.85	0.91	0.30	-0.40	-0.40	-0.14	-.999**	-0.89	0.17	-0.03	-0.02	-0.73	0.18	-0.71	0.07	-0.36	0.28	0.02	-0.68	-0.66	0.90	0.51	0.62	0.38	-0.29		0.35	0.00	0.55	0.85	0.01	1.000*	0.99	-0.99	-0.91
Acidobacteriota BS	-0.25	-0.29	-0.07	-0.01	0.87	-0.87	-0.64	0.00	0.42	.988*	-0.32	0.32	-0.61	0.72	-0.64	-0.89	0.76	-0.01	0.24	0.05	0.64	-0.18	-0.82	-0.76	0.07	-0.02	0.03		-0.94	0.16	0.88	-0.66	0.49	0.39	-0.36	-0.11
Nitrospirota RH	0.87	-0.41	0.29	0.87	-0.46	0.61	-0.49	0.16	-0.12	-0.28	.996**	-.989*	-0.05	0.39	0.60	0.68	0.31	0.87	0.84	0.75	0.22	0.31	0.00	0.11	-0.93	-0.86	-0.13	-0.32		0.00	-0.63	0.68	-0.12	-0.01	-0.02	-0.28
Nitrospirota BS	0.38	-0.25	0.56	0.88	0.06	-0.24	-.966*	-0.24	-0.14	0.53	0.65	-0.67	-0.77	0.94	-0.20	-0.01	0.69	0.88	0.93	0.45	0.40	0.49	-0.40	-0.22	-0.64	-0.90	0.29	0.45	0.62		0.34	0.62	0.80	0.85	-0.87	-0.97
BGU extent	-0.87	0.98	0.47	-0.45	-0.44	-0.28	0.94	-0.87	-0.71	-0.52	-0.53	0.49	-0.20	-0.97	-0.83	0.10	-0.98	-0.47	-0.78	-0.98	-0.92	0.49	0.83	0.75	0.84	0.48	0.85	-0.52	-0.59	-0.74		-0.49	0.84	0.78	-0.76	-0.57
BGU hotspot	0.93	-0.46	0.03	0.64	-0.52	0.84	-0.19	0.38	0.01	-0.54	0.91	-0.89	0.31	0.08	0.84	0.79	0.13	0.65	0.61	0.77	0.17	0.08	0.10	0.15	-0.88	-0.62	-0.36	-0.54	0.93	0.31	-0.61		0.06	0.16	-0.20	-0.44
LAP extent	-0.91	0.95	0.39	-0.53	-0.36	-0.36	0.96	-0.83	-0.65	-0.44	-0.60	0.57	-0.11	-0.99	-0.87	0.01	-0.95	-0.55	-0.83	-0.99	-0.88	0.41	0.77	0.69	0.88	0.56	0.81	-0.45	-0.66	-0.80	1.00	-0.68		0.99	-0.99	-0.92
LAP hotspot	0.84	-0.26	0.56	1.000**	-0.59	0.98	-0.75	-0.02	-0.29	-0.51	.997*	-.999*	-0.77	0.67	0.88	0.83	0.26	1.000**	0.92	0.65	0.09	0.55	0.11	0.24	-0.87	-1.000**	0.06	-0.51	0.99	0.94	-0.47	0.98	-0.54		-.999*	-0.96
GLU extent	-0.76	1.000*	0.64	-0.27	-0.61	-0.08	0.85	-0.95	-0.84	-0.68	-0.35	0.31	-0.39	-0.90	-0.70	0.29	-1.000*	-0.29	-0.64	-0.91	-0.98	0.65	0.92	0.86	0.71	0.30	0.94	-0.68	-0.42	-0.60	0.98	-0.45	0.96	-0.28		0.97
GLU hotspot	0.95	-0.50	0.33	0.96	-0.36	0.89	-0.89	0.24	-0.03	-0.27	0.98	-0.97	-0.58	0.84	0.97	0.66	0.50	0.97	0.99	0.82	0.34	0.31	-0.15	-0.02	-0.97	-0.97	-0.20	-0.27	0.99	1.00	-0.68	1.00	-0.74	0.97	-0.52	

Table S2.1.11. Pearson correlation coefficients of the correlations of plant growth, biochemical and microbial response variables of KW2 at 0-30 cm and 30-60 cm. Asterisks indicate significant correlation coefficients at: *$p \leq 0.05$; **$p \leq 0.01$; ***$p \leq 0.001$.

0-30 cm / 30-60 cm	DW root	NH_4^+ RH	NH_4^+ BS	NO_3^- RH	NO_3^- BS	DOC RH	DOC BS	pH RH	pH BS	P RH	P BS	K RH	K BS	BGU V_{max} RH	BGU V_{max} BS	LAP V_{max} RH	LAP V_{max} BS	C_{mic}	N_{mic}	RLD	SRL	Rdia	Chloroflexi RH	Chloroflexi BS	Gemmatimonadota RH	Gemmatimonadota BS	Acidobacteriota RH	Acidobacteriota BS	Nitrospirota RH	Nitrospirota BS	BGU extent	BGU hotspot	LAP extent	LAP hotspot	GLU extent	GLU hotspot
DW root		0.51	0.27	-0.04	0.32	0.02	-0.59	0.03	0.34	-0.61	-0.48	-0.71	-0.24	-0.25	0.02	0.52	0.19	-0.59	0.15	0.87	0.62	-0.68	-0.26	-0.13	-0.81	-0.88	-0.32	-.982*	-0.34	-0.94	-0.34	0.42	0.69	-0.31	-0.47	0.77
NH_4^+ RH	-0.06		0.93	0.32	.958*	0.83	0.21	0.02	0.68	0.36	0.14	0.11	0.50	0.29	-0.66	0.82	-0.39	-0.13	-0.61	0.12	-0.21	0.29	-0.79	-0.43	-0.03	-0.12	0.64	-0.34	0.29	-0.67	-0.95	0.00	0.99	0.58	0.43	0.97
NH_4^+ BS	0.16	0.24		0.11	0.88	.968*	0.24	-0.26	0.83	0.57	0.08	0.20	0.43	0.16	-0.55	0.89	-0.25	-0.19	-0.86	-0.20	-0.53	0.50	-0.62	-0.18	0.09	0.19	0.82	-0.10	0.20	-0.53	-0.96	-0.35	0.99	0.58	0.43	0.97
NO_3^- RH	0.81	0.53	0.20		0.55	0.11	0.76	0.92	-0.45	0.33	0.89	0.65	0.89	.969*	-0.88	-0.28	-.968*	0.82	0.20	0.12	0.20	0.32	-0.83	-.987*	0.56	-0.07	0.27	0.14	0.93	0.20	-0.63	0.69	0.26	0.97	.998*	0.14
NO_3^- BS	-0.55	0.75	-0.33	0.00		0.83	0.47	0.22	0.50	0.53	0.41	0.38	0.73	0.55	-0.85	0.65	-0.63	0.16	-0.57	0.00	-0.26	0.46	-0.91	-0.62	0.23	0.01	0.74	-0.14	0.55	-0.45	-1.000**	0.09	0.92	0.79	0.67	0.87
DOC RH	0.93	0.21	0.44	0.89	-0.43		0.39	-0.29	0.78	0.74	0.19	0.38	0.50	0.21	-0.56	0.79	-0.30	-0.05	-0.94	-0.44	-0.72	0.69	-0.56	-0.14	0.30	0.43	0.93	0.15	0.28	-0.31	-0.99	-0.49	0.95	0.72	0.59	0.91
DOC BS	0.94	-0.18	0.43	0.67	-0.74	0.92		0.54	-0.26	0.82	.963*	.986*	0.93	0.90	-0.82	-0.23	-0.89	0.90	-0.24	-0.55	-0.44	0.83	-0.63	-0.68	.951*	0.59	0.67	0.70	0.95	0.57	-0.50	0.10	0.10	0.92	0.97	-0.02
pH RH	0.20	0.72	0.83	0.54	0.13	0.54	0.31		-0.72	-0.01	0.75	0.43	0.64	0.83	-0.63	-0.54	-0.80	0.77	0.57	0.35	0.52	-0.02	-0.60	-0.90	0.37	-0.30	-0.13	0.01	0.76	0.24	-0.29	0.89	-0.12	0.81	0.90	-0.24
pH BS	0.71	-0.67	0.25	0.19	-.975*	0.57	0.84	-0.12		0.25	-0.46	-0.25	-0.13	-0.41	0.00	.968*	0.33	-0.66	-0.84	-0.16	-0.51	0.20	-0.11	0.37	-0.30	0.12	0.53	-0.25	-0.37	-0.65	-0.62	-0.64	0.89	0.01	-0.16	0.93
P RH	-0.27	-0.83	-0.69	-0.68	-0.26	-0.59	-0.30	-.973*	0.20		0.64	0.87	0.72	0.54	-0.63	0.19	-0.56	0.51	-0.73	-0.83	-0.86	.997**	-0.45	-0.26	0.85	0.84	0.94	0.75	0.64	0.40	-0.72	-0.45	0.37	0.99	.998*	0.26
P BS	-.975*	-0.12	-0.32	-0.89	0.46	-.989*	-0.93	-0.41	-0.62	0.48		0.92	0.93	.970*	-0.83	-0.39	-0.95	.964*	0.01	-0.34	-0.18	0.65	-0.66	-0.81	0.88	0.38	0.47	0.58	.986*	0.56	-0.42	0.35	0.02	0.89	0.95	-0.10
K RH	-0.37	-0.89	-0.42	-0.82	-0.39	-0.62	-0.28	-0.84	0.27	0.94	0.55		0.86	0.82	-0.72	-0.26	-0.80	0.87	-0.30	-0.68	-0.55	0.88	-0.50	-0.54	.988*	0.71	0.69	0.81	0.88	0.66	-0.42	-0.04	0.01	0.88	0.95	-0.10
K BS	-0.94	0.37	-0.20	-0.57	0.80	-0.83	-.963*	-0.04	-0.91	0.05	0.88	0.08		.954*	-.973*	-0.02	-.973*	0.79	-0.25	-0.27	-0.26	0.70	-0.87	-0.86	0.77	0.31	0.68	0.39	.970*	0.24	-0.74	0.29	0.40	1.00	1.00	0.29
BGU V_{max} RH	0.85	-0.56	0.15	0.38	-0.89	0.69	0.90	-0.11	.971*	0.13	-0.75	0.14	-.976*		-0.91	-0.28	-.995**	0.90	0.05	-0.13	-0.03	0.53	-0.80	-0.93	0.74	0.18	0.43	0.37	.992**	0.36	-0.57	0.51	0.19	0.95	0.99	0.07
BGU V_{max} BS	0.87	-0.15	-0.35	0.68	-0.34	0.67	0.67	-0.21	0.53	0.07	-0.77	-0.16	-0.78	0.71		-0.15	0.94	-0.65	0.28	0.11	0.17	-0.59	.962*	0.89	-0.60	-0.14	-0.66	-0.18	-0.91	-0.01	0.86	-0.34	-0.58	-0.99	-0.96	-0.49
LAP V_{max} RH	0.13	0.80	0.77	0.53	0.25	0.47	0.21	.992**	-0.24	-.981*	-0.34	-0.87	0.06	-0.22	-0.25		0.18	-0.62	-0.76	0.03	-0.35	0.13	-0.30	0.16	-0.35	-0.06	0.51	-0.41	-0.26	-0.78	-0.70	-0.43	0.93	0.12	-0.06	0.96
LAP V_{max} BS	-0.94	-0.09	0.11	-0.87	0.28	-0.84	-0.76	-0.10	-0.48	0.24	0.91	0.44	0.80	-0.67	-.950*	-0.06		-0.85	0.02	0.11	0.05	-0.54	0.86	0.94	-0.71	-0.16	-0.49	-0.31	-.987*	-0.27	0.66	-0.49	-0.29	-0.98	-1.000*	-0.18
C_{mic}	-0.90	-0.37	-0.33	-.972*	0.23	-.974*	-0.82	-0.55	-0.40	0.65	.967*	0.74	0.72	-0.56	-0.70	-0.51	0.88		0.20	-0.33	-0.09	0.54	-0.46	-0.72	0.87	0.38	0.27	0.64	0.91	0.72	-0.16	0.40	-0.25	0.73	0.84	-0.36
N_{mic}	-0.54	0.86	0.26	0.04	0.82	-0.24	-0.56	0.60	-0.86	-0.63	0.35	-0.59	0.74	-0.86	-0.62	0.69	0.42	0.11		0.62	0.87	-0.70	0.24	-0.19	-0.26	-0.60	-0.88	-0.28	-0.04	0.19	0.97	0.76	-0.98	-0.62	-0.48	-0.96
RLD	.997**	-0.07	0.22	0.80	-0.59	0.94	.961*	0.23	0.74	-0.29	-.979*	-0.37	-.952*	0.86	0.83	0.16	-0.91	-0.90	-0.54		0.93	-0.87	-0.12	-0.24	-0.74	-.999**	-0.67	-0.91	-0.25	-0.64	0.12	0.74	0.29	-0.70	-0.81	0.40
SRL	-.984*	0.02	0.00	-0.83	0.44	-0.89	-0.86	-0.11	-0.62	0.22	0.94	0.37	0.89	-0.79	-0.94	-0.05	.984*	0.89	0.52	-.968*		-0.86	0.01	-0.27	-0.57	-0.91	-0.83	-0.70	-0.15	-0.31	0.82	0.85	-0.51	-.999*	-0.98	-0.41
Rdia	0.80	-0.50	-0.37	0.41	-0.59	0.53	0.68	-0.43	0.73	0.35	-0.65	0.18	-0.84	0.85	0.93	-0.49	-0.80	-0.49	-0.86	0.77	-0.84		-0.39	-0.23	0.87	0.88	0.91	0.80	0.63	0.47	-0.65	-0.46	0.28	0.98	.999*	0.17
Chloroflexi RH	0.87	0.45	0.26	.992**	-0.12	0.94	0.75	0.54	0.30	-0.66	-0.94	-0.78	-0.66	0.48	0.70	0.51	-0.89	-.993**	-0.05	0.86	-0.87	0.46		0.88	-0.36	0.10	-0.56	0.09	-0.78	0.25	0.96	-0.43	-0.77	-0.93	-0.85	-0.69
Chloroflexi BS	-0.30	0.07	0.88	-0.28	-0.21	-0.03	0.02	0.60	0.04	-0.40	0.16	-0.08	0.17	-0.14	-0.73	0.56	0.57	0.16	0.35	-0.23	0.46	-0.64	-0.23		-0.44	0.20	-0.24	0.01	-0.88	-0.04	0.75	-0.73	-0.42	-.998*	-0.99	-0.31
Gemmatimonadota RH	0.70	-0.76	-0.15	0.16	-0.86	0.44	0.71	-0.44	0.92	0.45	-0.54	0.41	-0.87	0.94	0.71	-0.53	-0.57	-0.31	-.978*	0.70	-0.67	0.91	0.25	-0.33		0.78	0.63	0.89	0.82	0.76	-0.28	-0.11	-0.14	0.81	0.90	-0.25
Gemmatimonadota BS	0.59	-0.38	0.70	0.23	-0.89	0.64	0.83	0.33	0.86	-0.20	-0.60	0.00	-0.76	0.78	0.19	0.21	-0.28	-0.45	-0.50	0.64	-0.44	0.34	0.34	0.50	0.60		0.67	0.93	0.30	0.67	-0.13	-0.70	-0.29	0.70	0.82	-0.39
Acidobacteriota RH	0.91	0.21	0.50	0.88	-0.44	.998**	0.92	0.58	0.57	-0.62	-.978*	-0.63	-0.81	0.68	0.62	0.51	-0.80	-.964*	-0.22	0.93	-0.85	0.49	0.93	0.03	0.42	0.67		0.48	0.52	0.06	-0.95	-0.48	0.73	0.95	0.88	0.65
Acidobacteriota BS	0.85	-0.14	-0.38	0.67	-0.31	0.65	0.65	-0.23	0.51	0.08	-0.75	-0.15	-0.76	0.69	1.000**	-0.26	-0.95	-0.68	-0.61	0.82	-0.93	0.93	0.69	-0.75	0.70	0.16	0.60		0.46	0.89	0.11	-0.43	-0.51	0.52	0.66	-0.60
Nitrospirota RH	0.00	0.46	-0.74	0.32	0.71	-0.10	-0.35	-0.24	-0.56	0.02	0.03	-0.29	0.26	-0.37	0.39	-0.15	-0.34	-0.11	0.25	-0.07	-0.17	0.14	0.22	-0.82	-0.26	-0.81	-0.15	0.41		0.41	-0.56	0.40	0.18	0.95	0.99	0.06
Nitrospirota BS	0.65	0.72	0.32	.965*	0.17	0.81	0.53	0.71	-0.01	-0.84	-0.78	-0.94	-0.38	0.17	0.47	0.71	-0.71	-0.91	0.29	0.64	-0.66	0.16	0.94	-0.12	-0.09	0.14	0.81	0.47	0.32		0.43	-0.10	-0.76	0.20	0.37	-0.83
BGU extent	0.98	-0.06	-0.11	0.89	-0.97	0.84	0.89	0.04	0.99	-0.18	-0.91	-0.44	-0.98	.999*	0.97	-0.02	-.999*	-0.87	-0.77	0.96	-1.00	0.91	0.88	-0.59	0.92	0.55	0.80	0.96	0.46	0.75		-0.15	-0.91	-0.79	-0.68	-0.86
BGU hotspot	-0.79	-0.56	-0.34	-.990*	0.03	-0.92	-0.69	-0.65	-0.20	0.76	0.89	0.86	0.56	-0.37	-0.60	-0.63	0.81	.978*	-0.09	-0.79	0.79	-0.33	-.989*	0.14	-0.11	-0.31	-0.91	-0.59	-0.21	-.977*	-0.81		-0.26	0.72	0.83	-0.37
LAP extent	0.09	-0.97	-0.98	-0.17	-0.05	-0.26	-0.16	-0.94	0.18	0.88	0.12	0.72	-0.13	0.25	0.54	-0.96	-0.27	0.21	-0.84	0.03	-0.22	0.67	-0.18	-0.95	0.66	-0.63	-0.32	0.56	0.99	-0.41	0.30	0.31		0.48	0.32	0.99
LAP hotspot	-0.59	-0.89	-0.87	-0.77	0.62	-0.83	-0.76	-0.93	-0.51	0.98	0.74	.998*	0.55	-0.44	-0.14	-0.91	0.42	0.80	-0.28	-0.63	0.47	0.02	-0.78	-0.51	0.00	-0.98	-0.86	-0.12	0.64	-0.91	-0.39	0.86	0.76		0.99	0.37
GLU extent	0.69	0.83	0.80	0.85	-0.72	0.90	0.84	0.88	0.62	-0.94	-0.82	-.997*	-0.65	0.55	0.27	0.85	-0.54	-0.87	0.15	0.73	-0.59	0.11	0.86	0.39	0.13	.999*	0.92	0.25	-0.53	0.95	0.51	-0.92	-0.66	-0.99		0.21
GLU hotspot	0.90	-0.28	-0.32	0.76	-0.89	0.70	0.77	-0.18	0.94	0.04	-0.80	-0.24	-0.92	0.96	.999*	-0.23	-0.97	-0.74	-0.89	0.88	-0.95	0.98	0.76	-0.75	0.98	0.35	0.65	.998*	0.64	0.58	0.98	-0.66	0.51	-0.18	0.31	

Table S2.1.11. Pearson correlation coefficients of the correlations of plant growth, biochemical and microbial response variables of KW4 at 0-30 cm and 30-60 cm. Asterisks indicate significant correlation coefficients at: *$p \leq 0.05$; **$p \leq 0.01$; ***$p \leq 0.001$.

0-30 cm / 30-60 cm	DW root	NH_4^+ RH	NH_4^+ BS	NO_3^- RH	NO_3^- BS	DOC RH	DOC BS	pH RH	pH BS	P RH	P BS	K RH	K BS	BGU V_{max} RH	BGU V_{max} BS	LAP V_{max} RH	LAP V_{max} BS	C_{mic}	N_{mic}	RLD	SRL	Rdia	Chloroflexi RH	Chloroflexi BS	Gemmatimonadota RH	Gemmatimonadota BS	Acidobacteriota RH	Acidobacteriota BS	Nitrospirota RH	Nitrospirota BS	BGU extent	BGU hotspot	LAP extent	LAP hotspot	GLU extent	GLU hotspot
DW root		-0.76	0.50	0.15	0.25	-0.13	0.11	0.46	-0.05	0.33	-0.46	0.72	0.47	0.25	-0.63	-0.59	-0.53	0.29	0.56	0.79	-0.78	0.70	-.969*	-0.74	-0.05	-0.44	0.57	-0.59	0.43	-.979*	0.59	0.33	-0.84	-0.78	-0.54	-0.64
NH_4^+ RH	-0.49		0.15	0.52	0.44	0.74	-0.62	0.22	0.59	-0.02	0.21	-0.52	-0.82	0.16	0.18	0.88	0.73	0.38	0.06	-0.26	.960*	-0.84	0.88	0.64	0.42	0.88	-0.07	0.62	0.06	0.65	-0.99	-0.63	0.98	0.99	0.98	-0.10
NH_4^+ BS	0.15	0.66		0.81	0.87	0.70	-0.78	.986*	0.83	0.19	-0.16	0.18	-0.19	0.80	-0.87	0.12	-0.07	0.83	0.79	0.72	-0.01	0.11	-0.27	-0.46	0.20	0.39	0.92	-0.30	0.49	-0.65	-0.72	-0.54	0.42	0.51	0.76	-0.85
NO_3^- RH	-0.19	-0.51	-.972*		.993**	.957*	-0.67	0.89	0.72	0.56	-0.45	0.28	-0.72	0.39	-0.42	0.65	0.53	.988*	0.88	0.69	0.48	-0.46	0.04	0.14	0.71	0.82	0.51	0.32	0.77	-0.26	-.997*	-0.38	0.90	0.94	1.000*	-0.32
NO_3^- BS	0.25	-0.53	-0.79	0.86		0.93	-0.70	0.94	0.74	0.53	-0.43	0.30	-0.63	0.47	-0.52	0.55	0.43	.992**	0.91	0.74	0.38	-0.36	-0.04	0.02	0.64	0.75	0.61	0.21	0.76	-0.36	-0.98	-0.39	0.85	0.90	0.99	-0.42
DOC RH	0.16	-0.92	-0.68	0.50	0.31		-0.76	0.78	0.78	0.41	-0.26	0.03	-0.83	0.39	-0.29	0.79	0.64	0.90	0.71	0.45	0.69	-0.63	0.33	0.30	0.68	0.93	0.40	0.44	0.61	0.01	-.999*	-0.53	0.92	0.95	1.000**	-0.29
DOC BS	0.55	-.979*	-0.70	0.59	0.68	0.83		-0.75	-.997**	0.23	-0.34	0.43	0.35	-0.86	0.66	-0.36	-0.08	-0.60	-0.37	-0.16	-0.40	0.18	-0.35	0.18	-0.03	-0.58	-0.73	0.14	-0.06	0.09	0.76	0.93	-0.47	-0.56	-0.80	0.82
pH RH	-0.38	0.24	0.47	-0.61	-0.91	0.07	-0.43		0.80	0.33	-0.28	0.26	-0.33	0.70	-0.78	0.25	0.09	0.91	0.87	0.77	0.10	-0.02	-0.24	-0.33	0.36	0.50	0.84	-0.14	0.62	-0.59	-0.84	-0.47	0.58	0.66	0.87	-0.74
pH BS	0.11	-0.24	0.34	-0.55	-0.70	0.43	0.06	0.84		-0.17	0.28	-0.36	-0.35	0.86	-0.69	0.35	0.09	0.65	0.44	0.24	0.38	-0.16	0.29	-0.20	0.07	0.59	0.76	-0.14	0.13	-0.15	-0.77	-0.90	0.48	0.57	0.80	-0.81
P RH	0.79	-0.82	-0.48	0.44	0.74	0.53	0.91	-0.66	-0.15		-.983*	0.86	-0.56	-0.44	0.18	0.45	0.60	0.63	0.75	0.73	0.18	-0.41	-0.34	0.38	0.90	0.42	-0.13	0.57	0.95	-0.25	-0.51	0.55	0.79	0.72	0.46	0.71
P BS	0.85	0.03	0.59	-0.55	-0.06	-0.35	0.05	-0.25	0.02	0.40		-0.93	0.39	0.46	-0.15	-0.27	-0.46	-0.55	-0.72	-0.76	0.00	0.24	0.50	-0.25	-0.80	-0.24	0.12	-0.44	-0.92	0.37	0.33	-0.66	-0.65	-0.57	-0.28	-0.83
K RH	0.50	-0.88	-0.78	0.73	0.86	0.69	.958*	-0.66	-0.23	0.92	0.03		-0.05	-0.36	-0.04	-0.08	0.11	0.41	0.67	0.82	-0.36	0.12	-0.77	-0.08	0.55	-0.08	0.02	0.12	0.80	-0.62	0.14	0.73	0.23	0.12	-0.20	0.99
K BS	0.01	0.24	0.73	-0.86	-0.94	-0.07	-0.40	0.90	0.87	-0.47	0.20	-0.64		0.16	-0.30	-.990**	-.961*	-0.64	-0.45	-0.18	-0.91	0.95	-0.55	-0.78	-0.86	-.964*	0.18	-0.87	-0.58	-0.43	0.87	0.18	-0.99	-0.97	-0.84	-0.27
BGU V_{max} RH	-0.55	-0.26	-0.89	0.93	0.62	0.39	0.30	-0.35	-0.48	0.07	-0.81	0.44	-0.72		-0.91	-0.17	-0.43	0.37	0.27	0.20	-0.11	0.35	-0.03	-0.65	-0.37	0.10	0.92	-0.62	-0.13	-0.43	-0.35	-0.83	-0.01	0.09	0.40	-0.99
BGU V_{max} BS	0.18	-0.10	0.53	-0.71	-0.79	0.24	-0.08	0.84	.976*	-0.21	0.19	-0.36	0.94	-0.65		0.35	0.54	-0.46	-0.49	-0.53	0.40	-0.55	0.43	0.82	0.28	0.07	-.993**	0.73	-0.11	0.77	0.23	0.53	0.14	0.03	-0.29	1.000*
LAP V_{max} RH	-0.19	-0.72	-0.67	0.49	0.14	0.93	0.60	0.28	0.46	0.21	-0.64	0.46	0.01	0.52	0.25		.958**	0.55	0.33	0.04	.957*	-.974*	0.66	0.82	0.79	.958*	-0.24	0.87	0.46	0.54	-0.87	-0.24	0.99	0.97	0.84	0.27
LAP V_{max} BS	-0.16	0.76	0.94	-0.93	-0.91	-0.66	-0.84	0.66	0.39	-0.73	0.29	-0.93	0.79	-0.73	0.55	-0.53		0.46	0.31	0.07	0.88	-.974*	0.54	0.91	0.87	0.86	-0.44	.970*	0.54	0.54	-0.70	0.05	0.91	0.86	0.66	0.52
C_{mic}	0.05	0.83	0.92	-0.81	-0.59	-0.91	-0.81	0.20	-0.04	-0.51	0.55	-0.78	0.44	-0.73	0.17	-0.88	0.87		0.94	0.79	0.36	-0.36	-0.11	0.05	0.71	0.73	0.55	0.26	0.84	-0.39	-1.00	-0.27	0.90	0.94	1.000*	-0.33
N_{mic}	0.91	-0.49	0.31	-0.42	-0.09	0.27	0.47	0.03	0.50	0.60	0.77	0.30	0.39	-0.70	0.56	-0.02	0.06	0.06		0.95	0.08	-0.15	-0.42	-0.10	0.68	0.50	0.54	0.13	0.92	-0.61	-.999*	-0.01	0.91	0.95	1.000**	-0.30
RLD	0.81	-0.11	0.15	-0.05	0.46	-0.29	0.27	-0.73	-0.45	0.65	0.84	0.38	-0.36	-0.37	-0.33	-0.61	-0.16	0.28	0.53		-0.23	0.12	-0.69	-0.30	0.53	0.20	0.55	-0.07	0.87	-0.80	-0.98	0.20	0.84	0.90	0.99	-0.43
SRL	-0.27	0.68	0.12	0.12	0.26	-0.80	-0.52	-0.54	-0.87	-0.26	0.07	-0.26	-0.52	0.17	-0.77	-0.75	0.10	0.49	-0.57	0.35		-.958*	0.85	0.83	0.59	0.90	-0.29	0.81	0.19	0.72	-0.89	-0.39	0.99	0.98	0.86	0.22
Rdia	0.23	-0.43	0.19	-0.42	-0.54	0.58	0.25	0.73	.980*	0.04	0.04	-0.03	0.77	-0.41	0.93	0.56	0.22	-0.20	0.59	-0.38	-0.95		-0.72	-0.93	-0.75	-0.87	0.45	-0.95	-0.35	-0.69	0.74	0.11	-0.94	-0.89	-0.70	-0.46
Chloroflexi RH	0.76	-0.38	0.45	-0.60	-0.36	0.26	0.30	0.31	0.71	0.37	0.68	0.08	0.63	-0.79	0.78	0.04	0.26	0.14	.958*	0.30	-0.67	0.76		0.67	0.08	0.57	-0.36	0.54	-0.36	0.90	-0.93	-0.53	1.000**	0.99	0.90	0.14
Chloroflexi BS	-0.03	-0.35	0.11	-0.33	-0.59	0.59	0.15	0.83	.967*	-0.15	-0.21	-0.13	0.75	-0.24	0.89	0.66	0.22	-0.26	0.35	-0.61	-0.92	.964*	0.56		0.65	0.62	-0.75	.972*	0.21	0.80	-0.42	0.17	0.72	0.64	0.37	0.78
Gemmatimonadota RH	-0.09	-0.06	-0.63	0.79	0.87	-0.10	0.24	-0.89	-0.94	0.34	-0.18	0.50	-.984*	0.69	-.987*	-0.15	-0.68	-0.30	-0.48	0.36	0.66	-0.87	-0.71	-0.84		0.76	-0.19	0.81	0.88	0.08	-0.72	0.25	0.92	0.88	0.68	0.50
Gemmatimonadota BS	-0.37	0.39	0.61	-0.72	-.967**	-0.10	-0.57	.984*	0.78	-0.73	-0.16	-0.77	0.92	-0.45	0.81	0.11	0.78	0.37	0.01	-0.66	-0.40	0.64	0.30	0.73	-0.88		0.05	0.71	0.52	0.35	-0.97	-0.42	0.99	1.000**	0.95	0.00
Acidobacteriota RH	-0.86	0.15	-0.19	0.11	-0.41	0.25	-0.30	0.67	0.36	-0.67	-0.88	-0.38	0.28	0.44	0.24	0.58	0.13	-0.28	-0.61	-.994**	-0.26	0.28	-0.40	0.52	-0.27	0.60		-0.64	0.17	-0.73	-0.36	-0.58	-0.01	0.10	0.41	-0.99
Acidobacteriota BS	-0.06	-0.44	-0.02	-0.20	-0.49	0.68	0.24	0.77	0.93	-0.09	-0.29	-0.03	0.66	-0.12	0.82	0.75	0.10	-0.38	0.31	-0.64	-0.94	0.94	0.50	.991**	-0.76	0.65	0.55		0.43	0.64	-0.50	0.22	0.78	0.72	0.46	0.71
Nitrospirota RH	0.93	-0.36	0.06	-0.02	0.48	-0.04	0.48	-0.66	-0.26	0.80	0.84	0.53	-0.29	-0.39	-0.17	-0.39	-0.27	0.10	0.71	.960*	0.08	-0.14	0.48	-0.40	0.24	-0.63	-.977*	-0.41		-0.41	-0.83	0.30	0.98	0.95	0.80	0.33
Nitrospirota BS	-0.34	-0.65	-0.82	0.68	0.31	0.86	0.57	0.12	0.21	0.18	-0.77	0.50	-0.22	0.73	-0.01	.962*	-0.65	-0.93	-0.24	-0.61	-0.54	0.31	-0.22	0.45	0.10	-0.05	0.61	0.56	-0.44		-0.23	-0.13	0.57	0.48	0.18	0.88
BGU extent	0.94	-0.86	0.29	-0.15	0.43	-.999*	0.78	-0.67	-0.39	0.95	0.90	0.61	-0.27	-0.47	-0.24	-.997*	-0.14	0.60	0.68	1.00	0.44	-0.34	0.42	-0.60	0.27	-0.61	-1.000**	-0.68	1.000**	-0.90		0.63	-0.93	-0.96	-.999*	0.25
BGU hotspot	0.58	-0.83	-0.16	-0.05	-0.01	0.80	0.73	0.23	0.71	0.58	0.20	0.50	0.34	-0.24	0.63	0.62	-0.27	-0.50	0.77	0.00	-0.93	0.83	0.78	0.72	-0.50	0.11	-0.09	0.74	0.28	0.42	0.12		-0.30	-0.40	-0.67	0.91
LAP extent	0.43	-0.98	-0.45	0.57	0.93	-0.70	1.00	-.997*	-0.92	0.90	0.34	0.99	-0.86	0.26	-0.84	-0.67	-0.79	-0.12	-0.02	0.79	0.94	-0.90	-0.32	-0.99	0.86	-0.99	-0.73	-.998*	0.71	-0.35	0.72	-0.60		0.99	0.91	0.12
LAP hotspot	0.11	0.72	0.85	-0.92	-0.98	0.22	-0.80	0.89	0.99	-0.54	0.20	-0.92	1.000*	-0.73	1.000**	0.18	0.99	0.62	0.54	-0.35	-0.98	1.00	0.77	0.92	-1.000*	0.92	0.26	0.88	-0.24	-0.19	-0.25	0.93	-0.85		0.95	0.02
GLU extent	0.64	0.21	.999*	-0.98	-0.72	-0.36	-0.34	0.49	0.75	0.02	0.71	-0.56	0.82	-0.99	0.84	-0.39	0.89	0.95	0.91	0.23	-0.71	0.78	0.99	0.56	-0.83	0.55	-0.32	0.47	0.33	-0.70	0.32	0.98	-0.42	0.83		-0.30
GLU hotspot	-0.99	0.51	-0.71	0.60	0.04	0.90	-0.40	0.24	-0.09	-0.70	-1.000*	-0.16	-0.21	0.83	-0.24	0.91	-0.34	-0.91	-0.94	-0.83	0.03	-0.14	-0.80	0.16	0.22	0.17	0.88	0.26	-0.89	.999*	-0.88	-0.57	-0.31	-0.23	-0.73	

2.2. Study 2: Mutualistic interaction between arbuscular mycorrhiza fungi and soybean roots enhances drought resistant through regulating glucose exudation and rhizosphere expansion

Duyen Thi Thu Hoang[1a], Mehdi Rashtbari[1b], Luu The Anhc, Shang Wang[b], Dang Thanh Tu[a], Nguyen Viet Hiep[d], Bahar S. Razavi[b*]

[a] Climate Change and Development Program, VNU Vietnam-Japan University, Vietnam National University, Hanoi, Viet Nam
[b] Department of Soil and Plant Microbiome, Institute of Phytopathology, Christian-Albrechts University, Kiel, Germany
[c] VNU-Central Institute of Natural Resources and Environmental Studies, Vietnam National University, Hanoi, Viet Nam
[d] Microbiology Department, Soils and Fertilizers Research Instiute, Hanoi, Viet Nam

[§] *Two first authors equally contributed to this study.*

Status: Published in Soil Biology and Biochemistry 171 (2022) 108728

2.2.1. Abstract

Glucose is one of the low molecular weight components of root exudates to mediate the cross-talk between plants and microbes, but less is known about their contribution to drought resistance of plants and root-associated microbiome. To fill this knowledge gap, we optimized the visualization of glucose exudation and coupled it with another *in situ* tool – soil zymography - as well as destructive analysis of enzyme kinetics (β-glucosidase; acid phosphomonoesterase) and microbial biomass. This helped identify how microbial functionality - affected by drought and P limitation - will show more resistance in the hotspots of soybean rhizosphere (grown in the rhizoboxes for 10 weeks) associated with arbuscular mycorrhizal fungi (AMF) symbiosis than those without AMF.

Drought reduced glucose exudation, mainly allocated to root tips, and narrowed the rhizosphere enzymatic hotspot by three times. However, AMF inoculation enhanced glucose exudation compared to non-mycorrhizal plants and enlarged enzymatic hotspot area by 53% under drought condition. Despite the 50% reduction in β-glucosidase and acid phosphomonoesterase activities owing to water deficit, AMF symbiont triggered up to 36% enzyme activities in correlation with the non-mycorrhizal ones. Therefore, the drought resistance of these two enzymes was enhanced by up to 63% in mycorrhizal plants. The biomass of microbial phosphorus increased by 45% under drought AMF-conditioned plants.

We conclude that the cooperation between soybean and AMF induced the formation of favorable microsites around the root, specifically in overlapping localities between rhizosphere and mycorrhizosphere, characterized by enhanced glucose release, increasing rhizosphere expansion, high enzyme activities and shortened substrate turnover time. This, in turn, contributed to the stronger resistance of microbial functions (e.g., enzyme expression) to drought stress in the rhizosphere hotspots. Thus, in response to AMF inoculation and consequent high glucose availability, rhizosphere microorganisms increased P mining rate in those hotspots remaining active despite water scarcity.

Keywords: *glucose imaging, rhizosphere, mycorrhizosphere, zymography, microbial functional resistance.*

2.2.2. Introduction

Drought severity is projected to be more frequent in the future, posing major challenges for the persuasion of sustainable agriculture development globally (Mach et al., 2019). The induced water stress affects all aspects of plant growth, such as decreasing leaf area and size, hampering photosynthesis (Bruce et al., 2007), reducing the shoot/root ratio (Peña-Rojas et al., 2004, 2006) limiting aboveground to underground carbon (C) transfer (Fuchslueger et al., 2014, 2016; Hasibeder et al., 2015; Karlowsky et al., 2018), and C diffusion from roots to rhizosphere soil (Gorissen et al., 2004), indirectly affecting microbial activity (Kuzyakov and Blagodatskaya, 2015). In addition, water deficit triggers nutrient (e.g., phosphorus (P)) accumulation in soil, which is difficult for the plants to take up (Sardans and Peñuelas, 2004). Plants have evolved various strategies to counter the negative effects of drought and P deficiency, ranging from modification of root morphology to physiological (Wang et al., 2001), biochemical, and biophysical processes (Carminati et al., 2010). Most prominently, plants can mediate root exudate quality and quantity to facilitate their communication with rhizosphere microorganisms (Williams and de Vries, 2020), or form symbiosis with arbuscular mycorrhizal fungi (AMF) to increase water and P uptake (Doubková et al., 2012; 2013). If the mediation of exudates promotes the recovery of plants, microbial activities, and ecosystem functions after drought (Karlowsky et al., 2018), symbiosis with AMF enhances the buffering capacity of the plant to drought (Doubková et al., 2013). In fact, root exudates act as signals to attract symbionts as AMF to build symbiotic relationships (Peters & Long, 1988; Besserer et al., 2006). For example, drought increases organic acid exudation in maize, which is an effective chemoattractant for *Bacillus subtilis* (e.g., in the soybean rhizosphere; Allard-Massicotte et al., 2016) or a nutritional source for *Trichoderma spp.* (Zhang et al., 2014). Similarly, during drought, soybean may benefit from the symbiotic association with AMF, which enhances its osmoprotective properties (Pavithra & Yapa, 2018). In reality, soil systems with high spatio-temporal variability of properties are often subjected to combined stresses (Brook et al., 2008), which can, theoretically, affect plant-microbial cooperation strategy to overcome these limitations. However, the plant strategy to overcome drought by mediating symbiosis with AMF and regulating primary compounds (e.g., glucose) exudation within rhizosphere under nutrient deprivation is poorly investigated.

Glucose, the primary compound in exudates as an easy available sugar, is among the soluble carbohydrates that are adjusted by the roots to adapt to osmotic conditions (Sharp et al., 1990; Spollen et al., 2008; Voothuluru et al., 2016). On the other hand, the distribution of glucose also corresponds to the nutrient status of the rhizosphere (Marschner, 1998; Hinsinger, 2001). Water stress inhibits glucose exudation (Calvo et al., 2019), and instead stimulates the accumulation of this compatible solute in roots (Palta and Gregory, 1997) to maintain physiological processes such as stomatal conductance, photosynthetic rate (Jacob and Lawlor 1991; Ghannoum and Conroy 2007), and expansion growth (Morgan, 1984; Bohnert and Sheveleva, 1998; Hoffmann, 2010). In contrast, the root secretion of glucose tends to increase as a strategy of plants to deal with P deficiency (Carvalhais et al., 2011). Although the exuded glucose supposedly varies with plant growth stage (Vancura and Hovadik, 1965), plant species (Strickland et al., 2012), and environmental conditions (Calvo et al., 2019), its exudation pattern is still obscure, especially as plants suffer the combined effects of drought and P deficiency.

It is well known that glucose is a labile source of energy for microbial community within rhizosphere. Despite flavonoids released by plant roots act as a signal to attract AMF symbiont (Buee et al., 2000; Antunes et al., 2006), enriched glucose exudation makes rhizosphere more

attractive to soil microorganisms. The presence of such microbial communities in the rhizosphere facilitates nutrient transformation to meet the demands of plants and themselves by synthesizing different functioning enzymes. Consequently, the rhizosphere is one of the most critical microbial hotspots in the agroecosystem and probably in terrestrial ecosystems. However, the formation of such hotspots in the rhizosphere strongly depends on biotic factors mediated by root-microbial interactions (Razavi et al., 2016; Kuzyakov and Razavi, 2019) and affected by abiotic controls. In other words, the resistance of microorganisms affects the ability of the system to maintain ecosystem services even under critical stress conditions (Shade et al., 2012). To cover the costs of this resistance, energetic adaptation mechanisms (e.g., expression of enzymes) are required by individual microbial groups to redirect resources from growth to survival-related mechanisms (Schimel et al., 2007). Accordingly, the microsites with abundant resources (e.g., hotspots with high abundance of available C) exhibit strengthened resistance in soil ecosystems (Shu et al., 2019). Hence, the significant increase in the distribution of rhizosphere microbial hotspots under P-limitation and water-stress conditions can be used to evaluate the resistance and recovery threshold of plants with AMF symbiosis.

Here, we tested the following hypotheses: i) Drought reduces microbial energy resources (e.g. root exudate), thus, indirectly changing microbial activity. ii) Microbial functionality - affected by drought and P limitation - will show more resistance in the hotspots of soybean rhizosphere associated with AMF symbiosis than those without AMF, due to a higher abundance of the available substrate (e.g. glucose); iii) AMF increases the accessibility of plants to nutrient sources not only by their hypha system but also by enlarging enzymatic rhizosphere size that extends soil volume mined by plants and microbes for potentially available nutrients.

To clarify the hypotheses, soybeans (*Glycine max* L.) were grown in rhizoboxes containing limited-P soil in a greenhouse at 22 $^{\circ}$C under optimum water conditions (65% WHC) for 7 weeks, one more week at transition stage to drought condition followed by two weeks drought (25% WHC). Coupled with direct glucose imaging, soil zymography was implemented to demonstrate the mediation of C and P transformation and translocation by mycorrhizal roots and soil microbial communities to adapt to drought condition and restricted P availability. Additionally, microbial biomass P and kinetics of β-glucosidase and acid phosphomonoesterase were assayed to interpret the role of AMF symbiosis in the resistant capacity of microorganisms under water stress and P deprivation.

2.2.3. Materials and Methodologies

2.2.3.1. Soil sampling and experimental design

Soil was collected in January, 2020 from the depth of 0-20 cm of the Ap horizon of an arable sandy clay loam, Fluvisol, located in Quang Nam, a southern province of central region of Vietnam (15º49’11’’N, 108º09’77’’E). Roots and stones were separated and soil was immediately sealed in a plastic bag. The samples were kept cold (~4 °C) during transportation to the laboratory. Soil sampled were sieved through a 2 mm mesh in prior to the experiment. A small portion of soil was dried under 60 °C, ground and prepared for C and N content analysis.

The soil consisted of 61% sand, 18.4% silt, 20.6% clay, with a pH 6.8, OC 11.2 g kg^{-1}, TN 0.9 (g kg^{-1}), available P 28 (mg kg^{-1}). The soil C and N were measured by Isoprime 100 (Elementar, Germany). The total available P fraction (Olsen P) was determined by the method of DeLuca et al. (2015) where 0.5 g of fresh soil was extracted with 10 mL of 0.5M $NaHCO_3$ solution (Olsen et al., 1954).

2.2.3.2. Arbuscular mycorrhizal fungi colonization

Glomus mosseae inoculum was provided by Division of Microbiology, Soil and Fertilizers Research Institute, Vietnam. Briefly, arbuscular mycorrhizal fungi spores were isolated from

rhizopheric soil of pomelo growing in Gleyic Fluvisols (Flg) located in Phu Tho province, Vietnam. The fungus was propagated on maize root grown in greenhouse for 8 weeks (Tarafdar and Marschner, 1995), and the spores were surface sterilized to make inoculum for the experiment. We chose this fungal species because *Glomus mosseae (G. Mossea)* is a crucial AM fungus species in agricultural system (Benedetto et al., 2005) that is ubiquitous in worldwide ecosystems.

2.2.3.3. Plant and Experimental setup

The cultivar of soybean was *Glycine max L.* DT96 characterized with drought resistant capacity, which was provided by Agricultural Genetics Institute of Vietnam. Soybean seeds were sterilized with 70% ethanol and 10% hydrogen peroxide, and rinsed thrice with distilled water (Ibiang et al., 2017). These sterilized seeds were germinated on wet filter paper in a petri dish for three days before transplanting into rhizoboxes.

Treatments with and without AMF were set up in separate boxes. Zymography and glucose imaging were performed in different rhizoboxes to avoid cross effects of the two imaging methods. Thus, soil was packed in 24 transparent rhizoboxes (20 × 20 × 3 cm). The experiment consisted of four treatments (drought vs. optimum, AMF vs. no-AMF), each of which was replicated thrice to measure zymography, enzyme kinetics, and microbial biomass P. Simultaneously, another set of drought vs. optimum treatments with three replications inoculated with and without AMF was prepared for glucose imaging. To evaluate the effects of mycorrhiza on soybean drought resistance, 20 g of mycorrhiza inoculum (*Glomus mosseae*, > 100 cell g^{-1}) (Ruiz-Lozano et al., 2001) was added to 12 rhizoboxes.

The rhizoboxes were placed horizontally with one side open and then soil was slowly and continuously poured into the rhizoboxes through a 2 mm sieve to achieve a uniform soil packing. The open side was then closed, the samples were turned vertically, and they were gently shaken to achieve a stable soil packing. All the rhizoboxes were kept inclined at 45^{o} with the open side facing down like a door in the greenhouse chamber at 20-22 $^{\circ}$C and light intensity of 330 µmol m^{-2} s^{-1}. The emplacement of the rhizoboxes ensured root growth along the lower side of the boxes. The rhizoboxes were covered with aluminum foil to prevent algal growth. Soil moisture in each rhizobox was gravimetrically measured every two days to ensure 65% water holding capacity (WHC) during the first 7 weeks of the experiment, and distilled water was added if necessary. After that, drought condition (25% WHC) was set up in half of the 24 rhizoboxes by for two weeks (excluding 1 week of transition from 65%WHC to 25%WHC), the rest of the boxes were maintained at 65% WHC till harvest. Briefly, the growth of soybean was kept for 7 weeks at optimum moisture followed by 1 week at transition stage from optimum to drought and 2 more weeks at 25% WHC for drought treatment. The samples were collected after 10 weeks of the experiment (Appendix 1).

2.2.3.4. Staining arbuscular-mycorrhizal fungal colonizations in root

Root branches were randomly cut off from three plant replicates of each treatment. Root staining was implemented according to Vierheilig et al. (1998). Firstly, roots were boiled with KOH for 5 minutes and rinsed with tap water several times. Solution of black ink (Pelikan; Germany) and vinegar was used to boil the cleared roots for 3 minutes, followed by pure vinegar rinse. The stained arbuscules and their hyphae were observed and imaged under a light microscope (Vierheilig et al., 2005).

2.2.3.5. Glucose imaging: method optimization

The exudation of glucose was first visualized in gel-based approach which demonstrated a dependence of spatial and temporal pattern of glucose distribution on plant species, soil moisture, and root compartments (Voothuluru et al., 2018). *In situ* glucose imaging was

performed for AMF-inoculated and AMF non-inoculated rhizoboxes, which were divided into three droughts and three optimum conditions. Here, we optimized the method for soil matrix from protocols proposed by McLaughlin and Boyer (2004) and Voothuluru et al. (2018). Accordingly, phosphate powder was dissolved in distilled water to make a buffer solution of 0.05 M. 100 mL buffer solution was added to 0.00107 g glucose oxidase from *Aspergillus niger* (G7141-10KU, Sigma Aldrich, Germany), 0.003 g peroxidase from horseradish, and 0.005144 g Ampliflu red ($C_{14}H_{11}NO_4$, 90101-5MG-F, Sigma Aldrich, Germany) dissolved in 60 µL dimethylsulfoxid (Sigma Aldrich, $(CH_3)_2SO$). Parallelly, polyamide membrane filters (diameter 20 cm, pore size 0.45 µm - Tao Yuan, China) were cut to fit the size of the rhizobox. These membranes were saturated with the prepared solution prior to being attached to rooted sides of the rhizoboxes. In this study, glucose imaging was further developed by integrating the solution described above that becomes red when glucose oxidase and horseradish peroxidase (EC No. 232-668-6, Sigma Aldrich, Germany) catalyzes glucose-based conversion of colorless Ampliflu Red into magenta-colored resorufin, using membranes instead of gel. This modification enables glucose imaging at the soil surface and strongly reduces the diffusion artifacts occurring in gel.
After 20 minutes of incubation, membranes were quickly removed and placed in a dark room under UV light of 355 nm wavelength (an optimal incubation time should be tested in advance – time may differ between plants species). The magenta-colored area on the membrane indicated glucose exudation as hydrogen peroxide generated from the reaction between glucose and the enzyme glucose oxidase, catalyzed by horseradish peroxidase, converted colorless Ampliflu red into magenta color.

2.2.3.6. Soil Zymography

In order to localize hotspots of enzymatic activity at soil surface, the protocol of zymography was applied according to Razavi et al. (2019). In details, 4-methylumbelliferyl-phosphate (MUF-P, $C_{10}H_9O_6P$, EC No. 222-137-7, Sigma Aldrich, Germany) solution was prepared in Dimethyl sulfoxide (DMSO, $(CH_3)_2SO$, Sigma Aldrich, Germany) to prepare the solution of 10 mM. This substrate was used to detect acid phosphomoasterase activity.
The polyamide membrane filters (Tao Yuan, China) with large pore size of 0.45 µm were selected to reduce the restriction of enzyme diffusion through the pores. The cut membranes that match well with the door of rhizoboxes were soaked into the substrate solution. The membranes were directly applied to root-exposing side, and covered outside with aluminum foils to avoid dry out. After one hour of incubation, the membranes were lifted off and cleaned with a soft brush, then exposed to UV light of 355 nm wavelength excitation and 460 nm emission wavelength in a closed room. Beside analysis of rhizosphere size, the zymograms were used as a map to localize hotspot of acid phosphomoasterase activity (Fig. 2.2.1). The soil samples were collected from all the identified hotspots of each rhizobox and the mixed soils were split into 2 subsamples for further analysis (1 for enzyme kinetics, 1 for MBP).

2.2.3.7. Calibration lines

Glucose imaging was calibrated by soaking individual 2 cm^2 membrane in glucose solution at respective concentration of 0, 2, 4, 6, 8 and 10 mM and then placed in reaction mixture containing Ampliflu Red, glucose oxidase and horse radish peroxidase for 30 sec. These membranes were exposed under UV light in the same way as the samples. Calibrated values were used to quantify color intensity of the glucose release and relate glucose release to the gray-value. Fluorescent signals on an area basis were calculated based on the volume of substrate solution taken up by a fixed membrane size.
Zymography processing was calibrated by soaking individual 3 cm^2 membrane in MUF solution at respective concentration of 0.01, 0.2, 0.5, 1, 2, 4, 6 and 10 mM. These membranes

were exposed under UV light in the same way as the samples. Calibrated values were used to quantify color intensity of the zymograms and relate enzyme activity to the gray-value. Fluorescent signals of MUF on an area basis were calculated based on the volume of substrate solution taken up by a fixed membrane size.

2.2.3.8. Photography and processing glucose and zymography images

All the images were taken with a digital camera (Canon EOS 6D, Canon Inc.), with a Canon lens EF 24–105 mm 1: 4L IS with the setting of aperture and shutter speed at f/5.6 and 1/30 s respectively. The fixation of distance from the camera to UV light source and membranes was to ensure constancy in image qualification, comparable quality of image processing for all samples.

The image processing and analysis was conducted in ImageJ and Matlab. For image processing, all the taken images (glucose images and zymograms) were i) transformed to 16-bit grayscale value; ii) adjusted the background and contrast levels; iii) segmented roots and iv) converted grayvalue to enzyme activities and glucose intensity. The segmented roots and their radius were calculated using the Euclidean distance map function in Matlab (Menon et al., 2007; Zarebanadkouki and Carminati, 2014). The hotspot areas were determined as top 25% higher enzyme activities after subtracting background values at zero concentration of the calibration line from all zymograms (Ma et al., 2017).

Hotspot percentage was calculated based on the pixel size proportion of hot area to the entire image. Rhizosphere extent of each individual root was calculated from root surface.

2.2.3.9. Enzyme kinetics, substrate turnover time and resistance of enzyme activity under drought condition influenced by AMF

According to the zymograms, samples from the rhizosphere hotspots were collected. These samples were preserved at 5 ^{o}C and measured the next day. Supposing that drought restricted photosynthesis so may affect above-underground C translocation. On the other hand, AMF presence stimulated P uptake by plants under stressed conditions and P deficiencies. Therefore, two enzymes were selected to investigate the interaction between roots and microorganisms including: β-glucosidase and acid phosphomonoesterase. The kinetics of these two enzymes were determined using fluorescent substrates (Sigma Aldrich, Germany). MUF β-D-glucopyranoside (MUF-G) was used for the determination of β-glucosidase and 4-methylumbelliferyl-phosphate (MUF-P) for acid phosphomonoesterase. According to German et al., (2012), 1.0 g soil was suspended in 50 mL sterile water of which 50 µL suspension was pipetted in a 96-well microplate (Puregrade, Germany). Then, 50 µL MES hemisodium buffer (pH 6.5) (MES, $C_6H_{13}NO_4SNa_{0.5}$, Sigma Aldrich, Germany) and 100 µL respective substrate solution were added subsequently in each well. The activity of each enzyme was measured at 3 time points: 30, 60 and 120 min. using CLARIOstar plus (BMG LABTECH, Germany) at an excitation wavelength of 355 nm and an emission wavelength of 460 nm. Enzyme activities (V_{max}) were denoted as released MUF in nmol per g dry soil per hour (nmol MUF g^{-1} soil h^{-1}) (Awad et al., 2012) at the time point of 120 min. The linear increase of fluorescence overtime during the assay was properly checked and data obtained after 2 h was used for further calculation (German et al., 2011). Simultaneously, a range of MUF concentration of 0, 10, 20, 30, 40, 50, 100, 200 µM were prepared to calibrate the measurement.

The determination of K_m and V_{max} was conducted by fitting the measured values to Michaelis-Menten equation (1):

$$v = \frac{V_{max} \times [S]}{K_m + [S]} \qquad (1)$$

where v is the reaction rate, V_{max} is the maximum reaction rate at saturated substrate concentration, [S] is substrate concentration, K_m is the substrate concentration at which the reaction rate attains a half of maximum.

Based on V_{max}, K_m and [S] values, we calculated turnover time (Tt) of the added substrates according to equation (2) suggested by Panikov et al., (1992) and Larionova et al., (2007):

$$Tt\ (hours) = (K_m + S)/V_{max} \qquad (2)$$

Since drought triggers less proportion of C allocation to root rhizosphere (Gao et al., 2021), the low substrate concentration (equal to K_m) was chosen to calculate the turnover time of added substrates.

In order to evaluate the role of AMF in improving drought resistant capacity of soybean rhizosphere's enzyme activity, the resistance index (RS) was interpreted based on equation (3) (Orwin and Wardle, 2004):

$$RS\ (t_0) = 1 - \frac{2|D_0|}{C_0 + |D_0|} \qquad (3)$$

where D_0 is the amount of the difference in a biological function between the control soil (C_0) (here enzyme activity) and the drought soil at the end of disturbance (t_0). This resistance index is between -1 and +1, where +1 indicates no effects of disturbance (maximum resistance).

2.2.3.10. Microbial biomass phosphorus (MBP)

Microbial biomass phosphorus was determined by chloroform fumigation-extraction using anion exchange membrane (Kouno et al., 1995; Yevdokimov and Blagodatskaya, 2014). To prepare for the experiment, anion exchange membrane (AEM) strips were shaken with three sequential changes in 200 mL 0.5 mol L^{-1} $NaHCO_3$ for 24 h, then washed three times and kept in deionized water until use. Subsequently, each pair of 50-mL tube (for fumigation and non-fumigation purposes) contains the same sample equivalent to 3 g dry soil were filled with 30 mL of deionized water. The fumigated tube was added with 300 µl of chloroform to solubilize microbial biomass P. One anion exchange membrane (AEM) strip was placed in fumigated and non-fumigated tubes. These tubes were shaken for 24 h continuously to induce the recovery of inorganic P from the soil extract. After shaking, AEM strips were lifted out of the tubes and gently washed again in deionized water prior to being submerged into another centrifuge tube filled with 45 mL of 0.25 M H_2SO_4. Tubes containing membranes and 0.25 M H_2SO_4 were shaken for three hours to release membrane-fixed P back to the solution. 150 µL acid extract was mixed with 30 µl *Reagent 1* (prepared with 14.2 mmol L^{-1} ammonium molybdate tetrahydrate in H_2SO_4 3.1 M) and *Reagent 2* (prepared with 3.5 g L^{-1} aqueous polyvinyl alcohol reagent and malachite green) (D'Angelo et al., 2001) in disposable 96-well polystyrene microplates. These microplates were exposed to 40 ºC for 30 – 40 min in a dryer (thermostat) and read at 630 nm in CLARIOstar plus (BMG LABTECH, Germany).

2.2.3.11. Data analysis and statistics

All the statistical analyses were performed in Sigma-Plot 14.0. One-way ANOVA was applied to categorize hotspot boundary and hotspot intensity. The significant differences in enzyme activities, rhizosphere extent, hotspot percentage, substrate turnover time and drought resistance, microbial biomass P between droughts vs. optimum, with AMF vs. without AMF were confirmed by Two-Way ANOVA after checking normality and homogeneity of values. A probability level of $p < 0.05$ or $p < 0.001$ indicated the significance in comparison. Error bars indicate the standard error of the means.

2.2.4. Results

The staining technique with ink and vinegar demonstrated the colonization of AMF in mycorrhizal plant roots (Fig. S2.2.1). Our measurements showed that drought reduced the

shoot length by 1.3-1.5 times but the reduction of root length is less than shoot length. AMF inoculum strongly increased shoot length by 1.38 times at optimum condition and by 1.24 times in drought condition (Fig. S2.2.3).

2.2.4.1. Glucose exudation from root tips

In glucose imaging, decreasing the release of glucose was demonstrated in color bars in which white color showed the highest glucose exudation. Under optimum conditions, glucose was mainly exuded along the roots and root tips (Fig. 2.2.1). On the contrary, under drought condition, glucose exudation was more focused on the root tips. However, a higher release of glucose was observed in the rhizosphere under AMF-drought than control-drought.

2.2.4.2. Enzymatic hotspots and rhizosphere size

In the absence of AMF, drought reduced acid phosphomonoesterase hotspot percentage by three times compared to optimum condition, while AMF inoculation further reduced it to two times (Fig. 2.2.2a). The presence of AMF increased the hotspot area by 40% and 53% in optimum and drought conditions, respectively, compared to respective conditions without AMF. Enzymatic hotspot area increased by 9% under drought than optimum conditions with AMF symbiosis.

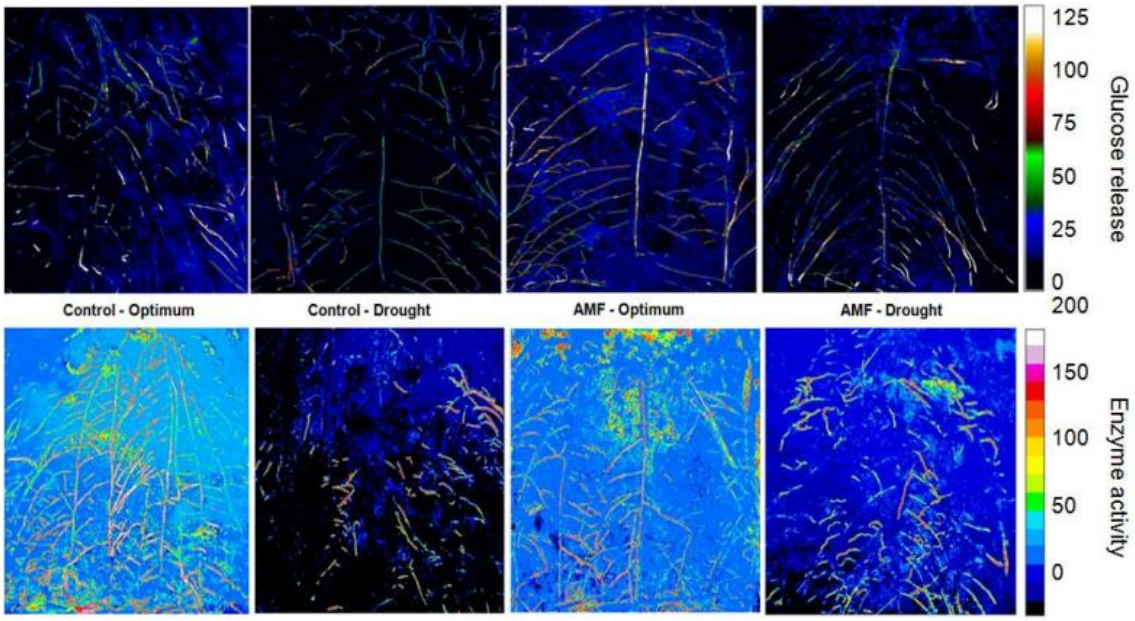

Figure 2.2.1. Upper row shows glucose release (nmol/cm^2), for treatment with and without AMF (control), under optimum and drought conditions. Lower row: shows zymograms of acid phosphomonoesterase (pmol cm^{-2} h $^{-1}$).

Water stress triggered a reduction of rhizosphere size by 78% when compared to the optimum condition (Fig. 2.2.2b). In contrast, in plants inoculated with AMF, rhizosphere extent under stress effects was almost the same as that under optimum condition (without AMF), and 71% higher than non-mycorrhizal rhizosphere under the same stress.

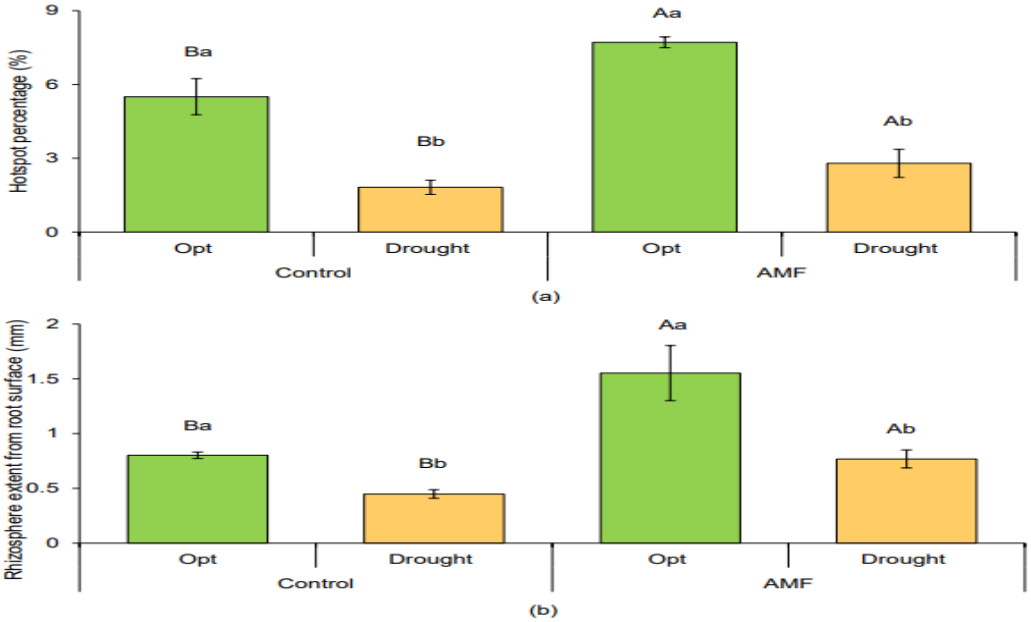

Figure 2.2.2. Hotspot percentage (a) and rhizosphere extent (b). Lower case letters: significant differences between optimum and drought at p < 0.05; upper case letters: significant differences between control and AMF at p < 0.05.

2.2.4.3. Enzyme kinetics, turnover time, and resistance to drought

Activities of β-glucosidase and acid phosphomonoesterase decreased by approximately 50% owing to water deficit, irrespective of AMF or non-AMF inoculation ($p < 0.001$, Fig. 2.2.3). K_m value of both enzymes considerably increased ($p < 0.001$) in mycorrhizal plants in comparison to non-mycorrhizal ones, regardless of optimum or drought conditions (Fig. S2.2.2).

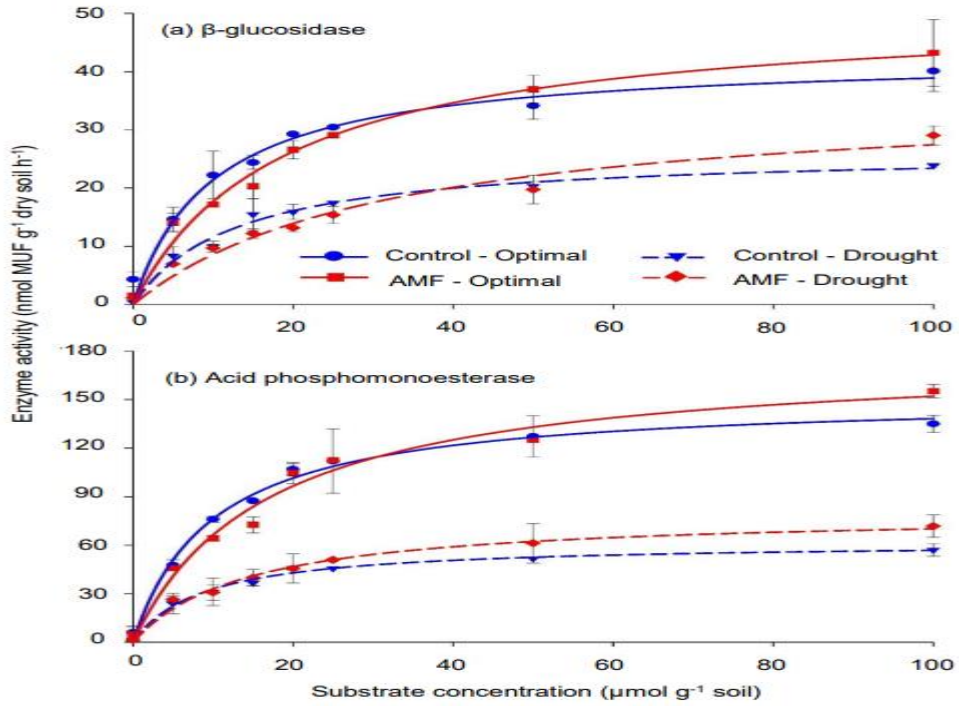

Figure 2.2.3. Michaelis-Menten kinetics (enzyme activity as a function of substrate concentration) for (a) β-glucosidase (GLU) and (b) acid phosphomonoesterase (PHOS). The bar indicated standard error.

While substrate turnover times of β-glucosidase and acid phosphomonoesterase were at least 56% shorter in optimum condition than in drought (p < 0.001, Fig. 2.2.4), AMF symbiont reduced the turnover time of these enzymes by up to 28%, especially under drought. Additionally, the drought resistance of β-glucosidase and acid phosphomonoesterase activities was enhanced by 63% and 57%, respectively, in mycorrhizal plants (p < 0.05, Fig. 2.2.5).

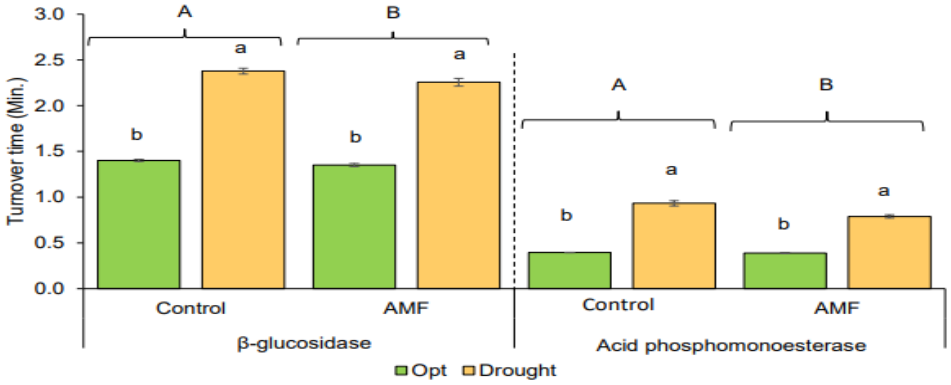

Figure 2.2.4. Substrate turnover time at optimum and drought condition with and without AMF inoculation. Lower case letters: significant differences between optimum and drought at p < 0.05; upper case letters: significant differences between control and AMF at p<0.05. GLU: β-glucosidase, PHOS: acid phosphomonoesterase.

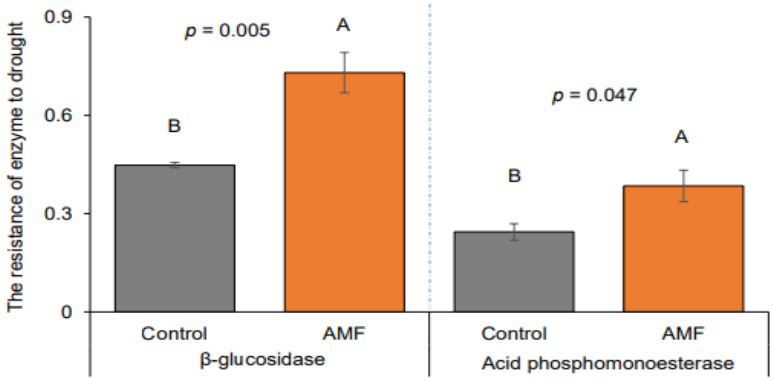

Figure 2.2.5. The resistance of enzyme activity to drought (i.e. RS (t0) = 1- (2|D_0| / (C_0 + |D_0|)). Letters indicate significant differences between control and AMF treatment of respective enzyme after Student's t test at p < 0.05.

2.2.4.4. Microbial biomass phosphorus

Drought resulted in a two-fold decrease of microbial biomass P (MBP) in both control and AMF treatments (Fig. 2.2.6). Nevertheless, biomass of microbial P increased by 50% and 45% under optimum and drought conditions, respectively, in plants inoculated with AMF.

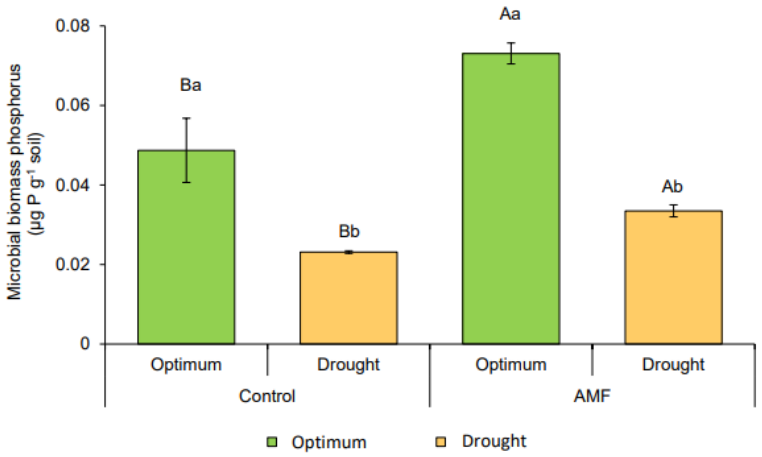

Figure 2.2.6. Microbial biomass phosphorus. Drought resulted in two-fold decrease of microbial biomass phosphorus (MBP) in both control and AMF treatments. Nevertheless, biomass of microbial phosphorus increased 50% and 45% in respective optimum and drought conditions as plant was inoculated with AMF. Lower case letters: significant differences between optimum and drought at $p < 0.05$; upper case letters: significant differences between control and AMF at $p < 0.05$.

2.2.5. Discussion

2.2.5.1. How AMF presence affected glucose exudation and enzymatic hotspot within rhizosphere?

In line with our first and second hypothesis, glucose exudation highly relied on moisture condition, as suggested by Vancura and Hovadik (1965) and Calvo et al. (2019). Under optimum condition, glucose was homogeneously exuded along the root as well as root tips, but drought dramatically reduced glucose exudation along with a total decrease in exudation (Liese et al., 2018), especially from the mature part of the root (Fig. 2.2.1). Remarkably, AMF strongly boosted glucose hotspots in comparison to non-mycorrhizal plants. Glucose exuded from root characterized by lability and ready utilization can be directly absorbed by AMF as a C source (Bago et al., 2000; Bücking et al., 2008) to stimulate AMF hyphae branching and lengthening. On the other hand, AMF may contribute to glucose release, for instance, by the expression of β-glucosidase and mobilizing oligo- and polysaccharides or glycosylated compounds. Therefore, the enhanced glucose exudation was attributed to the concomitant direct secretion from plant roots or product of β-glucosidase activity within rhizosphere. This accelerated glucose availability within the mycorrhizosphere (Kraigher *et al.*, 2013), the zone of influence in the vicinity of fungal hyphae (Tarafdar and Marschner, 1994), which compensates C deprivation of rhizobiota due to drought (Asensio et al., 2021). As a consequence, acid phosphomonoesterase hotspots percentage and rhizosphere extent increased by up to 53% and 71%, respectively, in mycorrhizal plants when compared with non-mycorrhizal plants under water scarcity (Fig. 2.2.2). AMF can play the role of root hairs and enlarge the overall extent of the absorbing surface of the host roots (40 times) (Muchovej, 2004; Pepe et al., 2016).

P is well known as one of the most essential nutrients for plant growth and is quickly taken up by plant roots resulting in a P depletion zone in the adhering vicinity of host roots (Lewis & Quirk, 1967; Hinsinger et al., 2009; Shen et al., 2011). However, water deficiency strongly inhibits soil P bioavailability (Sardan et al., 2007) in contrast to the increasing demand of P by plants under stress condition (He et al., 2014). The extension of the enzymatic rhizosphere is expected to compensate the P-depletion zone, especially under increasing water stress condition. The fungus mycelium system can approach microaggregate-trapped P and efficiently transport P into plant roots (Smith and Read, 2008; Schnepf et al., 2011). The spread

of external mycelium is coincidental with the synthesis of acid phosphomonoesterase by fungi (Tarafdar and Claassen, 1988; Dakora and Phillips, 2002) to facilitate P availability, which apparently contributed to higher hotspot percentage and rhizosphere extent in host plants than in non-host plants. Coupling with the glucose distribution pattern above, we conclude that plants sustain a mutual communication with rhizosphere microorganisms by diffusing more glucose along the plant roots associated with AMF as a strategy to adapt to water limitation. In turn, AMF boosts the P availability for plants in the enzymatic pathway by enlarging acid phosphomonoesterase hotspots and rhizosphere expansion. Consequently, shoot length increased by 1.24-1.37 times in AMF inoculation regardless of optimum or drought condition. Considering the fact that many hotspots have a mixed origin and mixed-use, it becomes more evident that the overlapping area between rhizosphere and mycorrhizosphere accelerates microbial activity around the roots (Fig. 2.2.7). Thus, AMF stimulated microbial-mediated processes and extended hotspots around the roots under water stress by forming favorable microsites for microorganisms which supported soybean performance.

2.2.5.2. How AMF symbiosis affected enzyme kinetics and its drought resistance?

In agreement with our second hypothesis, AMF symbiosis significantly enhanced β-glucosidase and acid phosphomonoesterase activities, compared with non-mycorrhizal plants, irrespective of optimal moisture or water deficiency ($p < 0.001$). This finding confirms that AMF promotes enzymatic activities, especially that of acid phosphomonoesterase (Welc et al., 2014) through possible stimulation of bacteria, fungi or plant roots (Joner and Jakobsen,1995; Yang et al., 2012; Nannipieri et al., 2011). C demand of AMF facilitates the synthesis of β-glucosidase by either bacteria or fungi (Pathan et al., 2017) to decompose root exudates containing carbohydrates and root slough-off. In addition, glomaline produced by AMF stores 4–5% of the total tropical soil C (Rillig et al., 2001) which promotes the β-glucosidase activity. Meanwhile, acid phosphomonoesterase was synthesized by both plant roots and fungal hyphae, leading to the increase in acid phosphomonoesterase activity in mycorrhizal plants. The higher *Km* values in AMF inoculated plant independent of water content indicated different enzyme systems with lower substrate affinity compared to control without AMF (Razavi et al., 2016b). The change of enzyme systems reflected a probable shift in dominant microbial populations toward species with lower affinity to celluloses and organic P-compounds as compared to the control (Zhang et al., 2020) indicating action of fast-growing microorganisms with low efficiency within the rhizosphere–mycorrhizosphere hotspots.

Our findings for both β-glucosidase and acid phosphomonoesterase was consistent with the results of a previous study on the reduction of enzyme activities as a result of water stress (Alster et al., 2013). This reduction might be the result of i) reduced diffusion of substrate to enzymes in suboptimal moisture (Nannipieri et al., 2002) and ii) adsorption of enzymes on soil particles (Steinweg et al., 2012) under drought.

At low substrate concentration (< 20 μmol g^{-1} soil), we detected a similar reaction rate of acid phosphomonoesterase under drought independent of AMF inoculation (Fig. 2.2.3). These results can be explained by an increase of *Km*, which is in the denominator of the Michaelis-Menten equation (1). Therefore, the positive effects of AMF on *Vmax* were canceled by the *Km* increase. A much greater increase in *Km* (substrate affinity decreased) than in *Vmax* canceled the differences in acid phosphomonoesterase activities at substrate concentrations below 20 μmol g^{-1} soil under drought. Thus, the decomposition of organic P-compounds under drought was accelerated only at substrate levels exceeding that threshold. Accordingly, increased turnover time of added substrates by enzymes, under drought demonstrates that the decomposition of soil organic matter was delayed under water stress condition due to lower activities of enzymes. AMF symbiont showed a faster degradation of substrates under drought condition, with up to 28% reduction in turnover time in the mycorrhizal rhizosphere. This

reduction is critical in improving C and nutrient transformation, especially P compounds within the rhizosphere, under water stress.

Effects of drought on soybean varies with its growth stage but most severe during vegetative and flowering timing (Desclausx et al., 2000) which showed more influences on shoot length than root length in our experiment (Fig. S2.2.3). As a result of AMF symbiosis, shoot length was significantly improved in comparison to plant without AMF. Moreover, AMF plays a leading role in enhancing drought-resistance of both β-glucosidase and acid phosphomonoesterase enzymes. As mentioned in a review by Dodd et al. (2000), greater allocation of sucrose to mycorrhizal roots maintains AMF growth and also retains sustainable plant production. The observed increased glucose excretion under drought treatment might have a function similar to that of sucrose in enhancing drought resistance of these two enzymes. Although the role of AMF hyphae in sustaining soil micro-aggregates is not within our research scope, we speculate that AMF-synthesized glomaline glues separate soil particles to make soil water-stable aggregates (Wu et al., 2008), facilitating drought resistance of β-glucosidase and acid phosphomonoesterase enzymes.

Given that drought dramatically reduced microbial biomass P (MBP) because of increasing P accumulation in soil accompanied with water limitation, AMF enormously improved MBP. Remarkably, AMF showed positive effects on MBP not only under drought but also under optimum conditions. This result implies that P is increasingly mobilized by AMF which was not only transported into the host plant but also served the soil microbes demand for P. This role of AMF is more critical as plants encounter simultaneous P deficiency and water limitation.

Overall, the stronger resistance of enzyme activities to drought in AMF-inoculated than in non-mycorrhizal suggests that microorganisms associated with mycorrhizal root have a higher capability to react to altered abiotic environmental conditions than those associated with non-mycorrhizal roots. The mycorrhization induced an interactive regulation of soybean glucose exudation and rhizosphere expansion for enzyme activities. This contributed to the resistance of microbial functions (e.g., enzyme expression) to drought stress in AMF-inoculated than in non-mycorrhizal soybean. AMF-inoculation suppressed adverse drought effects on plant and microbial nutrient mining, which has substantial implications for controlling microbial roles in organic matter decomposition and P cycling.

2.2.6. Acknowledgment

This study was funded by Vietnam National University, Hanoi (Project code: QG. 20.63). The method development of this work was motivated and supported by the German Federal Ministry of Education and Research (BMBF) (grant number 031B0910A). We gratefully acknowledge DAAD for supporting DTTH to have a short visit at the Department of Soil and Plant Microbiome, Institute of Phytopathology, University of Kiel, Germany.

2.2.7. References

Allard-Massicotte, R., Tessier, L., Lécuyer, F., Lakshmanan, V., Lucier, J.F., Garneau, D., Caudwell, L., Vlamakis, H., Bais, H.P., Beauregard, P.B., 2016. Bacillus subtilis early colonization of Arabidopsis thaliana roots involves multiple chemotaxis receptors. *MBio* 7, 1–10.

Alster, C.J., German, D.P., Lu, Y., and Allison, S.D., 2013. Microbial enzymatic responses to drought and to nitrogen addition in a southern California grassland. *Soil Biol. Biochem.* 64, 68–79.

Antunes, P.M., Rajcan, I., Goss, M.J., 2006. Specific flavonoids as interconnecting signals in the tripartite symbiosis formed by arbuscular mycorrhizal fungi, Bradyrhizobium japonicum (Kirchner) Jordan and soybean (Glycine max (L.) Merr.). Soil Biol. Biochem. 38, 533-543.

Awad, Y.M., Blagodatskaya, E., Ok, Y.S., Kuzyakov, Y., 2012. Effects of polyacrylamide, biopolymer, and biochar on decomposition of soil organic matter and plant residues as determined by 14C and enzyme activities. *Eur. J. Soil Biol.* 48, 1-10.

Bago, B., Pfeffer, P.E. & Shachar-Hill, Y., 2000. Carbon metabolism and transport in arbuscular mycorrhizas. *Plant Physiol*. 124, 949–958.

Benedetto, A., Magurno, F., Bonfante, P., Lanfranco, L., 2005. Expression profiles of a phosphate transporter gene (GmosPT) from the endomycorrhizal fungus Glomus mosseae. Mycorrhiza 15, 620–627.

Besserer, A., Puech-Pàges, V., Kiefer, P., Gómez-Roldán, V., Jauneau, A., Roy, S., Portais, J.C., Roux, C., Bécard, G., Séjalon-Delmas, N., 2006. Strigolactones stimulate arbuscular mycorrhizal fungi by activating mitochondria. *PLoS Biology* 4, 1239-1247.

Bohnert, H.J., Sheveleva, E.,1998. Plant stress adaptations – making metabolism move. *Current Opinion in Plant Biology* 1, 267–274.

Bruce, T.J.A., Matthes, M.C., Napier, J.A., Pickett, J.A., 2007. Stressful 'memories' of plants: evidence and possible mechanisms. *Plant Sci.* 173, 603-608.

Buee, M., Rossignol, M., Jauneau, A., Ranjeva, R., Bécard, G., 2000. The Pre-Symbiotic Growth of Arbuscular MycorrhizalFungi Is Induced by a Branching Factor PartiallyPurified from Plant Root Exudates. MPMI 13, 693–698.

Bücking, H., Abubaker, J., Govindarajulu, M., Tala, M., Pfeffer, P.E., Nagahashi, G., Lammers, P., Shachar-Hill, Y., 2008. Root exudates stimulate the uptake and metabolism of organic carbon in germinating spores of Glomus intraradices. *New Phytologist* 180, 684– 695.

Calvo OC, Franzaring J, Schmid I, Fangmeier A, 2019. Root exudation of carbohydrates and cations from barley in response to drought and elevated CO2. *Plant and Soil* 438, 127–142.

Carminati, A., Moradi, A.B., Vetterlein, D., Vontobel, P., Lehmann, E., Weller, U., Vogel, H.-J., Osward, S.E., 2010. Dynamics of soil water content in the rhizosphere. *Plant Soil* 332, 163–176.

Carvalhais, L.C., Dennis, P.G., Fedoseyenko, D., Hajirezaei, M-R., Borriss, R., von Wirén, N., 2011. Root exudation of sugars, amino acids, and organic acids by maize as affected by nitrogen, phosphorus, potassium, and iron deficiency. *J. Plant Nutr. Soil Sci.* 174, 3–11.

Dakora, F.D., Phillips, D.A., 2002. Root exudates as mediators of mineral acquisition in low-nutrient environments. *Plant and Soil* 245, 35– 47.

D'Angelo, E., Crutchfield, J., Vandiviere, M., 2001. Rapid, sensitive, microscale determination of phosphate in water and soil. *J Environ Qual* 30, 2206–2209.

DeLuca, T.H., Glanville, H.C., Harris, M., Emmett, B.A., Pingree, M.R.A., de Sosa, L.L., Cerda-Moreno, C., Jones, D.L., 2015. A novel biologically-based approach to evaluating soil phosphorus availability across complex landscapes. *Soil Biol. Biochem.* 88, 110-119.

Desclaux, D., Huynh, T.T., Roumet, P., 2000. Identification of soybean plant characteristics that indicate the timing of drought stress. Crop Science. 40, 716-722.

Dodd, J.C., Boddington, C.L., Rodriguez, A., Gonzalez-Chavez, C., Mansur, I., 2000. Mycelium of Arbuscular Mycorrhizal fungi (AMF) from different genera: form, function and detection. *Plant and Soil* 226, 131–151.

Doubková, P., Suda, J., and Sudova, R., 2012. The symbiosis with arbuscular mycorrhizal fungi contributes to plant tolerance to serpentine edaphic stress. *Soil Biol. Biochem.* 44, 56-64.

Doubková, P., Vlasáková, E., and Sudová, R., 2013. Arbuscular mycorrhizal symbiosis alleviates drought stress imposed on Knautia arvensis plants in serpentine soil. *Plant Soil* 370, 149–161.

Fuchslueger, L., Bahn, M., Fritz, K., Hasibeder, R., & Richter, A., 2014. Experimental drought reduces the transfer of recently fixed plant carbon to soil microbes and alters the bacterial community composition in a mountain meadow. *New Phytologist* 201, 916– 927.

Fuchslueger, L., Bahn, M., Hasibeder, R., Kienzl, S., Fritz, K., Schmitt, M., Watzka, M., Richter, A., 2016. Drought history affects grassland plant and microbial carbon turnover during and after a subsequent drought event. *Journal of Ecology* 104, 1453– 1465.

Gao, D., Joseph, J., Werner, R.A., Brunner, I., Zürcher, A., Hug, C., Wang, A., Zhao, C., Bai, E., Meusburger, K., Gessler, A., Hagedorn, F., 2021. Drought alters the carbon footprint of trees in soils—tracking the spatio-temporal fate of 13C-labelled assimilates in the soil of an old-growth pine forest. *Global Change Biology* 27, 2491-2506.

German, D.P., Marcelo, K.R.B., Stone, M.M., Allison, S.D., 2012. The Michaelis-Menten kinetics of soil extracellular enzymes in response to temperature: a cross-latitudinal study. *Global Change Biology* 18, 1468– 1479.

Ghannoum, O., Conroy, J.P., 2007. Phosphorus deficiency inhibits growth in parallel with photosynthesis in a C3 (Panicum laxum) but not two C4 (P. coloratum and Cenchrus ciliaris) grasses. *Functional Plant Biology* 34, 72-81.

George, T.S., Richardson, A.E., Simpson, R.J., 2005. Behaviour of plant-derived extracellular phytase upon addition to soil. *Soil Biol Biochem.* 37, 977-988.

Gorissen, A., Tietema, A., Joosten, N.N., Estiarte, M., Penuelas, J., Sowerby, A., Emmett, B.A., Beier, C., 2004. Climate change affects carbon allocation to the soil in shrublands. *Ecosystems* 7, 650-661.

Hasibeder, R., Fuchslueger, L., Richter, A., and Bahn, M., 2015. Summer drought alters carbon allocation to roots and root respiration in mountain grassland. *New Phytol.* 205, 1117–1127.

He, M. & Dijkstra, F.A., 2014. Drought effect on plant nitrogen and phosphorus: A meta-analysis. *New Phytol.* 204, 924–931.

Hinsinger, P., 2001. Bioavailability of soil inorganic P in therhizosphere as affected by root-induced chemical changes: areview. *Plant and Soil* 237, 173–195.

Hinsinger, P., Bengough, A.G., Vetterlein, D. & Young, I.M., 2009. Rhizosphere: biophysics, biogeochemistry and ecological relevance. *Plant Soil* 321, 117–152.

Hoffmann, C.M., 2010. Sucrose accumulation in sugar beet under drought stress. *Journal of Agronomy and Crop Science* 196, 243-252.

Ibiang, Y.B., Mitsumoto, H., and Sakamoto, K., 2017. Bradyrhizobia and arbuscular mycorrhizal fungi modulate manganese, iron, phosphorus, and polyphenols in soybean (Glycine max (L.) Merr.) under excess zinc. *Environ. Exp. Bot.* 137, 1–13.

Jacob, J., Lawlor, D.W., 1991. Stomatal and mesophyll limitations of photosynthesis in phosphate deficient sunflower, maize and wheat plants. *Journal of Experimental Botany* 42, 1003–1011.

Karlowsky, S., Augusti, A., Ingrisch, J., Akanda, M.K.U., Bahn, M., Gleixner, G., 2018. Drought-induced accumulation of root exudates supports post-drought recovery of microbes in mountain grassland. *Frontiers in Plant Science* 9, 1– 16.

Karmakar, K., Rana, A., Rajwar, A., Sahgal, M., Johri, B.N., 2015. Legume-Rhizobia Symbiosis Under Stress. In: Arora N. (eds) Plant Microbes Symbiosis: Applied Facets. *Springer*, New Delhi.

Keatinge, J.D.H., Easdown, W.J., Yang, R.Y., Chadha, M.L. & Shanmugasundaram, S., 2011. Overcoming chronic malnutrition in a future warming world: the key importance of mungbean and vegetable soybean. *Euphytica* 180, 129–141.

Kraigher, H., Bajc, M., Grebenc, T., 2013. Chapter 8 - mycorrhizosphere complexity. In: Matyssek, N.C.R., Cudlin, P., Mikkelsen, T.N., Tuovinen, J.P., Wieser, G., Paoletti, E. (eds): Developments in environmental science. *Elsevier*, pp 151–177.

Morgan, J.M., 1984. Osmoregulation and water stress in higher plants. *Ann. Rev. Plant Physio* 35, 299-319.

Pavithra, D., Yapa, N., 2018. Arbuscular mycorrhizal fungi inoculation enhances drought stress tolerance of plants. *Groundwater for Sustainable Development* 7, 490-494.

Peters, N.K. & Long, S.R., 1988. Alfalfa root exudates and compounds which promote or inhibit induction of Rhizobium meliloti nodulation genes. *Plant Physiology* 88, 396– 400.

Kandeler, E., Marschner, P., Tscherko, D., Gahoonia, T.S., Nielsen, N.E., 2002. Microbial community composition and functional diversity in the rhizosphere of maize. *Plant and Soil* 238, 301-312.

Kouno, K., Tuchiya, Y., Ando, T., 1995. Measurement of soil microbial biomass phosphorus by an anion-exchange membrane method. *Soil Biology & Biochemistry* 27, 1353– 1357.

Kuzyakov, Y., Razavi, B.S., 2019. Rhizosphere size and shape: Temporal dynamics and spatial stationarity. *Soil Biology & Biochemistry* 135, 343– 360.

Kuzyakov, Y., Blagodatskaya, E., 2015. Microbial hotspots and hot moments in soil: Concept & review. *Soil Biology & Biochemistry* 83, 184-199.

Larionova, A.A., Yevdokimov, I.V., Bykhovets, S.S., 2007. Temperature response of soil respiration is dependent on concentration of readily decomposable C. *Biogeosciences* 4, 1073– 1081.

Lewis, D.H. and Quirk, J.P., 1967. Phosphate diffusion in soil and uptake by plants. III. 31P movement and uptake by plants as indicated by 32P autoradiography. *Plant and Soil* 27, 445–453.

Liu, L., Chen, X., Hao, L., Zhang, G., Jin, Z., Li, C., Yang, Y., Rao, J., Chen, B., 2020. Traditional fermented soybean products: processing, flavor formation, nutritional and biological activities. *Critical Reviews in Food Science and Nutrition*. DOI: 10.1080/10408398.2020.1848792.

Ma, X., Razavi, B.S., Holz, M., Blagodatskaya, E., Kuzyakov, Y., 2017. Warming increases hotspot areas of enzyme activity and shortens the duration of hot moments in the root-detritusphere. *Soil Biology and Biochemistry* 107, 226-233.

Mach, K.J., Kraan, C.M., Adger, W.N., Buhaug, H., Burke, M., Fearon, J.D., Field, C.B., Hendrix, C.S., Maystadt, J-F., O'Loughlin, J., Roessler, P., Scheffran, J., Schultz, K.A., von Uexkull, N. 2019. Climate as a risk factor for armed conflict. *Nature* 571, 193–197.

Marschner, H., 1998. Role of root growth, arbuscular mycorrhiza and root exudates for the efficiency in nutrient acquisition. *Field Crops Research* 56, 203-207.

McLaughlin, J.E. & Boyer, J.S., 2004. Glucose localisation in maize ovaries when kernel number decreases at low water potential and sucrose is fed to the stems. *Annals of Botany* 94, 75– 86.

Menon, M., Robinson, B., Oswald, S.E., Kaestner, A., Abbaspour, K.C., Lehmann, E., Schulin, R., 2007. Visualization of root growth in heterogeneously contaminated soil using neutron radiography. *Eur. J. Soil Sci.* 58, 802-810.

Muchovej, R., 2004. Importance of mycorrhizae for agricultural crops. SS-AGR-170. Florida: Agronomy Department, Florida Cooperative Extension Service, Institute of Food and Agricultural Sciences, University of Florida.

Nannipieri, P., Kandeler, E., Ruggiero, P., 2002. Enzyme Activities and Microbiological and Biochemical Processes in Soil. Enzymes in the Environment. *Marcel Dekker*, New York, pp. 1-33.

Nannipieri, P., Giagnoni, L., Landi, L., Renella, G., 2011. Role of phosphatase enzymes in soil phosphorus in action. In: Bünemann E, Oberson A, Frossard E, editors. Springer Berlin Heidelberg, pp. 215–243.

Olsen, S.R., Cole, C.V., Watanabe, F.S., Dean, L.A., 1954. Estimation of Available Phosphorus in Soils by Extraction with Sodium Bicarbonate US Department of Agriculture Circular 939, US Department of Agriculture, Washington DC.

Orwin, K.H., and Wardle, D.A., 2004. New indices for quantifying the resistance and resilience of soil biota to exogenous disturbances. *Soil Biol. Biochem.* 36, 1907–1912.

Palta, J.A., and Gregory, P.J., 1997. Drought affects the fluxes of carbon to roots and soil in 13C pulse-labelled plants of wheat. *Soil Biol. Biochem.* 29, 1395–1403.

Pathan S.I., Žifčáková L., Ceccherini M.T., Pantani O.L., Větrovský T., Baldrian P., 2017. Seasonal variation and distribution of total and active microbial community of beta-glucosidase encoding genes in coniferous forest soil. Soil Biol. Biochem. 105, 71–80.

Panikov, N.S., Blagodatsky, S.A., Blagodatskaya, E., 1992. Determination of microbial mineralization activity in soil by modifed Wright and Hobbie method. *Biology and Fertility of Soils* 14, 280–287.

Peña-Rojas, K., Aranda, X., Fleck, I., 2004. Stomatal limitation to CO2 assimilation and down-regulation of photosynthesis in Quercus ilex resprouts in response to slowly imposed drought. *Tree Physiology* 24, 813– 822.

Peña-Rojas, K., Aranda, X., Jofre, R., Fleck, I., 2006. Leaf mosphology, photochemistry and water status changes in resprouting Quercus ilex under drought. *Functional Plant Biology* 32, 117– 130.

Pepe, A., Giovannetti, M. & Sbrana, C., 2016. Different levels of hyphal self incompatibility modulate interconnectedness of mycorrhizal networks in three arbuscular mycorrhizal fungi within the Glomeraceae. *Mycorrhiza* 26, 325–332.

Razavi, B.S., Zarebanadkouki, M., Blagodatskaya, E., Kuzyakov, Y., 2016. Rhizosphere shape of lentil and maize: spatial distribution of enzyme activities. *Soil Biol Biochem* 96, 229-237.

Razavi, B.S., Zhang, X., Bilyera, N., Guber, A., Zarebanadkouki, M., 2019. Soil zymography: Simple and reliable? Review of current knowledge and optimization of the method. *Rhizosphere* 11, 100161.

Rillig, M.C., Wright, S.F., Nichols, K.A., Schmidt, W.F., Torn, M.S., 2001. Large contribution of arbuscular mycorrhizal fungi to soil carbon pools in tropical forest soils. *Plant Soil* 233, 167-177.

Ruiz-Lozano, J.M., Collados, C., Barea, J.M., Azcón, R., 2001. Arbuscular mycorrhizal symbiosis can alleviate drought-induced nodule senescence in soybean plants. *New Phytologist* 151, 493-502.

Liese, R., Lübbe, T., Albers, N.W., Meier, I.C., 2018. The mycorrhizal type governs root exudation and nitrogen uptake of temperate tree species. *Tree Physiology* 38, 83–95.

Sardans, J., Peñuelas, J., 2004. Increasing drought decreases phosphorus availability in an evergreen Mediterranean forest. *Plant Soil* 267, 367–377.

Sardans, J., Peñuelas, J.. 2007. Drought changes phosphorus and potassium accumulation patterns in an evergreen Mediterranean forest. *Functional Ecology* 21, 191–201.

Schimel, J., Balser, T.C., Wallenstein, M., 2007. Microbial stress-response physiology and its implications for ecosystem function. *Ecology* 88, 1386-1394.

Schnepf, A., Leitner, D., Klepsch, S., Pellerin, S., and Mollier, A., 2011. "Modelling phosphorus dynamics in the soil-plant system," in Phosphorus in Action: Biological Processes in Soil Phosphorus Cycling, (eds.) Bünemann, E.K., Obserson, A., and Frossard, E. (Heidelberg: *Springer*), 113–133.

Shade, A., Peter, H., Allison, S.D., Baho, D.L., Berga, M., Bürgmann, H., Huber, D.H., Langenheder, S., Lennon, J.T., Martiny, J.B.H., Matulich, K.L., Schmidt, T.M., Handelsman, J., 2012. Fundamentals of microbial community resistance and resilience. *Front Microbiol* 3, 1–17.

Sharp, R.E., Hsiao, T.C., Silk, W.K., 1990. Growth of the maize primary root at low water potentials. II. Role of growth and deposition of hexose and potassium in osmotic adjustment. *Plant Physiol* 93, 1337–1346.

Shen, J.B., Yuan, L.X., Zhang, J.L., Li, H.G., Bai, Z.H., Chen, X.P., Zhang, W.F., Zhang, F.S., 2011. Phosphorus dynamics: from soil to plant. *Plant Physiology* 156, 997– 1005.

Shu, X., Hallett, P.D., Liu, M., Baggs, E.M., Hu, F., Griffiths, B.S., 2019. Resilience of soil functions to transient and persistent stresses is improved more by residue incorporation than the activity of earthworms. *Applied Soil Ecology* 139, 10-14.

Smith, S.E. and Read, D.J., 1997. Mycorrhizal Symbiosis, 2nd Edn. London: Academic Press.

Spollen, W.G., Tao, W., Valliyodan, B., Chen, K., Hejlek, L.G., Kim, J.J., Lenoble, M.E., Zhu, J., Bohnert, H.J., Henderson, D,, Schachtman, D.P., Davis, G.E., Springer, G.K., Sharp, R.E., Nguyen, H.T., 2008. Spatial distribution of transcript changes in the maize primary root elongation zone at low water potential. *BMC Plant Biol* 8, 32.

Steinweg, J.M., Dukes, J.S., Wallenstein, M.D., 2012. Modeling the effects of temperature and moisture on soil enzyme activity: linking laboratory assays to to continuous field data. *Soil Biol Biochem* 55, 85-92.

Strickland, M.S., Wickings, K., Bradford, M.A., 2012. The fate of glucose, a low molecularweight compound of root exudates, in the belowground foodweb of forests andpastures. *Soil Biol Biochem* 49, 23–29.

Tarafdar, J.C., Claasen, N., 1988. Organic phosphorus compounds as a phosphorus source for higher plants through the activity of phosphatases produced by plant roots and microorganisms. *Biology and Fertility of Soils* 5, 3308 – 3312.

Tarafdar, J.C., Marschner, H., 1994. Efficiency of VAM hyphae in utilization of organic phosphorus by wheat plants. *Soil Sci Plant Nutr* 40, 593–600.

Tarafdar, J.C., Marschner, H., 1995. Dual inoculation with Aspergillus fumigatus and Glomus mosseae enhances biomass production and nutrient uptake in wheat (Triticum aestivum L.) supplied with organic phosphorus as Na-phytate. Plant and Soil 173, 97-102.

Vancura, V., Hovadik, A., 1965. Root exudates of plants II. Composition of root exudates of some vegetables. *Plant Soil* 22, 21–32.

Verdoucq, L., Moriniere, J., Bevan, D.R., Esen, A., Vasella, A., Henrissat, B., Czjzek, M., 2004. Structural determinants of substrate specificity in family 1 β-glucosidases: novel insights from the crystal structure of sorghum dhurrinase-1, a plant β-glucosidase with strict specificity, in complex with its natural substrate. *J Biol Chem* 279, 31796–31803.

Vierheilig, H., Coughlan, A.P., Wyss, U. & Piche, Y., 1998. Ink and vinegar, a simple staining technique for arbuscular-mycorrhizal fungi. *Appl. Environ. Microbiol.* 64, 5004–5007.

Vierheilig, H., Schweiger, P., Brundrett, M., 2005. An overview of methods for the detection and observation of arbuscular mycorrhizal fungi in roots. *Physiologia Plantarum* 125, 393–404.

Voothuluru, P., Anderson, J.C., Sharp, R.E., Peck, S.C., 2016. Plasma membrane proteomics in the maize primary root growth zone: novel insights into root growth adaptation to water stress. *Plant, Cell & Environment* 39, 2043-2054.

Voothuluru, P., Braun, D.M., Boyer, J.S., 2018. An in vivo imaging assay detects spatial variability in glucose release from plant roots. *Plant Physiology* 178, 1002–1010.

Wang, W.X., Vinocur, B., Shoseyov, O., Altman, A., 2001. Biotechnology of plant osmotic stress tolerance: physiological and molecular considerations. Acta Hort 560: 285–292 Williams, A., de

Vries, F.T., 2020. Plant root exudation under drought: implications for ecosystem functioning. *New Phytologist* 225, 1899–1905.
Welc, M., Frossard, E., Egli, S., Bünemann, E.K., Jansa, J., 2014. Rhizosphere fungal assemblages and soil enzymatic activities in a 110- years alpine chronosequence. *Soil Biol. Biochem.* 74, 21-30.
Williams, A., de Vries, F.T., 2020. Plant root exudation under drought: implications for ecosystem functioning. *New Phytologist* 225, 1899-1905.
Wu, Q.S., Xia, R.X. and Zou, Y.N., 2008. Improved soil structure and citrus growth after inoculation with three arbuscular mycorrhizal fungi under drought stress. *Eur. J. Soil Biol.* 44, 122–128.
Yang SY, Grønlund M, Jakobsen I, Grotemeyer MS, Rentsch D, Miyao A, Hirochika H, Kumar CS, Sundaresan V, Salamin N, Catausan S, Mattes N, Heuer S, Paszkowski U (2012) Nonredundant regulation of rice arbuscular mycorrhizal symbiosis by two members of the PHOSPHATE TRANSPORTER1 gene family. Plant Cell 24: 4236–4251
Yevdokimov, I., Blagodatskaya, E., 2014. Determination of extractable and microbial P in soils with anion-exchange membranes. Goettingen, Germany.
Zarebanadkouki, M., Carminati, A., 2014. Reduced root water uptake after drying and rewetting. *J. Plant Nutr. Soil Sci.* 177, 227-236.
Zhang, H., Shi, L., Lu, H., Shao, Y., Liu, S., Fu, S., 2020. Drought promotes soil phosphorus transformation and reduces phosphorus bioavailability in a temperate forest. *Sci. Total Environ.* 732, 139295.
Zhang, F., Meng, X., Yang, X., Ran, W., Shen, Q., 2014. Quantification and role of organic acids in cucumber root exudates in Trichoderma harzianum T-E5 colonization. Plant physiology and Biochemistry 83, 250-257.

2.2.8. Graphical abstract

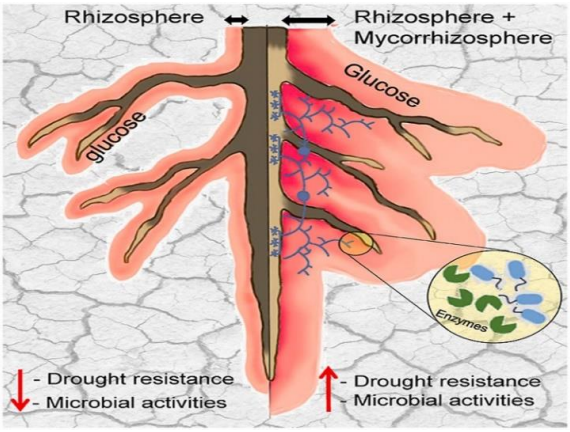

2.2.9. Appendix

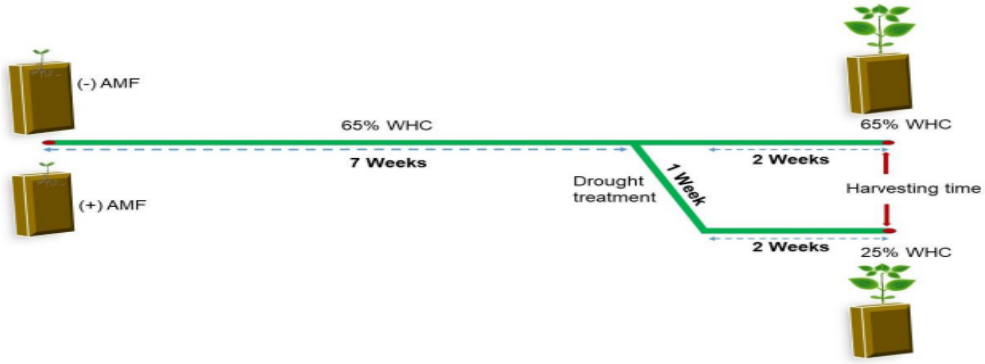

Appendix 2.2.1. Experiment design of soybean with four treatments: optimum (65% WHC) vs. drought (25% WHC) and AMF vs. no-AMF. Soybean grew under optimum condition for 8 weeks prior to a stress suffer for extra 2 weeks until harvest.

2.2.10. Supplementary figures

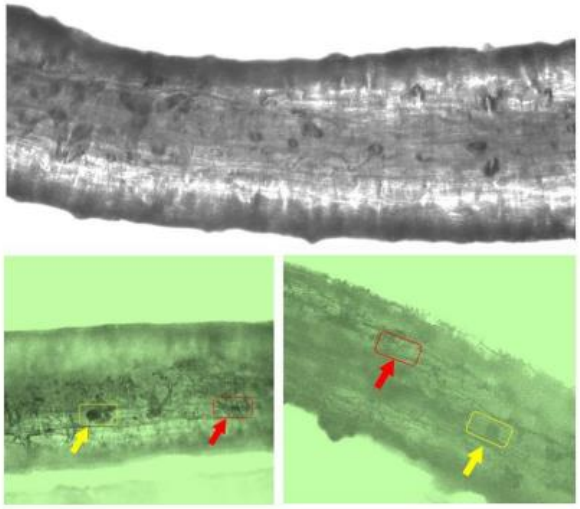

Figure S2.2.1. Arbuscular mycorrhiza fungi well accommodated in the roots. The image was taken using staining technique.

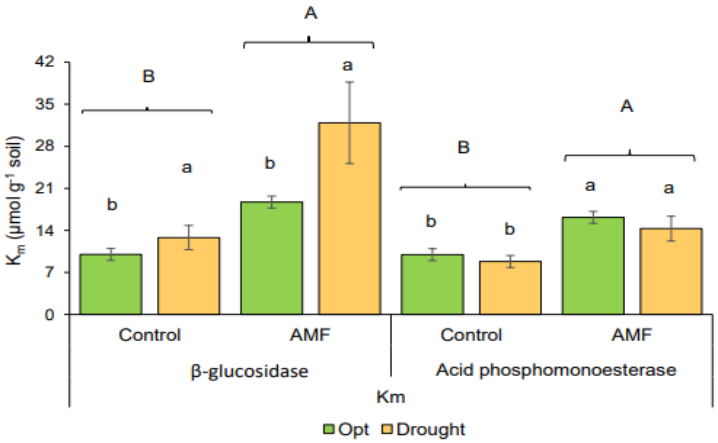

Figure S2.2.2. K_m values of β-glucosidase and acid phosphomonoesterase in mycorrhizal and non-mycorrhizal plants. Higher K_m value in mycorrhizal plants than non-mycorrhizal plants indicated different enzyme systems with lower substrate affinity. Lower case letters: significant differences between optimum (Opt) and drought at $p < 0.05$; upper case letters: significant differences between control and AMF at $p < 0.05$. GLU: β-glucosidase, PHOS: acid phosphomonoesterase.

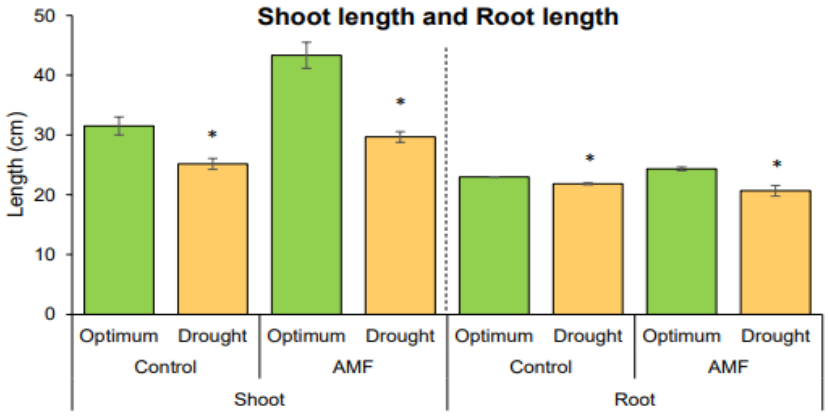

Figure S2.2.3. Drought reduced the shoot length by 1.3-1.5 times but the reduction of root length is less than shoot length. AMF inoculum strongly increased shoot length by 1.38 times at optimum condition and by 1.24 times at drought condition.

2.3. Study 3: Glucose Release and Enzyme Activity Are Affected by Successive Wheat Cultivation and Plant Developmental Stage

Mehdi Rashtbari[a*], Andrea Braun-Kiewnick[b], Kornelia Smalla[b], Bahar S. Razavi[a]
[a] *Department of Soil and Plant Microbiome, Institute of Phytopathology, Christian Albrechts University of Kiel, Kiel, Germany*
[b] *Institute for Epidemiology and Pathogen Diagnostics, Julius Kühn-Institute - Federal Research Centre for Cultivated Plants, Germany*

***** *corresponding author: mehdi.rashtbari@phytomed.uni-kiel.de*
https://orcid.org/0000-0002-8555-3450

Status: Revised version submitted to Geoderma

2.3.1. Abstract

Plants modify their rhizosphere through root exudates to recruit beneficial organisms, thus creating a protective zone around their roots. Changes in exudate compounds, such as glucose, can impact the abundance and activity of rhizosphere microorganisms. In this study, we investigated the presence of glucose in the rhizosphere of an economically important crop. We employed soil zymography, soil β-glucosidase enzyme kinetics, and microbial activity indices (such as respiration). Our aim was to offer new insights into microbial functionality by establishing connections between root exudation patterns and microbial activity. We conducted this study in the bulk soil and rhizosphere of first (W1) and third (W3) wheat after a break crop. Sampling occurred at two different times: t1 (four weeks after sowing, BBCH 13) and t2 (eight weeks after sowing, BBCH 29). W3 demonstrated a lower proportion of hotspots for glucose release at t2, with a 31.7% decline compared to W1. Additionally, presence of glucose at wheat root tips dropped by 19.4% in W3 compared to W1 at t1. At t2, the highest glucose presence at root tips was obtained in W1 with 403.3 nmol cm^{-2}, while W3 resulted in 20% less glucose presence. Accordingly, the maximum rate of β-glucosidase enzyme activity decreased by ~71% and 47% in the rhizosphere and bulk soil compartments at t2 compared to t1 in W1, while the respective values for W3 were ~82% and 83%, respectively. The microbial biomass C indicated a considerable decrease, resulting in lower enzyme activity for W3 compared to W1 samples. We concluded that successive wheat cultivation affected rhizosphere processes in terms of glucose exudation and enzyme activities, and that W3 not only resulted in lower glucose release and enzyme activity but also led to the production of less efficient enzymes with higher K_m values and lower catalytic efficiency. This may result in weaker, less healthy plants in successive wheat cultivation without a microbial protection zone around roots, leading to higher pathogen susceptibility and ultimately lower yields. Also, our method efficiently localized glucose exudation from wheat roots and has great potential to be expanded for the visualization of other sugars in the exudates.

Keywords: monoculture, root exudates, rotation, wheat, zymography

2.3.2. Introduction

Root exudates play a crucial role in shaping soil microbial community assembly (Zhalnina et al., 2018) and influencing biogeochemical processes that impact plant growth (Bakker et al., 2018; Blagodatskaya et al., 2021). These processes encompass C and nutrient dynamics, as well as the root-soil defense system (Kuzyakov and Razavi, 2019). The rhizosphere, the soil

zone surrounding plant roots, is characterized by a dynamic interaction between the rhizosphere microbiome and roots (Kennedy and de Luna, 2005, Giongo et al., 2024). Plants release a range of organic substances derived from photosynthesis into the rhizosphere, stimulating the proliferation of specific microbial groups in a plant species and soil type-dependent manner. This results in the formation of an environment rich in organic compounds. This dynamic environment can either stimulate or inhibit microbial communities, depending on the availability and composition of these compounds (Berg and Smalla, 2009; Hinsinger et al., 2011). Numerous studies have demonstrated that plants shape the composition and diversity of microbial communities in the rhizosphere through exudate-mediated interactions (Houlden et al., 2008; Chen et al., 2019). Moreover, plants can remodel the rhizosphere microbial communities in response to pathogen attacks (Li et al., 2020).

Boyer et al., (2010) reported that wheat (*Triticum aestivum*) and barley (*Hordeum vulgare*) release about 1 to 11 percent of their fixed C into the soil through rhizodeposition. This process involves the secretion of primary metabolites, such as sugars, amino acids, and organic acids, which make up the majority of root exudates (Canarini et al., 2019). Notably, Derrien et al., (2004) used stable C isotope tracing to show that up to 21% of the C fixed during wheat photosynthesis is released through root exudation. Glucose, a dominant sugar in root exudates of various plant species (Gunina and Kuzyakov, 2015), accounts for approximately 40-50% of exudates (Hütsch et al., 2002). As glucose is readily available in root exudates (Jones et al., 2009), it can directly influence the proliferation and function of potentially beneficial microorganisms in the rhizosphere (Finzi et al., 2015).

There is significant competition among microorganisms in the rhizosphere for nutrients and niches, which depend on these resources (Wang et al., 2021). As crops continue to grow, developmental senescence causes a decrease in root exudation and glucose production (Prudence et al., 2021). This intensifies competition on the root surface and reduces enzyme activity, which is directly related to the amount of available substrate (Allison and Vitousek 2005). This competition can lead to a decline in the abundance and activity of plant-beneficial microorganisms, as supported by studies such as Peralta et al. (2018), which observed reduced activity of antagonistic microorganisms. This reduction significantly impacts the rhizosphere microbiome, consequently affecting their function and ultimately influencing plant performance.

Glucose, a prevalent soluble carbohydrate abundant in root exudates, plays a pivotal role in facilitating root adaptation to dynamic environmental conditions (Canarini et al., 2019). Its consistent presence amid fluctuations in root exudate composition due to varying soil moisture, temperature, and nutrient availability underscores its significance in driving microbial activity within the rhizosphere (Hütsch et al., 2002). The influence of glucose extends beyond its role as a mere energy source. Studies have suggested its involvement in modulating root exudation patterns in response to environmental cues, thereby shaping the rhizosphere's microbial community structure (Smith and Read, 2008). For instance, glucose availability has been linked to alterations in microbial diversity and enzymatic activities, influencing nutrient cycling processes and potentially affecting plant nutrient uptake (Qi et al., 2022). Wild et al. (2014) found that glucose can actively engage in soil carbon metabolism processes by serving as both a carbon and energy source. Studies conducted in pure cultures have demonstrated that glucose molecules engage with microbial chemoreceptors, eliciting diverse biochemical responses. This finding holds significance for the study of soil microbes (Kirby, 2009).

The complexity of the rhizosphere extends beyond glucose availability, as the amount and composition of root exudates are subject to modulation by a range of biotic and abiotic factors (Gargallo-Garriga et al., 2018). Plant-mediated manipulation of microbial populations through sugar secretion, as seen in studies by Pascale et al., (2020), exemplifies the dynamic

interactions that occur. Additionally, the role of pathogens cannot be underestimated, as they harness sugar fluxes from plant roots to potentially enhance their growth and increase plant susceptibility to infection (Meteier et al., 2019). The intricate orchestration of these processes becomes evident through observations of increased glucose efflux into the root apoplast during the activation of sugar transporters, potentially serving as a strategy employed by pathogens (Chen et al., 2010; 2015).

Changes in exudate composition have implications for plant health, soil properties, and rhizosphere microorganisms. Higher sugar content in root exudates may be associated with pathogen resistance in plants, as sugars provide energy for defense responses and interact with hormonal signalling pathways (Meteier et al., 2019). For instance, elevated glucose levels in root exudates of Arabidopsis thaliana enhance the activity of defense enzymes against fungal pathogens (Naseem et al., 2012). However, root exudates can have differential effects on beneficial microorganisms and soil-borne pathogens (Jones et al., 2004), and the specific factors contributing to these effects in wheat root exudates are not well understood. Successive cultivation of wheat with other crops often leads to yield decline due to biotic and abiotic stressors, such as pathogen accumulation/attack and droughts, affecting water and nutrient uptake (Sieling et al., 2005).

This study aimed to investigate the impact of successive wheat cultivation on glucose release from roots and microbial activity. Glucose imaging, soil zymography, microbial respiration, and enzyme kinetics were optimized and utilized to quantify these effects. The hypothesis is that successive wheat cultivation would decrease glucose release, leading to reduced microbial activity and biomass. Additionally, a decline in soil microbial enzyme production in the third wheat (W3) compared to the first wheat (W1) was expected. To test the hypothesis, wheat plants (*Tritium aestivum*) were grown in rhizoboxes filled with soil from either W1 or W3 under optimal water conditions in a greenhouse. Glucose imaging (Hoang et al., 2022) and soil zymography (Spohn and Kuzyakov, 2014) were employed to investigate the role of soil microbial communities in C transformation and translocation. The study also measured microbial biomass C and the kinetics of the β-glucosidase enzyme responsible for glucose release from complex organic molecules in soil (German et al., 2012).

2.3.3. Materials and Methods

2.3.3.1. Experimental design

In this study, soil samples were collected from the Ap horizon (0-20 cm) of soil at the Hohenschulen experimental field site (54°19′05″N, 9°58′38″E) in Germany from six different plots at the beginning of the growing season. The soil samples were collected from two distinct wheat rotational positions: the first wheat position (referred to as W1), represented the first wheat cultivation after the break crop of winter oilseed rape, and the subsequent third wheat (wheat grown continuously for three years referred to as W3) addressing the continuous cultivation of wheat three years in a row following the same break crop. The details on the crop rotational trials and wheat rotational positions are described in Arnhold et al. (2023). The soil had a pH of 6.7 and the following properties: pseudogleyic sandy loam (Luvisol), 21% clay, 35% silt, 44% sand, 1.3% organic C, 0.15% total N, 9 $mg.kg^{-1}$ available P, and 15 $mg.kg^{-1}$ available K (Sieling et al., 2005).

The soil samples were then transported to a greenhouse facility at Kiel University, where they were sieved through a 2 mm mesh and filled into transparent rhizoboxes (20 × 20 × 3 cm) (Fig. S2.3.1). The rhizoboxes were arranged in a randomized design, with a total of six rhizoboxes filled with soil from W1 and another six filled with soil from W3, each treatment comprising three replicates. After filling the rhizoboxes with soil samples, healthy seeds of the wheat cultivar 'Nordkap' were selected and sterilized before being germinated on wet filter paper for three days at room temperature. One seed was then planted 1.5 cm deep into each

rhizobox. The rhizoboxes were placed in a greenhouse chamber, inclined at a 45° angle with the removable side facing down. The temperature was maintained at 22°C with a 12-hour day/light cycle and a light intensity of 300 mmol m^{-2} s^{-1}. The rhizoboxes were covered with aluminium foil to reduce evaporation and prevent algae growth. Soil moisture was monitored gravimetrically every two days and adjusted to maintain 70% water holding capacity (WHC) throughout the two-month experiment by adding sterile distilled water as needed.

Due to the limited space and resources in the rhizoboxes, plants were harvested at two time points: four weeks (t1, BBCH 13) and eight weeks (t2, BBCH 29) after sowing through destructive sampling. This approach ensured a consistent and comparable temporal assessment of enzyme activities and plant root exudates in W1 and W3.

2.3.3.2. Glucose imaging

Soil glucose imaging is a method used to visualize and quantify the amount of glucose exuded from plant roots. This method was optimized based on the protocols developed by McLaughlin and Boyer (2004) and Voothuluru et al. (2018) and is useful for studying plant root exudation and interactions with the surrounding soil. The process involves preparing a reaction mixture solution by dissolving phosphate powder (Sigma P7994) in distilled water to make a 100 mL buffer solution of 0.05 M (pH 7.4). To this solution, 1.7 unit/ml of glucose oxidase from *Aspergillus niger* (Sigma G7141), 1.5 unit/ml of peroxidase from horseradish (Sigma P8125), and 200 μM of Ampliflu red (Sigma 90101) dissolved in 60 μL of Dimethylsulfoxide were added.

Polyamide membrane filters with a diameter of 20 cm and a pore size of 0.45 mm (Tao Yuan, China) were cut to fit the size of the rhizobox and then saturated with the prepared reaction mixture solution. These membranes are then attached to the rooted side of each rhizobox. After an optimal incubation time (one hour for wheat), the membranes were quickly removed and placed in a dark room under UV light of 355 nm wavelength.

The magenta-colored area on the membrane indicates the presence of glucose exudation, as hydrogen peroxide was generated from a reaction between glucose and glucose oxidase enzymes. Horseradish peroxidase then catalyses the conversion of colorless Ampliflu red into magenta colored and fluorescent resorufin (Zhou et al., 1997). Glucose imaging was conducted for all rhizoboxes in two sampling times foe W1 and W3.

2.3.3.3. β -glucosidase Zymography

Zymography was performed to measure β-glucosidase activity, following the protocol developed by Razavi et al., (2019). Firstly, a fluorescent solution of 4-methylumbelliferyl-β-glucoside (MUF-β) (Sigma Aldrich, Germany) was prepared in 4-morpholineethane sulfonic acid (MES) with a concentration of 12 mM. The added substrate was cleaved by soil β-glucosidase enzymes, generating fluorescent signals under UV light, which was used to detect β-glucosidase activity.

To reduce enzyme diffusion through the pores, the polyamide membrane filters (Tao Yuan, China) with a pore size of 0.45 mm were utilized (Razavi et al., 2016). These membranes were soaked in the fluorescent solution and then directly applied to the root-exposing side of the rhizoboxes. They were then covered with aluminium foil to prevent exposure to light and drying out. After incubation for one hour, the membranes were quickly removed, cleaned with a soft brush, and exposed to UV light of 355 nm wavelength excitation in a dark room.

2.3.3.4. Calibration and image analysis

All images were captured using a Canon EOS 6D digital camera with a Canon lens EF 24–105 mm 1: 4L IS II USM. The aperture and shutter speed were set to f/5.6 and 1/10 sec (for glucose imaging) and 1/8 sec (for zymography), respectively. To create the calibration lines for glucose

imaging, membranes of 4 cm^2 were soaked in glucose solutions of varying concentrations (0, 2, 4, 6, 8, and 10 mM). The membranes were used to measure the fluorescent signals of glucose release on an area basis, calculated based on the volume of substrate solution taken up by a fixed membrane size.

For zymography processing, individual 4 cm^2 membranes were soaked in MUF solutions of varying concentrations (0, 0.2, 0.5, 1, 2, 4, 6, 8, and 10 mM), then exposed to UV light in the same way as the samples. Calibrated values were used to quantify the colour intensity and relate β-glucosidase activity to the grey value. Fluorescent signals of MUF on an area basis were calculated based on the volume of substrate solution taken up by a fixed membrane size. The images were processed and analysed using the ImageJ software package. All captured images were transformed to a 16-bit grayscale value, adjusted for background and contrast levels, segmented roots, and converted grey values to enzyme activities/glucose release rate. We used the "Adjust Brightness and Contrast" tool in ImageJ software to adjust the background and contrast levels in captured images to ensure that the grey values of the roots were within the 0-255 range. The lower and upper threshold levels were set to remove background noise and ensure clear visibility of roots. Finally, grey values were converted to enzyme activities/glucose release rates using a calibration curve generated from known concentrations. This allowed for quantification of enzymatic activities or glucose release rates in each image.

Mean+2SD was applied to identify and separate hotspots within each image which comprised three steps: dividing the greyscale histogram into two distributions with normal greyscale values, pinpointing the greyscale range associated with the hotspots, and subsequently mapping these hotspots onto the original image (Bilyera et al., 2020). This method allowed for the application of individualized thresholds to account for variations in enzyme activity and glucose release distribution within each image, ensuring that hotspot determination was tailored to the specific characteristics of the respective image. The rhizosphere extent of each root was calculated from the root surface for mature roots (>2 cm from the tip) and root tips (0–2 cm) for glucose release and β-glucosidase activity (soil zymograms). To measure the rhizosphere extent, five horizontal transects (angle to the root ~90°) were randomly drawn across five randomly selected roots for glucose release images and beta-glucosidase zymograms using ImageJ. In total, this yielded 25 lines per image as pseudo-replicates, and their mean was used for each rhizobox as a true replicate (Bilyera et al., 2021).

2.3.3.5. Enzyme kinetics, substrate affinity, and catalytic efficiency

After uprooting the plants from the rhizoboxes, rhizosphere samples were obtained by immediately removing attached soil particles from roots using toothbrushes (Hamel et al., 2019). To do this, the entire root was placed on a sterile surface, and the soil was brushed off the root surface using a clean toothbrush. The soil was then collected in a conical tube and stored at 5 °C. Bulk soil (without roots) was also collected from the boxes and stored in the same way for comparative purposes. All samples for enzyme kinetics were measured the next day. The kinetics of β-glucosidase were determined using β-D-glucopyranoside (MUF-G) fluorescent substrate (Sigma Aldrich, Germany). According to German et al., (2011), 1.0 g of soil was suspended in 50 mL of distilled water, and 50 µL aliquots were pipetted into labelled wells of a 96-well microplate (Thermo Fisher, Denmark). Then, 50 µL of MES buffer (pH 6.5) and 100 µL of the respective substrate solution were added to each well. The enzyme activity was measured at three time points: 30, 60, and 120 min using CLARIOstar plus (BMG LABTECH, Germany) at an excitation wavelength of 355 nm and an emission wavelength of 460 nm. We determined enzyme activities over a range of substrate concentrations from low to high (0, 20, 40, 60, 80, 100, 200, and 400 µmol g^{-1} soil) to ensure the appropriate saturating concentration. Enzyme activity (V_{max}) were expressed as released MUF in nmol per g dry soil

per hour (nmol MUF g^{-1} soil h^{-1}) (Awad et al., 2012), and affinity constants for β-glucosidase (K_m) were expressed in µmol substrate per g dry soil (µmol g^{-1} soil). Simultaneously, a range of MUF concentrations (0, 10, 20, 30, 40, 50, 100, and 200 nM) were prepared to calibrate the measurement. The Michaelis-Menten equation was used to determine the parameters of β-glucosidase enzyme activity (V):

$$V = \frac{V_{max}[S]}{K_{m+}[S]} \quad (1)$$

V_{max} represents the maximum enzyme activity, which is a function of enzyme concentration. K_m is the substrate concentration at half-maximal enzyme activity, and S is the substrate concentration. To calculate catalytic efficiency, we used the V_{max}-to-K_m ratio (Panikov et al., 1992). Additionally, we calculated the substrate turnover time using equation (2), where T_t represents the turnover time in hours, employing the highest substrate concentration within our experimental range (400 µmol g^{-1} soil) (Hoang et al., 2020).

$$T_t = \frac{K_m \times [S]}{V_{max}} \quad (2)$$

2.3.3.6. Basal respiration and substrate-induced respiration

The MicroResp™ system (Chapman et al., 2007) was utilized to measure basal respiration (BR) and substrate-induced respiration (SIR). For BR, we used distilled water, while SIR was measured using glucose as a readily available C source. The system comprises a 1.2-mL deep well plate containing fresh soil and C source, and a carbon dioxide detection microplate. The detection plate was read by a CLARIOstar Plus microplate reader (BMG LABTECH, Germany) at 0 and 6 hours after incubation at 25°C, with a wavelength of 570 nm. The absorbance readings were converted to CO_2 concentration using a standard calibration line.

The microbial biomass C (C_{mic}) was calculated by determining the rate of glucose-induced respiration after incubation using the formula developed by Anderson and Domsch (1990):

C_{mic} (µg C g^{-1} soil) = (µl CO_2 g^{-1} soil h^{-1}) × 40.04

The metabolic quotient (qCO_2), which indirectly reflects microbial maintenance expenses, availability, and efficiency of microbial substrate utilization, was determined by calculating the ratio of BR to C_{mic} (Anderson and Domsch, 1990).

2.3.3.7. Data analysis

All statistical analyses were conducted using Sigma-Plot 14.0 software. To test for significant differences in enzyme activities, substrate affinity, catalytic efficiency, substrate turnover time, rhizosphere extent, hotspot percentage, respiration, microbial biomass C, and qCO_2 between W1 and W3 soil samples collected at two different sampling times (t1 and t2), two-way ANOVA was performed after checking normality and homogeneity of variance values. A significance level of $p<0.05$ was used to determine the significance of treatment comparisons. The standard error of the means is represented by the error bars.

2.3.4. Results

2.3.4.1. Hotspot area and rhizosphere extent in W3 were significantly lower compared to W1 at t2

The spatial distribution of glucose release and β-glucosidase activity was found to be influenced by successive wheat plantation, particularly at t2, as shown in Figure 2.3.1. At t1, there was no significant difference in the total area of β-glucosidase activity hotspots in the rhizosphere of W3 and W1 soil samples. However, at t2, W3 samples showed a 25.2% lower proportion of hotspots (4.26% vs 5.70%, respectively; $p<0.01$) compared to W1. Furthermore, at t2, W3 exhibited the lowest proportion of glucose release hotspots, covering 1.83% of the

total soil surface area. This represents a 31.7% decline compared to W1 ($p<0.05$) (see Figure 2.3.2a).

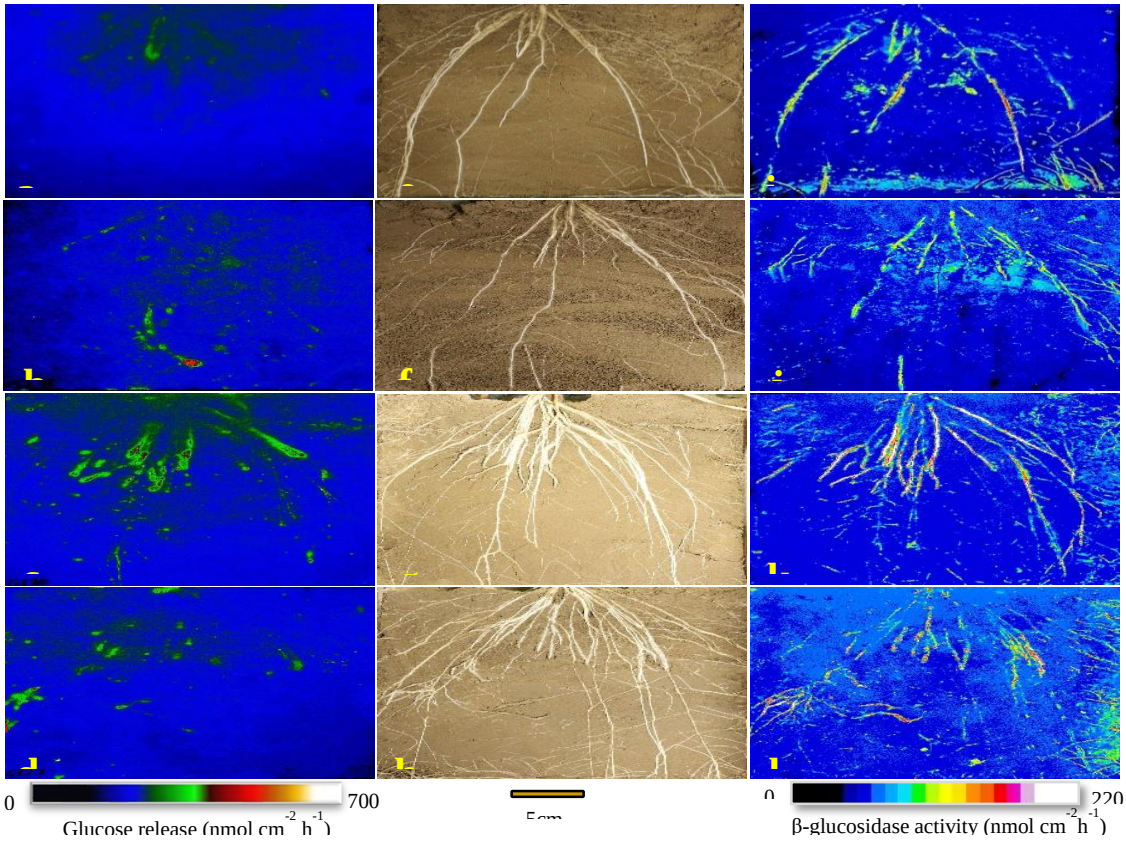

Figure 2.3.1. Spatial distribution of glucose release (a-d); β-glucosidase activity (i-l) and original images of the wheat root (e-h) at T1W1 (top row), T1W3 (second row), T2W1 (third row), T2W3 (lower row), respectively (T1: four weeks (BBCH 13), and T2: eight weeks after sowing (BBCH 29); W1: first and W3: third wheat after break crop.

Although the rhizosphere extent for glucose release was higher in W3 compared to W1 at t1, from 0.48 mm to 0.66 mm, there was a significant decrease during the later plant stage, with a 39.7% decline ($p<0.01$). On the other hand, the β-glucosidase activity around the wheat roots at t1 indicated a 33% decrease from W1 to W3. The decline in enzyme activity was observed over time, indicating lower enzyme activity at t2 compared to t1. However, it's noteworthy that the rate of decrease in W3 at t2, in comparison to W1, was not as pronounced as observed at t1. The highest and lowest extents of enzyme activity were observed in W1 at t1 and in W3 at t2, with values of 0.45 mm and 0.17 mm, respectively ($p<0.05$) (see Figure 2.3.2b). As the plants developed, it was observed that W3 wheat plants released less glucose from their root samples. This decrease in glucose release affected both the hotspot percentage and the extent of enzyme activity around the roots.

2.3.4.2. Glucose releasing rate and β-glucosidase activity are lower in W3 at t2 than in W1

The results showed that W3 wheat plants had a consistently lower in glucose release rate in both root tips and mature roots, especially at t2, compared to W1 ($p<0.05$). At t1, glucose release at wheat root tips decreased by 19.4% in W3 compared to W1. However, at t2, W1 had higher glucose release at root tips with 403.3 $nmol^{-1}$ cm^{-2}, while W3 resulted in 20% lower glucose release. A similar trend was observed for glucose release from mature roots, which decreased by 18.5% and 17.4% at t1 and t2, respectively, in W3 compared to W1 (Fig. 2.3.3a). The wheat crop rotational positions minimally affected β-glucosidase activity at t1 for both

root tips and mature roots. Subsequently, at t2, a noticeable declining trend in enzyme activity was observed from W1 to W3, leading to an 11.4% decrease in root tip activity and a 13.6% decrease in mature root enzyme activity. W1 displayed higher enzyme activity for root tips (153.85 nmol MUFcm^{-2}h^{-1}) and mature roots (159.64 nmol MUFcm^{-2}h^{-1}) ($p<0.01$; Fig. 2.3.3b). Thus, the highest glucose release at T2 was accompanied by the highest β-glucosidase activity.

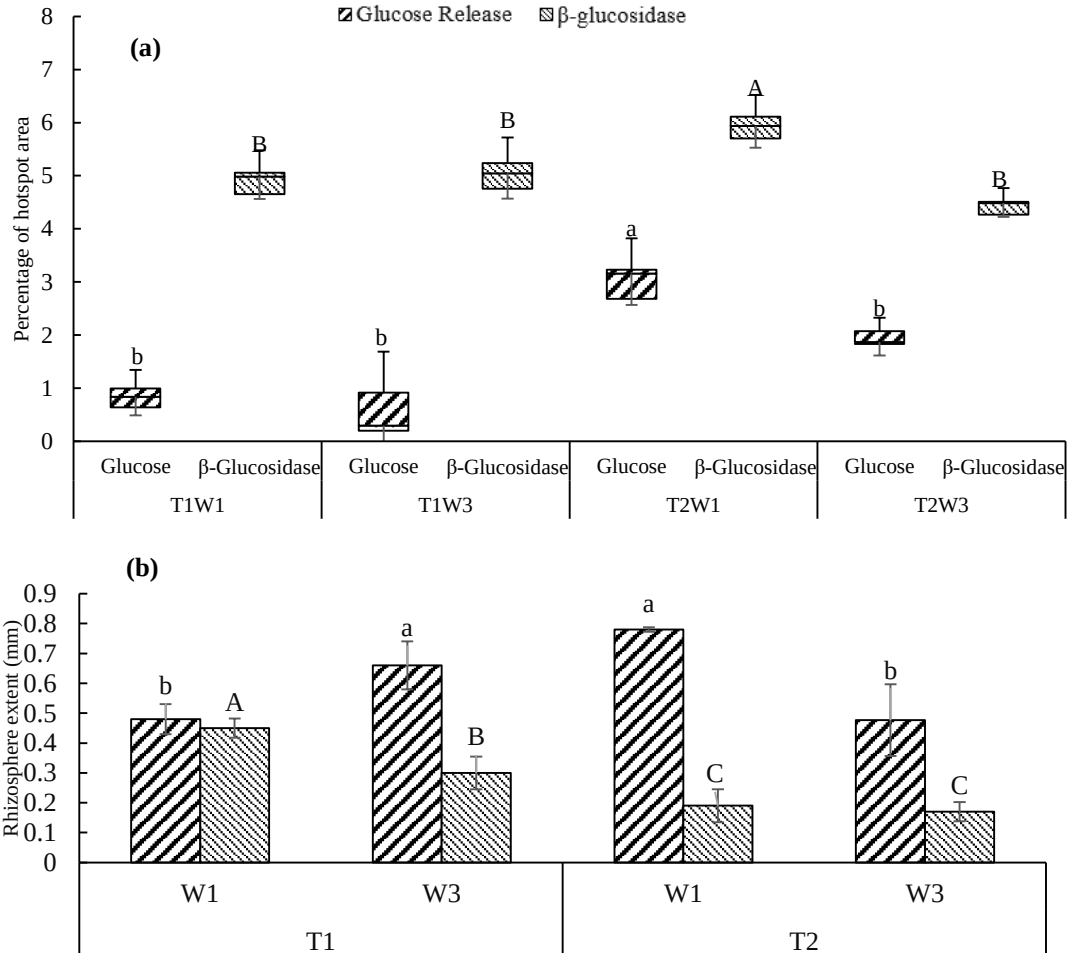

Figure 2.3.2. (a) Comparison of the percentage of hotspot area and (b) rhizosphere extent for glucose release and β-glucosidase activity in the first (W1) and third (W3) wheat after break crop at two sampling dates (T1: four weeks (BBCH 13), and T2: eight weeks after sowing (BBCH 29)). Lower-case letters denote significant differences between treatments in terms of glucose release and upper-case letters denote significant differences between treatments in terms of β-glucosidase activity according to two- way ANOVA at $p<0.05$.

2.3.4.3. Enzyme kinetics were the lowest at t2 in W1 and W3

The maximum rate (V_{max}) of β-glucosidase activity in the rhizosphere and bulk soil was strongly influenced by the sampling dates, which corresponded to different stages of plant development ($p<0.01$). At t1, soil samples from W3 had a higher V_{max} compared to W1 samples, showing 86.51 nmol MUF g^{-1}h^{-1} in rhizosphere and 113.9 nmol MUF g^{-1}h^{-1} in bulk soil samples, respectively. The increase in the bulk soil V_{max} was substantial (~60%). W1 samples had a lower V_{max} in bulk soil than in the rhizosphere (41.78 vs. 70.2 nmol MUF g^{-1}h^{-1}), while the Vmax in bulk soil samples of W3 was higher than rhizosphere samples (113.9 vs. 86.51 nmol MUF g^{-1}h^{-1}, respectively; Fig. 2.3.4). However, at t2, compared to t1, there was a notable and significant decrease in the V_{max} values observed for both rhizosphere and bulk soil samples. There was no statistical difference between W1 and W3, but the decreasing rate of V_{max} was not equal in W1 and W3 crop rotations. The maximum rate of β-glucosidase activity

decreased by ~71% and 47% in the rhizosphere and bulk soil compartments at t2 in W1 compared to t1, while the respective values for W3 were ~82% and 83%, respectively (Fig. 2.3.4). Although K_m values increased in W3 compared to W1 at t1 for bulk soil, there were no significant differences between K_m values at both sampling dates and crop rotations for rhizosphere soil. However, catalytic efficiency decreased at t2 for rhizosphere, and there were no prominent differences between W1 and W3 at both sampling times ($p<0.01$; Fig. 2.3.5). At t1, W3 resulted in higher turnover time (86h for rhizosphere and 400h for bulk soil), indicating lower enzyme efficiency in this crop rotational position compared to W1. Changes in turnover time at t2 were not statistically considerable for the rhizosphere. However, substrate turnover time increased two-fold for rhizosphere soil at W3 owing to plant growth ($p<0.01$; Fig. 2.3.6). Hence, successive wheat rotation considerably decreased enzyme efficiency. Developing the plants to later growth stages sharply declined the maximum rate of β-glucosidase activity, and substrate utilization was growth-dependent, especially in W3.

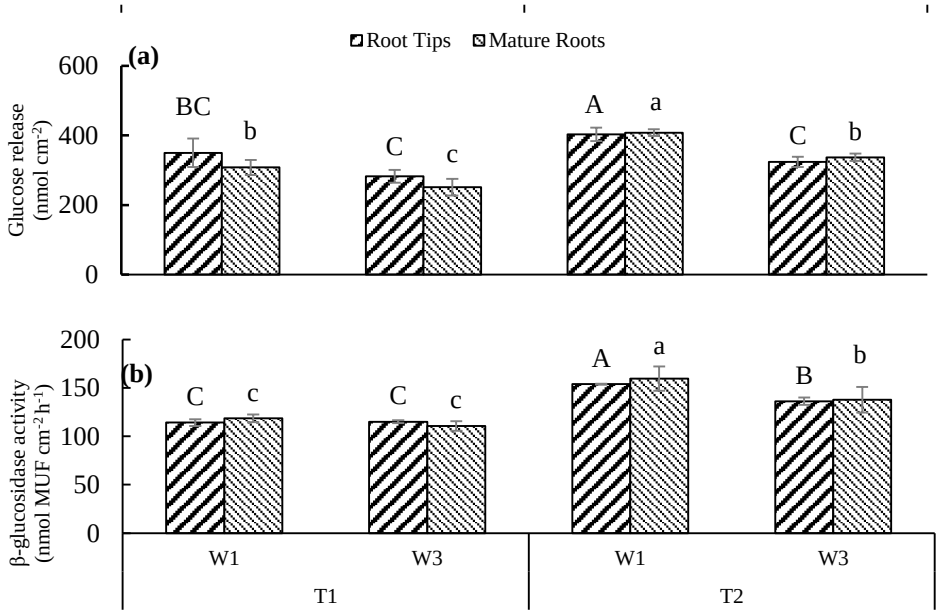

Figure 2.3.3. (a) Glucose releasing rate and (b) β-glucosidase activity in the first (W1) and third (W3) wheat after break crop at two sampling times (T1: four weeks (BBCH 13), and T2: eight weeks after sowing (BBCH 29)). Lower-case letters denote significant differences between treatments for mature root and upper-case letters denote significant differences between treatments for root tips according to two-way ANOVA at $p<0.05$.

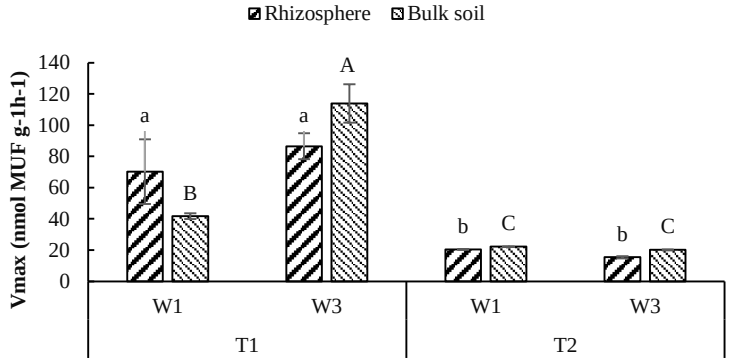

Figure 2.3.4. V_{max} values of β-glucosidase in different soil compartments in the first (W1) and third (W3) wheat after break crop at two sampling times (T1: four weeks (BBCH 13), and T2: eight weeks after sowing (BBCH 29)). Lower-case letters denote significant differences between treatments for rhizosphere and upper-case letters denote significant differences between treatments for bulk soil samples according to two-way ANOVA at $p<0.05$.

2.3.4.4. Microbial biomass C, microbial quotient, and respiration are less efficient in W3

The microbial biomass C (MBC) was significantly lower in W3 at both sampling times compared to W1 ($p<0.05$). At t1, higher MBC was observed in W1, which was 9.62 µg g^{-1} soil, while it was 5.92 µg g^{-1} soil in W3. Similarly, at t2, the MBC in W3 decreased by 32% (Fig. 2.3.7). Moreover, soil basal respiration increased at t2, but no significant difference was observed between W1 and W3 ($p<0.01$). W1 exhibited higher basal respiration by 0.114 µg CO2 $g^{-1}h^{-1}$, which was 10.5% higher than that observed in W3. At both sampling times, the microbial quotient in W3 was significantly higher compared to W1, with higher microbial quotient observed at t2 in W3, which was 0.018 µg CO_2-C mg^{-1} MBC h^{-1}, indicating a ~28% increase compared to W1 at the same sampling date ($p<0.01$; Fig. 2.3.8). The decrease in microbial biomass C in W3 accompanied by a higher microbial quotient might suggest harsh growth conditions for the soil microbial community in W3 compared to W1.

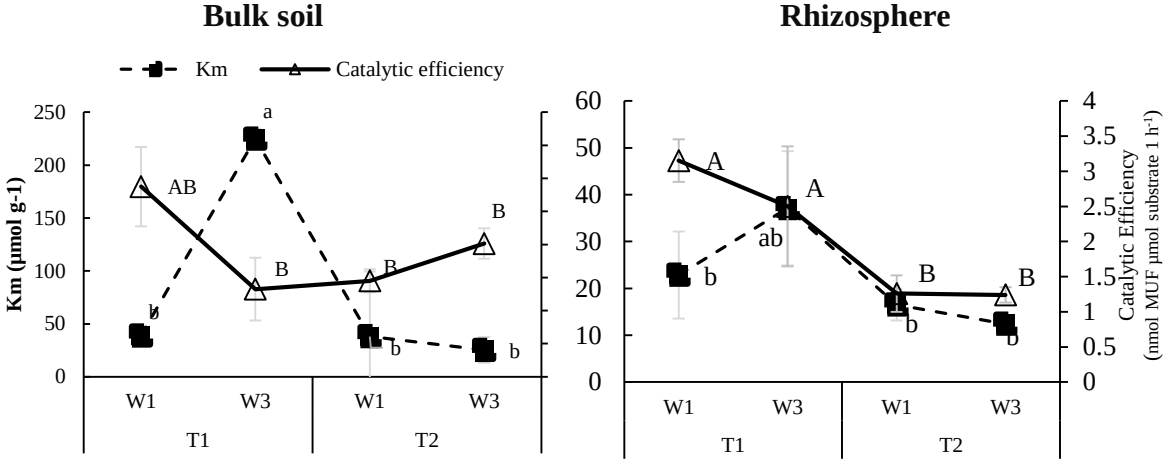

Figure 2.3.5. K_m values and catalytic efficiency of β-glucosidase in different soil compartments in the first (W1) and third (W3) wheat after break crop at two sampling times (T1: four weeks (BBCH 13), and T2: eight weeks after sowing (BBCH 29)). Lower-case letters denote significant differences between treatments in terms of K_m and upper-case letters denote significant differences between treatments in terms of catalytic efficiency according to two-way ANOVA at $p<0.05$.

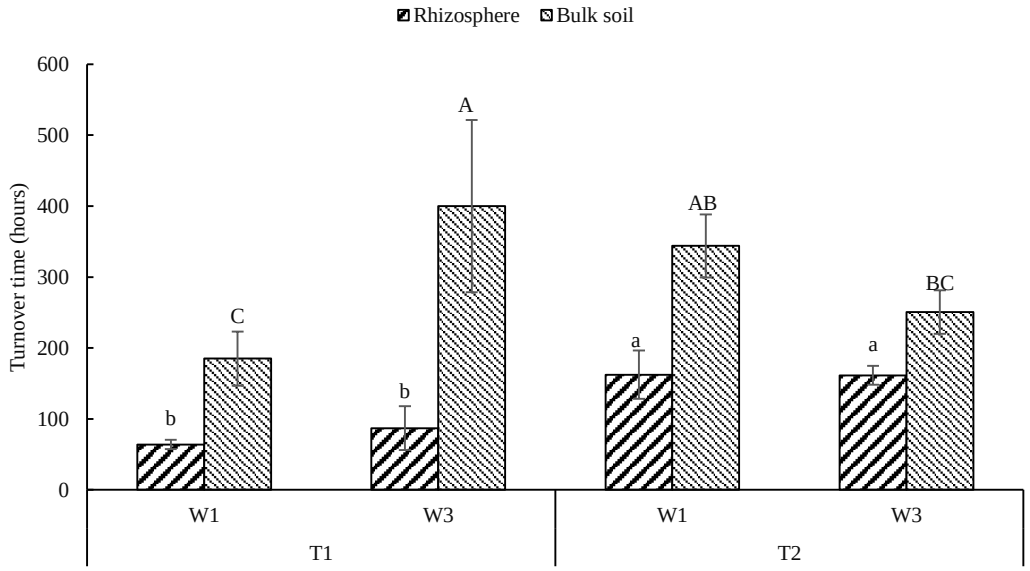

Figure 2.3.6. Turnover time of the β-glucosidase at a substrate concentration of 200 µmol g^{-1} soil in different soil compartments in the first (W1) and third (W3) wheat after break crop at two sampling times (T1: four weeks (BBCH 13), and T2: eight weeks after sowing (BBCH 29)). Lower-case letters denote significant differences between treatments for rhizosphere and upper-case letters denote significant differences between treatments for bulk soil samples according to two-way ANOVA at $p<0.05$.

2.3.5. Discussion

2.3.5.1. Glucose release

In accordance with our first hypothesis, successive wheat cultivation resulted in a substantial reduction in glucose release from roots and a decrease in rhizosphere expansion at t2 (as depicted in Figs. 2.3.1, 2.3.2, and 2.3.3). However, this trend was not observed in plants at t1. The age of the plant is an essential factor that determines the extent and type of exudation (Olanrewaju et al., 2019), which varies throughout its life cycle (Gargallo-Garriga et al., 2018). As plants progress through their life cycle, the composition and quantity of root exudates can vary substantially (Gargallo-Garriga et al., 2018). The observed discrepancy between t1 and t2 may be attributed, in part, to the evolving physiological state of the plant, influencing its exudation patterns (Ulrich et al., 2022). Numerous studies have documented that issues associated with consecutive monoculture in plants arise from alterations in the soil microbial community triggered by the presence of root exudates (Wu et al., 2015; Li et al., 2015) which in turn could affect root exudation pattern. A growing body of research indicates that root exudates play a crucial role in shaping the special microbial communities within the rhizosphere (Huang et al., 2014; Paterson et al., 2007). Subsequently, these plant-associated microorganisms have the potential to exert influence on both plant growth and overall plant health. Also, decaying roots create a favourable environment for necrotrophic pathogens and contribute to increasing fungal colonization (Häffner et al., 2014; Olanrewaju et al., 2019) and can modify the fungal community within the rhizosphere, leading to the proliferation of host-specific pathogenic fungi at the cost of beneficial fungi associated with plant health (Wu et al., 2016).

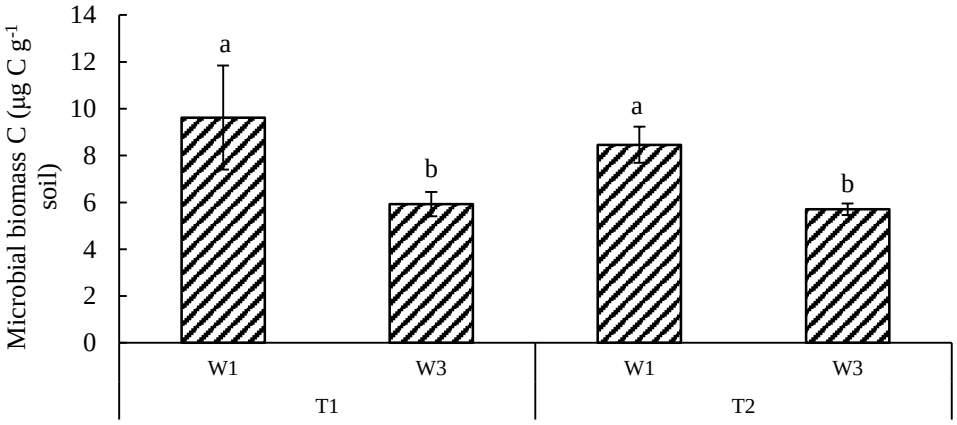

Figure 2.3.7. Microbial biomass C in wheat rhizosphere soil in the first (W1) and third (W3) wheat after break crop at two sampling times (T1: four weeks (BBCH 13), and T2: eight weeks after sowing (BBCH 29)). Lower-case letters denote significant differences between treatments according to two-way ANOVA at $p<0.05$.

The decrease in glucose release from wheat roots (as observed in Fig. 2.3.2) coupled with a decrease in C availability due to root senescence, leads to competition for C in the rhizosphere among beneficial microbes and soil-borne pathogens (Bressan and Figueiredo, 2008). Plant root exudates contain a variety of compounds, including sugars, that can have antimicrobial properties and regulate the microbial community in the soil (Dennis et al., 2010). In a similar study, Braun-Kiewnick et al., (unpublished data) showed increased concentrations of *Gaeumannomyces tritici* DNA by species-specific qPCR in W3 rhizosphere samples compared to W1 at later plant stages such as flowering and ripening compared to the tillering stage, confirming the higher relative abundance of an important soil-borne pathogen in W3. When plants are under pathogen attack, they may increase the release of certain compounds in their root exudates as a defence mechanism (Song et al., 2021). However, the response of plants

to pathogen attack can vary depending on the specific pathogen, plant species, and environmental conditions. Jalali and Suryanarayana (1971) showed that healthy wheat plants secrete considerably higher amounts of glucose than infected plants. The lower concentrations of released glucose in W3 were confirmed by its lower proportion of hotspot and lower rhizosphere extent during t2 (as illustrated in Figs. 1 and 2). This suggests that the plant's rhizosphere development and activity, as reflected by the extent and intensity of hotspots, may have played a role in the observed differences in glucose release between W3 and the other treatments. Root exudates, such as glucose, substantially affect the initiation and development of plant-microbe interactions in the rhizosphere (Hage-Ahmed et al., 2013). Therefore, the composition and extent of root exudates will affect soil-borne pathogens differently (Jones et al., 2004). Bakker et al., (2013) reported that pathogens have sophisticated mechanisms to receive sugar fluxes from the host plant. Moreover, pathogens can modify the expression of the SWEET family of sugar transporters to obtain the sugars necessary for their growth (Chen et al., 2010). The plant, by reducing rhizosphere size, is engineering density gradients of soil biochemical properties to establish a protection zone against pathogen invasion. In other words, plants can regulate their glucose release and modify plant-pathogen interactions towards a healthy relationship.

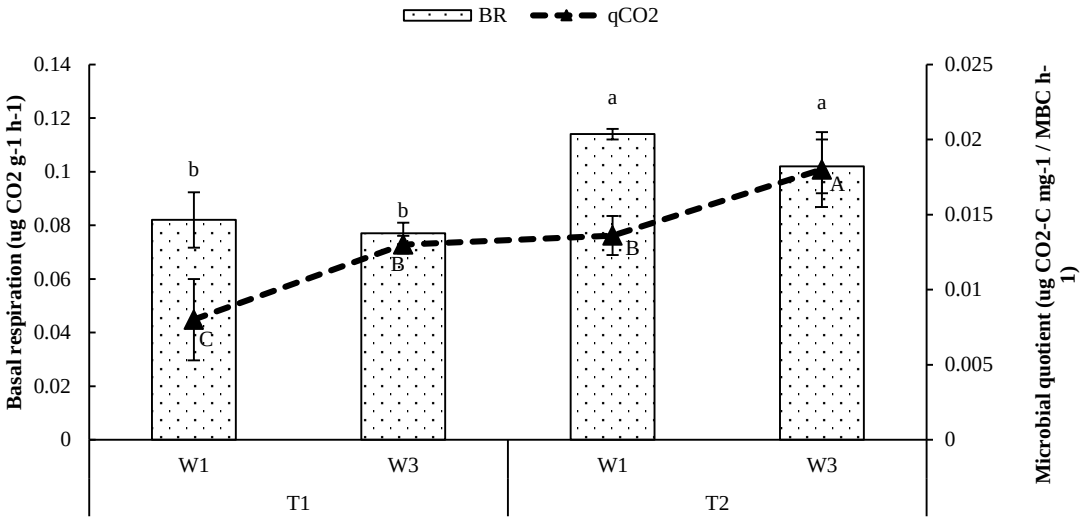

Figure 2.3.8. Basal respiration (bar charts) and microbial quotient values (dashed line) in wheat rhizosphere soil in the first (W1) and third (W3) wheat after break crop at two sampling times (T1: four weeks (BBCH 13), and T2: eight weeks after sowing (BBCH 29)). Lower-case letters denote significant differences between treatments in terms of basal respiration and upper-case letters denote significant differences between treatments in terms of microbial quotient according to two-way ANOVA at $p<0.05$.

Our results also showed that the root and shoot dry weight significantly decreased in W3 compared to W1 at both sampling times (Fig. S2.3.2). Furthermore, wheat plants in successive cultivation reduced root-released glucose to regulate their rhizosphere microbiome. The reduced glucose release observed in our study corresponded to a decrease in microbial activity within the rhizosphere. This, in turn, may have contributed to a diminished penetration of soil-borne pathogens into the roots, as suggested by Jalali and Suryanarayana (1971). Successive wheat plantation accelerated root senescence (Arnhold et al., 2023), created a harsh environment for soil microbes, and potentially paved the way for higher abundance of wheat soil-borne pathogens, ultimately affecting wheat yield. These findings suggest that the observed decrease in root and shoot dry weight may be a result of the lower glucose release and reduced microbial activity in the rhizosphere of the third wheat, potentially leading to a less efficient uptake of nutrients and water by the plants. Braun-Kiewnick et al., (unpublished

data) studying the bacterial and archaeal communities in the wheat rhizosphere and rhizoplane from the same soils found a significantly lower diversity in W3 compared to W1 at tillering stage confirming a shift in the plant-associated microbiota due to successive wheat cultivation, which might be related to changing root exudate patterns.

Our study found a decrease in microbial biomass C and enzyme activity in the third wheat (W3) compared to the first wheat (W1), which may be attributed to the higher pathogen levels in W3. This is consistent with previous studies that have shown that monoculture can lead to increased disease incidence and severity due to the build-up of pathogens in the soil (Mazzola, 2002).

The microbial community in the rhizosphere plays a crucial role in nutrient availability, which can influence the growth and activity of beneficial and pathogenic microorganisms in the soil (Chen et al., 2015; Manck-Götzenberger and Requena, 2016). Modification of root exudates and up- or down-regulation of sugar transporters, especially the SWEET family, can also influence both beneficial and pathogenic interactions (Chen et al., 2015). Therefore, the decrease in microbial biomass C and enzyme activity in W3 found in the present study may have affected the production of biocontrol compounds by antagonistic microorganisms in the soil (Peralta et al., 2018).

2.3.5.2. β -glucosidase activity

At t2, there was a significant decrease in the maximum rate (V_{max}) of β-glucosidase for both W1 and W3 compared to t1 (Fig. 2.3.4). Microorganisms prioritize survival and allocate their available resources accordingly (Zhang et al., 2019), investing less energy in enzyme production when there is no limitation (Allison and Vitousek, 2005). Our results showed that the glucose release rate substantially increased at t2 for both root tips and mature roots (Fig. 2.3.3a). However, the released glucose in the rhizosphere can have a different stimulatory effect on microbial activity (Baudoin et al., 2003) and can have an inhibitory effect on β-glucosidase activity, probably due to the end-product (glucose) (Zhang et al., 2019), thereby lowering the catalytic efficiency for the enzyme at t2 (Fig. 2.3.5).

While there was a significant decrease in V_{max} of β-glucosidase at t2 compared to t1 for both W1 and W3, the decrease was more pronounced for W3 (Fig. 2.3.4), likely because W3 had lower glucose release at both sampling times compared to W1 (Fig. 2.3.3a). The decrease in β-glucosidase activity can be attributed to the decline in glucose release. The decrease in glucose release in W3 at t2 might have resulted in a decrease in microbial biomass C (Fig. 2.3.7). Enzyme activity reflects the current or recently active microbial community members (Hargreaves and Hofmockel, 2014). Our results indicate that the decrease in microbial biomass C also resulted in a decrease in β-glucosidase activity, consistent with Hansen et al. (2019) who reported that higher rhizosphere β-glucosidase activity was typically accompanied by a greater microbial biomass. At t2, microbial communities may have allocated more energy to maintenance (Hargreaves and Hofmockel, 2014). Therefore, especially in W3, the limited C sources were allocated to respiration or microbial growth, resulting in lower microbial biomass and, consequently, lower enzyme production than W1.

Despite the difference in V_{max}, the K_m and catalytic efficiency remained stable in both W1 and W3 (Fig. 2.3.5). β-glucosidases hydrolyze the non-reducing end of β-D-glucosyl residues and release β-D-glucose (Cañizares et al., 2011). Higher glucose release at t2 (Fig. 2.3.3) resulted in non-competitive inhibition of β-glucosidase (Yang et al., 2015), where non-competitive inhibitor (glucose) reacts close to the active site and changes the shape of the enzyme (Dick, 2011). Moreover, released glucose prevents the hydrolyzed substrate from leaving (Yeoman et al., 2010). This type of enzyme inhibition results in a decline of V_{max} but stable K_m values (Datta et al., 2017). Alternatively, constant K_m can be explained by the expression of multiple isoenzymes (Bradford, 2013). Such isoenzyme expression leads to an

optimal balance between the static character of the enzyme (responsible for maintaining constant efficiency at a specific condition) and functional capacity, given similar flexibilities of isoenzymes under their respective optimal working conditions (e.g., low enzyme expression) (Razavi et al., 2017; Zavodszky et al., 1998). An increase in turnover time indicates a decline in enzyme efficiency. Therefore, maintaining a constant K_m value was not an effective strategy to ensure efficient catalysis.

Contrary to our expectations, we observed that, the bulk soil exhibited the highest enzyme activity, while the rhizosphere displayed more efficient enzymatic activity in terms of Km, catalytic efficiency, and turnover time. This unexpected result may be attributed to the presence of different microbial communities and enzyme types in the rhizosphere and bulk soil (Philippot et al., 2013). The rhizosphere is known to harbor a more intense dynamicity and active microbial community than the bulk soil, which may contribute to the higher enzymatic efficiency in this zone (Chaparro et al., 2014; Braun-Kiewnick et al. (unpublished data). Additionally, the rhizosphere is enriched with plant root exudates, which can stimulate the growth and activity of specific microbial groups that are capable of producing more efficient enzymes (Chaparro et al., 2014). Further investigations are required to identify the specific microbial groups and enzymes responsible for the observed differences in enzyme activity between the rhizosphere and bulk soil, especially for the W1 and W3t at t1, where bulk soil had higher V_{max} in W3. These findings highlight the complex and dynamic nature of the rhizosphere, and the need for a more comprehensive understanding of the factors influencing microbial activity and enzymatic efficiency in soil (Álvarez-Solís and Anzueto-Martínez, 2004).

2.3.5.3. Microbial biomass C and microbial quotient

The microbial biomass C in the rhizosphere soils of W3 was considerably lower than in W1, possibly due to a reduction in glucose release from the wheat and a lack of active C input to the rhizosphere from the plant (Prudence et al., 2021). Moreover, during the initiation of root senescence, the composition of root exudates changes significantly, mainly because of the diversion of N to the developing grains, which affects the composition and abundance of rhizosphere microbiomes (Zhalnina et al., 2018).

While our study revealed substantial differences in glucose release (Figs. 2.3.1, 2.3.2 and 2.3.3) and enzyme properties (Figs. 4, 5 and 6) between t1 and t2, the observation of no significant difference in microbial biomass C (Fig. 2.3.7) merits further discussion. The absence of a marked change in microbial biomass C could be attributed to the complex interplay of various factors influencing microbial dynamics. The observed alterations in glucose release and enzyme activities may not necessarily translate directly into detectable changes in microbial biomass within the relatively short time-span considered in our study. Microbial responses to changes in root exudates are influenced by factors such as microbial turnover rates, nutrient availability, and the overall microbial community structure, which can buffer or delay observable shifts in microbial biomass C (Fierer et al., 2007). Additionally, microbial biomass turnover rates and the turnover of labile carbon sources like glucose contribute to the overall microbial biomass C dynamics (Anderson and Domsch, 1989). The specific mechanisms governing microbial responses to changes in root exudates are complex and can be influenced by numerous factors, including microbial community composition, substrate preferences, and competition for resources (Bais et al., 2006; Allison and Martiny, 2008).

The decrease in glucose release from the roots at W3 led to accelerated wheat root senescence (as shown in Fig. 2.3.1) and the presence of decayed roots, which in turn resulted in an increase in necrotrophic pathogens around the root. The findings of Braun-Kiewnick et al., (unpublished data) in the same soil samples indicated that the number of antagonists against

wheat pathogens was significantly higher in W3, but the abundance of bacteria isolated in W1 and W3 was not significantly different. However, hydrolytic enzyme profiles of isolated bacteria (cellulase, ß-1,3 glucanase) was significantly higher in W1, indicating functionally more active bacteria in W1 compared to W3. In light of the observed increase in wheat pathogens and senesced roots, it is plausible that the root environment became less favorable for maintaining a diverse and functionally active microbial community (as shown in Fig. 2.3.8). To elaborate, the ratio between soil microbial biomass C and basal respiration, denoted as qCO2, serves as an indicator of the physiological state of the soil microbiota (Serafini et al., 2022) and indicates how effectively microorganisms in the soil use the available C (Fterich et al., 2012). A higher qCO2 at t2 in W3 suggests that the microbial community associated with W3 roots experienced a more stressful condition in the rhizosphere. Under such circumstances, increased respiration was required to sustain a unit of microbial biomass (Fterich et al., 2012). This contrasts with the lower qCO2 levels observed in W1 soils, indicating higher stability (Pinzari et al., 1999) and a more efficient utilization of available substrates by the microbial biomass. Thus, the microbiome associated with the roots at t2 and in W3 was more sensitive to the surrounding environment in the rhizosphere.

2.3.6. Conclusion

Overall, our study sheds light on the rhizosphere processes in successive wheat cultivation, revealing a significant impact on root processes. Specifically, the reduction in the release rate of key root exudates, notably glucose, alters the competitive dynamics on the root surface. The observed decrease in glucose release, coupled with constrained rhizosphere expansion, leads to a substantial reduction in microbial biomass C, resulting in lower enzyme activity. Maintaining the expansion of the rhizosphere is a plant strategy under biotic stress since the rhizosphere and its hotspots are essential microbial habitats that determine the processes, dynamics, and cycling of C in terrestrial ecosystems. The findings of this study suggest that successive wheat cultivation changes root primary compound exudation, leading to declining glucose release, creating a harsh environment for beneficial soil microbes and accelerating root senescence, ultimately resulting in wheat yield decline.

2.3.7. Acknowledgment

This study was carried out as part of the RhizoWheat project (Research program BONARES) and received financial support from the BMBF. The authors express their gratitude to the German Federal Ministry of Education and Research (BMBF) for providing funding for this research (grant number 031B0910A).

2.3.8. Statements and Declarations

The authors declare that they have no known competing financial interests or personal relationships that could have appeared to influence the work reported in this paper.

2.3.9. References

Allison, S. D., Martiny, J. B. H. 2008. Resistance, resilience, and redundancy in microbial communities. PNAS. 105(1), 11512–11519. https://doi.org/10.1073/pnas.0801925105

Allison, S.D., Vitousek, P.M., 2005. Responses of extracellular enzymes to simple and complex nutrient inputs. Soil Biol. Biochem. 37(5), 937-944. doi:https://doi.org/10.1016/j.soilbio.2004.09.014

Álvarez-Solís, J., Anzueto-Martínez, M.D.J., 2004. Soil microbial activity under different corn cropping systems in the highlands of Chiapas, México. Agrociencia. 38, 13-22.

Anderson, T. H., Domsch, K. H. 1989. Ratios of microbial biomass carbon to total organic carbon in arable soils. Soil Biol. Biochem. 21(4), 471–479. https://doi.org/10.1016/0038-0717(89)90117-X

Anderson, T.H., Domsch, K.H., 1990. Application of eco-physiological quotients (qCO2 and qD) on microbial biomasses from soils of different cropping histories. Soil Biol. Biochem. 22(2), 251-255. doi:https://doi.org/10.1016/0038-0717(90)90094-G

Arnhold, J., Grunwald, D., Braun-Kiewnick, A., Koch, H.J. 2023. Effect of crop rotational position and nitrogen supply on root development and yield formation of winter wheat. Front Plant Sci. 14:1265994. doi:10.3389/fpls.2023.1265994.

Averill, C., Finzi, A., 2011. Plant regulation of microbial enzyme production *in situ*. Soil Biol. Biochem. 43(12), 2457-2460. https://doi.org/10.1016/j.soilbio.2011.09.002

Awad, Y.M., Blagodatskaya, E., Ok, Y.S., Kuzyakov, Y., 2012. Effects of polyacrylamide, biopolymer, and biochar on decomposition of soil organic matter and plant residues as determined by 14C and enzyme activities. Eur. J. Soil Sci. 48, 1-10. doi:https://doi.org/10.1016/j.ejsobi.2011.09.005

Bais, H. P., Weir, T. L., Perry, L. G., Gilroy, S., Vivanco, J. M. 2006. The role of root exudates in rhizosphere interactions with plants and other organisms. Annu. Rev. Plant Biol. 57, 233–266. https://doi.org/10.1146/annurev.arplant.57.032905.105159

Bakker, P., Berendsen, R., Doornbos, R., Wintermans, P., Pieterse, C., 2013. The rhizosphere revisited: root microbiomics. Front. Plant Sci. 4:165. doi:10.3389/fpls.2013.00165

Bakker, P., Pieterse, C.M.J., de Jonge, R., Berendsen, R.L., 2018. The Soil-Borne Legacy. Cell. 172(6), 1178-1180. doi:10.1016/j.cell.2018.02.024

Baudoin, E., Benizri, E., Guckert, A., 2003. Impact of artificial root exudates on the bacterial community structure in bulk soil and maize rhizosphere. Soil Biol. Biochem. 35(9), 1183-1192. doi:https://doi.org/10.1016/S0038-0717(03)00179-2

Berg, G., Smalla, K., 2009. Plant species and soil type cooperatively shape the structure and function of microbial communities in the rhizosphere. FEMS Microbiol. Ecol. 68(1), 1-13. https://doi.org/10.1111/j.1574-6941.2009.00654.x

Bilyera, N., Zhang, X., Duddek, P., Fan, L., Banfield, C.C., Schlüter, S., Carminati, A., Kaestner, A., Ahmed, M.A., Kuzyakov, Y., Dippold, M.A., Spielvogel, S., Razavi, B.S., 2021. Maize genotype-specific exudation strategies: An adaptive mechanism to increase microbial activity in the rhizosphere. Soil Biol. Biochem. 162, 108426. doi:https://doi.org/10.1016/j.soilbio.2021.108426

Birt, H.W.G, Tharp, C.L., Custer, G.F., Dini-Andreote, F., 2022. Root phenotypes as modulators of microbial microhabitats. Front. Plant Sci. 13:1003868. doi: 10.3389/fpls.2022.1003868

Blagodatskaya, E., Tarkka, M., Knief, C., Koller, R., Peth, S., Schmidt, V., Spielvogel, S., Uteau, D., Weber, M., Razavi, B.S., 2021. Bridging Microbial Functional Traits with Localized Process Rates at Soil Interfaces. Front Microbiol, 12, 625697. doi:10.3389/fmicb.2021.625697

Boyer, J., Silk, W., Watt, M., 2010. Path of water for root growth. Funct. Plant Biol. 37(12), 1105-1116. doi:10.1071/fp10108

Bradford, M., 2013. Thermal adaptation of decomposer communities in warming soils. Front. Microbiol. 4. doi:10.3389/fmicb.2013.00333

Bressan, W., Figueiredo, J.E.F., 2008. Efficacy and dose–response relationship in biocontrol of Fusarium disease in maize by Streptomyces spp. Eur. J. Plant Pathol. 120(3), 311-316. doi:10.1007/s10658-007-9220-y

Canarini, A., Kaiser, C., Merchant, A., Richter, A., Wanek, W., 2019. Root Exudation of Primary Metabolites: Mechanisms and Their Roles in Plant Responses to Environmental Stimuli. Front. Plant Sci. 10. doi:10.3389/fpls.2019.00157

Cañizares, R., Benitez, E., Ogunseitan, O.A., 2011. Molecular analyses of β-glucosidase diversity and function in soil. Eur. J. Soil Biol. 47(1), 1-8. doi:https://doi.org/10.1016/j.ejsobi.2010.11.002

Chaparro, J. M., Badri, D.V., Vivanco, J.M., 2014. Rhizosphere microbiome assemblage is affected by plant development. The ISME J. 8(4), 790-803.

Chapman, S., Campbell, C., Artz, R., 2007. Assessing CLPPs using MicroResp™. J. Soils Sediments. 7, 406-410. doi:10.1065/jss2007.10.259.

Chen, H.Y., Huh, J.H., Yu, Y.C., Ho, L.H., Chen, L.Q., Tholl, D., Frommer, W.B., Guo, W.J., 2015. The Arabidopsis vacuolar sugar transporter SWEET2 limits carbon sequestration from roots and restricts Pythium infection. Plant J. 83(6),1046-58. doi:10.1111/tpj.12948

Chen, L.Q., Hou, B.H., Lalonde, S., Takanaga, H., Hartung, M., Qu, X.Q., Guo, W.J., Kim, J.G., Underwood, W., Chaudhuri, B., Chermak, D., Antony, G., White, F.F., Somerville, S.C., Mudgett,

M.B., Frommer, W., 2010. Sugar transporters for intercellular exchange and nutrition of pathogens. Nature. 468, 527–532. doi:10.1038/nature09606
Chen, S., Waghmode, T.R., Sun, R., Kuramae, E.E., Hu, C., Liu, B. 2019. Root-associated microbiomes of wheat under the combined effect of plant development and nitrogen fertilization. Microbiome, S. 136. DOI: 10.1186/s40168-019-0750-2.
Datta, R., Anand, S., Moulick, A., Baraniya, D., Imran Pathan, S., Rejsek, K., Vranova, V., Sharma, M., Kelkar, A., Formánek, P., 2017. How enzymes are adsorbed on soil solid phase and factors limiting its activity: A Review. Int. Agrophys. 31(2), 287-302. doi:10.1515/intag-2016-0049
Dennis P.G., Miller, A.J., Hirsch, P.R., 2010. Are root exudates more important than other sources of rhizodeposits in structuring rhizosphere bacterial communities? FEMS Microbiol. Ecol. 72 (3), 313–327. https://doi.org/10.1111/j.1574-6941.2010.00860.x
Derrien, D., Marol, C., Balabane, M. Balesdent, J., 2006. The turnover of carbohydrate carbon in a cultivated soil estimated by 13C natural abundances. Eur. J. Soil Sci. 57, 547-557. https://doi.org/10.1111/j.1365-2389.2006.00811.x
Dick, W.A., 2011. Kinetics of Soil Enzyme Reactions. In Methods of Soil Enzymology, R.P. Dick (Ed.). https://doi.org/10.2136/sssabookser9.c3
Fierer, N., Bradford, M. A., Jackson, R. B. 2007. Toward an ecological classification of soil bacteria. Ecology, 88(6), 1354–1364. https://doi.org/10.1890/05-1839
Finzi, A.C., Abramoff, R.Z., Spiller, K.S., Brzostek, E.R., Darby, B.A., Kramer, M.A., Phillips, R.P., 2015. Rhizosphere processes are quantitatively important components of terrestrial carbon and nutrient cycles. Glob Chang Biol. 21(5), 2082-2094. doi:10.1111/gcb.12816
Fterich, A., Mosbah, M., Mars, M., 2012. Impact of grazing on soil microbial communities along a chronosequence of *Acacia tortilis* subsp. raddiana in arid soils in Tunisia. Eur. J. Soil Biol. 50, 56–63. doi:10.1016/j.ejsobi.2011.12.002
Gargallo-Garriga, A., Preece, C., Sardans, J., Oravec, M., Urban, O., Peñuelas, J., 2018. Root exudate metabolomes change under drought and show limited capacity for recovery. Sci. Rep. 8(1), 12696. doi:10.1038/s41598-018-30150-0
German, D.P., Marcelo, K.R.B., Stone, M.M., Allison, S.D., 2012. The Michaelis–Menten kinetics of soil extracellular enzymes in response to temperature: a cross-latitudinal study. Glob Chang Biol. 18(4), 1468-1479. doi:https://doi.org/10.1111/j.1365-2486.2011.02615.x
German, D.P., Weintraub, M.N., Grandy, A.S., Lauber, C.L., Rinkes, Z.L., Allison, S.D., 2011. Optimization of hydrolytic and oxidative enzyme methods for ecosystem studies. Soil Biol. Biochem. 43(7), 1387-1397. doi:https://doi.org/10.1016/j.soilbio.2011.03.017
Giongo, A., Arnhold, J., Grunwald, D., Smalla, K., Braun-Kiewnick, A. 2024 Soil depths and microhabitats shape soil and root-associated bacterial and archaeal communities more than crop rotation in wheat. Front. Microbiomes. 3:1335791. doi: 10.3389/frmbi.2024.1335791
Gunina, A., Kuzyakov, Y., 2015. Sugars in soil and sweets for microorganisms: Review of origin, content, composition and fate. Soil Biol. Biochem. 90, 87-100. doi:https://doi.org/10.1016/j.soilbio.2015.07.021
Häffner, E., Karlovsky, P., Splivallo, R., Traczewska, A., and Diederichsen, E., 2014. ERECTA, salicylic acid, abscisic acid, and jasmonic acid modulate quantitative disease resistance of Arabidopsis thaliana to Verticillium longisporum. BMC Plant Biol. 14(1), 85. doi:10.1186/1471-2229-14-85
Hage-Ahmed, K., Moyses, A., Voglgruber, A., Hadacek, F., Steinkellner, S., 2013. Alterations in Root Exudation of Intercropped Tomato Mediated by the Arbuscular Mycorrhizal Fungus Glomus mosseae and the Soilborne Pathogen *Fusarium oxysporum* f.sp. lycopersici. J Phytopathol. 161(11-12), 763-773. doi:https://doi.org/10.1111/jph.12130.
Hamel, C., Gan, Y., Messer, D., Bainard, L.D., 2019. Soil 16S DNA sequence data and corresponding soil property and wheat yield data from a 72-plot field experiment involving pulses and wheat crops grown in rotations in the semiarid prairie. Data Br. 23, 103790. doi:10.1016/j.dib.2019.103790
Hansen, J.C., Schillinger, W.F., Sullivan, T.S., Paulitz, T.C., 2019. Soil Microbial Biomass and Fungi Reduced with Canola Introduced into Long-Term Monoculture Wheat Rotations. Front. Microbiol. 10:1488. doi: 10.3389/fmicb.2019.01488doi:10.3389/fmicb.2019.01488
Hardina, Neate, S., Jabaji-Hare, S., Olphel-Keller, K., 2004. FEMS Microbiol. Ecol. 47(2), 143-152. DOI: 10.1016/S0168-6496(03)00255-1

Hargreaves, S.K., Hofmockel, K.S., 2014. Physiological shifts in the microbial community drive changes in enzyme activity in a perennial agroecosystem. Biogeochemistry. 117(1), 67-79. doi:10.1007/s10533-013-9893-6

Hinsinger, P., Betencourt, E., Bernard, L., Brauman, A., Plassard, C., Shen, J., Tang, X., Zhang, F., 2011. P for Two, Sharing a Scarce Resource: Soil Phosphorus Acquisition in the Rhizosphere of Intercropped Species. Plant Physiol. 156, 1078-1086. doi:10.1104/pp.111.175331

Hoang, D.T., Maranguit, D., Kuzyakov, Y., Razavi, B.S., 2020. Accelerated microbial activity, turnover and efficiency in the drilosphere is depth dependent. Soil Biol. Biochem. 147, 107852. doi:https://doi.org/10.1016/j.soilbio.2020.107852

Hoang, D.T., Rashtbari, M., Anh, L.T., Wang, S., Tu, D.T., Hiep, N.V., Razavi, B.S., 2022. Mutualistic interaction between arbuscular mycorrhiza fungi and soybean roots enhances drought resistant through regulating glucose exudation and rhizosphere expansion. Soil Biol. Biochem. 171, 108728. doi:https://doi.org/10.1016/j.soilbio.2022.108728

Houlden, A., Timms-Wilson, T.M., Day, M.J., Bailey, M.J., 2008. Influence of plant developmental stage on microbial community structure and activity in the rhizosphere of three field crops. FEMS Microbiol. Ecol. 65(2), 193-201. doi:10.1111/j.1574-6941.2008.00535.x

Huang, X. F., Chaparro, J. M., Reardon, K. F., Zhang, R., Shen, Q., Vivanco, J. M. 2014. Rhizosphere interactions: root exudates, microbes, and microbial communities. Botany. 92, 267–275. https://doi.org/10.1139/cjb-2013-0225

Hütsch, B.W., Augustin, J., Merbach, W., 2002. Plant rhizodeposition — an important source for carbon turnover in soils. J. Plant. Nutr. Soil Sci. 165(4), 397-407. doi:https://doi.org/10.1002/1522-2624(200208)165:4<397::AID-JPLN397>3.0.CO;2-C

Jalali, B.L., Suryanarayana, D., 1971. Shift in the carbohydrate spectrum of root exudates of wheat in relation to its root-rot disease. Plant Soil. 34, 261-267. https://doi.org/10.1007/BF01372783

Jones, D.L., Hodge, A., Kuzyakov, Y., 2004. Plant and mycorrhizal regulation of rhizodeposition. New Phytol. 163(3), 459-480. doi:10.1111/j.1469-8137.2004.01130.x

Jones, D.L., Nguyen, C., Finlay, R.D., 2009. Carbon flow in the rhizosphere: carbon trading at the soil–root interface. Plant Soil. 321(1), 5-33. doi:10.1007/s11104-009-9925-0

Kennedy, A.C., de Luna, L.Z., 2005. Rhizosphere. In D. Hillel (Ed.), Encyclopedia of Soils in the Environment (pp. 399-406). Oxford: Elsevier. https://doi.org/10.1016/B0-12-348530-4/00163-6

Kirby, J.R. 2009. Chemotaxis-Like Regulatory Systems: Unique Roles in Diverse Bacteria. Annu. Rev. Microbiol. 63, 45–59. Doi:0066-4227/09/1013-0045$20.00.

Kuzyakov, Y., Razavi, B.S., 2019. Rhizosphere size and shape: Temporal dynamics and spatial stationarity. Soil Biol. Biochem. 135, 343-360. doi:https://doi.org/10.1016/j.soilbio.2019.05.011

Kwak, Y.S., Weller, D.M., 2013. Take-all of Wheat and Natural Disease Suppression: A Review. Plant Pathol J. 29(2),125-35. doi: 10.5423/PPJ.SI.07.2012.0112.

Li, X., Chang-feng, D., Ke, H., Tao-lin, Z., Ya-nan, Z., Ling, Z., Yi-ru, Y., Jin-guang, L., Xing, W. 2014. Soil sickness of peanuts is attributable to modifications in soil microbes induced by peanut root exudates rather than to direct allelopathy. Soil Biol. Biochem. 78, 149-159. https://doi.org/10.1016/j.soilbio.2014.07.019

Li, Y.J., Hu, Q.P., 2020. Studying of the promotion mechanism of Bacillus subtilis QM3 on wheat seed germination based on β-amylase. Open Life Sci. 15(1), 553-560. doi:10.1515/biol-2020-0062

Manck-Götzenberger, J., Requena, N., 2016. Arbuscular mycorrhiza Symbiosis Induces a Major Transcriptional Reprogramming of the Potato SWEET Sugar Transporter Family. Front. Plant Sci. 7:487. doi: 10.3389/fpls.2016.00487

Mazzola, M., 2002. Mechanisms of natural soil suppressiveness to soilborne diseases. Antonie Van Leeuwenhoek 81, 557–564 (2002). https://doi.org/10.1023/A:1020557523557

McLaughlin, J.E., Boyer, J.S., 2004. Glucose localization in maize ovaries when kernel number decreases at low water potential and sucrose is fed to the stems. Ann Bot. 94(1), 75-86. doi:10.1093/aob/mch123

Meteier, E., La Camera, S., Goddard, M.L., Laloue, H., Mestre, P., Chong, J., 2019. Overexpression of the VvSWEET4 Transporter in Grapevine Hairy Roots Increases Sugar Transport and Contents and Enhances Resistance to *Pythium irregulare*, a Soilborne Pathogen. Front. Plant Sci. 10:884. doi: 10.3389/fpls.2019.00884

Naseem, M., Philippi, N., Hussain, A., Wangorsch, G., Ahmed, N., Dandekar, T., 2012. Integrated systems view on networking by hormones in Arabidopsis immunity reveals multiple crosstalk for cytokinin. Plant Cell, 24(4), 1793-1814. DOI: 10.1105/tpc.112.098335

Olanrewaju, O.S., Ayangbenro, A.S., Glick, BR., Babalola, O.O., 2019. Plant health: feedback effect of root exudates-rhizobiome interactions. Appl. Microbiol. Biotechnol. 103(3), 1155-1166. doi:10.1007/s00253-018-9556-6

Panikov, N.S., Blagodatsky, S.A., Blagodatskaya, J.V., Glagolev, M.V., 1992. Determination of microbial mineralization activity in soil by modified Wright and Hobbie method. Biol. Fertil. Soils. 14(4), 280-287. doi:10.1007/BF00395464

Pascale, A., Proietti, S., Pantelides, I.S., Stringlis, I.A., 2020. Modulation of the Root Microbiome by Plant Molecules: The Basis for Targeted Disease Suppression and Plant Growth Promotion. Front. Plant Sci. 10:1741. doi: 10.3389/fpls.2019.01741

Paterson, E., Gebbing, T., Abel, C., Sim, A., Telfer, G. 2007. Rhizodeposition shapes rhizosphere microbial community structure in organic soil. New Phytol. **173**, 600–610. https://doi.org/10.1111/j.1469-8137.2006.01931.x

Peralta, A.L., Sun, Y., McDaniel, M.D., Lennon, J.T., 2018. Crop rotational diversity increases disease suppressive capacity of soil microbiomes. Ecosphere, 9(5), e02235. doi:https://doi.org/10.1002/ecs2.2235

Philippot, L., Raaijmakers, J.M., Lemanceau, P., Van Der Putten, W.H., 2013. Going back to the roots: the microbial ecology of the rhizosphere. Nat. Rev. Microbiol. 11(11), 789-799. https://doi.org/10.1038/nrmicro3109

Pinzari, F., Trinchera, A., Benedetti, A., Sequi, P., 1999. Use of biochemical indices in the mediterranean environment: comparison among soils under different forest vegetation. J. Microbiol. Methods. 36(1), 21-28. doi:https://doi.org/10.1016/S0167-7012(99)00007-X

Prudence, S.M.M., Newitt, J.T., Worsley, S.F., Macey, M.C., Murrell, J.C., Lehtovirta-Morley, L.E., Hutchings, M.I., 2021. Soil, senescence and exudate utilisation: characterisation of the Paragon var. spring bread wheat root microbiome. Environ. Microbiomes. 16(1), 12. doi:10.1186/s40793-021-00381-2

Qi, B., Zhang K., Qin, S., Lyu, D., He, J. 2022. Glucose addition promotes C fixation and bacteria diversity in C-poor soils, improves root morphology, and enhances key N metabolism in apple roots. PLoS One. 19;17(1):e0262691. doi: 10.1371/journal.pone.0262691

Razavi, B.S., Liu, S., Kuzyakov, Y., 2017. Hot experience for cold-adapted microorganisms: Temperature sensitivity of soil enzymes. Soil Biol. Biochem. 105, 236-243. doi:https://doi.org/10.1016/j.soilbio.2016.11.026

Razavi, B.S., Zarebanadkouki, M., Blagodatskaya, E., Kuzyakov, Y., 2016. Rhizosphere shape of lentil and maize: Spatial distribution of enzyme activities. Soil Biol. Biochem. 96, 229-237. doi:https://doi.org/10.1016/j.soilbio.2016.02.020

Razavi, B.S., Zhang, X., Bilyera, N., Guber, A., Zarebanadkouki, M., 2019. Soil zymography: Simple and reliable? Review of current knowledge and optimization of the method. Rhizosphere, 11, 100161. doi:https://doi.org/10.1016/j.rhisph.2019.100161

Serafini, C.G., Clerici, N.J., Della-Flora, I.K., Dupont, G.K., da Costa Cabrera, L., Daroit, D.J., 2022. Effects of atrazine on soil microbial indicators and the evaluation of herbicide attenuation in microcosms. J. Soils Sediments. 22(4), 1165-1175. doi:10.1007/s11368-021-03121-8

Sieling, K., Stahl, C., Winkelmann, C., Christen, O., 2005. Growth and yield of winter wheat in the first 3 years of a monoculture under varying N fertilization in NW Germany. Eur J Agron. 22(1), 71-84. doi:https://doi.org/10.1016/j.eja.2003.12.004.

Smith, S.E., Read, D., 2008. The Symbionts Forming Arbuscular Mycorrhizas. Mycorrhizal Symbiosis 3rd Edn. London: Academic Press, 13–41. https://doi.org/10.1016/B978-0-12-370526-6.X5001-6

Song, S., Liu, Y., Wang, N.R., Haney, C.H., 2021. Mechanisms in plant–microbiome interactions: lessons from model systems. Curr. Opin. Plant Biol. 62, 102003. https://doi.org/10.1016/j.pbi.2021.102003

Spohn, M., Kuzyakov, Y., 2014. Spatial and temporal dynamics of hotspots of enzyme activity in soil as affected by living and dead roots—a soil zymography analysis. Plant Soil. 379, 67-77. doi:10.1007/s11104-014-2041-9

Ulrich, D. E. M., Clendinen, C. S., Alongi, F., Mueller, R. C., Chu, R. K., Toyoda, J., Gallegos-Graves, V., Goemann, H. M., Peyton, B., Sevanto, S., Dunbar, J. 2022. Root exudate composition reflects drought severity gradient in blue grama (Bouteloua gracilis). Sci Rep. 22;12(1):12581. doi: 10.1038/s41598-022-16408-8. PMID: 35869127; PMCID: PMC9307599.

Voothuluru, P., Braun, D.M., Boyer, J.S., 2018. An in Vivo Imaging Assay Detects Spatial Variability in Glucose Release from Plant Roots. Plant physiol. 178(3), 1002-1010. doi:10.1104/pp.18.00614

Wang, H., Liu, R., You, M.P., Barbetti, M.J., Chen, Y., 2021. Pathogen Biocontrol Using Plant Growth-Promoting Bacteria (PGPR): Role of Bacterial Diversity. Microorganisms. 9(9):1988. doi: 10.3390/microorganisms9091988.

Wild, B., Schnecker, J., Alves, R.J., Baruskov, P., Bartya, J., Čapek, P., Gentsch, N., Gittel, A., Guggenberger, G., Lashchinskiy, N., Mikutta, R., Rusalimova, O., Šantrůčková, H., Shibistova, T., Urich. T., Watzka, M., Zrazhevskaya, G., Richter, A. 2014. Input of easily available organic C and N stimulates microbial decomposition of soil organic matter in arctic permafrost soil. Soil Biol. Biochem. 75: 143-151. https://doi.org/10.1016/j.soilbio.2014.04.014.

Wu, L., Chen, J., Wu, H., Wang, J., Wu, Y., Lin, S., Khan, M.U., Zhang, Z., Lin, W. 2016. Effects of consecutive monoculture of *Pseudostellaria heterophylla* on soil fungal community as determined by pyrosequencing. Sci Rep. 24;6:26601. doi: 10.1038/srep26601. PMID: 27216019; PMCID: PMC4877567.

Yang, Y., Zhang, X., Yin, Q., Fang, W., Fang, Z., Wang, X., Zhang, X., Xiao, Y., 2015. A mechanism of glucose tolerance and stimulation of GH1 β-glucosidases. Sci. Rep. 5(1), 17296. doi:10.1038/srep17296

Yeoman, C.J., Han, Y., Dodd, D., Schroeder, C.M., Mackie, R.I., Cann, I.K.O., 2010. Chapter 1 - Thermostable Enzymes as Biocatalysts in the Biofuel Industry. Adv Appl Microbiol. 70:1-55. doi: 10.1016/S0065-2164(10)70001-0

Zavodszky, P., Kardos, J., Svingor, Á., Petsko, G.A., 1998. Adjustment of conformational flexibility is a key event in the thermal adaptation of proteins. Proc. Natl. Acad. Sci. 95(13), 7406-7411. https://doi.org/10.1073/pnas.95.13.7406

Zhalnina, K., Louie, K. B., Hao, Z., Mansoori, N., da Rocha, U. N., Shi, S., Cho, H., Karaoz, U., Loque, D., Bowen, B.P., Firestone, M.K., Northen, T.R., Brodie, E.L., 2018. Dynamic root exudate chemistry and microbial substrate preferences drive patterns in rhizosphere microbial community assembly. Nat. Microbiol. 3(4), 470-480. doi:10.1038/s41564-018-0129-3

Zhang, X., Dippold, M.A., Kuzyakov, Y., Razavi, B.S., 2019. Spatial pattern of enzyme activities depends on root exudate composition. Soil Biol. Biochem. 133, 83-93. doi:https://doi.org/10.1016/j.soilbio.2019.02.010

Zhou, M., Diwu, Z., Panchuk-Voloshina, N., Haugland, R.P., 1997. A stable non-fluorescent derivative of resorufin for the fluorometric determination of trace hydrogen peroxide: applications in detecting the activity of phagocyte NADPH oxidase and other oxidases. Anal Biochem. 253(2), 162-168. doi:10.1006/abio.1997.2391

2.3.10. Graphical abstract

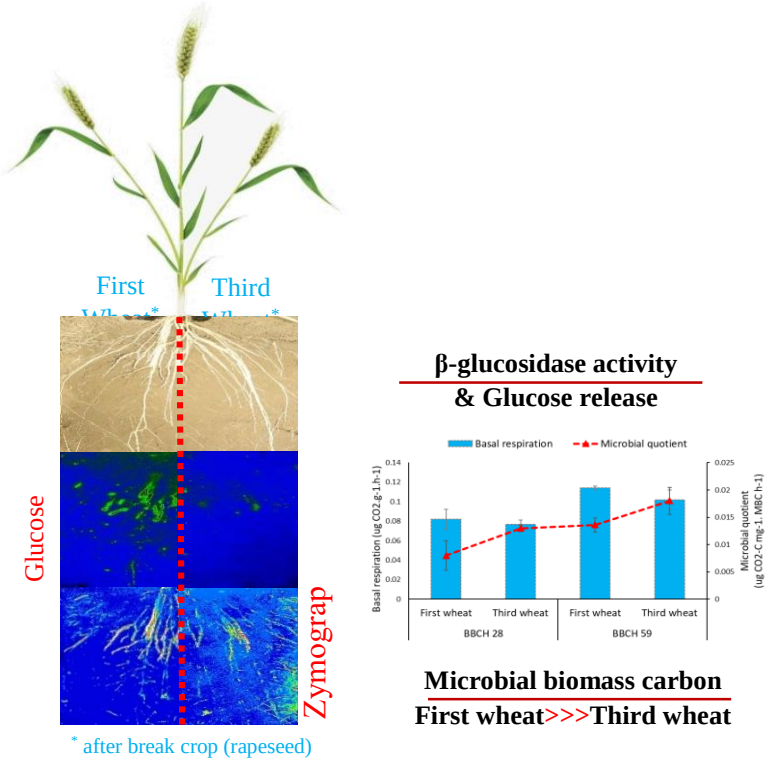

2.3.11. Supplementary Figures

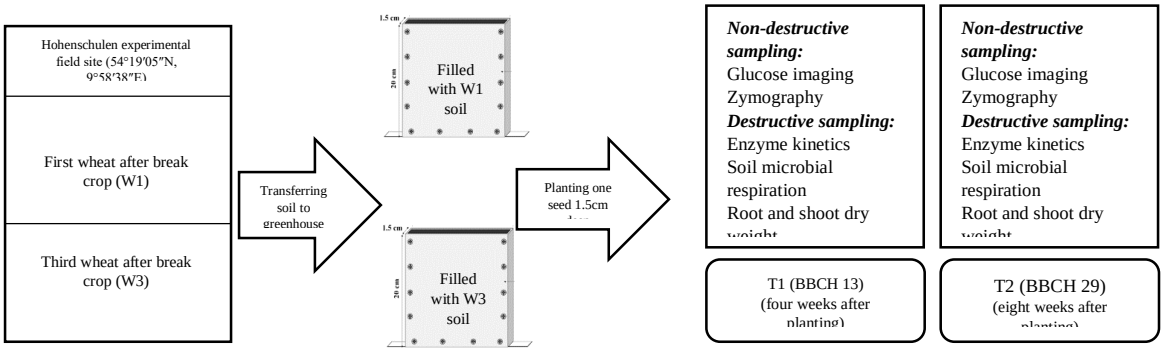

Figure S2.3.1- Experimental Design and Methodology

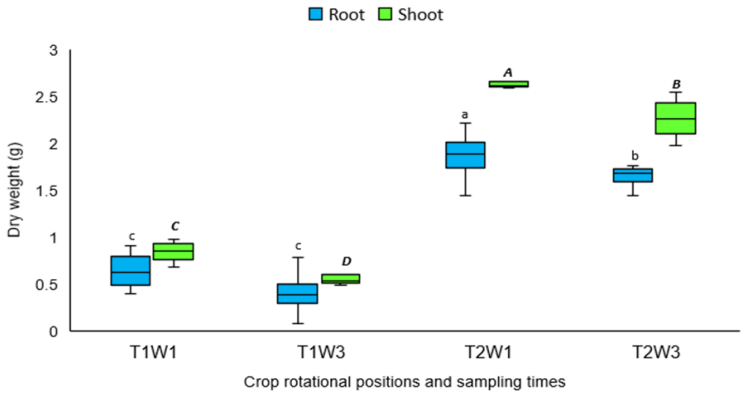

Figure S2.3.2- Wheat root and shoot dry weight in the first (W1) and third (W3) wheat after break crop at two sampling times (T1: four weeks (BBCH 13), and T2: eight weeks after sowing (BBCH 29)). Lower-case letters denote significant differences between treatments in terms of wheat root dry weight and upper-case letters denote significant differences between treatments in terms of wheat shoot dry weight according to two- way ANOVA at $p<0.05$.

2.4. Study 4: A SWEET Challenge: Less Sugars for Rhizospheric Microbiome Under the Successive Wheat Rotation

Mehdi Rashtbari[1*], Seyed Sajjad Hoseini[2], Ahmad Samir Azimi[3], Markus Schemmel[4], Zheng Zhou[4], Lingyue Han[4], Daguang Cai[4], Bahar S. Razavi[4]

[1] Department of Soil and Plant Microbiome, Institute of Phytopathology, Christian Albrechts University of Kiel, Kiel, Germany; [2]Department of Soil Science, Faculty of Agriculture, Ferdowsi University of Mashhad, Mashhad, Iran; [3]Biogeochemistry of Agroecosystems, Department of Crop Science, University of Göttingen, Göttingen, Germany; [4]Department of Molecular Phytopathology and Biotechnology, Institute of Phytopathology, Christian-Albrechts-University of Kiel, Kiel, Germany.

***** *corresponding author: mehdi.rashtbari@phytomed.uni-kiel.de*

Status: In preparation

2.4.1. Summary

- Considering the crucial role of root exudates, we hypothesized that continuous wheat cultivation would lead to lower glucose release, resulting in lower microbial growth, activity, and biomass.
- For the first time *in situ* glucose imaging was optimized for studying the interactions in the first (W1) and third (W3) wheat after break crop plots in the field. Glucose imaging method combined with soil microbial respiration, enzyme kinetics and the quantification SWEET genes expression levels in wheat plants.
- W3 had the lowest proportion of hotspots for glucose release with 1.35 % of the total soil surface area, indicating a 17.7 % decline compared to W1. Also, the expressions of functional orthologous genes of SWEET1a in wheat roots were significantly upregulated in W3 compared to W1. The growing microbial biomass in the rhizosphere soil of W1 was about five times higher than W3.
- Differences in SWEET gene expression and shift in glucose release is linked to altered root physiology and exudation processes, potentially reflecting the plant's strategy to create a less favourable environment for opportunistic pathogens. Hence, this study provides novel insights into the complex interactions between continuous wheat cultivation, root exudation, microbial dynamics, gene expression, and enzymatic activities.

Keywords: monoculture, root exudates, SWEET genes, wheat rotation, glucose, enzyme, microbial growth

2.4.2. Introduction

Plant adaptes strategies to sustain rhizospheric microbial growth and proliferation and to coopt soil born pathogens under stress condition mostley trough the exudate regulations (Baker *et al*., 2012). Root exudation is a complex process by which plants respond to changing environmental conditions, allocating carbon to roots and subsequently to the soil (Canarini *et al*., 2019; Oburger & Jones, 2018). This initiates a cascade of feedback loops between root and soil microbiome (Vetterlein *et al*., 2020). The extensive input of easily degradable substances and labile carbon such as sugars (e.g. glucose comprising ~ 40-50% of root secretions) (Hütsch *et al*., 2002; Dennis *et al*., 2010) provides a significant energy source for microorganisms

(Hinsinger *et al*., 2009), inducing higher microbial abundance and activities in the rhizosphere than in root free soil (Kuzyakov and Razavi, 2019). Root exudation improve plant performance by altering the soil environment (Zhao *et al*., 2021) and creating faivorable microbial hotspots – micro-habitats within the rhizosphere – a small volume of soil influenced by living roots (Hinsinger *et al*., 2009).

While soil microbial communities play a crucial role in regulating ecosystem services, such as carbon and nutrient cycling (Blagodatskaya *et al*., 2020), the exudates changes alter the structure, diversity, and function of the microorganisms, (Chaparro *et al*., 2014). This suggests that root exudation stimulates the production of extracellular enzymes in the rhizosphere (Zhang *et al*., 2019), hence, controls nutrient acquisition (Bais *et al*., 2006). Thus, higher enzyme activities in the rhizosphere are dependent on soil microbial activity, the direct release of enzymes by roots, and root exudates (Zhang *et al*., 2021). However, the accumulation of root secretions in the soil around the root not only shapes specific beneficial microbial groups it can also attract plant pathogens and increase microbial competition for nutrients (Jones *et al*., 2009). Detailed knowledge about the allocation and localization of photosynthetic sugars released from roots is an important prerequisite for understanding the complex interactions between plants and the rhizosphere microbiome in agroecosystems.

Fixed carbaon during photosynthesis will be transported from leaves (source tissues) to non-photosynthesic part of plants – such as root (sink tissues). In other word, photosynthetically produced sugars are transported over long distances as sucrose via phloem flow, driven by concentration gradients resulting from differences in turgor (Canarini *et al*., 2019; Liu *et al*., 2021b). Prior to entering sink cells, sucrose is hydrolyzed irreversibly into glucose and fructose by sucrose invertase (Liu *et al*., 2021a; Paulsen *et al*., 2019). In order to be released into the soil environment, glucose must cross at least one plasma membrane, which is impermeable to uncharged polar glucose molecules (Yang & Hinner, 2015). Plant SWEET (sugars will be eventually effluxed transporter) sugar transporters play different physiological roles during plant growth and development, including maintatining the uptake of glucose from the apoplast to the parenchyma cells in sink tissues (Ho *et al*., 2019). Specific transmembrane proteins mediate transmembrane absorption of these molecules, forming small pores through the lipid bilayer (Sasse *et al*., 2018; Paulsen *et al*., 2019). Once in the apoplast, diffusion primarily controls glucose efflux from the root to the soil (Canarini *et al*., 2019).

The SWEET transporter family includes potential candidates for sugar exudation, such as glucose, from plant roots to feed microbiota (Chen *et al*., 2015). These efflux carriers may permit sugar exudate regulation via gene expression up/downregulation or post-translational modification (Badri *et al*., 2008; Canarini *et al*., 2019). SWEETs are ubiquitous, bidirectional, pH-dependent carriers (Chen *et al*., 2010), classified into four clades; clade I and II members prefer hexose (Chandran, 2015; Chen *et al*., 2012). In plants, SWEETs are predominantly localized to the plasma membrane and facilitate sugar efflux from the cytosol to the apoplast (Anjali *et al*., 2020; Eom *et al*., 2015). They also contribute to pathogen susceptibility (Chen *et al*., 2010), as pathogen-produced transcription activator-like (TAL) effectors target the SWEET gene to obtain sugars for nutrition (Asai & Kobayashi, 2016; Cohn *et al*., 2014). Chen *et al*. (2015) demonstrated increased glucose efflux into the root apoplast due to SWEET gene expression activation by pathogens. Despite the essentiality of this process in plant-soil-microbiome system and its effect on shaping of rhizosphereic biota, a complete understanding of mechanism involved and the pathways from leave to the action takers – soil microorganisms is lacking.

Wheat (*Triticum aestivum*) is an important crop worldwide, and the increasing demand for wheat requires more intensive cropping systems, such as monoculture (Gan *et al*., 2014). However, continuous cultivation of wheat contributes to a decline in grain yield and quality (Debaeke *et al*., 1996), possibly due to increased proliferation of agrophages (pests and fungal

pathogens), (Woźniak, 2019). Hence, in the present study, we aimed to investigate and quantify the effects of continuous wheat rotations on glucose release, microbial growth and activity, and expression of sugar transporter genes.

We tested the following hypotheses: i) continuous wheat cultivation results in differently expressed sugar transporter genes in plant roots and leaves; ii) the variation in SWEET gene expression results in lower glucose release by root, causing lower microbial growth, activity, and biomass in the rhizosphere; iii) a decrease in glucose release in continuous wheat will be accompanied by a decline in microbial functionality reflected in lower enzyme expression and reduction of enzymatic efficiency. To test these hypotheses, a specific field installation root windows (Bilyera *et al*., 2021) in the first (W1) and third (W3) wheat after break crop plots in the Hohenschulen field at CAU Kiel was performed. To identify and localize glucose hotspots, direct *in situ* glucose imaging (Hoang-Rashtbari *et al*., 2022) combined by expression of sugar transporter genes in root and leaf sample as well as destractive analysis of soil microbial growth kintetics and enzyme kinetics (including the activity of α- and β-glucosidase, leucine aminopeptidase and acid phosphatase enzymes) were performed.

2.4.3. Materials and Methods

2.4.3.1. Soil description and experimental setup

A field experiment was conducted at the Hohenschulen experimental field site (54°19′05″N, 9°58′38″E), which is owned by the Christian-Albrechts-University of Kiel, Germany. The soil at the site was pseudogleyic sandy loam (Luvisol), with 21% clay and 35% silt, 44% sand, a pH of 6.7, and organic carbon content of 1.3%, total nitrogen content of 0.15%, and available phosphorous and potassium contents of 9 $mg.kg^{-1}$ and 15 $mg.kg^{-1}$, respectively (Sieling *et al*., 2005).

Soil samples for enzyme and microbial growth kinetics were taken from the Ap horizon of a sandy loam soil (0-20 cm) from two distinct wheat rotational positions: the first wheat position (referred to as W1), represented the first wheat cultivation after the break crop of winter oilseed rape, and the subsequent third wheat (wheat grown continuously for three years referred to as W3) addressing the continuous cultivation of wheat three years in a row following the same break crop in 2021. The details on the crop rotational trials and wheat rotational positions are described in Arnhold *et al*. (2023). The samples were sieved through a 2 mm mesh and stored at 4°C. Plant leaf and root sampling, as well as *in situ* glucose imaging, were carried out in four replications at BBCH 59 (when the flag leaf was fully extended and photosynthesis was optimal).

2.4.3.2. Installing root windows and *in situ* glucose imaging

At the tillering stage (BBCH 28) under the field condition, the root windows were built at an angle of 90° to the soil surface next to the wheat plants. Root windows (30 × 30 cm) consisting of a transparent acrylic sheet (3-5 mm thick) were fixed in place by two vertical steel rods and backfilled with soil to remove air gaps.

Soil *in situ* glucose imaging was applied on all plots according to Hoang *et al*. (2022). Accordingly, phosphate powder (Sigma P7994) was dissolved in distilled water to make a buffer solution of 0.05 M. 100 mL buffer solution (pH 7.4). It was added respectively with 1.7 unit/ml glucose oxidase from Aspergillus niger (Sigma G7141), 1.5 unit/ml peroxidase from horseradish (Sigma P8125), and 200 µM Ampliflu red (Sigma 90101) dissolved in 60 µL Dimethylsulfoxide. Installed rhizotrones were gently removed to avoid cutting roots. Polyamide membrane filters (pore size 0.45 mm - Tao Yuan, China) were cut into 10 ×10 cm. These membranes were saturated with the prepared reaction mixture solution before being attached to the rooted area. After 20 minutes of incubation (an optimal incubation time was tested in advance – time may differ between plants species (Hoang *et al*., 2022), membranes

were promptly removed and placed in a dark container and immediately transferred to the dark room under UV light of 355 nm wavelength. The magenta-colored area on the membrane indicated glucose exudation as hydrogen peroxide generated from a reaction between glucose and glucose oxidase enzymes, which was catalyzed by horseradish peroxidase to convert colorless Ampliflu red into magenta color resorufin (Zhou *et al*., 1997).
All images were taken with a digital camera (Canon EOS 6D, Canon Inc.) and a Canon lens EF 24–105 mm 1: 4L IS II USM with the setting of aperture and shutter speed at f/5.6 and 1/10 sec, respectively.

The calibration lines for glucose imaging were prepared by soaking a 4 cm^2 membrane in glucose solution at respective concentrations of 0, 2, 4, 6, 8, and 10 mM. The membranes were soaked in the respective reaction mixture solution. Fluorescent signals of glucose release on an area basis were calculated based on the volume of substrate solution taken up by a fixed membrane size. The image processing and analysis were conducted using the software package ImageJ.

Mean+2SD was applied to identify and separate hotspots within each image which comprised three steps: dividing the greyscale histogram into two distributions with normal greyscale values, pinpointing the greyscale range associated with the hotspots, and subsequently mapping these hotspots onto the original image (Bilyera *et al*., 2020). The glucose release was determined for mature roots and root tips where the flux of primary metabolites through root exudation is mainly located, and the plants to communicate more with soil microorganisms (Canarini *et al*., 2019; Zhang *et al*., 2020). Five horizontal transects (angle to the root ~90°) were randomly drawn across five selected roots in the image using ImageJ to measure the glucose release. This yielded 25 lines per image as pseudo-replicates, and their mean was used for each replicate (as a true replicate) (Razavi *et al*., 2019).

2.4.3.3. Expression analysis by RT-qPCR

Total RNA from wheat leaf and root tissues was extracted with TRIzol® reagent (Thermo Fisher Scientific, Germany) according to the manufacturer's instructions. The tissues were homogenized with pestles in liquid nitrogen, and then incubated for 5 min at room temperature. Subsequently, 200 µl of chloroform was added, vigorously vortexed, and centrifuged at 10,000 rpm for 15 min at 4 °C. The resulting clear supernatant was carefully transferred to a new 1.5 ml tube and incubated on ice for 30 min before being centrifuged at 12,000 rpm for 15 min at 4 °C. The supernatant was discarded, and the RNA pellet was washed twice with 1 ml 80% DEPC-ethanol and 1 ml 100% ethanol, followed by centrifugation at 12,000 rpm for 5 min at 4 °C, and subsequent supernatant removal. The RNA pellet was air-dried and dissolved in 50 µl DEPC-water. Quality and concentration control of total RNA were performed using gel electrophoresis and NanoVue Plus Spectrophotometer (GE Healthcare Life Science), respectively. Total RNA samples of three independent biological replicates were used for further experimentation.
Complementary DNA (cDNA) was synthesized from 1 µg total RNA in 20 µl reaction volume using RevertAid First Strand cDNA Synthesis Kit (Thermo Fisher Scientific, Germany) at 42 °C for 1 h. Approximately 50 ng of the synthesized cDNA was used as a template for RT-qPCR reactions, conducted with qPCR SyGreen Mix (2X) (Nippon Genetics, Germany). The quantification of *TaeSWEET1a* expression levels was performed using the following program: 10 min 95 °C; 40 × 15 s 95 °C, 30 s 59 °C, 30 s 72 °C; 10 s 95 °C, melting curve from 65 °C to 95 °C. The normalization of expression levels was carried out using *GADPH* as the internal reference gene. Each data point represents the mean of three independent biological replicates, with each replicate measured in duplicate. Primers used for RT-qPCR quantification assays are detailed in Table S1.

2.4.3.4. Kinetics of the substrate-induced respiration

Total and active microbial biomass was characterized by Substrate Induced Growth Respiration (SIGR) (Blagodatskaya *et al*., 2014). Accordingly, 0.5 g fresh soil was amended with a mixture of glucose (10 mg g^{-1}) and mineral salts (1.9 mg g^{-1} $(NH_4)_2SO_4$, 2.25 mg g K_2HPO_4 and 3.8 mg g^{-1} $MgSO_4.7H_2O$) in order to induce unlimited growth. There were samples amended with distilled water as a control. Soil samples were incubated in the modified rapid automated bacterial impedance technique (RABIT) system (Don Whitley Scientific, UK) at 25°C, and the CO_2 production rate was monitored every six minutes. Equation (3) was used to estimate the specific growth rate (μ) of soil microorganisms:

$$CO_2 = A + B \times \exp(\mu t) \quad (3)$$

Where A is the initial respiration rate uncoupled from ATP production, B is the initial rate of couple (growth) respiration, and t is the time (Blagodatsky *et al*., 2000). The total microbial biomass (TMB) and growing microbial biomass (GMB) at time zero were given by Eqs. (4) and (5):

$$TMB = \frac{B}{r_0 Q} \quad (4)$$

$$GMB = TMB \times r_0 \quad (5)$$

where r_0 is the physiological state index of the microbial biomass (MB) before substrate addition and was calculated according to Eq. (6):

$$r_0 = \frac{B(\lambda-1)}{A+B(\lambda-1)} \quad (6)$$

where λ = 0.9, which has been accepted as a basic stoichiometric constant (Panikov & Sizova, 1996). Q is the total specific respiration activity:

$$Q = \frac{\mu}{\lambda Y CO_2} \quad (7)$$

YCO2 is the microbial yield per unit of glucose-C consumed, which was assumed to be a mean value of 0.6 (Panikov & Sizova, 1996). The theory of microbial growth kinetics has been presented in detail earlier (Panikov, 1991).

The duration of the lag period (t_{lag}) was determined as the time interval between the glucose addition and the moment when the increasing rate of growth-related respiration becomes as high as the rate of respiration uncoupled from ATP generation. It was calculated by using the parameters of the approximated curve of the respiration rate of microorganisms with the equation (8) (Blagodatskaya *et al*., 2009);

$$T_{lag} = \frac{ln(A/B)}{\mu_m} \quad (8)$$

In addition, the kinetic approach allowed the assessment of generation time (T_g) of both actively growing and total microbial populations consuming glucose. The estimation of T_g for actively growing biomass is based on specific growth rates, i.e.:

$$T_g = \frac{ln(2)}{\mu_m} \quad (9)$$

2.4.3.5. Enzyme kinetics, substrate affinity, and catalytic efficiency

After removing plant roots from the plots, rhizosphere samples were collected by detaching tightly adhered soil particles immediately from roots using toothbrushes (Hamel *et al*., 2019). Briefly, the complete root was put on a sterile surface, and the soil was brushed off the root surface using a clean toothbrush. The loosely attached soil to the roots after shaking off the plant roots was collected as root-affected soil samples. The soil was collected in a conical tube and stored at 4°C. The root-free soil was collected as bulk soil for comparative purposes and stored the same way. All samples for enzyme kinetics were measured the next day.

The kinetics of hydrolytic enzymes involved in C, N, and P cycles were measured by fluorimetric microplate assays of 4-methylumbelliferone (MUF) and 7-amino-4-methyl coumarin (AMC) (Dorodnikov *et al*., 2009). Three types of fluorogenic substrates based on

MUF and one type based on AMC were used to assess enzymatic activities; 4-methylumbelliferyl-β-D-glucoside to detect β-glucosidase activity, 4-methylumbelliferyl-α-D-glucoside to detect α-glucosidase activity, 4-methylumbelliferylphosphate to detect acid phosphomonoesterase activity, and L-Leucine-7-amino-4-methylcoumarin to detect leucine aminopeptidase activity. All substrates and chemicals were purchased from Sigma (Germany).

According to (German *et al*., 2011), 1.0 g of soil was suspended in 50 mL distilled water, of which 50 µL aliquots were pipetted into labeled wells of a 96-well microplate (Thermo Fisher, Denmark). Then, 50 µL buffer (MES/Trizma) and 100 µL respective substrate solution were added to each well. The activity of enzymes was measured at three time points: 30, 60, and 120 min using CLARIOstar plus (BMG LABTECH, Germany) at an excitation wavelength of 355 nm and an emission wavelength of 460 nm. We determined enzyme activities over a range of substrate concentrations from low to high (0, 20, 40, 60, 80, 100, 200, and 400 µmol g^{-1} soil) to ensure the appropriate saturating concentration (Razavi *et al*. 2016a).

Enzyme activities (V_{max}) were denoted as released MUF/AMC in nmol per g dry soil per hour (nmol MUF/AMC g^{-1} soil h^{-1}) (Awad *et al*., 2012) and affinity constant for each enzyme (K_m) expressed in µmol substrate per g dry soil (µmol g^{-1} soil). Simultaneously, MUF/AMC concentrations of 0, 10, 20, 30, 40, 50, 100, and 200 nM were prepared to calibrate the measurement. The Michaelis-Menten equation (Michaelis-Menten, 1913) was used to determine the parameters of the activity of the enzyme (V):

$$V = \frac{V_{max}[S]}{K_m + [S]} \quad (1)$$

where V_{max} is the maximum enzyme activity (a function of enzyme concentration), S is the substrate concentration, and K_m is the substrate concentration at half-maximal enzyme activity. Both V_{max} and K_m parameters were approximated by the Michaelis-Menten equation (1) with the non-linear regression routine of SigmaPlot (v. 12.3). Catalytic efficiency was calculated as the V_{max}-to-K_m ratio (Panikov *et al*., 1992). The substrate turnover rate was calculated by equation (2), where T_t is the turnover time (hours) (Hoang *et al*., 2020).

$$T_t = \frac{K_m \times [S]}{V_{max} + [S]} \quad (2)$$

2.4.3.6. Data analysis

All the statistical analyses were performed in SAS v. 9.2, and all graphs were drawn using Excel 2016. Significant differences in enzyme activities, substrate affinity, catalytic efficiency, substrate turnover time, rhizosphere extent, hotspot percentage, substrate-induced growth respiration kinetics parameters, and differentially expressed SWEET genes between W1 and W3 soil samples were confirmed by Two-Way ANOVA after checking normality and homogeneity of variance values. A probability of $p < 0.05$ was used as the significance level between treatment comparisons. Error bars indicate the standard error of the means.

2.4.4. Results

2.4.4.1. Lower glucose release in W3 compared to W1

The spatial pattern of glucose release was affected by continuous wheat cultivation (Fig. 2.4.1). W3 had the lowest proportion of hotspots for glucose release with 1.35 % of the total soil surface area, indicating a 17.7 % decline compared to W1 ($p<0.05$) (Fig. 2.4.2a). Glucose release rate for wheat root tips and mature roots showed that W3 demonstrated a consistent decrease in both compartments compared to W1 and the highest glucose release at root tips was obtained in W1 with 593.5 $nmol^{-1}$ cm^{-2} ($p<0.05$). However, as shown in Figure 2b, glucose release increased enormously in root tips compared to mature roots in W1 and W3. In W1, glucose release at wheat root tips increased by 30.2 % compared to mature roots, while in W3, root tips had 35.6 % higher glucose release than mature roots (Fig. 2.4.2b).

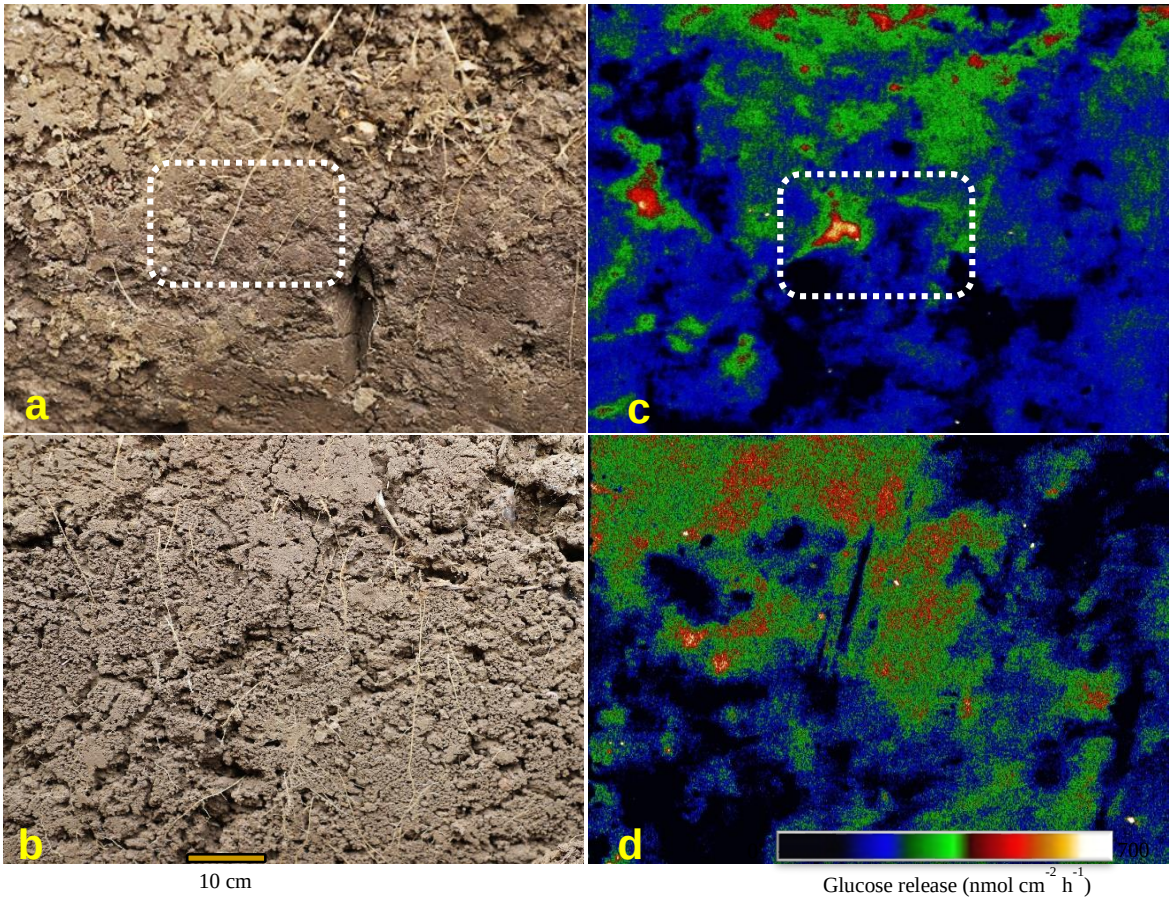

Figure 2.4.1. Original images of the wheat root (a, b) and spatial distribution of glucose release (c, d) at W1 (top row) and W3 (lower row), respectively (W1: first and W3: third wheat after break crop).

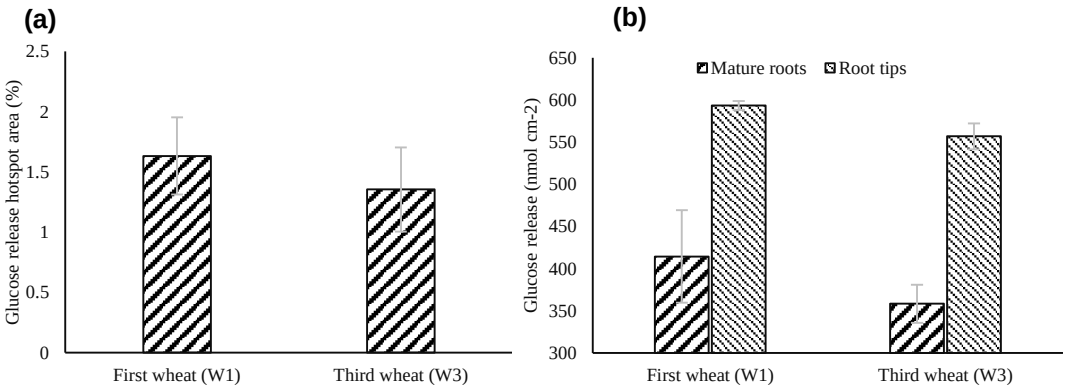

Figure 2.4.2. (a) Comparison of the percentage of hotspot area and (b) mean glucose releasing rate in the whole area and region of interest (ROI) in the first (W1) and third (W3) wheat after break crop. Error bars represent standard error of means (n = 4).

2.4.4.2. Gene expression

Table 2.4.1 provided some information regarding SWEET genes identified in wheat roots and leaves in continuous wheat cultivation compared to W1. Results showed that the expressions of functional orthologous genes of SWEET1a in wheat roots were significantly upregulated in W3 compared to W1. The expressions of these orthologous genes were also checked by real-time quantitative PCR. It was found that these genes were upregulated under continuous wheat cultivation (Fig. 2.4.3a). However, there was a reverse expression pattern for SWEET genes in wheat plant leaves in W3 compared to W1. We found downregulation of genes, especially for

SWEET 2a. Also, all orthologous genes of SWEET13 showed downregulation in continuous wheat cultivation compared to W1 (Fig. 2.4.3b).

Table 2.4.1- Information about the SWEET genes identified in wheat leaf and root

	Gene name	Gene ID	Length (bp)	Locus on Chromosome
Leaf	SWEET 13 (1)	TraesCS6D03G0847700	1376	6D
	SWEET 13 (2)	TraesCS6A03G0966400	1473	6A
	SWEET 13 (3)	TraesCS6D03G0847200	1375	6D
	SWEET 2a	TraesCS6B03G0449300	1246	6B
Root	SWEET 1a (1)	TraesCS1D03G0639100	1055	1D
	SWEET 1a (2)	TraesCS1A03G0674900	1277	1A

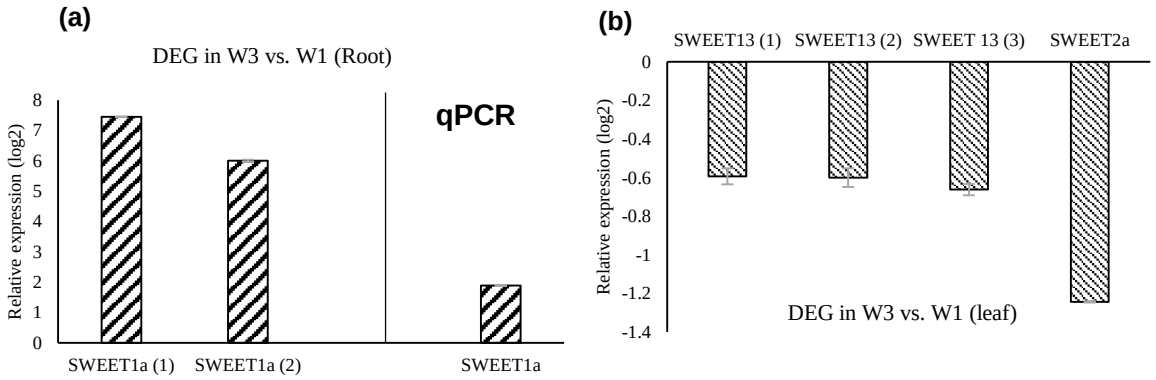

Figure 2.4.3. Relative expression of differentially expressed SWEET genes in wheat (a) roots and (b) leaves in W3 vs. W1 (W1: first and W3: third wheat after break crop). Error bars represent standard error of means.

2.4.4.3. Substrate-induced respiration kinetics

Total microbial biomass dropped by 11.8 and 4.8 % in W3 in the rhizosphere and bulk soils compared to W1 (respectively; Fig. 2.4.4a). The Growing microbial biomass in the rhizosphere soil of W1 was about five times higher than W3, and different crop rotations did not affect growing microbial biomass in bulk soil compartment (Fig. 2.4.4b). The GMB/TMB ratio was also strongly affected by crop rotation, and W1 had the higher ratios in both rhizosphere and bulk soil (0.14 and 0.002, respectively; Fig. 2.4.4c). The specific growth rates (μ) considerably increased in W3 in the rhizosphere compartment compared to W1 (0.17 and 0.23 h^{-1}) and both W1 and W3 had similar specific growth rates in bulk soil samples (about 0.26 h^{-1}; Fig. 2.4.4d). Despite a slower specific growth rate, a seven times shorter lag period was observed in W1 vs W3 rhizosphere soil. Similar lag periods were observed for bulk soil samples in W1 and W3 (15.49 and 15.64 h, respectively; Fig. 2.4.4e). Generation time of actively growing microbial community-consuming substrate during incubation of soils with glucose and nutrients in W3 declined by 24.2 % compared to W1 in rhizosphere soil and the difference in Tg in bulk soil for W1 and W3 was negligible (2.66 and 2.58 h, respectively; Fig. 2.4.4f).

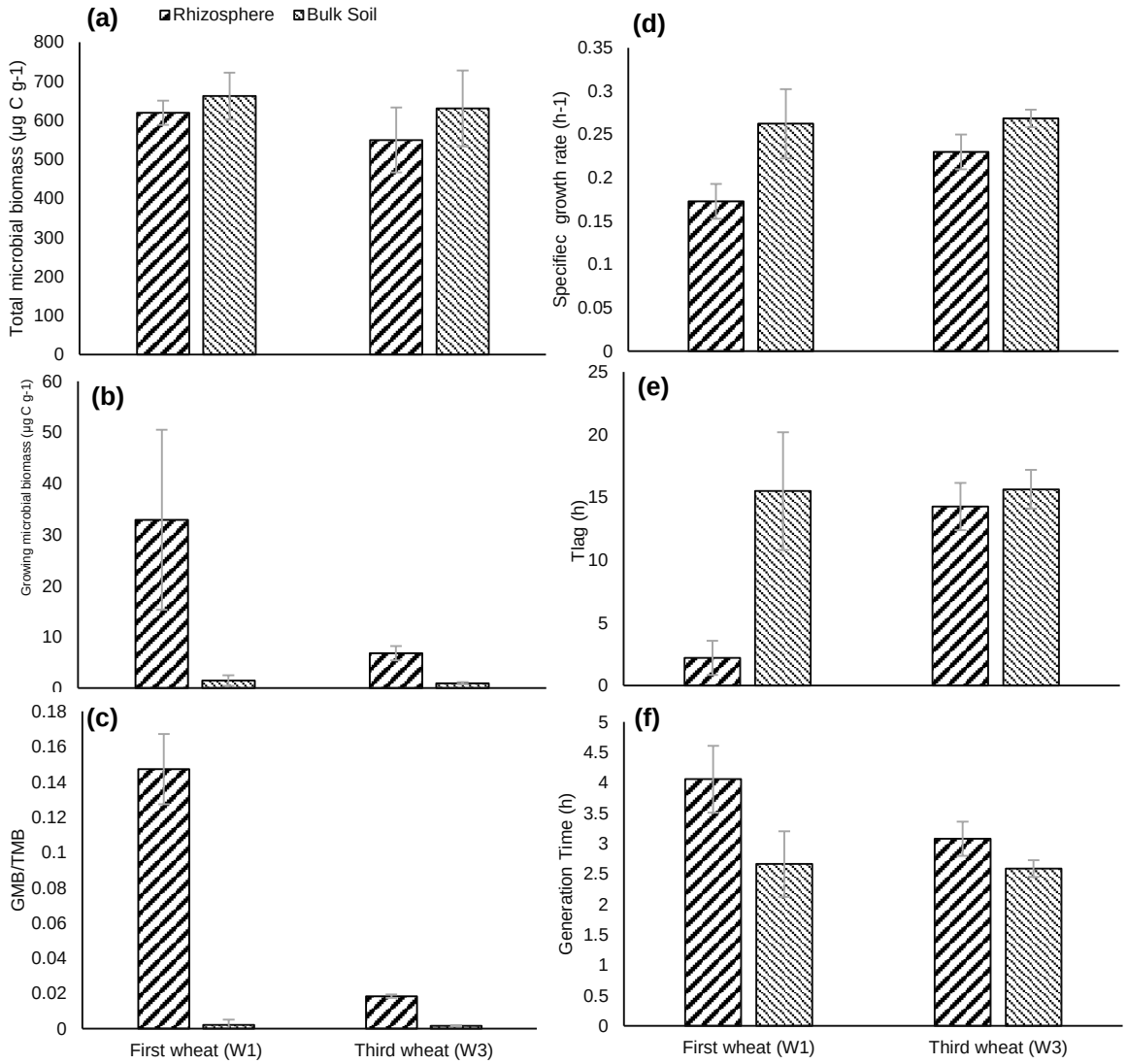

Figure 2.4.4. Total microbial biomass (TMB) (a), actively growing microbial biomass (GMB) (b), Specific growth rates (µ) of soil microorganisms (d), their lag time (T_{lag}) (e) and generation time (T_g) (f) in rhizosphere and bulk soil samples of the first (W1) and third (W3) wheat after break crop during incubation at 25°C. Error bars represent standard error of means (n = 3).

2.4.4.4. Enzyme kinetics is the lowest at T2 in both wheat crop rotations

Wheat rotational positions strongly affected the maximum rate (V_{max}) of extracellular enzymes in the rhizosphere, root affected, and bulk soil (p<0.01; Fig. 2.4.5). For β-glucosidase activity, soil samples from W1 resulted in a higher V_{max} compared to W3 samples, demonstrating 145.5, 148.5 and 74.6 nmol MUF $g^{-1}h^{-1}$ in the rhizosphere, root affected and bulk soil samples, respectively. W3 resulted in a 23.7 and 45 % decrease in V_{max} value compared to W1 in rhizosphere and bulk soil, respectively (Fig. 2.4.5a). Despite no difference between soil compartments in terms of α-glucosidase activity in W1, the rhizosphere soil had the lowest V_{max} value in W3 with 49.6 nmol MUF $g^{-1}h^{-1}$ indicating 47 % decrease compared to W1 (Fig. 2.4.5b).

Leucine aminopeptidase showed different trends in soil compartments at W1 and W3. While the highest V_{max} value was observed in rhizosphere soil in W1 with 128.8 nmol AMC $g^{-1}h^{-1}$, the V_{max} value in this compartment decreased by 44.8 % and had the lowest value in W3 with 71.1 nmol AMC $g^{-1}h^{-1}$. The highest value was observed in bulk soil with 97.7 nmol AMC $g^{-1}h^{-1}$ (Fig. 2.4.5c). Contrary to leucine aminopeptidase; there was no statistical difference

between rhizosphere and bulk soil in W1 for acid phosphatase V_{max} value. The activity of acid phosphatase at W3 decreased in BS and RH compartments by 8.6 and 15.7 %, respectively. Root-affected soil had the lowest V_{max} value in both crop rotational positions with 315.8 and 275.3 nmol MUF $g^{-1}h^{-1}$, respectively, indicating a 12.8 % drop in W3 vs W1 (Fig. 2.4.5d).

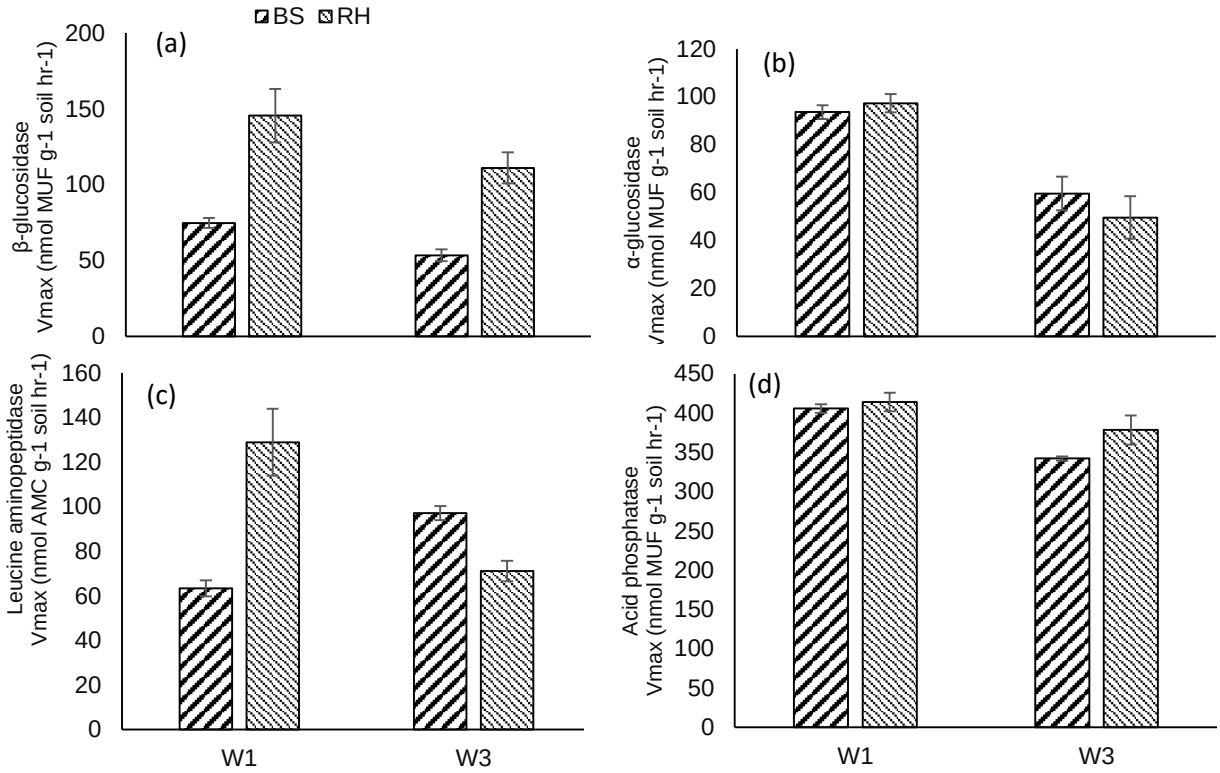

Figure 2.4.5. V_{max} values of β-glucosidase (a), α-glucosidase (b), leucine aminopeptidase (c) and acid phosphatase (d) in different wheat soil compartments (BS: bulk soil, RA: root affected soil, RH: rhizosphere) in the first (W1) and (W3) third wheat after break crop). Lower-case letters denote significant differences between treatments according to ANOVA at p<0.05.

There was a decreasing trend in β-glucosidase K_m values from bulk soil to root-affected and rhizosphere soil in W1 and W3. The same trend was also observed for catalytic efficiency values. However, the catalytic efficiency of β-glucosidase in rhizosphere soil in W3 decreased by 17.5 % compared to W1. The lowest catalytic efficiency was observed in bulk soil in W3 with 1.94 nmol MUF μmol substrate^{-1} h^{-1}. Accordingly, the lowest substrate turnover time was observed in W1 rhizosphere soil with 2.08 h (Fig. 2.4.6a). Results for catalytic efficiency values for α-glucosidase, leucine aminopeptidase, and acid phosphatase showed that, in both crop rotational positions, there was a slight decrease in efficiency from bulk soil to root affected soil and then drastically increased in rhizosphere soil. According to the results, these enzymes were less efficient in root affect soils than bulk and rhizosphere soils. Results for substrate turnover time support these findings (Fig. 2.4.6b, b, c). Overall results showed that the RH compartment had the highest enzyme activity and a downward trend from rhizosphere to bulk soil compartments for enzyme activities.

2.4.5. Discussion

2.4.5.1. Glucose release

The observed differences in glucose release between W1 and W3 underscore the impact of crop rotation on root exudation patterns. Continuous wheat cultivation reduced glucose release in the rhizosphere (Figs. 2.4.1, 2.4.2a). The substantial reduction in glucose hotspots in W3

compared to W1 could be attributed to changes in root physiology and exudation processes. This result aligns with Chen *et al*. (2022) who have highlighted the impact of crop rotation in altering root exudation patterns. This indicates that the development and dynamics of the rhizosphere, as demonstrated by the intensity of hotspots, potentially contributed to the observed variations in glucose release between W3 and W1. Root-secreted compounds, including glucose, have a significant impact on initiating and fostering plant-microbe interactions within the rhizosphere (Hage-Ahmed *et al*., 2013). Consequently, the composition and quantity of root exudates can lead to distinct responses from soil-borne pathogens (Jones *et al*., 2004). In line with this, Bakker *et al*. (2013) pointed out that pathogens employ intricate mechanisms to exploit sugar fluxes from the host plant. Additionally, pathogens have the capability to manipulate the expression of sugar transporters from the SWEET gene family to secure the sugars essential for their proliferation (Chen *et al*., 2010).

Especially, as monoculture practices can lead to escalated disease occurrence and severity, primarily due to the accumulation of pathogens in the soil. Hence, by reducing the released glucose amount, plants strategically establish gradients of soil biochemical attributes to establish a protective buffer against pathogenic invasions. Essentially, plants can regulate the release of glucose and modify the dynamics of plant-pathogen interactions to foster a mutually beneficial association. Our results revealed a decline in microbial biomass carbon and enzyme activity in the case of the W3, in comparison to the first wheat (W1) which might be attributed to the heightened levels of pathogens in the third wheat cycle (Mazzola *et al*., 2002).

The lower glucose release rate in both root tip and mature root compartments of W3, along with the higher glucose release in root tips compared to mature roots (Fig. 2.4.2b), suggests a potential shift in resource allocation strategies driven by crop rotation. The initial section of the plant root, known as the root tip, serves as the pioneering element in the plant's interaction with a novel soil milieu and assumes a pivotal function in reacting to environmental cues. An increasing body of research has demonstrated that the root tip functions as a central hub for perceiving external nutrient levels and subsequently effecting changes in the arrangement of the root system and shaping rhizosphere hotspots (Grover *et al*., 2021; Razavi *et al*., 2016b). Higher release of glucose in root tips contributes to increase in microbial community persistence in the rhizosphere (Nwachukwu *et al*., 2021) which allows the plant to more effectively uptake nutrient, even in continuous wheat cultivation.

2.4.5.2. Gene Expression

The observed differential expression of SWEET genes in wheat roots and leaves highlights the intricate interplay between crop rotation and plant-microbe interactions. The expressions of functional orthologous genes of SWEET1a in wheat roots were significantly upregulated in W3 compared to W1 which further confirmed by real-time quantitative PCR (Fig. 2.4.3a). SWEET1a, belonging to clade I of the SWEET family, acts as a low affinity (Km ~100 mM) glucose-specific carrier with a passive diffusion manner and involved in the redistribution of sugars within the root system and the uptake of glucose into unloading cells as part of the sugar unloading mechanism in sink organs (Chen *et al*., 2010; Ho *et al*., 2019). The upregulation of these genes in W3 wheat roots may reflect the need for energy and carbon sources required for nutrient uptake and root development. Also, this upregulation could be linked to altered root exudation patterns and the demand for nutrient acquisition in the rhizosphere of W3 (Wen *et al*., 2022).

Conversely, the expressions of functional orthologous genes of SWEET13 and SWEET2a in wheat leaves were significantly downregulated in W3 compared to W1 (Fig. 2.4.3b). These genes are involved in the export of sugars (such as glucose and sucrose) produced during photosynthesis from the mesophyll cells of wheat leaves to other plant tissues (Breia *et al*., 2021) and may play important roles in sugar partitioning during seed development

(Xie *et al*., 2019). SWEET2 transporters retrieve sugars from the cytosol to the vacuole to limit their leakage to the extracellular space where they may feed the pathogen (Chen *et al*., 2015). This downregulation, especially for SWEET2a, could reflect a complex response to changes in root exudation and nutrient availability, potentially impacting plant growth and stress responses. Also, the downregulation of these genes may indicate a decreased sugar export from the source tissues (leaves) to the rest of the plant and might be a result of reduced photosynthetic activity or altered resource allocation in continuous wheat cultivation. This is consistent with Zhang *et al*. (2021) who found decrease in photosynthesis rate and efficiency in monoculture compared to intercropping and crop rotation shade-demanding crop *Amorphophallus xiei*.

2.4.5.3. Response of substrate-induced respiration kinetics

The findings derived from this investigation illuminate the complex interconnections among crop rotation, microbial dynamics, and soil health within agroecosystems. The observed changes in microbial biomass, growth rates, and substrate utilization patterns under different crop rotations have important implications for nutrient cycling, microbial activity, and sustainable agricultural practices. The substantial reduction in total and growing microbial biomass observed in the rhizosphere and bulk soils of W3 compared to W1 (Fig. 2.4.4a and b) signifies the strong influence of crop rotation on soil microbial communities. This reduction could be attributed to a range of factors, including altered root exudation patterns (Figs. 2.4.1 and 2.4.2) which might result in shifts in nutrient availability (Ma *et al*., 2022), and modifications in microbial community composition (Sasse *et al*., 2018). The finding that the rhizosphere soil of W1 had a significantly higher growing microbial biomass compared to W3 supports the idea that different crop rotations can create distinct microbial habitats with varying nutrient dynamics (Li *et al*., 2021). Microbial communities in the rhizosphere soil serve as a bridge connecting plants and the soil, potentially mirroring soil nutrient conditions and exerting an impact on plant growth (Haldar and Sengupta, 2015) and might be affected by different factors like crop rotation (Qiao *et al*., 2019). Decreased growing microbial biomass in the rhizosphere of continuous wheat cultivation caused by decline in soil nutrient availability (Jiang *et al*., 2019) and decreased root exudation are the primary reasons for the challenges associated with consecutive cultivation (Li *et al*., 2021).

The GMB/TMB ratio, which indicates the proportion of actively growing microbial biomass relative to the total microbial biomass, exhibited notable changes due to crop rotation. The higher GMB/TMB ratio in W1, particularly in the rhizosphere soil (Fig. 2.4.4c), suggests that this rotation fostered a more favorable environment for microbial growth and activity (Zhang *et al*., 2022). The observed variations in GMB/TMB ratios might be indicative of shifts in microbial community structure and function, potentially driven by differences in nutrient availability and root exudates.

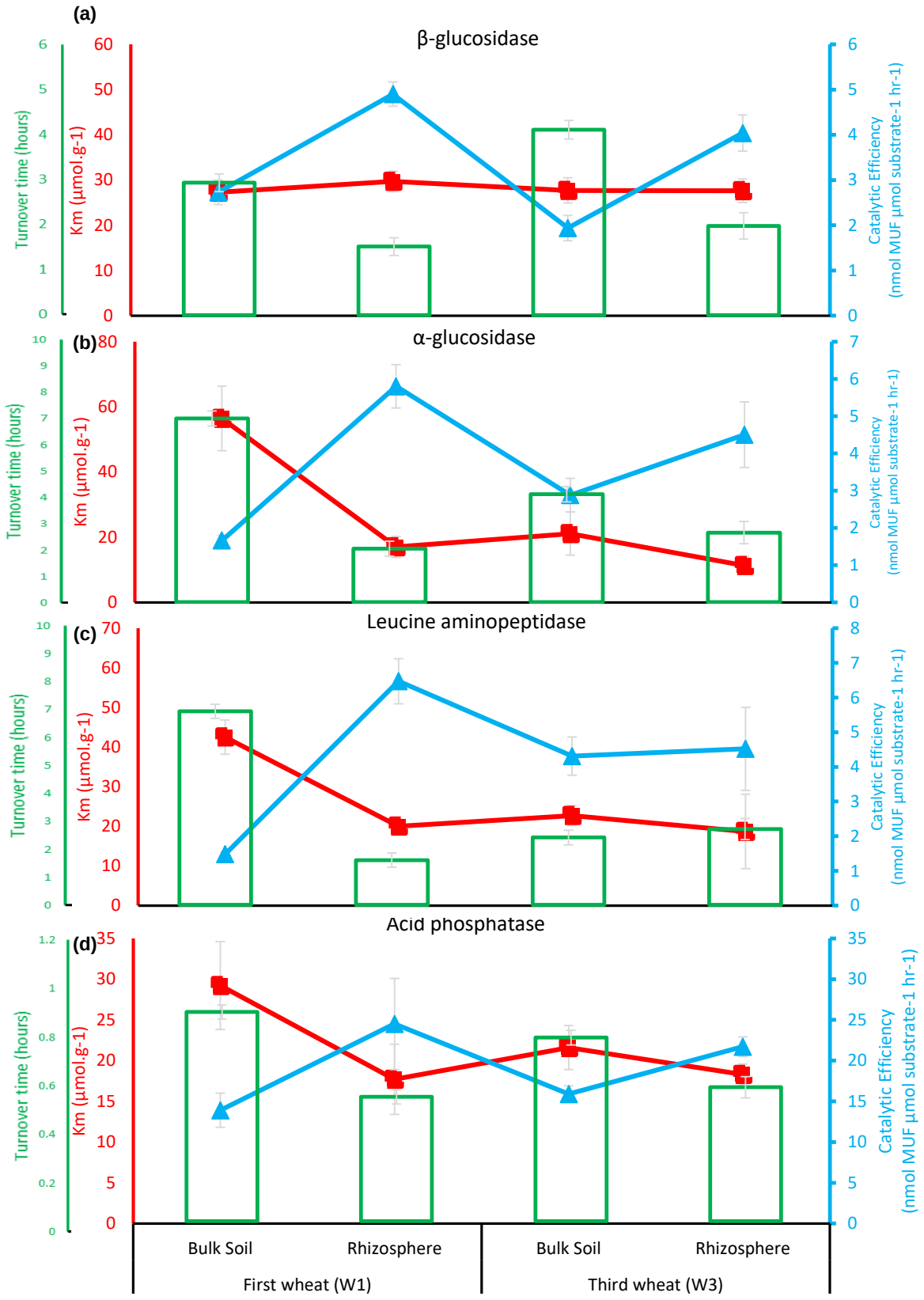

Figure 2.4.6. ***Km*** **values, catalytic efficiency and substrate turn over time of β-glucosidase (a), α-glucosidase (b), leucine aminopeptidase (c) and acid phosphatase (d) in different wheat soil compartments in the first (W1) and (W3) third wheat after break crop). Error bars represent standard error of means (n = 4).**

The results clearly demonstrate a shift in microbial communities towards less efficient microorganisms in W3 compared to W1, evident in both the rhizosphere and bulk soil compartments. This underscores the unique microbial reactions triggered by continuous wheat cultivation (Fig. 2.4.4d-f). The r- and K-strategist framework can be employed to explore soil bacterial ecology, enabling comprehension of bacterial interactions (Pascault *et al*., 2013; Pan *et al*., 2022). In ecosystems that have been disturbed, structures primarily influenced by r-strategists emerge, displaying traits associated with rapid growth. Conversely, in undisturbed and mature ecosystems, communities dominated by K-strategists prevail, characterized by their lower maximum-specific growth rates (Pianka, 1970). Alterations in the proportions of r- and K-strategists within microbial communities serve as valuable indicators of how soil microorganisms respond to stressors (Simonin *et al*., 2017). According to the findings illustrated in Fig. 2.4.4c, continuous wheat cultivation markedly diminished both the growing and active microbial biomass. These findings suggest that due to a decrease in glucose release (as observed in Figs. 2.4.1 and 2.4.2) and alterations in gene expression patterns within wheat roots and leaves (as depicted in Fig. 2.4.3), successive wheat cultivation practices fostered a harsh and unstable soil environment surrounding the roots. Given that soil microbes frequently face limitations in carbon availability (Soong *et al*., 2020), the reduced carbon supply resulting from diminished glucose release during continuous wheat cultivation could potentially contribute to a decline in the proliferation of growing microbial biomass (Singh *et al*., 2010), ultimately leading to an uncrowded environment with less competition. This circumstance may favor the predominance of opportunistic r-strategists, characterized by fast growth rates and low resource affinities, as highlighted in previous studies (Erbilgin *et al*., 2017; Yin *et al*., 2022). This is consistent with the observed trends in the catalytic efficiency of enzymes (as shown in Fig. 2.4.6), wherein these fast-growers can outcompete the slower-growing K-strategists (Blagodatskaya *et al*., 2009; Sun *et al*., 2021).

2.4.5.4. Enzyme kinetics is the lowest at T2 in both wheat crop rotations

Enzymes play a crucial role as essential agents that facilitate the breakdown of intricate organic compounds, allowing the release of nutrients and carbon, which are then made accessible for uptake by both plants and microbiomes. The enzymatic activities within the rhizosphere, root-affected, and bulk soil compartments of different wheat plant rotational positions unveil the intricate interplay between crop rotation and soil microbial functionality. The variations observed in maximum rate and catalytic efficiency values of extracellular enzymes reflect the diverse responses of microbial communities to changing growth conditions and nutrient availability. In all studied enzymes, rhizosphere soil had higher V_{max} in wheat rotational positions than bulk soil samples (Fig. 2.4.5). The elevated enzyme activity in the rhizosphere in comparison to other compartments is attributed not solely to microbial activity but also to the direct contribution of enzymes released by roots. This root-mediated influence encompasses root secretions composed of high molecular weight substances (>1000 Da), such as enzymes, or is a result of root cell lysis (Oburger and Jones, 2018). Roor exudates seem to play a key role in the effect of monoculture cultivation. Continuous wheat cultivation strongly decreased glucose release (Figs. 2.4.1 and 2.4.2) and also resulted in a substantial drop in growing microbial biomass and dominatcy of less efficient g microbial community (Fig. 2.4.4). Together, they influenced soil enzymatic activity and resulted in lower V_{max} for all enzymes compare to the first wheat after break crop (Fig. 2.4.5). Other studies also showed significantly lower soil microbial biomass in monoculture systems (McDaniel and Grandy, 2016) and strong impact of continuous cultivation on the richness and diversity of the soil microbial community. Decreased soil enzyme activities and efficiency have been reported by Dou *et al*. (2016) who investigated the impact of continuous cropping of sorghum, cotton and corn on soil enzyme activities after 26 years of cropping on alkaline phosphatase, and -d-glucosidase. Lower

enzyme activity and efficiency in continuous cropping from the first wheat after break crop might be due to the fact that most labile organic matter is lost and the limitation of diversity in the rates of residue production and their distribution across the soil profile (Wright *et al*., 2007; Nourbakhsh, 2007). All these in turn would negatively impact microbial functionality, reflected in the reduction of expression of different types of enzymes.

2.4.6. Conclusion

In summary, our study offers novel insights into the complex interplay between continuous wheat cultivation, root exudation patterns, microbial dynamics, gene expression, and enzymatic activities within the rhizosphere and bulk soil compartments. Notably, our research introduced a pioneering approach by conducting glucose imaging in the field setting for the first time, shedding light on the dynamics of glucose release from wheat roots. The decline in glucose release observed under continuous wheat cultivation (W3) compared to the first wheat after a break crop (W1) underscores the significance of root exudates in shaping rhizosphere interactions. This shift in glucose release could be linked to altered root physiology and exudation processes, potentially reflecting the plant's strategy to create a less favorable environment for potential pathogens. The differential expression of SWEET genes in wheat roots and leaves further adds to the novelty of our findings. The upregulation of SWEET1a orthologous genes in W3 roots suggests a demand for energy and carbon sources for nutrient uptake, while the downregulation of certain genes in leaves could indicate shifts in resource allocation strategies. The microbial responses we observed, including changes in microbial biomass, growth rates, and substrate utilization patterns, highlight the intricate microbial community dynamics influenced by continuous wheat cultivation. These shifts in microbial composition are mirrored in the altered enzymatic activities observed across different compartments.

Our study not only contributes to the understanding of how continuous wheat cultivation shapes plant-soil-microbe interactions but also introduces novel techniques, like *in situ* glucose imaging, to assess these interactions in the field. These insights carry implications for sustainable agricultural practices, nutrient cycling, and ecosystem health. By revealing the complex cascade of effects triggered by continuous cultivation, we provide valuable perspectives for optimizing management strategies and maintaining productive ecosystems in the face of evolving agricultural practices.

2.4.7. Acknowledgment

This study was carried out as part of the RhizoWheat project (Research program BonaRes) and received financial support from the BMBF. The authors express their gratitude to the German Federal Ministry of Education and Research (BMBF) for providing funding for this research (grant number 031B0910A).

2.4.8. Statements and Declarations

The authors declare that they have no known competing financial interests or personal relationships that could have appeared to influence the work reported in this paper.

2.4.9. References

Anjali A, Fatima U, Manu MS, Ramasamy S, Senthil-Kumar M. 2020. Structure and regulation of SWEET transporters in plants: an update. *Plant Physiology and Biochemstry* **156**: 1–6. https://doi.org/10.1016/j.plaphy.2020.08.043.

Arnhold J, Grunwald D, Braun-Kiewnick A, Koch HJ. 2023. Effect of crop rotational position and nitrogen supply on root development and yield formation of winter wheat. *Frontiers in Plant Science* **14**:1265994. doi:10.3389/fpls.2023.1265994.

Asai Y, Kobayashi Y. 2016. Increased Expression of the Tomato SISWEET15 Gene During Grey Mold Infection and the Possible Involvement of the Sugar Efflux to Apoplasm in the Disease Susceptibility. *Journal of Plant Pathology & Microbiology* **7(1)**: 1-8. https://doi.org/10.4172/2157-7471.1000329.

Awad YM, Blagodatskaya E, Ok YS, Kuzyakov Y. 2012. Effects of polyacrylamide, biopolymer, and biochar on decomposition of soil organic matter and plant residues as determined by 14C and enzyme activities. *European Journal of Soil Biology* **48**: 1-10. https://doi.org/https://doi.org/10.1016/j.ejsobi.2011.09.005.

Badri DV, Loyola-Vargas VM, Du J, Stermitz FR, Broeckling CD, Iglesias-Andreu L, Vivanco JM. 2008. Transcriptome analysis of Arabidopsis roots treated with signaling compounds: a focus on signal transduction, metabolic regulation and secretion. *New Phytologist* **179(1)**: 209-223. https://doi.org/https://doi.org/10.1111/j.1469-8137.2008.02458.x.

Bais HP, Weir TL, Perry LG, Gilroy S, Vivanco JM. 2006. The role of root exudates in rhizosphere interactions with plants and other organisms. *Annual Review of Plant Biology* **57**: 233–266. https://doi.org/10.1146/annurev.arplant.57.032905.105159.

Bakker P, Berendsen R, Doornbos R, Wintermans P, Pieterse C. 2013. The rhizosphere revisited: root microbiomics. *Frontiers in Plant Science* **4**:165. doi:10.3389/fpls.2013.00165.

Blagodatskaya EV, Blagodatsky SA, Anderson TH, Kuzyakov Y. 2009. Contrasting effects of glucose, living roots and maize straw on microbial growth kinetics and substrate availability in soil. *European Journal of Soil Science* **60(2)**: 186-197. https://doi.org/https://doi.org/10.1111/j.1365-2389.2008.01103.x.

Blagodatskaya E, Blagodatsky S, Anderson T H, Kuzyakov Y. 2014. Microbial growth and carbon use efficiency in the rhizosphere and root-free soil. *PLoS One* **9(4)**: e93282. https://doi.org/10.1371/journal.pone.0093282

Blagodatsky SA, Heinemeyer O, Richter J. 2000. Estimating the active and total soil microbial biomass by kinetic respiration analysis. *Biology and Fertility of Soils* **32(1)**: 73-81. https://doi.org/10.1007/s003740000219

Breia R, Conde A, Badim H, Fortes AM, Gerós H, Granell A. 2021. Plant SWEETs: from sugar transport to plant-pathogen interaction and more unexpected physiological roles. *Plant Physiology* **186(2)**: 836-852. doi: 10.1093/plphys/kiab127.

Canarini A, Kaiser C, Merchant A, Richter A, Wanek W. 2019. Root Exudation of Primary Metabolites: Mechanisms and Their Roles in Plant Responses to Environmental Stimuli [Review]. *Frontiers in Plant Science* **10**: 157. https://doi.org/10.3389/fpls.2019.00157.

Cesco S, Neumann G, Tomasi N, Pinton R, Weisskopf L. 2010. Release of plant-borne flavonoids into the rhizosphere and their role in plant nutrition. *Plant and Soil* **329(1)**: 1-25. https://doi.org/10.1007/s11104-009-0266-9.

Chandran D. 2015. Co-option of developmentally regulated plant SWEET transporters for pathogen nutrition and abiotic stress tolerance. *IUBMB Life*, **67(7)**: 461-471. https://doi.org/https://doi.org/10.1002/iub.1394.

Chaparro JM, Badri DV, Vivanco JM. 2014. Rhizosphere microbiome assemblage is affected by plant development. *The ISME Journal* **8(4)**: 790-803. https://doi.org/10.1038/ismej.2013.196.

Chen S, Wang L, Gao J, Zhao Y, Wang Y, Qi J, Peng Z, Chen B, Pan H, Wang Z, Gao H, Jiao S, Wei G. 2022. Agricultural Management Drive Bacterial Community Assembly in Different Compartments of Soybean Soil-Plant Continuum. *Frontiers in Microbiology* **13**: 868307. doi: 10.3389/fmicb.2022.868307.

Chen HY, Huh JH, Yu YC, Ho LH, Chen LQ, Tholl D, Frommer WB, Guo WJ. 2015. The Arabidopsis vacuolar sugar transporter SWEET2 limits carbon sequestration from roots and restricts Pythium infection. *The Plant Journal* **83(6)**: 1046-1058. https://doi.org/10.1111/tpj.12948.

Chen LQ, Hou BH, Lalonde S, Takanaga H, Hartung ML, Qu XQ, Guo WJ, Kim JG, Underwood W, Chaudhuri B, Chermak D, Antony G, White FF, Somerville SC, Mudgett MB, Frommer WB. 2010. Sugar transporters for intercellular exchange and nutrition of pathogens. *Nature* **468(7323)**: 527-532. https://doi.org/10.1038/nature09606.

Chen, LQ, Qu XQ, Hou BH, Sosso D, Osorio S, Fernie AR, Frommer WB. 2012. Sucrose Efflux Mediated by SWEET Proteins as a Key Step for Phloem Transport. *Science* **335(6065)**: 207-211. https://doi.org/10.1126/science.1213351.

Cohn M, Bart RS, Shybut M, Dahlbeck D, Gomez M Morbitzer R, Hou BH, Frommer WB, Lahaye T, Staskawicz BJ. 2014. *Xanthomonas axonopodis* Virulence Is Promoted by a Transcription Activator-Like Effector–Mediated Induction of a SWEET Sugar Transporter in Cassava. *Molecular Plant-Microbe Interactions* **27(11)**: 1186-1198. https://doi.org/10.1094/MPMI-06-14-0161-R.

Debaeke P, Aussenac T, Fabre JL, Hilaire A, Pujol B, Thuries L. 1996. Grain nitrogen content of winter bread wheat (*Triticum aestivum* L.) as related to crop management and to the previous crop. *European Journal of Agronomy* **5(3)**: 273-286. https://doi.org/https://doi.org/10.1016/S1161-0301(96)02038-2.

Dennis PG, Miller AJ, Hirsch PR. 2010. Are root exudates more important than other sources of rhizodeposits in structuring rhizosphere bacterial communities? *FEMS Microbiology Ecology* **72(3)**: 313-327. https://doi.org/10.1111/j.1574-6941.2010.00860.x.

Dorodnikov M, Blagodatskaya E, Blagodatsky S, Marhan S, Fangmeier A, Kuzyakov Y. 2009. Stimulation of microbial extracellular enzyme activities by elevated CO_2 depends on soil aggregate size. *Global Change Biology* **15(6)**:1603–14. https://doi.org/10.1111/j.1365-2486.2009.01844.x.

Dou F, Wright AL, Mylavarapu RS, Jiang X, Matocha JE. 2016. Soil enzyme activities and organic matter composition affected by 26 years of continuous cropping. *Pedosphere* **26**:618–625. https://doi.org/10.1016/S1002-0160(15)60070-4.

Eom JS, Chen LQ, Sosso D, Julius BT, Lin IW, Qu XQ, Braun DM, Frommer WB. 2015. SWEETs, transporters for intracellular and intercellular sugar translocation. *Current Opinion in Plant Biology* **25**: 53-62. https://doi.org/https://doi.org/10.1016/j.pbi.2015.04.005.

Erbilgin O, Bowen BP, Kosina SM, Jenkins S, Lau RK, Northen TR. 2017. Dynamic substrate preferences predict metabolic properties of a simple microbial consortium. *BMC bioinformatics* **18**: 1-12. https://doi.org/10.1186/s12859-017-1478-2.

Gan Y, Liang C, Chai Q, Lemke RL, Campbell CA, Zentner RP. 2014. Improving farming practices reduces the carbon footprint of spring wheat production. *Nature Communications* **5(1)**: 5012. https://doi.org/10.1038/ncomms6012.

German DP, Marcelo KRB, Stone, MM, Allison SD. 2012. The Michaelis–Menten kinetics of soil extracellular enzymes in response to temperature: a cross-latitudinal study. *Global Change Biology* **18(4)**: 1468-1479. https://doi.org/10.1111/j.1365-2486.2011.02615.x.

German DP, Weintraub MN, Grandy AS, Lauber CL, Rinkes ZL, Allison SD. 2011. Optimization of hydrolytic and oxidative enzyme methods for ecosystem studies. *Soil Biology and Biochemistry* **43(7)**: 1387-1397. https://doi.org/https://doi.org/10.1016/j.soilbio.2011.03.017.

Ghani MI, Ali A, Atif MJ, Pathan SI, Pietramellara G, Ali M, Amin B, Cheng Z. 2022. Diversified crop rotation improves continuous monocropping eggplant production by altering the soil microbial community and biochemical properties. *Plant and Soil* **480(1)**: 603-624. https://doi.org/10.1007/s11104-022-05606-y.

Grover M, Bodhankar S, Sharma A, Sharma P, Singh J, Nain L. 2021. PGPR mediated alterations in root traits: way toward sustainable crop production. *Frontiers in Sustainable Food Systems* **4**: 618230. https://doi.org/10.3389/fsufs.2020.618230.

Hage-Ahmed K, Moyses A, Voglgruber A, Hadacek F, Steinkellner S. 2013. Alterations in Root Exudation of Intercropped Tomato Mediated by the Arbuscular Mycorrhizal Fungus Glomus mosseae and the Soilborne Pathogen *Fusarium oxysporum* f.sp. lycopersici. *Journal of Phytopathology*. **161(11-12)**: 763-773. doi:https://doi.org/10.1111/jph.12130.

Haldar S, Sengupta S. 2015. Plant-microbe Cross-talk in the Rhizosphere: Insight and Biotechnological Potential. *The Open Microbiology Journal* **31(9)**:1-7. doi: 10.2174/1874285801509010001.

Hamel C, Gan Y, Messer D, Bainard LD. 2019. Soil 16S DNA sequence data and corresponding soil property and wheat yield data from a 72-plot field experiment involving pulses and wheat crops grown in rotations in the semiarid prairie. *Data in Brief* **23**: 103790. https://doi.org/10.1016/j.dib.2019.103790.

Ho LH, Klemens PAW, Neuhaus HE, Ko HY, Hsieh SY, Guo WJ. 2019. SlSWEET1a is involved in glucose import to young leaves in tomato plants. *Journal of Experimental Botany* **70(12)**:3241-3254. doi: 10.1093/jxb/erz154.

Hoang DTT, Rashtbari M, Anh LT, Wang S, Tu DT, Hiep NV, Razavi BS. 2022. Mutualistic interaction between arbuscular mycorrhiza fungi and soybean roots enhances drought resistant through regulating glucose exudation and rhizosphere expansion. *Soil Biology and Biochemistry* **171**: 108728. https://doi.org/https://doi.org/10.1016/j.soilbio.2022.108728

Hoang DT, Maranguit D, Kuzyakov Y, Razavi BS. 2020. Accelerated microbial activity, turnover and efficiency in the drilosphere is depth dependent. *Soil Biology and Biochemistry* **147**, 107852. https://doi.org/https://doi.org/10.1016/j.soilbio.2020.107852

Hu L, Robert CAM, Cadot S, Zhang X, Ye M, Li B, Manzo D, Chervet N, Steinger T, van der Heijden MGA, Schlaeppi K, Erb M. 2018. Root exudate metabolites drive plant-soil feedbacks on growth and defense by shaping the rhizosphere microbiota. *Nature Communications* **9(1)**: 2738. https://doi.org/10.1038/s41467-018-05122-7

Huang X, Liu H, Ma B. 2022. The Current Progresses in the Genes and Networks Regulating Cotton Plant Architecture. *Frontiers in Plant Science* **13**: 882583. doi: 10.3389/fpls.2022.882583.

Hütsch BW, Augustin J, Merbach W. 2002. Plant rhizodeposition — an important source for carbon turnover in soils. *Journal of Plant Nutrition and Soil Science* **165(4)**: 397-407. https://doi.org/10.1002/1522-2624(200208)165:4%3C397::AID-JPLN397%3E3.0.CO;2-C.

Jiang Y, Arafat Y, Letuma P, Ali L, Tayyab M, Waqas M, Li Y, Lin W, Lin S, Lin W. 2019. Restoration of long-term monoculture degraded tea orchard by green and goat manures applications system. *Sustainability* **11**: 1011. doi: 10.3390/su11041011.

Jones DL, Nguyen C, Finlay RD. 2009. Carbon flow in the rhizosphere: carbon trading at the soil–root interface. *Plant and Soil* **321(1)**: 5-33. https://doi.org/10.1007/s11104-009-9925-0.

Jones DL, Hodge A, Kuzyakov Y. 2004. Plant and mycorrhizal regulation of rhizodeposition. *New Phytologist* **163(3)**: 459-480. doi:10.1111/j.1469-8137.2004.01130.x.

Li M, Guo J, Ren T, Luo G, Shen Q, Lu J, Guo S, Ling N. 2021. Crop rotation history constrains soil biodiversity and multifunctionality relationships. *Agriculture, Ecosystems & Environment* **319**: 107550. https://doi.org/10.1016/j.agee.2021.107550.

Liu C, Song Y, Dong X, Wang X, Ma X, Zhao G, Zang S. 2021a. Soil Enzyme Activities and Their Relationships With Soil C, N, and P in Peatlands From Different Types of Permafrost Regions, Northeast China. *Frontiers in Environmental Science* **9**:670769. doi: 10.3389/fenvs.2021.670769.

Liu H, Li C, Qiao L, Hu L, Wang X, Wang J, Ruan X, Yang G, Yin G, Wang C, Sun Z, Ma K, Li L. 2021b. The Sugar Transporter family in wheat (*Triticum aestivum*. L): genome-wide identification, classification, and expression profiling during stress in seedlings. *PeerJ* **9**: e11371. https://doi.org/10.7717/peerj.11371.

Ma W, Tang S, Dengzeng Z, Zhang D, Zhang T, Ma X. 2022. Root exudates contribute to belowground ecosystem hotspots: A review. *Frontiers in Microbiology* **13**:937940. doi: 10.3389/fmicb.2022.937940.

Ma X, Zarebanadkouki M, Kuzyakov Y, Blagodatskaya E, Pausch J, Razavi BS. 2018. Spatial patterns of enzyme activities in the rhizosphere: Effects of root hairs and root radius. *Soil Biology and Biochemistry* **118**: 69-78. https://doi.org/10.1016/j.soilbio.2017.12.009.

Mazzola M. 2002. Mechanisms of natural soil suppressiveness to soilborne diseases. *Antonie Van Leeuwenhoek* **81**: 557–564. https://doi.org/10.1023/A:1020557523557.

McDaniel MD, Grandy AS. 2016. Soil microbial biomass and function are altered by 12 years of crop rotation. *Soil* **2**: 583–599, https://doi.org/10.5194/soil-2-583-2016.

Michaelis L, Menten ML. 1913. Die kinetik der invertinwirkung. *Biochemische Zeitschrift* **49**: 333-369.

Nourbakhsh F. 2007. Decoupling of soil biological properties by deforestation. *Agriculture, Ecosystems & Environment* **121(4)**: 435-438. https://doi.org/10.1016/j.agee.2006.11.010.

Nwachukwu BC, Ayangbenro AS, Babalola OO. Effects of soil properties and carbon substrates on bacterial diversity of two sunflower farms. *AMB Express* **12**: 47. https://doi.org/10.1186/s13568-022-01388-9.

Oburger E, Jones DL. 2018. Sampling root exudates – Mission impossible? *Rhizosphere* **6**: 116-133. https://doi.org/https://doi.org/10.1016/j.rhisph.2018.06.004.

Pan Y, Kang P, Tan M, Hu J, Zhang Y, Zhang J, Song N, Li X. 2022. Root exudates and rhizosphere soil bacterial relationships of *Nitraria tangutorum* are linked to k-strategists' bacterial community under salt stress. *Frontiers in Plant Science* **13**:997292. doi: 10.3389/fpls.2022.997292.

Panikov NS. 1991. Kinetics, Microbial Growth. In: Flickinger, M. C. and Drew, S. W., Eds. Encyclopedia of Bioprocess Technology: Fermentation, Biocatalysts and Bioseparation. New York: John Wiley & Sons, Inc., 1513-1543.

Panikov NS, Sizova MV. 1996. A kinetic method for estimating the biomass of microbial functional groups in soil. *Journal of Microbiological Methods* **24(3)**: 219-230. https://doi.org/10.1016/0167-7012(95)00074-7 .

Panikov, N. S., Blagodatsky, S. A., Blagodatskaya, J. V., & Glagolev, M. V. (1992). Determination of microbial mineralization activity in soil by modified Wright and Hobbie method. Biology and Fertility of Soils, 14(4), 280-287. https://doi.org/10.1007/BF00395464

Pascault N., Ranjard L., Kaisermann A., Bachar D., Christen R., Terrat S., *et al*.. (2013). Stimulation of different functional groups of bacteria by various plant residues as a driver of soil priming effect. *Ecosystems* 16, 810–822. doi: 10.1007/s10021-013-9650-7

Paulsen, P. A., Custódio, T. F., & Pedersen, B. P. (2019). Crystal structure of the plant symporter STP10 illuminates sugar uptake mechanism in monosaccharide transporter superfamily. Nature Communications, 10(1), 407. https://doi.org/10.1038/s41467-018-08176-9

Pianka, E. R. (1970). On r and K selection. *American Naturalist, 102*, 592–597.

Qiao, C., Penton, C., Xiong, W., Liu, C., Wang, R., Liu, Z., Xu, X., Li, R., & Shen, Q. (2019). Reshaping the rhizosphere microbiome by bio-organic amendment to enhance crop yield in a maize-cabbage rotation system. *Applied Soil Ecology*, *142*, 136-146. https://doi.org/10.1016/j.apsoil.2019.04.014

Razavi, B. S., Zhang, X., Bilyera, N., Guber, A., & Zarebanadkouki, M. (2019). Soil zymography: Simple and reliable? Review of current knowledge and optimization of the method. Rhizosphere, 11, 100161. https://doi.org/https://doi.org/10.1016/j.rhisph.2019.100161

Razavi, B.S., Blogdatskaya, E., Kuzyakov, Y. 2016a. Temperature selects for static soil enzyme systems to maintain high catalytic efficiency. Soil Biology and Biochemistry. 97: 15-22. http://dx.doi.org/10.1016/j.soilbio.2016.02.018.

Razavi, B.S., Zarebanadkouki, M., Blogdatskaya, E., Kuzyakov, Y. 2016b. Rhizosphere shape of lentil and maize: Spatial distribution of enzyme activities. Soil Biology and Biochemistry. 96: 229-237. http://dx.doi.org/10.1016/j.soilbio.2016.02.020.

Sasse, J., Martinoia, E., & Northen, T. (2018). Feed Your Friends: Do Plant Exudates Shape the Root Microbiome? Trends in Plant Science, 23(1), 25-41. https://doi.org/https://doi.org/10.1016/j.tplants.2017.09.003

Sasse, J., Martinoia, E., and Northen, T. (2018). Feed your friends: do plant exudates shape the root microbiome? *Trends Plant Sci.* 23, 25–41. doi: 10.1016/j.tplants.2017.09.003

Sieling, K., Stahl, C., Winkelmann, C., & Christen, O. (2005). Growth and yield of winter wheat in the first 3 years of a monoculture under varying N fertilization in NW Germany. European Journal of Agronomy, 22(1), 71-84. https://doi.org/https://doi.org/10.1016/j.eja.2003.12.004

Simonin, M., Nunan, N., Bloor, J. M. G., Pouteau, V., & Niboyet, A. (2017). Short-term responses and resistance of soil microbial community structure to elevated CO2 and N addition in grassland mesocosms. *FEMS Microbiology Letters*, **364**, fnx077. https://doi.org/10.1093/femsle/fnx077

Singh, B. K., Bardgett, R. D., Smith, P., & Reay, D. S. (2010). Microorganisms and climate change: Terrestrial feedbacks and mitigation options. *Nature Reviews Microbiology*, **8**, 779–790. https://doi.org/10.1038/nrmicro2439

Soong JL, Fuchslueger L, Marañon-Jimenez S, Torn MS, Janssens IA, Penuelas J, Richter A. Microbial carbon limitation: The need for integrating microorganisms into our understanding of ecosystem carbon cycling. Glob Chang Biol. 2020 Apr;26(4):1953-1961. doi: 10.1111/gcb.14962.

Sun, Y, Wang, C, Yang, J, Liao, J, Chen, HYH, Ruan, H. Elevated CO_2 shifts soil microbial communities from *K*- to *r*-strategists. *Global Ecol Biogeogr*. 2021; 30: 961–972. https://doi.org/10.1111/geb.13281.

Vetterlein D, Carminati A, Kögel-Knabner I, Bienert GP, Smalla K, Oburger E, Schnepf A, Banitz T, Tarkka MT and Schlüter S (2020) Rhizosphere Spatiotemporal Organization–A Key to Rhizosphere Functions. Front. Agron. 2:8. doi: 10.3389/fagro.2020.00008.

Wen, Z., White, P.J., Shen, J. and Lambers, H. (2022), Linking root exudation to belowground economic traits for resource acquisition. New Phytol, 233: 1620-1635. https://doi.org/10.1111/nph.17854

Woźniak, A. (2019). Effect of Crop Rotation and Cereal Monoculture on the Yield and Quality of Winter Wheat Grain and on Crop Infestation with Weeds and Soil Properties. International Journal of Plant Production, 13(3), 177-182. https://doi.org/10.1007/s42106-019-00044-w

Wright, A.L., Dou, F., Hons, F.M. 2007. Soil organic C and N distribution for wheat cropping systems after 20 years of conservation tillage in central Texas. Agriculture, Ecosystems & Environment. 121(4): 376-382. https://doi.org/10.1016/j.agee.2006.11.011

Xie H, Wang D, Qin Y, Ma A, Fu J, Qin Y, Hu G, Zhao J (2019) Genome-wide identification and expression analysis of SWEET gene family in *Litchi chinensis* reveal the involvement of *LcSWEET2a/3b* in early seed development. BMC Plant Biol **19**: 499.
Yang, N. J., & Hinner, M. J. (2015). Getting Across the Cell Membrane: An Overview for Small Molecules, Peptides, and Proteins. In A. Gautier & M. J. Hinner (Eds.), Site-Specific Protein Labeling: Methods and Protocols (pp. 29-53). Springer New York. https://doi.org/10.1007/978-1-4939-2272-7_3
Yin, Q., Sun, Y., Li, B., Feng, Z., Wu, G. 2022. The r/K selection theory and its application in biological wastewater treatment processes. Science of The Total Environment. 824: 153836. https://doi.org/10.1016/j.scitotenv.2022.153836.
Zhalnina, K., Louie, K. B., Hao, Z., Mansoori, N., da Rocha, U. N., Shi, S., Cho, H., Karaoz, U., Loqué, D., Bowen, B. P., Firestone, M. K., Northen, T. R., & Brodie, E. L. (2018). Dynamic root exudate chemistry and microbial substrate preferences drive patterns in rhizosphere microbial community assembly. Nature Microbiology, 3(4), 470-480. https://doi.org/10.1038/s41564-018-0129-3
Zhang J, Shuang S, Zhang L, Xie S and Chen J (2021) Photosynthetic and Photoprotective Responses to Steady-State and Fluctuating Light in the Shade-Demanding Crop *Amorphophallus xiei* Grown in Intercropping and Monoculture Systems. *Front. Plant Sci.* 12:663473. doi: 10.3389/fpls.2021.663473
Zhang Y, Wang J, Yang J, Li Y, Zhang W, Liu S, Yang G, Yan Z, Liu Y. Microwave-Assisted Enzymatic Extraction, Partial Characterization, and Antioxidant Potential of Polysaccharides from Sagittaria trifolia Tuber. Chem Biodivers. 2022 Aug;19(8):e202200219. doi: 10.1002/cbdv.202200219.
Zhang, X., Dippold, M. A., Kuzyakov, Y., & Razavi, B. S. (2019). Spatial pattern of enzyme activities depends on root exudate composition. Soil Biology and Biochemistry, 133, 83-93. https://doi.org/https://doi.org/10.1016/j.soilbio.2019.02.010
Zhang, X., Kuzyakov Y, Zang H, Dippold MA, Shi L, Spielvogel S, Razavi BS. 2020. Rhizosphere hotspots: root hairs and warming control microbial efficiency, carbon utilization and energy production. *Soil Biology and Biochemistry* **148**: 107872. https://doi.org/10.1016/j.soilbio.2020.107872
Zhao, M., Zhao, J., Yuan, J., Hale, L., Wen, T., Huang, Q., Vivanco, J. M., Zhou, J., Kowalchuk, G. A., & Shen, Q. (2021). Root exudates drive soil-microbe-nutrient feedbacks in response to plant growth [https://doi.org/10.1111/pce.13928]. Plant, Cell & Environment, 44(2), 613-628. https://doi.org/https://doi.org/10.1111/pce.13928
Zhou, M., Diwu, Z., Panchuk-Voloshina, N., & Haugland, R. P. (1997). A stable nonfluorescent derivative of resorufin for the fluorometric determination of trace hydrogen peroxide: applications in detecting the activity of phagocyte NADPH oxidase and other oxidases. Anal Biochem, 253(2), 162-168. https://doi.org/10.1006/abio.1997.2391

2.4.10. Supplementary table

Table S2.4.1- Primer used in this study

Name	Forward primer	Reverse primer	Product length
TaeSWEET1a	CGTCTTCTCCATCTGCATGTAC	GATGGCGTAGAGGATGAGCT	220bp
GADPH	CCTTCCGTGTTCCCACTGTTG	ATGCCCTTGAGGTTTCCCTC	124bp

2.5. Study 5: Different Crop Rotation Scenarios Affected Enzyme Kinetics Pattern in a Loess Soil

Mehdi Rashtbari[1], Jessica Arnhold[2], Dennis Grunwald[2], Heinz-Josef Koch[2], Bahar S. Razavi[1]

[1]Department of Soil and Plant Microbiome, Institute of Phytopathology, University of Kiel, Germany;
[2]Department of Agronomy, Institute of Sugar Beet Research, Göttingen, Germany

***** *corresponding author: mehdi.rashtbari@phytomed.uni-kiel.de*

Status: In preparation

2.5.1. Abstract

Continuous wheat cultivation leads to crop productivity decrease. Soil carbon availability is one of the main determinants of microbial activity and temporal variation in carbon inputs results in change in the microbial activity and functionality. Therefore, this study aims to elucidate and quantify the effects of the first and second wheat after break crop and long-term wheat monoculture, on soil enzymatic activity and microbial growth. We hypothesized that the long-term wheat rotation leads to the production of less efficient enzymes accompanied by the decline of enzyme production. We performed spatial sampling in frame of a field study at the experimental farm Harste, (IFZ, Göttingen). A soil sampling from rhizosphere (RH), and bulk soil (BS), at two sampling times, BBCH 29 (end of tillering) and BBCH 69-71 (the flowering stage) as 1st (W1) and 2nd (W2) wheat after break crop and wheat monoculture (WM) was performed. The kinetic parameters of enzymes involved in C, N and P cycles and also microbial growth kinetics were determined. Results showed there was considerable decrease in V_{max} in WM compared to W1 and W2 in RH and RA compartments for β-glucosidase and in RA for LAP. The highest decrease in wheat monoculture compared to the W1 was observed in RH by ~34 % for β-glucosidase and 26.2 % in BS for β-glucosidase. The substrate affinity (K_m) for β-glucosidase in BS and RA strongly decreased in WM compared to W1 and W2, while in RH a 38 and 18.6 % increase was observed in W2 and WM compared to W1, respectively. the bulk soil exhibited a higher total microbial biomass than the rhizosphere soil at t1 in WM and t2 in W1 and WM. at t2, W2 and WM had significantly higher μ compared to W1 in the bulk soil (an increase of 21.6% and 14.7%, respectively). The general trend of catalytic efficiency demonstrated a gradual decrease with wheat rotation as a function of distance from root to bulk soil. Overall results showed that RH compartment had the highest enzyme activity and there was a downward trend from rhizosphere to bulk soil compartments for enzyme activities. We concluded that continuous cultivation of wheat suppressed microbial activity and functional efficiency and not only resulted to lower enzyme activity, but also led to production of less efficient enzymes.

Keywords: biomass, efficiency, enzymes, function, growth, monoculture

2.5.2. Introduction

Soils constitute a diverse habitat characterized by an intricate amalgamation of minerals, organic matter, and a complex network of water- and air-filled pore spaces (Joos and De Tender, 2022). This environment serves as the dwelling place for a rich abundance and diversity of organisms, pivotal in executing fundamental soil processes and functions. Among these processes, the primary contributors are the microorganisms inhabiting both the bulk soil and the rhizosphere (the region surrounding plant roots) (Philippot et al., 2013). Accounting

for as much as 95% of total soil biomass (van Leeuwen et al., 2017), soil microbes, despite their relatively low presence in the soil matrix, wield substantial influence over sustainable crop productivity and play essential roles in soil ecosystems. They govern crucial activities such as nutrient cycling, organic matter decomposition, and the preservation of soil fertility (Wu et al., 2024). Concurrently, soil microbes significantly contribute to the regulation of soil-borne diseases affecting crops. The inhibition of pathogen infection in roots arises from intricate interactions with other soil microorganisms (Duran et al., 2017), often manifested through the production of inhibitory secondary metabolites and enzymes (Garbeva et al., 2011; Meisner and de Boer, 2018). This dual role underscores the multifaceted importance of soil microorganisms, not only as drivers of essential soil processes but also as key players in the protection and health maintenance of agricultural systems.

Enzymes within the soil matrix play a pivotal role in upholding the quality, functional diversity, and nutrient cycling of ecosystems (Kandeler et al., 1999; Liu et al., 2021). Primarily of microbial origin, these enzymes are also secreted by plant roots and soil fauna, contributing to the complex biochemical landscape of the soil environment (Telesiński et al., 2021). With their elevated catalytic capacity, soil enzymes regulate essential reactions in soils, governing microbial cycles, stabilizing soil structure, facilitating the formation of soil organic matter (SOM), and driving nutrient cycling (Mir et al., 2023; Erdel et al., 2023). A consensus among researchers underscores the significance of enzyme activity as the most sensitive indicator of soil ecochemical status. This heightened sensitivity arises from the integral role enzymes play in all microbiological reactions, encompassing the cycles of soil nutrients, and their rapid response to changes induced by natural or anthropogenic factors (Antonious et al., 2020; Telesiński et al., 2019). Consequently, the assessment of enzyme activities emerges as a reliable and robust indicator for discerning the extent of soil deterioration attributable to various environmental attributes and anthropogenic factors (Rao et al., 2014). This emphasis on enzyme activity underscores its potential as a valuable metric for evaluating the impact of diverse stressors on soil health and ecosystem functionality.

Monocropping, the recurrent cultivation of the same crop over successive years, has become a prevalent practice in intensive and large-scale agriculture (Tilman et al., 2011). This continuous cultivation approach has been associated with various soil challenges, including the disruption of soil microbial communities, degradation of soil properties, and a decline in soil enzyme activity (She et al., 2017; Yu et al., 2024). Extensive research has demonstrated the profound impact of different cropping systems on the structure of the soil microbial community (Rao et al., 2021). Earlier researches has underscored the significant impact of various cropping systems on the structure of the soil microbial community (Li et al., 2021). Specifically, investigations have revealed substantial alterations in both composition and function of the soil bacterial community due to the introduction of break crop in a prolonged continuous cropping system (Rao et al., 2021; Sun et al., 2023). Notably, soils characterized by higher ratios of bacteria to fungi exhibited more resilient bacterial structures and demonstrated increased resistance to soil-borne diseases (Liu et al., 2015). This emphasizes the intricate relationship between soil microbial composition, cropping practices, and their consequences for soil health and disease resistance. Following continuous monocropping, a notable shift from bacterial to fungal dominance occurs, with the abundance and diversity of the fungal community showing a negative correlation with soil health (Han et al., 2010). The ramifications of such shifts extend to plant health, as exemplified by studies on continuous peanut cropping, where the abundance of beneficial *Burkholderiales* and *Pseudomonadales* decreases while detrimental *Fusarium solani* and *Fusarium oxysporum* increase, ultimately impacting crop yield negatively (Chen et al., 2020). Similar trends have been observed in the continuous cropping of buckwheat, where the accumulation of detrimental microorganisms further underscores the challenges associated with prolonged monocropping practices (Yu et al., 2024; Wang et al., 2019).

Moreover, continuous cropping systems exert broader effects on soil properties and enzyme activity, influencing the structure of rhizosphere microbial communities (Song et al., 2018 Zhou et al., 2018). The imbalance in the soil microbial community emerges as a pivotal issue leading to obstacles in continuous cropping and subsequent reductions in crop yields (Li et al., 2022). Understanding and mitigating the complex interactions within soil ecosystems under monocropping scenarios are critical for sustainable agricultural practices and long-term soil health management.

Meier et al. (2021) highlighted that rhizosphere microbiomes exhibit responsiveness to host species. Simultaneously, various cropping systems have been identified to influence microbial species and the relative abundances of soil-enriched microorganisms (Castle et al., 2021) and therefore their functions. Therefore, the comprehensive analysis of soil microbial properties and enzyme activity stands as a crucial avenue for investigating the consequences of land conversions and prioritizing scientifically informed soil management practices. Therefore, in the present study, we aimed to investigate and quantify the effects of different wheat rotational positions including the first (W1) and second (W2) winter wheat (*Tritium aestivum*) after break crop of winter oilseed rape and a long-term winter wheat monoculture of 18 years on microbial growth and different enzymes kinetics involved in carbon (C), nitrogen (N) and phosphorous (P) cycles. We hypothesize that: i) wheat monoculture and continuous wheat cultivation leads to lower microbial growth, activity, and biomass; ii) a decrease in microbial growth and biomass in wheat monoculture will be accompanied by a decline in enzyme production and efficiency.

2.5.3. Materials and Methods

2.5.3.1. Soil description and experimental setup

A field experiment was conducted at the field site is located near Harste (51°36′23.5″N, 9°51′55.8″E), in Central Germany. The soil type is a silty loam Luvisol derived from Loess (IUSS Working Group WRB, 2015). Long-term (1991–2020) mean annual precipitation is 624 mm and mean annual temperature is 9.4°C (DWD, 2022; Arnhold et al., 2023).

Soil samples for enzyme and microbial growth kinetics were taken from the Ap horizon (0-20 cm) from three distinct wheat rotational positions: the first wheat position (referred to as W1), represented the first wheat cultivation after the break crop of winter oilseed rape, and the subsequent second wheat (wheat grown continuously for two years referred to as W3) addressing the continuous cultivation of wheat two years in a row following the same break crop in 2022 and a long-term wheat monoculture of 18 years. The details on the crop rotational trials and wheat rotational positions are described in Arnhold et al. (2023).

2.5.3.2. Soil sampling

After uprooting the plants, loosely adhered root soil was removed by vigorously shaking the total root mass collected from field at BBCH 28 (end of tillering) BBCH 69-71 (flowering stage). After this procedure, the roots still had a layer of soil attached to them (rhizosphere, or RH). The complete root system was placed on a sterile surface, and the RH soil was gently brushed off the root surface with a sterile toothbrush (Hamel et al., 2019). Bulk soil (without roots) was also collected in a conical tube and stored at 5 °C, in the same way as RA and RH. The details on sampling scheme are described in Giongo et al. (2023).

2.5.3.3. Kinetics of the substrate-induced respiration

Total and active microbial biomass was characterized by Substrate Induced Growth Respiration (SIGR) (Blagodatskaya et al., 2014). Accordingly, 0.5 g fresh soil was amended with a mixture of glucose (10 mg g^{-1}) and mineral salts (1.9 mg g^{-1} $(NH_4)_2SO_4$, 2.25 mg g K_2HPO_4 and 3.8 mg g^{-1} $MgSO_4.7H_2O$) in order to induce unlimited growth. There were samples amended with

distilled water as a control. Soil samples were incubated in the modified rapid automated bacterial impedance technique (RABIT) system (Don Whitley Scientific, UK) at 25°C, and the CO_2 production rate was monitored every six minutes. Equation (3) was used to estimate the specific growth rate (μ) of soil microorganisms:

$$CO_2 = A + B \times \exp(\mu t) \quad (3)$$

Where A is the initial respiration rate uncoupled from ATP production, B is the initial rate of couple (growth) respiration, and t is the time (Blagodatsky et al., 2000). The total microbial biomass (TMB) and growing microbial biomass (GMB) at time zero were given by Eqs. (4) and (5):

$$TMB = \frac{B}{r_0 Q} \quad (4)$$

$$GMB = TMB \times r_0 \quad (5)$$

where r_0 is the physiological state index of the microbial biomass (MB) before substrate addition and was calculated according to Eq. (6):

$$r_0 = \frac{B(\lambda-1)}{A+B(\lambda-1)} \quad (6)$$

where λ = 0.9, which has been accepted as a basic stoichiometric constant (Panikov & Sizova, 1996). Q is the total specific respiration activity:

$$Q = \frac{\mu}{\lambda Y CO_2} \quad (7)$$

YCO_2 is the microbial yield per unit of glucose-C consumed, which was assumed to be a mean value of 0.6 (Panikov & Sizova, 1996). The theory of microbial growth kinetics has been presented in detail earlier (Panikov, 1991).

The duration of the lag period (t_{lag}) was determined as the time interval between the glucose addition and the moment when the increasing rate of growth-related respiration becomes as high as the rate of respiration uncoupled from ATP generation. It was calculated by using the parameters of the approximated curve of the respiration rate of microorganisms with the equation (8) (Blagodatskaya et al., 2009);

$$T_{lag} = \frac{ln(A/B)}{\mu_m} \quad (8)$$

In addition, the kinetic approach allowed the assessment of generation time (T_g) of both actively growing and total microbial populations consuming glucose. The estimation of T_g for actively growing biomass is based on specific growth rates, i.e.:

$$T_g = \frac{ln(2)}{\mu_m} \quad (9)$$

2.5.3.4. Enzyme kinetics, substrate affinity, and catalytic efficiency

The kinetics of hydrolytic enzymes involved in C, N, and P cycles were measured by fluorimetric microplate assays of 4-methylumbelliferone (MUF) and 7-amino-4-methyl coumarin (AMC) (Dorodnikov et al., 2009). Three types of fluorogenic substrates based on MUF and one type based on AMC were used to assess enzymatic activities; 4-methylumbelliferyl-β-D-glucoside to detect β-glucosidase activity, 4-methylumbelliferyl-α-D-glucoside to detect α-glucosidase activity, 4-methylumbelliferylphosphate to detect acid phosphomonoesterase activity, and L-Leucine-7-amino-4-methylcoumarin to detect leucine aminopeptidase activity. All substrates and chemicals were purchased from Sigma (Germany). According to (German et al., 2011), 1.0 g of soil was suspended in 50 mL distilled water, of which 50 µL aliquots were pipetted into labeled wells of a 96-well microplate (Thermo Fisher, Denmark). Then, 50 µL buffer (MES/Trizma) and 100 µL respective substrate solution were added to each well. The activity of enzymes was measured at three-time points: 30, 60, and 120 min using CLARIOstar plus (BMG LABTECH, Germany) at an excitation wavelength of 355 nm and an emission wavelength of 460 nm. We determined enzyme activities over a range

of substrate concentrations from low to high (0, 20, 40, 60, 80, 100, 200, and 400 µmol g^{-1} soil) to ensure the appropriate saturating concentration.

Enzyme activities (V_{max}) were denoted as released MUF/AMC in nmol per g dry soil per hour (nmol MUF/AMC g^{-1} soil h^{-1}) (Awad et al., 2012) and affinity constant for each enzyme (K_m) expressed in µmol substrate per g dry soil (µmol g^{-1} soil). Simultaneously, MUF/AMC concentrations of 0, 10, 20, 30, 40, 50, 100, and 200 nM were prepared to calibrate the measurement. The Michaelis-Menten equation (Michaelis-Menten, 1913) was used to determine the parameters of the activity of the enzyme (V):

$$V = \frac{V_{max}[S]}{K_m + [S]} \quad (1)$$

where V_{max} is the maximum enzyme activity (a function of enzyme concentration), S is the substrate concentration, and K_m is the substrate concentration at half-maximal enzyme activity. Both V_{max} and K_m parameters were approximated by the Michaelis-Menten equation (1) with the non-linear regression routine of SigmaPlot (v. 12.3). Catalytic efficiency was calculated as the V_{max}-to-K_m ratio (Panikov et al., 1992). The substrate turnover rate was calculated by equation (2), where T_t is the turnover time (hours) (Hoang et al., 2020).

$$T_t = \frac{K_m \times [S]}{V_{max} + [S]} \quad (2)$$

2.5.5. Data analysis

All the statistical analyses were performed in SAS v9.2. Significant differences in enzyme activities, substrate affinity, catalytic efficiency, substrate turnover time, and substrate-induced growth respiration kinetics parameters between W1, W2 and WM soil samples were confirmed by Two-Way ANOVA after checking normality and homogeneity of variance values. A probability of $p < 0.05$ was used as the significance level between treatment comparisons. Error bars indicate the standard error of the means.

2.5.6. Results

2.5.6.1. Microbial growth kinetics

At t1, different wheat rotational positions had a substantial impact on the total microbial biomass in the rhizosphere compartment, with a 42.5% and 42.8% decrease in WM compared to W2 and W1, respectively. Notably, the bulk soil exhibited a higher total microbial biomass than the rhizosphere soil at t1 in WM and t2 in W1 and WM (Fig. 2.5.1a). The trend in growing microbial biomass varied at both t1 and t2. In both sampling times, the rhizosphere soil showed significantly higher growing microbial biomass compared to the bulk soil. While wheat monoculture significantly increased growing microbial biomass at t1, by t2, the rhizosphere soil of W1 exhibited approximately 2.5 times higher growth compared to WM. Crop rotations did not have a significant effect on growing microbial biomass in the bulk soil compartment (Fig. 2.5.1b).

The GMB/TMB ratio was strongly influenced by crop rotation at t1, with WM having higher ratios in both rhizosphere and bulk soil (0.08 and 0.002, respectively). Although W1 had the highest ratio at t2 in both bulk and rhizosphere soil compartments, there was no significant difference between wheat rotational positions (Fig. 2.5.1c). Specific growth rates (µ) considerably decreased in WM in the rhizosphere compartment compared to W1 at t1 (0.22 and 0.27 h^{-1}). There were no significant differences in specific growth rates among wheat rotational positions in bulk soil samples at t1. The decreasing trend in rhizosphere soil persisted at t2 with no strong difference between wheat rotational positions. However, at t2, W2 and WM had significantly higher µ compared to W1 in the bulk soil (an increase of 21.6% and 14.7%, respectively, Fig. 2.5.1d).

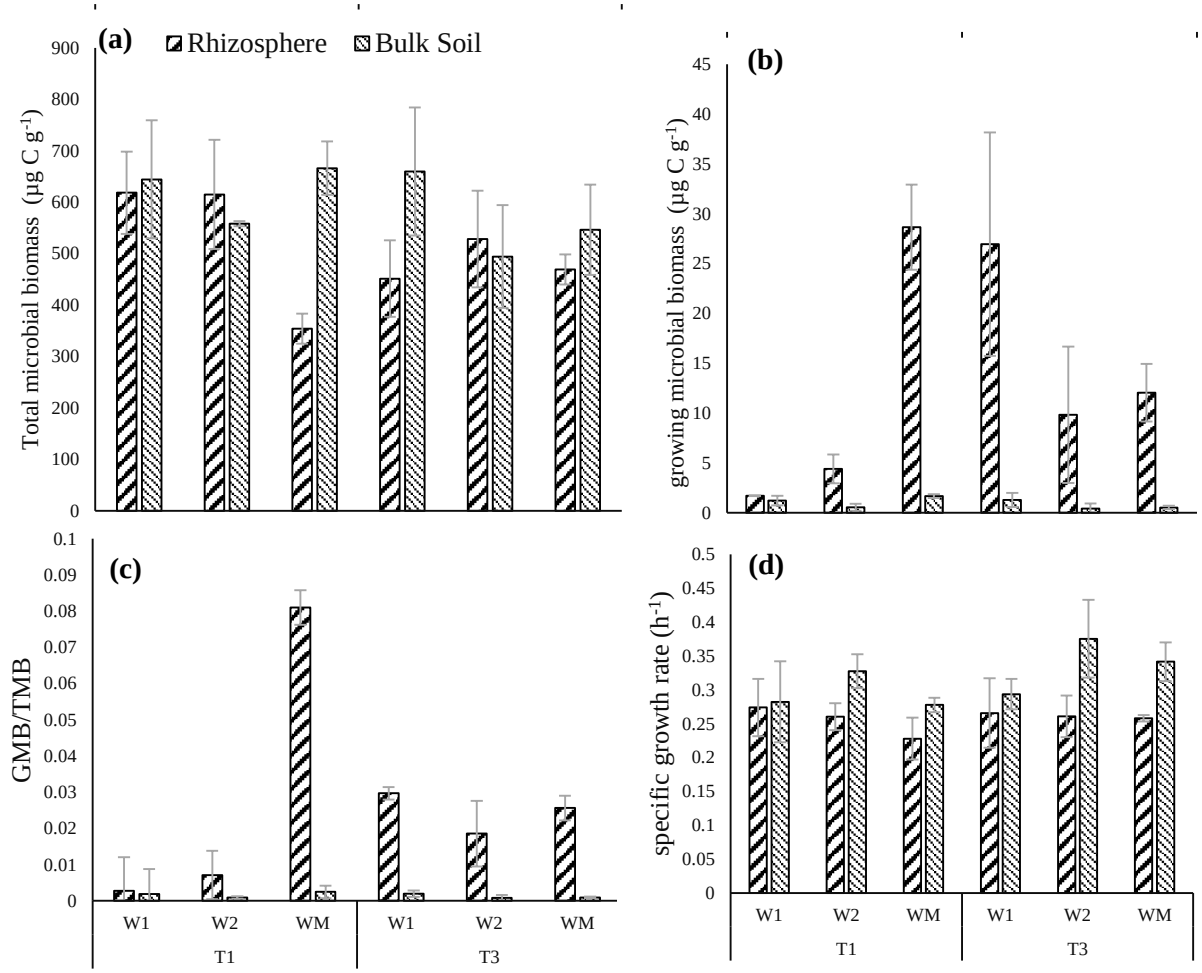

Figure 2.5.1. Total microbial biomass (TMB) (a), actively growing microbial biomass (GMB) (b), the ration of GMB/TMB (c) and Specific growth rates (µ) of soil microorganisms (d) in different wheat soil compartments (BS: bulk soil, RH: rhizosphere) in the first (W1), second (W2) winter wheat after oilseed rape break crop and long-term wheat monoculture (WM) at two sampling times, T1 (BBCH 29) and T2 (BBCH 59). Error bars represent standard error of means (n = 3) according to ANOVA at p<0.05.

A reverse trend was observed in the lag time of soil microbial biomass between t1 and t2. At t1, there was a decreasing trend from W1 to W2 and WM, with wheat monoculture significantly reducing lag time (10.43, 5.85, and 0.16 hours, respectively). However, at t2, we observed an increasing trend, and WM exhibited about four times longer lag period compared to W1 in the rhizosphere soil. No significant differences were found between wheat rotational positions in the bulk soil compartment (Fig. 2.5.2a). The generation time of the actively growing microbial community, consuming substrate during soil incubation with glucose and nutrients, declined by 14.3% in WM compared to W1 in both rhizosphere and bulk soil at t2. The difference in generation time between W1 and WM was negligible at t1 (Fig. 2.52b).

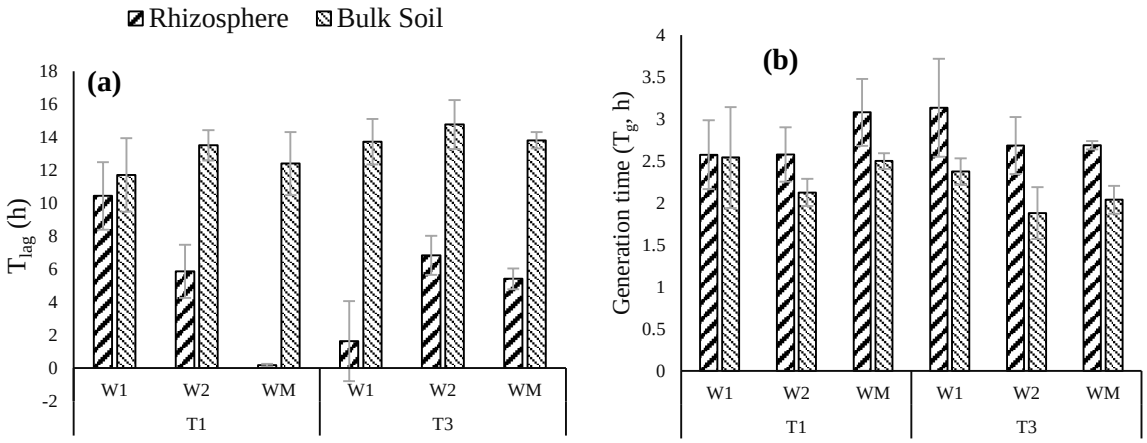

Figure 2.5.2. the lag time of soil microbial biomass (T_{lag}) (a), their generation time (T_g) (b), in different wheat soil compartments (BS: bulk soil, RH: rhizosphere) in the first (W1), second (W2) winter wheat after oilseed rape break crop and long-term wheat monoculture (WM) at two sampling times, T1 (BBCH 29) and T2 (BBCH 59). Error bars represent standard error of means (n = 3) according to ANOVA at p<0.05.

2.5.6.2. Enzyme kinetics

Wheat plant rotational positions significantly influenced the maximum rate (V_{max}) of extracellular enzymes in the rhizosphere, root-affected, and bulk soil (p<0.01; Fig. 2.5.3). In terms of α-glucosidase activity at t1, continuous wheat cultivation markedly increased the enzyme activity in all sampling compartments. However, a reverse trend was observed at t2, with WM showing the lowest V_{max} compared to W1 and W2. Notably, at t2, the rhizosphere soil exhibited the highest V_{max} value compared to both bulk soil (BS) compartment (Fig. 2.5.3a). For β-glucosidase activity, no substantial differences were observed between wheat rotational positions in BS samples. However, the rhizosphere (RH) had the highest value in WM (113.03 nmol MUF $g^{-1}h^{-1}$), indicating a 31.4% and 13.2% decrease compared to W1 and W2, respectively. In the second sampling time, WM significantly decreased β-glucosidase activity in all studied compartments. The lowest V_{max} was observed in wheat monoculture with values of 56.67 and 67.98 nmol MUF $g^{-1}h^{-1}$ in BS and RH compartments, respectively (Fig. 2.5.3b).

Leucine aminopeptidase activity displayed an increasing trend from bulk soil to rhizosphere soil. In the bulk soil (BS) at t1, W1 exhibited the highest V_{max} at 114.4 nmol AMC $g^{-1}h^{-1}$, with a 29.8% and 15.9% decrease in W2 and WM, respectively. At t2, wheat monoculture resulted in significantly higher V_{max} in BS. In the rhizosphere (RH) compartment, at both sampling times, WM consistently showed the lowest V_{max} for leucine aminopeptidase activity (Fig. 2.5.3c). In contrast to the other studied enzymes, wheat monoculture led to a substantial increase in acid phosphatase compared to the first and second wheat after the break crop. Moreover, the rhizosphere soil exhibited higher enzyme activity compared to both bulk soil (BS) compartment. In rhizosphere (RH) compartment, WM demonstrated the highest enzyme activity at t2, with values of 73.8 and 83.1 nmol MUF $g^{-1}h^{-1}$, respectively. At the second sampling time, W1 displayed the lowest acid phosphatase activity in RH (Fig. 2.5.3d).

At t2, the rhizosphere (RH) exhibited the most efficient α-glucosidase with low substrate affinity in both W1 and WM. Additionally, the bulk soil in WM displayed the lowest catalytic efficiency. Throughout both sampling times, W2 resulted in the lowest catalytic efficiency overall (Fig. 2.5.4a). For β-glucosidase, there was a decreasing trend in K_m values from bulk soil to rhizosphere soil in all wheat rotational positions. At t1, WM had the lowest K_m and the highest catalytic efficiency, with wheat monoculture displaying more efficient β-glucosidase enzymes compared to WM. However, at t2, the RH compartment in W1 had the highest catalytic efficiency, reaching 4.4 nmol MUF μmol substrate$^{-1}h^{-1}$. With plant growth, wheat

monoculture resulted in lower enzyme efficiency, and there were no significant differences between W2 and WM (Fig. 2.5.4b).

The same trend was observed for catalytic efficiency values for leucine aminopeptidase at the second sampling time. W1 in the RH compartment exhibited the highest catalytic efficiency, and continuous wheat cultivation led to a decline in enzyme efficiency. At t1, W2 had more efficient enzymes, and the bulk soil in WM had the highest K_m and the lowest efficiency (Fig. 2.5.4c). A different trend was observed for catalytic efficiency and K_m values for acid phosphatase, where wheat monoculture at both sampling times led to more efficient enzymes. At t2, RH soil in WM had the highest catalytic efficiency values, reaching 2.9 nmol MUF µmol substrate^{-1}h^{-1}, corresponding to a 38.6% and 6.2% increase compared to W1 and W2, respectively (Fig. 2.5.4d).

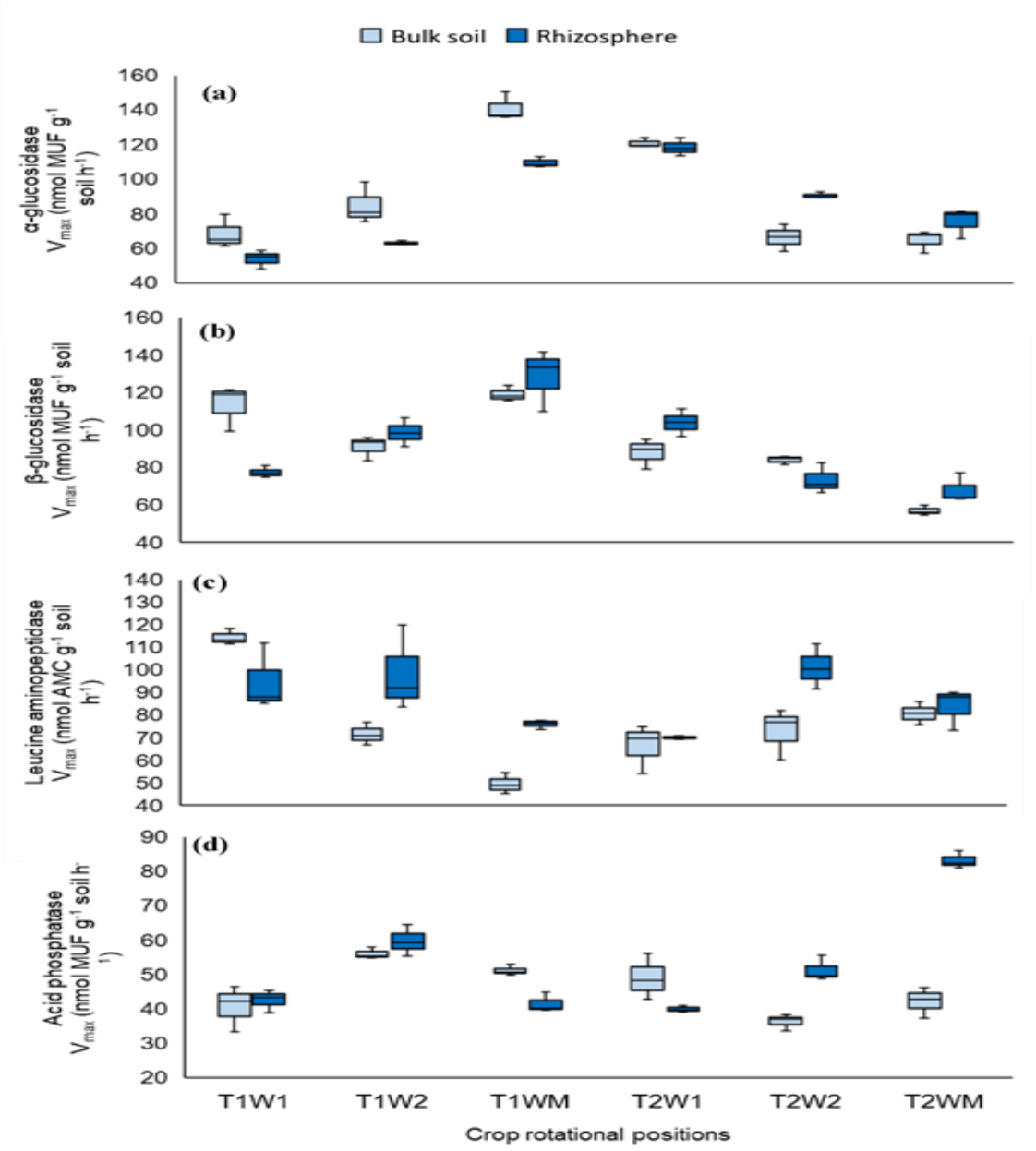

Figure 2.5.3. V_{max} values of α-glucosidase (a), β-glucosidase (b), leucine aminopeptidase (c) and acid phosphatase (d) in different wheat soil compartments (BS: bulk soil, RH: rhizosphere) in the first (W1), second (W2) winter wheat after oilseed rape break crop and long-term wheat monoculture (WM) at two sampling times, T1 (BBCH 29) and T2 (BBCH 59). Error bars represent standard error of means (n = 3) according to ANOVA at $p<0.05$.

Based on the results in Fig. 2.5.5, enzymes exhibited higher efficiency in terms of substrate turnover time at t2 compared to t1. At t1, the rhizosphere (RH) soil in WM had the lowest substrate turnover time for α-glucosidase. However, at t2, there was no significant difference between W1 and WM (Fig. 2.5.5a). For β-glucosidase at t1, WM showed lower turnover time in both RH and bulk soil (BS) compared to W1 and W2. However, at t2, in the RH compartment, the lowest turnover time was observed in W1, with a 2.51-hour turnover time, which increased by 56% and 45.5% in W2 and WM, respectively (Fig. 2.5.5b).

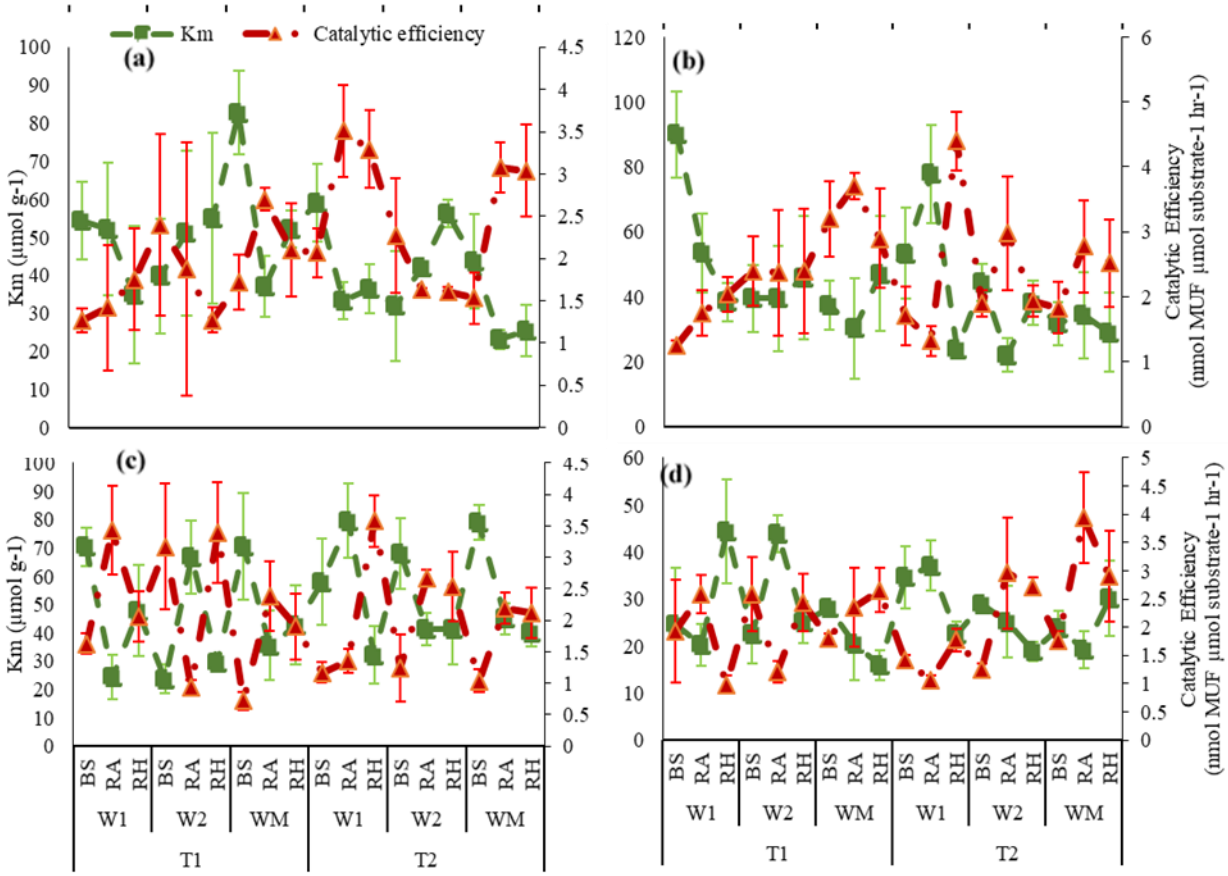

Figure 2.5.4. K_m values and catalytic efficiency of α-glucosidase (a), β-glucosidase (b), leucine aminopeptidase (c) and acid phosphatase (d) in different wheat soil compartments (BS: bulk soil, RH: rhizosphere) in the first (W1), second (W2) winter wheat after oilseed rape break crop and long-term wheat monoculture (WM) at two sampling times, T1 (BBCH 29) and T2 (BBCH 59). Error bars represent standard error of means (n = 3) according to ANOVA at p<0.05.

In BS at t1, the highest substrate turnover time was observed in WM for leucine aminopeptidase, significantly higher than W1 and W2. Also, in RH soil at t2, the turnover time was lower than in BS. However, there were no significant differences between wheat rotational positions in both BS and RH compartments (Fig. 2.5.5c). At t2, rhizosphere soil exhibited the highest turnover time for acid phosphatase enzyme, reaching 3.96 hours in WM, which had no significant difference with W2. In all sampling compartments and at both sampling times, RH in WM consistently had the lowest substrate turnover time (Fig. 2.5.5d).

2.5.7. Discussion

2.5.7.1. Microbial growth kinetics

This study unravels dynamic shifts in microbial biomass, growth, and activity influenced by various wheat rotational positions across two sampling times (t1 and t2; Fig. 2.5.1), revealing the intricate interplay between crop rotation and soil microbial ecology. Previous studies,

including those by Venter et al. (2016) and Sun et al. (2023), support the complexity of this relationship. At t1, the rhizosphere significantly impacted total microbial biomass, with wheat monoculture (WM) exhibiting a marked decrease compared to other rotational positions (Fig. 2.5.1a). This aligns with Mayer et al.'s (2019) findings of reduced rhizosphere microbial biomass in monoculture systems. Despite this, growing microbial biomass remained consistently higher in the rhizosphere than in bulk soil, indicating localized enrichment by root exudates (Wang et al., 2022).

While wheat monoculture enhanced microbial growth in the rhizosphere at t1, a notable shift occurred by t2. The rhizosphere soil of W1 (first year wheat) exhibited a remarkable growth increase, surpassing WM by approximately 2.5 times (Fig. 2.5.1). This hints at an adaptive and growth-promoting effect of W1 on the rhizosphere microbiome, consistent with Liu et al.'s (2023) observations of enhanced microbial activity in rotational systems compared to monoculture. These findings underscore the temporal dynamics and intricate relationships between wheat rotational positions and microbial responses, emphasizing the need for a comprehensive understanding of soil microbial communities in sustainable agricultural practices.

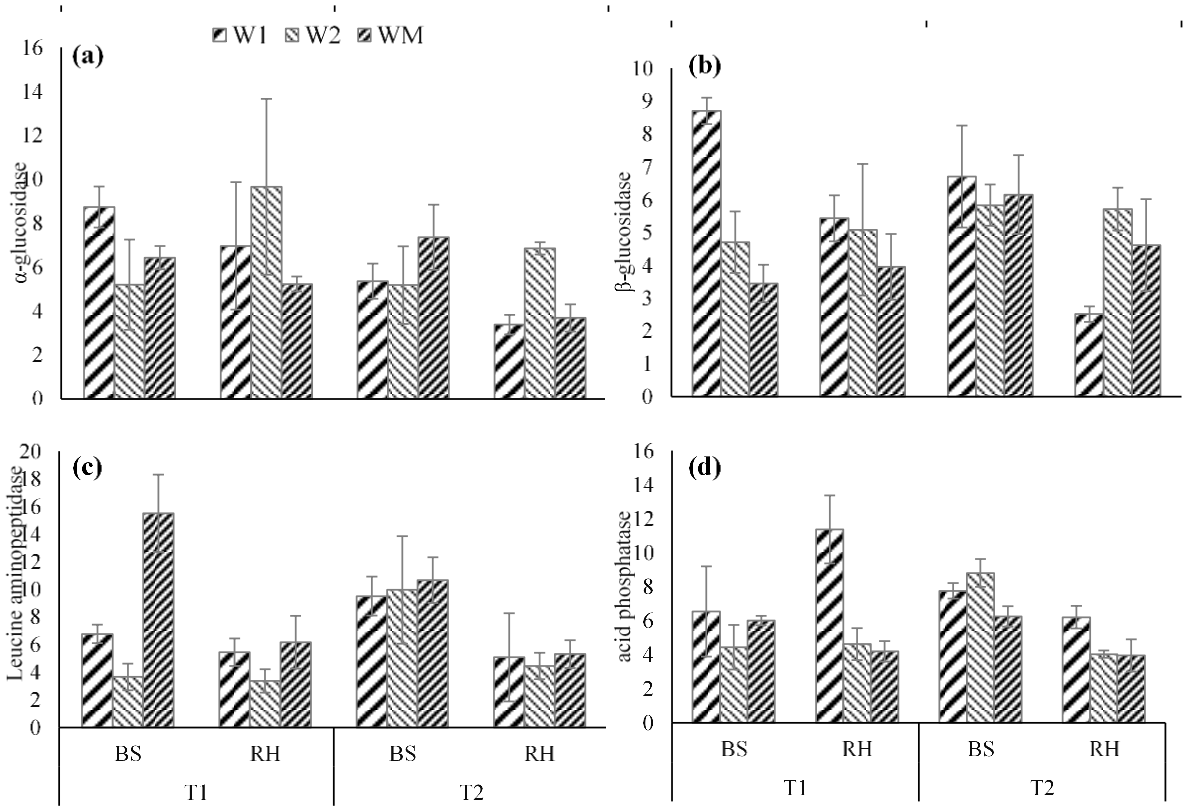

Figure 2.5.5. Substrate turnover time values of α-glucosidase (a), β-glucosidase (b), leucine aminopeptidase (c) and acid phosphatase (d) in different wheat soil compartments (BS: bulk soil, RH: rhizosphere) in the first (W1), second (W2) winter wheat after oilseed rape break crop and long-term wheat monoculture (WM) at two sampling times, T1 (BBCH 29) and T2 (BBCH 59). Error bars represent standard error of means (n = 3) according to ANOVA at $p<0.05$

The GMB/TMB ratio, reflecting microbial efficiency in resource utilization, was notably influenced by crop rotation at t1 (Fig. 2.5.1c). Wheat monoculture showed higher ratios in both the rhizosphere and bulk soil, suggesting a potential trade-off between growth and efficiency (Fierer et al., 2007). Although W1 had the highest ratio at t2, the absence of significant

differences across rotations suggests a convergence in microbial efficiency over time, possibly due to community adjustments (Sun et al., 2023).
Specific growth rates (μ) exhibited significant decreases in the rhizosphere of WM at t1, persisting at t2, hinting at a potential stress response or resource limitation in the monoculture system (Liu et al., 2023). Conversely, W2 (second year wheat) and WM displayed significantly higher μ in bulk soil at t2, indicating a shift in microbial dynamics and potential proliferation in bulk soil. The observed changes in lag time, with WM showing a fourfold increase in the rhizosphere by t2, further support the dynamic and potentially stressed response of the monoculture microbiome. The decline in generation time within WM at t2 suggests alterations in microbial metabolic activities, potentially in response to resource availability or stress adaptation (Wright et al., 2021).
The significant reduction in lag time for WM rhizosphere at t1, compared to other rotations, suggests a rapid and efficient activation of microbial biomass, possibly reflecting a readily available resource pool (e.g., root exudates) at t1, as observed in studies by Yahya et al. (2021). However, the unexpected increase in lag time for WM rhizosphere at t2 compared to W1 suggests a potential shift in the functional dynamics of the microbial community, attributable to various factors such as resource depletion, stress adaptation, and changes in community composition.
The decline in generation time of actively growing microbial communities in WM at t2, compared to W1 (Fig. 2.5.2), implies the adaptability of the microbial community to different rotational positions. This rapid growth strategy might be a response to resource limitations in the monoculture system, allowing for faster resource acquisition and biomass accumulation in response to reduced soil fertility (Croft et al., 2015). The negligible difference in generation time between W1 and WM at t1 suggests an initial stability or similarity in the metabolic activities of the microbial communities. However, as the experiment progressed, the differences in resource availability and potential stress factors in the monoculture system likely led to the observed divergence in generation times.

2.5.7.2. Enzyme kinetics

Continuous wheat cultivation (WM) exhibited contrasting effects on α-glucosidase activity depending on the sampling time and soil compartment. At t1, WM increased activity across all compartments (Fig. 2.5.3), potentially reflecting readily available resources for this readily degradable substrate (Sinsabaugh et al., 2002). However, at t2, WM exhibited the lowest activity, suggesting potential resource depletion or changes in microbial community composition in the monoculture system (Yahya et al., 2021). Notably, the rhizosphere consistently displayed higher activity compared to bulk soil, highlighting the localized enrichment of enzymes due to root exudates (Dhungaha et al., 2023). While the rhizosphere displayed the most efficient enzyme (low K_m) at t2 in both W1 and WM, WM bulk soil had the lowest efficiency throughout the study, suggesting potential spatial and temporal variability in enzyme efficiency within the different compartments and wheat rotations (Wang et al., 2023).
Similar to α-glucosidase, WM showed variable effects on β-glucosidase activity. At t1, WM had the highest activity in the rhizosphere, displaying the highest catalytic efficiency. However, this advantage diminished by t2, with W1 rhizosphere exhibiting the highest efficiency, potentially indicating efficient utilization of complex carbohydrates by specific microbial groups (Sinsabaugh et al., 2002). By t2, WM displayed the lowest activity in all compartments, suggesting potential limitations or shifts in resource availability in the monoculture over time. The decline in β-glucosidase activity in WM at t2, coupled with lower efficiency compared to W1 rhizosphere, indicates potential limitations or shifts in resource availability for the monoculture system over time.

Unlike other enzymes, WM consistently had lower leucine aminopeptidase activity in the rhizosphere, indicating limited access or utilization of protein-derived substrates. Conversely, WM displayed the highest acid phosphatase activity in the rhizosphere at t2, with W1 rhizosphere displaying the highest efficiency at t2, while WM generally had lower efficiency. This suggests a potential adaptation towards utilizing more recalcitrant organic phosphorus sources (Sinsabaugh et al., 2008; Chen et al., 2021).

2.5.8. Conclusion

This study revealed intricate connections between soil microbial dynamics and crop rotation practices. Wheat monoculture (WM) significantly affected microbial biomass, growth, and enzyme activity across different compartments and sampling times, highlighting the complex and dynamic nature of these interactions. WM initially decreased rhizosphere biomass but eventually promoted microbial growth compared to other rotations, highlighting the potential for both suppression and adaptation within the microbiome. Also, WM displayed higher growth-to-maintenance ratios, potentially prioritizing growth over resource utilization. However, rotational differences in efficiency converged over time, suggesting community adjustments. These findings emphasize the importance of understanding the temporal dynamics and intricate relationships between crop rotation and soil microbial responses for sustainable agricultural practices. Further research exploring the underlying mechanisms and long-term impacts of different cropping systems on soil microbial communities is crucial.

2.5.9. Acknowledgment

This study was carried out as part of the RhizoWheat project (Research program BonaRes) and received financial support from the BMBF. The authors express their gratitude to the German Federal Ministry of Education and Research (BMBF) for providing funding for this research (grant number 031B0910A).

2.5.10. Statements and Declarations

The authors declare that they have no known competing financial interests or personal relationships that could have appeared to influence the work reported in this paper.

2.5.11. References

Antonious G.F., Turley E.T., Dawood M.H. 2020. Monitoring soil enzymes activity before and after animal manure application. *Agriculture.* **10**:166. doi: 10.3390/agriculture10050166.

Arnhold, J., Grunwald, D., Braun-Kiewnick, A., Koch, H.J. 2023. Effect of crop rotational position and nitrogen supply on root development and yield formation of winter wheat. Front Plant Sci. 14:1265994. doi:10.3389/fpls.2023.1265994.

Blagodatskaya, E. V., Blagodatsky, S. A., Anderson, T. H., & Kuzyakov, Y. (2009). Contrasting effects of glucose, living roots and maize straw on microbial growth kinetics and substrate availability in soil [https://doi.org/10.1111/j.1365-2389.2008.01103.x]. European Journal of Soil Science, 60(2), 186-197. https://doi.org/https://doi.org/10.1111/j.1365-2389.2008.01103.x

Blagodatskaya, E., Blagodatsky, S., Anderson, T. H., & Kuzyakov, Y. (2014). Microbial growth and carbon use efficiency in the rhizosphere and root-free soil. PLoS One, 9(4), e93282. https://doi.org/10.1371/journal.pone.0093282

Blagodatsky, S. A., Heinemeyer, O., & Richter, J. (2000). Estimating the active and total soil microbial biomass by kinetic respiration analysis. Biology and Fertility of Soils, 32(1), 73-81. https://doi.org/10.1007/s003740000219

Castle, S. C., Samac, D. A., Gutknecht, J. L., Sadowsky, M. J., Rosen, C. J., Schlatter, D., & Kinkel, L. L. (2021). Impacts of cover crops and nitrogen fertilization on agricultural soil fungal and bacterial communities. *Plant and Soil*, *466*(1-2), 139-150.

Chen YP, Tsai CF, Rekha PD, Ghate SD, Huang HY, Hsu YH, Liaw LL, Young CC. Agricultural management practices influence the soil enzyme activity and bacterial community structure in tea plantations. Bot Stud. 2021 May 18;62(1):8. doi: 10.1186/s40529-021-00314-9.

Chen, M.N., Zhang, J.C., Liu, H., Wang, M., Pan, L.J., Chen, N., Wang, T., Jing, Y., Chi, X. Y., Du, B.H., 2020. Long-term continuously monocropped peanut significantly disturbed the balance of soil fungal communities. J. Microbiol. 58, 563–573. https:// doi.org/10.1007/s12275-020-9573-x

Croft, S.A., Pitchford, J.W., Hodge, A. 2015. Fishing for nutrients in heterogeneous landscapes: modelling plant growth trade-offs in monocultures and mixed communities. AoB PLANTS. 7: plv 109. https://doi.org/10.1093/aobpla/plv109.

Dhungana, I., Kantar, M.B., Nguyen, N.H. 2023. Root exudate composition from different plant species influences the growth of rhizosphere bacteria. Rhizosphere. 25: 100645. https://doi.org/10.1016/j.rhisph.2022.100645.

Duran, P., Jorquera, M., Viscardi, S., Carrion, V. J., de la Luz Mora, M., and Pozo, M. J. (2017). Screening and characterization of potentially suppressive soils against Gaeumannomyces graminis under extensive wheat cropping by Chilean indigenous communities. Front. Microbiol. 8:1552. doi: 10.3389/fmicb. 2017.01552

DWD (2022) German meteorological service. Available at: https://opendata.dwd.de/ climate_environment/CDC/observations_Germany/climate/multi_annual/mean_ 91-20

Erdel E, Şimşek U, Kesimci TG. 2023. Effects of Fungi on Soil Organic Carbon and Soil Enzyme Activity under Agricultural and Pasture Land of Eastern Türkiye. *Sustainability*. 2023; 15(3):1765. https://doi.org/10.3390/su15031765

Fierer, N., Bradford, M.A. and Jackson, R.B. (2007), Toward an ecological classification of soil bacteria. Ecology, 88: 1354-1364. https://doi.org/10.1890/05-1839

Garbeva, P., Hol, W. H. G., Termorshuizen, A. J., Kowalchuk, G. A., and de Boer, W. (2011). Fungistasis and general soil biostasis – A new synthesis. Soil Biol. Biochem. 43, 469–477. doi: 10.1016/j.soilbio.2010. 11.020

German, D. P., Weintraub, M. N., Grandy, A. S., Lauber, C. L., Rinkes, Z. L., & Allison, S. D. (2011). Optimization of hydrolytic and oxidative enzyme methods for ecosystem studies. Soil Biology and Biochemistry, 43(7), 1387-1397. https://doi.org/https://doi.org/10.1016/j.soilbio.2011.03.017

Giongo A, Arnhold J, Grunwald D, Smalla K and Braun-Kiewnick A (2024) Soil depths and microhabitats shape soil and root-associated bacterial and archaeal communities more than crop rotation in wheat. Front. Microbiomes 3:1335791. doi: 10.3389/frmbi.2024.1335791

Hamel, C., Gan, Y., Messer, D., Bainard, L.D., 2019. Soil 16S DNA sequence data and corresponding soil property and wheat yield data from a 72-plot field experiment involving pulses and wheat crops grown in rotations in the semiarid prairie. Data Br. 23, 103790. doi:10.1016/j.dib.2019.103790

Han, Q.H., Xin, S.L., Hong, H., 2010. Characterization of an antimicrobial material from a newly isolated bacillus amyloliquefaciens from mangrove for biocontrol of capsicum bacterial wilt. Biol. Control 54, 359–365. https://doi.org/10.1016/j. biocontrol.2010.06.015

Hoang, D.T., Maranguit, D., Kuzyakov, Y., Razavi, B.S., 2020. Accelerated microbial activity, turnover and efficiency in the drilosphere is depth dependent. Soil Biol. Biochem. 147, 107852. doi:https://doi.org/10.1016/j.soilbio.2020.107852

IUSS Working Group WRB (2015). "World Reference Base for Soil Resources 2014,legends for soil maps," in World soil resources reports (Rome: FAO). update 2015. International soil classification system for naming soils and creating

Joos, L., De Tender, C. 2022. Soil under stress: The importance of soil life and how it is influenced by (micro)plastic pollution. Computational and Structural Biotechnology Journal. 20: 1554–1566. https://doi.org/10.1016/j.csbj.2022.03.041

Kandeler, E., Stemmer, M., and Klimanek, E.-M. (1999). Response of Soil Microbial Biomass, Urease and Xylanase within Particle Size Fractions to Long-Term Soil Management. *Soil Biol. Biochem.* 31 (2), 261–273. doi:10.1016/S0038-0717(98)00115-1

Li, G., Li, P., Wu, M., Liu, K., Evangelos, P., Liu, J., Liu, M., Li, Z., 2022. Variation in rhizosphere microbial communities and its association with the nodulation ability of peanut. Arch. Agron Soil Sci. 69, 759–770. https://doi.org/10.1080/ 03650340.2022.2033734.

Li, T., Li, Y., Shi, Z., Wang, S., Wang, Z., Liu, Y., ... & Liao, Y. (2021). Crop development has more influence on shaping rhizobacteria of wheat than tillage practice and crop rotation pattern in an arid agroecosystem. *Applied Soil Ecology*, *165*, 104016.

Liu C, Song Y, Dong X, Wang X, Ma X, Zhao G and Zang S (2021) Soil Enzyme Activities and Their Relationships With Soil C, N, and P in Peatlands From Different Types of Permafrost Regions, Northeast China. *Front. Environ. Sci.* 9:670769. doi: 10.3389/fenvs.2021.670769

Liu, L., Sun, C., Liu, S., Chai, R., Huang, W., Liu, X., Tang, C., Zhang, Y., 2015a. Bioorganic fertilizer enhances soil suppressive capacity against bacterial wilt of tomato. PLoS One 10, e0121304. https://doi.org/10.1371/journal.pone.0121304.

Liu, Q., Zhao, Y., Li, T., Chen, L., Chen, Y., Sui, P. 2023. Changes in soil microbial biomass, diversity, and activity with crop rotation in cropping systems: A global synthesis. Applied Soil Ecology. 186: 104815. https://doi.org/10.1016/j.apsoil.2023.104815.

Liu, Y., Song, X., Wang, K., He, Z., Pan, Y., Li, J., Hai, X., Dong, L., Shangguan, Z.,
& Deng, L. (2023). Changes in soil microbial metabolic activity following long-term forest succession on the central Loess Plateau, China. *Land Degradation & Development*, 34(3), 723–735. https://doi.org/10.1002/ldr.4489

Mayer, Z.; Sasvári, Z.; Szentpéteri, V.; Pethőné Rétháti, B.; Vajna, B.; Posta, K. Effect of Long-Term Cropping Systems on the Diversity of the Soil Bacterial Communities. *Agronomy* **2019**, *9*, 878. https://doi.org/10.3390/agronomy9120878

Meier MA, Lopez-Guerrero MG, Guo M, Schmer MR, Herr JR, Schnable JC, Alfano JR, Yang J. 2021. Rhizosphere microbiomes in a historical maize-soybean rotation system respond to host species and nitrogen fertilization at the genus and subgenus levels. Appl Environ Microbiol 87:e03132-20. https://doi.org/10.1128/AEM.03132-20

Meisner A and de Boer W (2018) Strategies to Maintain Natural Biocontrol of Soil-Borne Crop Diseases During Severe Drought and Rainfall Events. Front. Microbiol. 9:2279. doi: 10.3389/fmicb.2018.02279

Michaelis, L. and Menten, M. L. (1913) Die Kinetik der Invertinwirkung Biochem. Z. 49, 333– 369.

Mir YH, Ganie MA, Shah TI, Bangroo SA, Mir SA, Shah AM, Wani FJ, Qin A, Rahman SU. Soil microbial and enzyme activities in different land use systems of the Northwestern Himalayas. PeerJ. 2023 Sep 26;11:e15993. doi: 10.7717/peerj.15993.

Panikov, N. (1991). Kinetics, Microbial Growth. In: Flickinger, M. C. and Drew, S. W., Eds. Encyclopedia of Bioprocess Technology: Fermentation, Biocatalysts and Bioseparation. New York: John Wiley & Sons, Inc., 1513-1543.

Panikov, N. S., & Sizova, M. V. (1996). A kinetic method for estimating the biomass of microbial functional groups in soil. Journal of Microbiological Methods, 24(3), 219-230. https://doi.org/https://doi.org/10.1016/0167-7012(95)00074-7

Philippot L, Raaijmakers JM, Lemanceau P, van der Putten WH. Going back to the roots: the microbial ecology of the rhizosphere. Nat Rev Microbiol 2013; 11:789–99. https://doi.org/10.1038/nrmicro3109.

Rao MA, Scelza R, Acevedo F, Diez MC, Gianfreda L. 2014. Enzymes as useful tools for environmental purposes. Chemosphere. 107:145-162. doi: 10.1016/j.chemosphere.2013.12.059. Epub 2014 Jan 8. PMID: 24411841.

Rao, D., Meng, F., Yan, X., Zhang, M., Yao, X., Kim, K. S., ... & Zhang, W. (2021). Changes in soil microbial activity, bacterial community composition and function in a long-term continuous soybean cropping system after corn insertion and fertilization. *Frontiers in Microbiology*, *12*, 638326.

She, S., Niu, J., Zhang, C., Xiao, Y., Chen, W., Dai, L., ... & Yin, H. (2017). Significant relationship between soil bacterial community structure and incidence of bacterial wilt disease under continuous cropping system. *Archives of microbiology*, *199*, 267-275.

Sinsabaugh, R. L., Carreiro, M. M., & Repert, D. A. (2002). Allocation of extracellular enzymatic activity in relation to litter composition, N deposition, and mass loss. *Biogeochemistry*, *60*, 1-24.

Sinsabaugh, R.L., Lauber, C.L., Weintraub, M.N., Ahmed, B., Allison, S.D., Crenshaw, C., Contosta, A.R., Cusack, D., Frey, S., Gallo, M.E., Gartner, T.B., Hobbie, S.E., Holland, K., Keeler, B.L., Powers, J.S., Stursova, M., Takacs-Vesbach, C., Waldrop, M.P., Wallenstein, M.D., Zak, D.R. and Zeglin, L.H. (2008), Stoichiometry of soil enzyme activity at global scale. Ecology Letters, 11: 1252-1264. https://doi.org/10.1111/j.1461-0248.2008.01245.x

Song X, Pan Y, Li L, Wu X, Wang Y. 2018. Composition and diversity of rhizosphere fungal community in Coptis chinensis Franch. continuous cropping fields. PLoS One. 2018 Mar 14;13(3):e0193811. doi: 10.1371/journal.pone.0193811.

Sun L, Wang S, Narsing Rao MP, Shi Y, Lian Z-H, Jin P-J, Wang W, Li Y-M, Wang K-K, Banerjee A, Cui X-Y and Wei D (2023) The shift of soil microbial community induced by cropping sequence affect soil properties and crop yield. *Front. Microbiol*. 14:1095688. doi: 10.3389/fmicb.2023.1095688.

Sun, Q.; Zhang, P.; Zhao, Z.; Li, X.; Sun, X.; Jiang, W. 2023. Continuous Wheat/Soybean Cropping Influences Soybean Yield and Rhizosphere Microbial Community Structure and Function. Agronomy 2023, 13, 28. https://doi.org/10.3390/ agronomy13010028

Telesiński A, Pawłowska B, Biczak R, Śnieg M, Wróbel J, Dunikowska D, Meller E. 2021. Enzymatic Activity and Its Relationship with Organic Matter Characterization and Ecotoxicity to *Aliivibrio fischeri* of Soil Samples Exposed to Tetrabutylphosphonium Bromide. Sensors (Basel). 2021 Feb 24;21(5):1565. doi: 10.3390/s21051565.

Telesiński A., Krzyśko-Łupicka T., Cybulska K., Pawłowska B., Biczak R., Śnieg M., Wróbel J. 2019. Comparison of oxidoreductive enzyme activities in three coal tar creosote-contaminated soils. *Soil Res.* **57**:814–824. doi: 10.1071/SR19040.

Tilman, D., Balzer, C., Hill, J., & Befort, B. L. (2011). Global food demand and the sustainable intensification of agriculture. *Proceedings of the national academy of sciences*, *108*(50), 20260-20264.

Van Leeuwen, J. P., Djukic, I., Bloem, J., Lehtinen, T., Hemerik, L., De Ruiter, P. C., & Lair, G. J. (2017). Effects of land use on soil microbial biomass, activity and community structure at different soil depths in the Danube floodplain. European journal of soil biology, 79, 14-20.

Venter, Z.S., Jacobs, K., Hawkins, H.J. 2016. The impact of crop rotation on soil microbial diversity: A meta-analysis. Pedobiologia. 59(4(: 215-223. https://doi.org/10.1016/j.pedobi.2016.04.001.

Wang J, Chen S, Sun R, Liu B, Waghmode T, Hu C. Spatial and temporal dynamics of the bacterial community under experimental warming in field-grown wheat. PeerJ. 2023 Jun 14;11:e15428. doi: 10.7717/peerj.

Wang, Y., Zhang, Y., Li, Z.Z., Zhao, Q., Huang, X.Y., Huang, K.F., 2019. Effect of continuous cropping on the rhizosphere soil and growth of common buckwheat. Plant Prod. Sci. 23, 81–90. https://doi.org/10.1080/1343943X.2019.1685895

Wright, A. J., L. Mommer, K. Barry, and J. van Ruijven. 2021. Stress gradients and biodiversity: monoculture vulnerability drives stronger biodiversity effects during drought years. *Ecology* 102(1):e03193. 10.1002/ecy.3193

Wu, H., Cui, H., Fu, C., Li, R., Qi, F., Liu, Z., Yang, G., Xiao, K., Qiao, M. 2024. Unveiling the crucial role of soil microorganisms in carbon cycling: A review. Science of The Total Environment. 909: 168627. https://doi.org/10.1016/j.scitotenv.2023.168627.

Yahya M, Islam Eu, Rasul M, Farooq I, Mahreen N, Tawab A, Irfan M, Rajput L, Amin I and Yasmin S (2021) Differential Root Exudation and Architecture for Improved Growth of Wheat Mediated by Phosphate Solubilizing Bacteria. *Front. Microbiol.* 12:744094. doi: 10.3389/fmicb.2021.744094

Yang T, Evans B and Bainard LD (2021) Pulse Frequency in Crop Rotations Alters Soil Microbial Community Networks and the Relative Abundance of Fungal Plant Pathogens. *Front. Microbiol.* 12:667394. doi: 10.3389/fmicb.2021.667394

Yu, T., Hou, X., fang, X., Razavi, B., Zang, H., Zeng, Z., Yang, Y. 2024. Short-term continuous monocropping reduces peanut yield mainly via altering soil enzyme activity and fungal community. Environmental Research. 245 (15): 117977. https://doi.org/10.1016/j.envres.2023.117977.

Zhou, X., Wang, Z., Jia, H., Li, L., Wu, F., 2018. Continuously monocropped Jerusalem Artichoke changed soil bacterial community composition and ammonia-oxidizing and denitrifying bacteria abundances. Front. Microbiol. 9 https://doi.org/10.3389/ fmicb.2018.00705.

Acknowledgments

I express my deepest gratitude to my esteemed supervisor, Jun. Prof. Dr. Bahar Razavi, for her unwavering guidance, invaluable insights, and continuous support throughout my doctoral journey. Her expertise, encouragement, and commitment to academic excellence have played a pivotal role in shaping the trajectory of my research and academic growth.

This study was carried out as part of the RhizoWheat project (Research program BONARES) and received financial support from the BMBF. The authors express their gratitude to the German Federal Ministry of Education and Research (BMBF) for providing funding for this research (grant number 031B0910A).

A heartfelt appreciation goes to all my colleagues involved in the Rhizowheat project. I also would like to express my sincere gratitude to Prof. Cai and all my friends at the Institute of Phytopathology, Kiel University. The collaborative spirit and shared dedication to advancing knowledge in our field have made this academic endeavor both enriching and rewarding.

I extend my sincere appreciation to all my friends at the Christian-Albrechts-University of Kiel (CAU), with special mentions for Hamed Kashi and Shang Wang. I also would like to extend my appreciation to Nikolaus Kaloterakis from Forschungszentrum Jülich (FZJ). Their shared experiences have enriched my academic and personal life, creating a supportive community that has made the academic journey more enjoyable.

Exceptional thanks are reserved for my wife, Sanam, and my daughter, Hida, who have been unwavering pillars of support throughout this challenging journey. Their boundless patience, understanding, and encouragement have provided the strength and motivation needed during the demanding phases of my doctoral studies. Their love and support have made this academic pursuit a shared family achievement.

Heartfelt gratitude goes out to my cherished family in Iran. Despite the physical distance, your love has provided a source of strength, motivation, and comfort. This achievement is a testament to the shared commitment and resilience of our familial bonds, and I am deeply thankful for the continuous support from my great family in Iran.

I am grateful for the collective contributions and collaborative spirit of everyone mentioned above, which have significantly enriched the depth and quality of my doctoral research. Your support and encouragement have been instrumental in reaching this milestone, and I am truly thankful for the shared journey and companionship.